γδ T Cells:
Friend or Foe in Melanoma under Immune Checkpoint Blockade?

Dissertation

der Mathematisch-Naturwissenschaftlichen Fakultät
der Eberhard Karls Universität Tübingen
zur Erlangung des Grades eines
Doktors der Naturwissenschaften
(Dr. rer. nat.)

vorgelegt von
M.Sc Nicola Herold (geboren Beucke)
aus Würzburg

Tübingen
2023

Gedruckt mit Genehmigung der Mathematisch-Naturwissenschaftlichen Fakultät der Eberhard Karls Universität Tübingen.

Tag der mündlichen Qualifikation:	22.01.2024
Dekan:	Prof. Dr. Thilo Stehle
1. Berichterstatter/-in:	PD Dr. Kilian Wistuba-Hamprecht
2. Berichterstatter/-in:	Prof. Dr. Hans-Georg Rammensee

Table of contents

List of abbreviations

AJCC	American Joint Committee on Cancer
ADCC	Antibody-dependent cellular cytotoxicity
APC	Antigen-presenting cell
B2M	β2 microglobulin
BTN	Butyrophilin
BTNL	Butyrophilin-like
CAR	Chimeric antigen receptor
CTLA-4	Cytotoxic T-lymphocyte-associated protein 4
DETC	Dendritic epidermal T cells
DNAM-1	DNAX accessory molecule-1
DOT	Delta One T
EPCR	Endothelial protein C receptor
FFPE	Formaldehyde-fixed paraffin-embedded
HMBPP	(E)-4-Hydroxy-3-methyl-but-2-enyl pyrophosphate
ICB	Immune checkpoint blockade
ICS	Intracellular cytokine staining
IHC	Immunohistochemistry
IPP	Isopentenyl pyrophosphate
irAE	Immune-related adverse events
LAG-3	Lymphocyte-activation gene 3
LFA-1	Lymphocyte function-associated antigen 1
MICA	Major histocompatibility complex class I chain-related A
OMIP	Optimized Multicolor Immunofluorescence Panel
OS	Overall survival
PD-1	Programmed cell death protein 1
PD-L1	Programmed cell death ligand 1
PD-L2	Programmed cell death ligand 2
PFA	Paraformaldehyde
PFS	Progression free survival
ROI	Region of interest
SKCM	Skin Cutaneous Melanoma
TCGA	The Cancer Genome Atlas
TEGs	T cells engineered with defined γδ TCRs
T_{EM}	T effector memory
T_{EMRA}	T effector memory re-expressing CD45RA
TIGIT	T cell immunoreceptor with Ig and ITIM domains
TIL	Tumor-infiltrating lymphocyte
TIM-3	T cell immunoglobulin and mucin domain 3
TME	Tumor microenvironment
TRAIL	Tumor necrosis factor-related apoptosis-inducing ligand

1. Abstract

Immune checkpoint blockade was the first treatment to significantly prolong the survival of melanoma patients with distant metastases and nowadays has become standard of care. Therapeutic antagonistic antibodies targeting PD-1 block binding to its ligands and are able to reinvigorate exhausted T cells. However, PD-1 expression is not limited to αβ T cells, but can also be found on γδ T cells making this heterogeneous population of unconventional T cells a further target of anti-PD-1 therapy.

Since γδ T cells are a less-well-studied T cell population, we looked into the pitfalls one might encounter when investigating these cells using polychromatic flow or mass cytometry, applying commercially available kits for magnetic cell isolation or when performing immunohistochemical staining. In this context, a careful selection of the utilized antibodies is of particular importance in order to avoid bias in the phenotypic or functional characterization and the drawn conclusions. Furthermore, we adapted an assay developed for αβ T cells to the γδ T cell subset, allowing a more rapid detection of functional Vδ1 and Vδ2 T cells based on the assessment of integrin activation. In addition to that we implemented the identification of γδ T cells in a high dimensional in situ imaging approach. This enables in-depth investigation of the phenotypic profile of tissue-resident and tumor-infiltrating innate-like Vγ9Vδ2 and adaptive-like Vδ1 T cells and their microenvironment. Building on this, future studies might elucidate the role and interplay of γδ T cells in solid malignancies and uncover potential targets of immunotherapy.

In parallel, we examined the role of γδ T cells in late-stage melanoma patients undergoing anti-PD-1 therapy, since a durable response is only achieved in a fraction of patients. Peripheral blood mononuclear cells and tumor-infiltrating lymphocytes were used to study the phenotype, functionality and TCR repertoire of Vδ1 and Vδ2 T cells. High frequencies of peripheral Vδ1 T cells were linked to poor overall survival and a late-differentiated potentially senescent-like phenotype that is presumably not responsive to immune checkpoint blockade. However, the abundance of Vδ1 T cells in the tumor was linked to prolonged overall survival and the senescent-like phenotype showed a lower prevalence at the tumor site. This supports the currently ongoing endeavors taking advantage of Vδ1 T cells for cancer immunotherapy.

2. Zusammenfassung

Immuncheckpointblockade ist die erste Therapie, die zu einer signifikanten Verlängerung des Gesamtüberlebens bei Patienten mit metastasiertem Melanom führte und ist heutzutage Erstlinientherapiestandard. Therapeutische, antagonistische Antikörper blockieren die Interaktion zwischen PD-1 und seinen Liganden wodurch erschöpfte T-Zellen reaktiviert werden können. PD-1 wird jedoch nicht nur von klassischen αβ T-Zellen exprimiert, sondern ist auch auf γδ T-Zellen vorzufinden. Dies macht die heterogene, unkonventionelle γδ T-Zell Population zu einem weiteren Angriffspunkt der anti-PD-1 Therapie.

Da γδ T-Zellen weniger gut untersucht sind, haben wir zunächst mögliche Fallstricke betrachtet, die einem bei massen- oder durchflusszytometrischen Analysen, bei der Verwendung kommerziell verfügbarer Kits zur magnetischen Zellisolation oder in der Immunhistochemie begegnen können. In diesem Zusammenhang ist es besonders wichtig auf eine sorgfältige Auswahl der eingesetzten Antikörper zu achten, um einen Bias bei der phänotypischen und funktionellen Charakterisierung sowie den daraus resultierenden Schlussfolgerungen zu vermeiden. Darüber hinaus haben wir einen Assay, der auf der Detektion von aktivierten Integrinen basiert und ursprünglich für αβ T-Zellen entwickelt wurde, adaptiert, was eine raschere Bestimmung von funktionellen Vδ1 und Vδ2 T-Zellen ermöglicht. Zudem haben wir die Identifikation von γδ T-Zellen in der hoch-dimensionalen in-situ Bildgebung implementiert. Dies erlaubt eine detaillierte Untersuchung des phänotypischen Profils von gewebsständigen und tumorinfiltrierenden Vγ9Vδ2 und Vδ1 T-Zellen sowie deren Mikroumgebung. Zukünftige Studien könnten darauf aufbauend die Rolle und das Zusammenspiel von γδ T-Zellen in soliden Tumoren beleuchten und potenzielle Angriffspunkte für Immuntherapien identifizieren.

Parallel dazu haben wir analysiert, welche Rolle γδ T-Zellen in Patienten mit fortgeschrittenem Melanom unter anti-PD-1 Therapie spielen, da nur ein geringer Anteil der Patienten ein anhaltendes Therapieansprechen zeigt. Mononukleäre Zellen des peripheren Blutes und tumorinfiltrierende Lymphozyten wurden mit Hinblick auf den Phänotyp, die Funktionalität und das TCR Repertoire der Vδ1 und Vδ2 T-Zellen untersucht. Hohe Frequenzen an peripheren Vδ1 T-Zellen stehen in Zusammenhang mit einem schlechtem Gesamtüberleben sowie der Dominanz eines spät-differenzierten potentiell Seneszenz-ähnlichen Phänotyps, der mutmaßlich nicht auf die Immuncheckpointblockade anspricht. Die Abundanz von tumorinfiltrierenden Vδ1 T-Zellen war jedoch positiv mit dem Überleben verknüpft und der Seneszenz-ähnliche Phänotyp zeigte eine verringerte Prävalenz im Tumor. Insgesamt unterstützen unsere Ergebnisse damit die zurzeit laufenden Bestrebungen zur Nutzung von Vδ1 T-Zellen in der Krebsimmuntherapie.

3. Publications and manuscripts

(1) Pitfalls in the characterization of circulating and tissue-resident human γδ T cells (2020). **Beucke N**, Wesch D, Oberg HH, Peters C, Bochem J, Weide B, Garbe C, Pawelec G, Sebens S, Röcken C, Hashimoto H, Löffler MW, Nocerino P, Kordasti S, Kabelitz D, Schilbach K, Wistuba-Hamprecht K. **Journal of Leukocyte Biology** 107(6): 1097-1105. PMID: 31967358.

(2) Accurate determination of γδ T cells in multi-channel mass and flow cytometry (2020). **Beucke N**, Wistuba-Hamprecht K. Letter to the Editor - **Cytometry Part B: Clinical Cytometry** 100(3): 288-289. PMID: 32469457.

(3) Integrin activation enables rapid detection of functional $V\delta1^+$ and $V\delta2^+$ γδ T cells (2022). **Herold N**, Schöllhorn A, Feile A, Gaißler A, Mohrholz A, Pawelec G, Löffler MW, Dimitrov S, Gouttefangeas C, Wistuba-Hamprecht K. **European Journal of Immunology** 52(5): 730-736. PMID: 35133647.

(4) High-dimensional in situ proteomics imaging to assess γδ T cells in spatial biology (2024). **Herold N**, Bruhns M, Babaei S, Spreuer J, Castagna A, Yurttas C, Scheuermann S, Seitz C, Königsrainer A, Jurmeister P, Löffler MW, Claassen M, Wistuba-Hamprecht K. **Journal of Leukocyte Biology.**

(5) A Vδ1 T cell subset is responsive to PD-1 blockade and associated with survival in melanoma (2024). **Herold N**, Bochem J, Leyens J, Wingerter S, Forchhammer S, Spreuer J, Deseke M, Yurttas C, Nocerino P, Antunes dos Reis R, Amaral T, Wagner NB, Thiel K, Soffel D, Bieber K, Terheyden P, Wesch D, Oberg HH, Sebens S, Claassen M, Königsrainer A, Garbe C, Pawelec P, Meier F, Löffler MW, Weide B, Prinz I, Ravens S, Kordasti S, Eigentler TK, Wistuba-Hamprecht K. **Submitted manuscript.**

Not embedded in this thesis:

(6) Genetic Influence on the Peripheral Differentiation Signature of $V\delta2^+$ γδ and $CD4^+$ αβ T Cells in Adults (2021). **Beucke N**, Wingerter S, Hähnel K, Larsen LA, Christensen K, Pawelec G, Wistuba-Hamprecht K**. Cells** 10(2): 373. PMID: 33670279.

4. Personal contribution

(1) Pitfalls in the characterization of circulating and tissue-resident human γδ T cells

Study conceptualization
Investigation
Data curation and formal analysis
Writing of the original draft
Review, editing and revision

(2) Accurate determination of γδ T cells in multi-channel mass and flow cytometry

Writing of the original draft
Review, editing and revision

(3) Integrin activation enables rapid detection of functional $V\delta1^+$ and $V\delta2^+$ γδ T cells

Study conceptualization
Investigation
Data curation and formal analysis
Writing of the original draft
Review, editing and revision

(4) High-dimensional in situ proteomics imaging to assess γδ T cells in spatial biology

Study conceptualization
Investigation
Data curation and formal analysis
Review, editing and revision

(5) A Vδ1 T cell subset is responsive to PD-1 blockade and associated with survival in melanoma

Study conceptualization
Investigation
Data curation and formal analysis
Writing of the original draft
Review, editing and revision

5. Introduction

5.1 Melanoma

The worldwide incidence of melanoma, the deadliest and most aggressive type of skin cancer, has been rising over the past decades and continues to [1]. Melanoma arises from malignant transformation of melanocytes, pigment-producing cells located primarily in the epidermis, but also found in the eye and at mucosal sites. The American Joint Committee on Cancer (AJCC) staging system categorizes patients into stage I-IV, based on characteristics of the primary tumor, involvement of lymph nodes and the presence of distant metastases. Local disease is defined as stage I-II, node-positive disease as stage III and patients with metastatic spread to distant sites are classified as stage IV [2]. Despite recent improvements in therapy increasing the 5-year survival rate of stage IV patients remarkably from less than 5% [3] to around 50% [4], prognosis for this patient group remains poor. Melanoma is characterized by one of the highest prevalence of somatic mutations [5], rendering these tumors highly immunogenic and a substantial proportion of this mutational burden is associated with exposure to ultraviolet radiation [6].

5.2 Immune checkpoint blockade

Melanoma has been historically treatment-resistant and among the group of most refractory cancers [7]. Immunotherapy utilizing monoclonal antagonistic antibodies blocking the engagement of the inhibitory checkpoint receptor cytotoxic T-lymphocyte-associated protein 4 (CTLA-4) was the first therapy to significantly extend the survival of patients with advanced disease [8]. Furthermore, melanoma was the first disease in which the efficacy of immune checkpoint blockade (ICB) was demonstrated [9] and durable clinical responses after treatment discontinuation have been reported [10], reshaping the field of immunotherapy. Nowadays, therapeutic blockade of programmed cell death protein 1 (PD-1) alone or in combination with CTLA-4 is first-line treatment in metastatic melanoma [7] and has been approved for multiple other malignancies. Moreover, ICB has been extended to the neo-adjuvant and adjuvant setting to reduce the risk of disease recurrence and several clinical trials are ongoing [11]. However, not all patients respond (primary resistance) to these systemic therapies, only a fraction derives long-lasting benefit (secondary resistance) and the minority experiences complete remission. Since the stimulation of the immune system is not tumor-specific, there is an increased risk of all-grade immune-related adverse events (irAE) and high rates of grade 3-4 irAE leading to treatment discontinuation [12]. Therefore it is important to understand the underlying biology and mechanisms determining response [13], identify patients who are likely to (not) respond [14] and explore new avenues of immunotherapy. Numerous ongoing clinical trials are evaluating the potential of targeting

novel immune checkpoints like Lymphocyte-Activation Gene 3 (LAG-3), T cell immunoglobulin and mucin domain 3 (TIM-3), T cell immunoreceptor with Ig and ITIM domains (TIGIT) and B7 Homolog 3 either as monotherapies or in dual/triple blockade regimens with PD-1 to potentiate the therapeutic effect [15, 16]. In 2022 the RELATIVITY-047 trial led to FDA approval of dual checkpoint inhibition of PD-1 and LAG-3, showing a comparable benefit to combination therapy with CTLA-4 and a favorable safety profile [17, 18].

5.3 PD-1

Though ipilimumab targeting CTLA-4 has been approved first, anti-PD-1 monotherapy or in combination with ipilimumab showed improved overall survival (OS) in the KEYNOTE-006 study [19] and Check-Mate-067 trial [20], respectively. The PD-1 pathway has a multifaceted physiologic role maintaining immune homeostasis and peripheral self-tolerance, limiting pro-inflammatory responses and protecting against autoimmunity [21]. PD-1 is inducibly and transiently expressed on T cells upon activation. Its´ cognate ligands programmed cell death ligand 1 (PD-L1) and 2 (PD-L2) are widely expressed on immune cells as well as in non-lymphoid tissue and on tumor cells [22]. The rationale behind anti-PD-1 therapy is that abrogation of this inhibitory regulatory mechanism should allow tumor-reactive T cells to mount an effective anti-tumor response.

Persistent expression of PD-1 has been linked to CD8 T cell exhaustion, a process occurring in adaptation to chronic antigen exposure as for example occurring in chronic viral infections or in the tumor setting [23]. Exhausted cells are characterized by a loss of effector function and impaired proliferative capacity, thereby unable to control tumor growth. However, exhaustion is not a fixed state and does not describe a uniform population. Instead, it is a dynamic process in which long-term persisting PD-1^{low} progenitor CD8 T cells with self-renewal ability yet low cytotoxicity, give rise to short-lived PD-1^{high} terminally exhausted CD8 T cells with high cytotoxic activity, but limited expansion capacity [24, 25]. Since these terminally exhausted T cells, showing a sustained co-expression of multiple co-inhibitory immune receptors including CTLA-4, TIM-3 and TIGIT, are only transient effectors, tumor control is only temporary [24, 26]. Progenitor exhausted CD8 T cells are permissive to PD-1/PD-L1 therapy, while terminally exhausted cells are considered unresponsive [25, 27, 28]. Reinvigoration of exhausted T cells is rapid and can be detected in patients as early as one week after the initial dose of ICB [29]. A higher proportion of progenitor exhausted CD8 T cells within the tumor-infiltrating lymphocytes (TILs) has been associated with a longer OS and progression free survival (PFS) in melanoma patients undergoing anti-PD-1 therapy [30]. The response to anti-PD-1 treatment is not restricted to the tumor microenvironment (TME), it

also depends on immunomodulation of the peripheral blood and lymphoid compartment and the communication between blood, tumor and tumor draining lymph nodes [25]. Furthermore, the response to PD-1 blockade likely extends to other subsets beyond exhausted CD8 T cells, for example effector memory CD8 T cells, other PD-1 expressing T cells, macrophages and dendritic cells.

5.4 γδ T cells

γδ T cells are an evolutionary conserved third lineage of lymphocytes, besides αβ T cells and B cells, carrying a somatically rearranged antigen receptor [31]. Expression of the inhibitory checkpoint receptor PD-1 on γδ T cells makes this population of non-classical T cells a further, less well-studied, target of ICB.

5.4.1 γδ T cell subsets

The numerically minor γδ T cell compartment comprises heterogeneous subsets with distinct functionalities and is commonly delineated based on γ- and in particular δ-chain usage. The TCRγδ gene family encompasses eight TRDV genes of which Vδ1, Vδ2 and Vδ3 are exclusive to TCRδ, while Vδ4-8 are shared with the TCRα locus. Out of the 14 TRGV genes, only six are functional, namely Vγ2,3,4,5,8,9 [32]. One can distinguish between innate-like Vγ9Vδ2 and adaptive-like non-Vγ9Vδ2 T cells mainly represented by Vδ1 T cells [33, 34]. Vγ9Vδ2 T cells predominate in the peripheral blood and are characterized by a semi-invariant TCR repertoire with restricted CDR3 length containing prevalent conserved public sequences shared between individuals [33]. Vδ1 T cells are also present in blood but show a higher prevalence in tissue especially at barrier sites [35]. Their TCR repertoire is private, highly diverse and often shaped by stable, focused clonal expansions [34, 36].

5.4.2 γδ T cell development and differentiation

The first T cells to develop in the fetus are Vγ9Vδ2 T cells generated at extrathymic sites, including the fetal liver and potentially the primitive gut, coincidently with or shortly after the start of hematopoiesis between 6-9 weeks after gestation [37, 38]. Vδ1 T cells are generated later in gestation in the fetal thymus. In the thymus, αβ and γδ T cells develop from a common precursor. Successful rearrangement of the γ- and δ-chain by VJ or VDJ recombination, respectively, allows commitment to the γδ lineage [32, 39]. Fate decision between the αβ and γδ lineage warrants further investigation, yet is likely to follow a signal strength-based instructional model [32].

Vδ1 T cells follow an adaptive differentiation program paralleling CD8 T cell differentiation [40] and concurring with TCR-dependent clonal expansion, downregulation of secondary

lymphoid homing receptors and increased expression of effector molecules [41]. In contrast to that, Vγ9Vδ2 T cells show a rather innate-like behavior with polyclonal expansions [33, 42]. However, there is still heterogeneity in the expression profile of classical T cell differentiation markers like CD45RA, CD27, CD28 and CD16, which is linked to functional properties [43, 44].

5.5 Target recognition via the γδ TCR

A few years ago a MHC-restricted human γδ TCR recognizing a MART-1-derived peptide was discovered [45]. However, this is a rare case and γδ T cells are in general considered not MHC-restricted and instead recognize qualitatively distinct antigens. Compared to αβ T cells, γδ T cells harbor a greater diversity in CDR3 length and composition and are therefore likely able to bind to more diverse antigens [31], thereby broadening the scope of antigens recognized by T cells, though the cognate antigens for most γδ TCRs are yet to be determined. The so far discovered TCR ligands as well as the expression of NK receptors indicate a major contribution to discrimination between normal and stress conditions through recognition of self-molecules reflecting a dysregulated state or alterations due to infection or cellular stress [46]. γδ TCRs are marked by diverse and unusual binding modes and differ in their receptor affinities. Furthermore, some γδ TCRs show cross-reactivity or dual specificity, thereby being able to intrinsically combine innate and adaptive immunity.

5.5.1 Recognition by Vγ9Vδ2 T cells

Vγ9Vδ2 T cells recognize low molecular mass, non-peptidic, organic pyrophosphate antigens – termed phosphoantigens – in a butyrophilin-dependent manner. Phosphoantigens can be of endogenous origin arising from the mevalonate pathway. For example, isopentenyl pyrophosphate (IPP) may accumulate in cancer cells due to a dysregulated metabolism or as a consequence of treatment with nitrogen-containing bisphosphonates, commonly used in the context of bone disorders, inhibiting the enzyme farnesyl pyrophosphate synthase [47, 48]. Besides that, foreign phosphoantigens like (E)-4-Hydroxy-3-methyl-but-2-enyl pyrophosphate (HMBPP) are generated by plasmodium parasites and numerous species of bacteria as intermediate of the non-mevalonate pathway of isoprenoid biosynthesis [49]. Phosphoantigens do not interact directly with the Vγ9Vδ2 TCR instead recognition is mediated by butyrophilins (BTNs). BTNs are structural relatives of the B7 family of immune-regulatory molecules and four of them - BTN2A1 and the three BTN3A isoforms A1, A2 and A3 – are known to be involved in the activation of γδ T cells [50]. BTN2A1 and BTN3A1 are closely associated on the cell surface, phosphoantigen binding to the intracellular domain of BTN3A1 induces a conformational change and BTN2A1 then directly binds to a germline-encoded region of the Vγ9 chain. Moreover, the CDR2δ and CDR3γ/δ regions are required

for phosphoantigen sensing, though the interaction partner has not yet been elucidated [51, 52]. In addition to that, differences in antitumor reactivity between individual Vγ9Vδ2 clones are linked to the composition of the CDR3 domain [53].

5.5.2 Recognition by non-Vγ9Vδ2 T cells

Target recognition by non-Vγ9Vδ2 T cells is in general less well understood and limited to knowledge on some individual clones. A commonly observed pattern is the recognition of MHC and MHC-related molecules, often in an antigen-independent manner, although affinity can be modulated by the bound antigen [54].

Members of the CD1 family present lipid antigens, are structurally related to MHC class I and are recognized by various γδ T cell clones. CD1a is bound by a Vγ3Vδ1 TCR via an atypical end-to-side docking independent of lipid antigen presentation [55] and several Vδ1 clones recognize CD1b with different binding modalities depending on or independent of the carried lipid [56]. The affinity of different Vδ1 TCRs to CD1c and CD1d is modulated by the bound lipid antigen that can be of endogenous or exogenous origin [57, 58]. The MHC class I-related molecule MR1 presents vitamin B-derived metabolites and is recognized by a diverse population of γδ T cells carrying Vδ1, Vδ3 or Vδ5 chains combined with different γ chains. These γδ TCRs can recognize empty MR1, though the loaded antigen affects affinity, and utilize diverse binding modes including an unusual recognition of the underside of the MR1 antigen-binding cleft [59]. The highly polymorphic major histocompatibility complex class I chain-related A (MICA) molecules, members of the ULBP family – both also ligands for NKG2D – and endothelial protein C receptor (EPCR) are expressed upon cellular stress and can be directly recognized by the γδ TCR [46, 60].

Apart from MHC-related molecules, several other ligands have been described, including the algae protein phycoerythrin [61], annexin A2 [62] and the human MutS homolog 2 [63]. Furthermore, paralleling BTN-mediated recognition of phosphoantigens, butyrophilin-like 3 (BTNL3) and BTNL8 are enriched in the gut epithelium, form heterodimers and BTNL3 directly binds to germline-encoded regions of a Vγ4 TCR [64]. Reactivity to EPCR, a lipid carrier with structural similarity to CD1, can also be combined with responsiveness to BTNL3 as shown for a Vγ4 clone [65]. Likewise, a Vγ4Vδ1 TCR with dual specificity for CD1b and BTNL3/BTNL8 has been described [56]. Taken together, antigen recognition via the γδ TCR cannot be generalized (yet) and many of the so far known ligands are only recognized by particular clones.

5.6 γδ T cells in cancer

γδ T cells are pleiotropic effectors with the ability to exert anti- as well as pro-tumor functions and tumor-infiltrating γδ T cells have been associated with favorable and unfavorable prognosis depending on the subset and malignancy [66]. Besides their somatically rearranged TCR, γδ T cells can utilize germline-encoded natural killer receptors for recognition of cancer cells.

5.6.1 Anti-tumor functions of γδ T cells

Direct killing of cancer cells can be exerted by triggering apoptosis through the perforin-granzyme axis. γδ T cells secrete cytotoxic granules containing perforin, which leads to pore-formation, and granzyme B, a pro-apoptotic serine protease. In addition to that, apoptosis can be induced via engagement of death receptors by the membrane-bound death receptor ligands FasL and tumor necrosis factor-related apoptosis-inducing ligand (TRAIL). Moreover, γδ T cells expressing the Fc receptor CD16 can bind to antibodies coating a target cell and elicit antibody-dependent cellular cytotoxicity (ADCC) [66, 67].

Besides their direct anti-tumor reactivity, γδ T cells employ a variety of indirect mechanisms thereby orchestrating the anti-tumor immune response. These unconventional T cells can mimic dendritic cell functions and induce priming of αβ T cells. Activated Vγ9Vδ2 T cells can express antigen-presenting and costimulatory molecules at levels similar to professional antigen-presenting cells (APCs) and antigen presentation induces proliferation and differentiation of naive CD4 and CD8 T cells [68] [69]. Humoral immunity is modulated by γδ T cells providing B cell help [70, 71] and release of the pro-inflammatory type 1 cytokines IFN-γ and TNF is, amongst other functions of these pleiotropic effector molecules, involved in dendritic cell maturation [72]. Furthermore, NK cells can be stimulated by the interaction of 4-1BB with its ligand 4-1BBL, expressed on the surface of activated γδ T cells [73].

In addition to the γδ TCR, γδ T cells can express NK cell receptors including killer activation receptors for example NKG2D, NKp30/44/46 and killer inhibitory receptors like NKG2A. These receptors can act in synergy with the TCR enabling γδ T cells to combine T cell- and NK cell-related mechanisms to recognize their target [74]. NKG2D is expressed on most γδ T cells and allows recognition of transformed cells upregulating MICA, MICB or ULBPs [75]. The NK receptor DNAX accessory molecule-1 (DNAM-1) is also widely expressed and its binding to Nectin-like-5 has been shown to be involved in the cytotoxicity against hepatocellular carcinoma cells [76]. Circulating γδ T cells show no constitutive expression of Nkp30, Nkp44 and Nkp46, but expression can be induced and is associated with enhanced cytotoxicity against tumor cells [77, 78]. Furthermore, Nkp46-expressing Vδ1 T cells are

present in the healthy intestine, able to infiltrate colorectal cancer tissue and exhibit a high cytotoxic potential [79].

5.6.2 Pro-tumor functions of γδ T cells

IL-17, secreted by γδ T cells can support angiogenesis, promote metastasis and recruit immunosuppressive myeloid cells. However, most of this knowledge stems from mouse experiments and it is controversially discussed whether and to what extent the tumor-promoting function of γδ T cells in humans is mediated by IL-17 [67, 80]. An immunosuppressive Vδ1 subset expressing CD73, producing IL-10 and able to inhibit the proliferation of αβ T cells has been identified in breast cancer [81]. Furthermore, a breast cancer-infiltrating Vδ1 population caused impairment of dendritic cell maturation and suppressed the proliferation of naive and effector T cells [82]. Moreover, γδ T cells can produce IL-4, galectin-1 and -9, which might suppress the anti-tumor activity of other γδ and CD8 T cells [67]. Inconsistent results regarding the relationship between FoxP3 expression and regulatory activity of γδ T cells have been reported, therefore FoxP3 should not be relied on as an indicator of regulatory potential [83, 84].

5.6.3 γδ T cells in melanoma

γδ T cells are known to infiltrate primary melanoma as well as metastases, though they are mainly found in earlier disease stages [85, 86]. The majority of the infiltrating Vδ1 and Vδ2 T cells are of the T effector memory (T_{EM}) or terminally-differentiated T effector memory re-expressing CD45RA (T_{EMRA}) phenotype [86]. Infiltration of Vδ1 T cells in necrotizing choroidal melanoma and a higher proportion of intratumoral γδ T cells in cutaneous melanoma have been associated with prolonged OS [87, 88]. Furthermore, polyclonal Vδ1 and Vδ2 T cell lines generated from tumor-infiltrating lymphocytes were able to exert cytotoxicity against a melanoma cell line [86]. Concerning the circulating compartment of γδ T cells in melanoma patients, reduced numbers of Vδ2 T cells have been described in non-metastatic [89, 90] as well as in stage III and IV patients [91]. Moreover, an accumulation of $CD28^-$ γδ T cells expressing high levels of perforin in stage I-III patients [92] and increased frequencies of T_{EM} and $CD57^+$ γδ T cells in the peripheral blood of metastatic patients have been observed [91]. High frequencies of Vδ1 T cells in late-stage patients are negatively associated with OS [93], also in the context of immune therapy with ipilimumab [94]. In addition to that, high Vδ1 levels are linked to an accumulation of late-differentiated Vδ1 T cells with a T_{EMRA} phenotype [94].

5.7 γδ T cell-based cancer immunotherapy

Overall the tumor-suppressive functions of γδ T cells seem to prevail, despite some reports regarding their tumor-promoting features [95], and a considerable variety of γδ T cell-based immunotherapy approaches targeting hematologic malignancies as well as solid tumors are under development. The focus thereof has been shifting from adoptive transfer of expanded autologous Vγ9Vδ2 T cells and bisphosphonate treatment to more advanced approaches and targeting of the Vδ1 compartment. Due to their tissue-resident nature, Vδ1 T cells might more efficiently traffic to and persist at the tumor site [96]. Currently, several clinical trials exploring antibody-based cell engagers or adoptive cell therapy in various malignancies are ongoing [97].

5.7.1 Antibody-based cell engagers

An agonistic anti-BTN3A antibody, binding all three isoforms, is able to mimic the conformational change induced by phosphoantigens and thereby selectively sensitizes cells for recognition by Vγ9Vδ2 T cells. Due to the ability to bind all BTN3A isoforms, cells predominantly expressing the BTN3A2 isoform, which lacks the phosphoantigen-sensing domain, can also be targeted [98]. Furthermore, a number of bispecific antibodies engaging the Vγ9 TCR and different tumor-antigens for example HER2, CD40, CD123 and EGFR are explored at the clinical or preclinical level [95]. These constructs are designed to promote the activation and accumulation of Vγ9 T cells at the tumor site.

5.7.2 Adoptive cell therapy

Previous clinical trials investigating the autologous adoptive transfer of expanded Vγ9Vδ2 T cells revealed a good safety profile, though limited therapeutic efficacy [99]. Nowadays, most approaches employ allogeneic instead of autologous adoptive cell therapy, since there is a low risk of graft-versus-host disease due to the lack of MHC restriction and to circumvent the limitation of variable expansion capacity of γδ T cells from different patients [100].
Besides an improved expansion protocol for Vγ9Vδ2 T cells utilizing vitamin C and IL-15 [101], a clinical-grade protocol for the expansion and differentiation of Vδ1 T cells has been developed [78]. Moreover, several genetically engineered γδ T cell products based on Vδ1 or Vδ2 T cells carrying a modified chimeric antigen receptor (CAR) have been designed. These include CD19- and CD20-directed CAR γδ T cells as well as a CAR containing an external region of NKG2D and a CAR directed against glypican-3 [95, 102]. In order to transfer the innate-like phosphoantigen responsiveness of Vγ9Vδ2 T cells to αβ T cells, T cells engineered with defined γδ TCRs (TEGs) were generated by retroviral transduction. These TEGs carry a defined high affinity Vγ9Vδ2 TCR allowing them to sense metabolic

dysregulation and thereby target a broad range of malignancies [103, 104]. Beyond that, chemotherapy-resistant γδ T cells have been developed by introducing a methylguanine DNA methyltransferase transgene conferring resistance to temozolomide. This enables the modified γδ T cells to survive in the presence of temozolomide and to recognize NKG2D ligands, which can be transiently upregulated on tumor cells due to the DNA damage induced by this alkylating agent [105].

6. Aim of the thesis

Approval of ipilimumab, an immune checkpoint inhibitor directed against CTLA-4, in 2011 led to a breakthrough in the treatment of melanoma patients with distant metastases. Later, antagonistic antibodies targeting PD-1 followed and ICB became first-line treatment. However, durable clinical responses are achieved only in a fraction of patients, stressing the importance of better understanding the underlying biology. γδ T cells are also a target of anti-PD-1 therapy but have been less well-studied in this context which prompted us to investigate these unconventional T cells and their role in cancer immunosurveillance in more detail.

On the one hand, we aim to illustrate which difficulties and pitfalls one might be confronted with when studying this minor T cell subset by applying commonly used laboratory techniques like polychromatic flow cytometry, immunohistochemistry (IHC) or magnetic cell isolation. These considerations shall support entry to and improve comparability in the growing field of γδ T cell immunology. Furthermore, we intend to advance these methods by adapting an integrin-based activation assay to the γδ T cell population and by implementing the detection of innate-like Vγ9Vδ2 and adaptive-like Vδ1 T cells in a high-dimensional imaging approach. Building on this, future studies could create a detailed profile of tumor-infiltrating γδ T cells and provide a better understanding of the surrounding tumor microenvironment, potentially resulting in the identification of new targets for cancer immunotherapy.

On the other hand, we aim to elucidate which role γδ T cells play in metastasized melanoma in the context of ICB to gain insight into factors impacting patients' response or resistance. By in-depth investigation of the phenotypic profile in independent patient cohorts, we intend to robustly determine which subsets of γδ T cells are associated with clinical outcome. Comparative analysis of the functionality and TCR repertoire before and during therapy should enable us to examine potential alterations or impairments of the γδ T cell population in melanoma patients and whether the γδ T cell compartment can be shaped by ICB. This, along with comparison of the peripheral blood population to the tumor site, will allow us to better understand the contribution of γδ T cells to tumor immunity and with regard to their potential for use in novel therapeutic approaches.

7. Results and discussion

7.1 Methodological considerations and establishment of novel approaches for the comprehensive investigation of γδ T cells

Due to their pleiotropic functions and lack of MHC restriction γδ T cells are of rising interest also with regard to exploitation for cancer immunotherapy. Besides cancer, these unconventional T cells are involved in inflammation, auto-immune and infectious disease. However, compared to αβ T cells, γδ T cells are a less-well-studied T cell population, also reflected by the limited number of commercially available reagents. Furthermore, in some instances, conflicting data has been reported regarding their pro- or anti-tumor function and their association with favorable or unfavorable clinical outcome. Therefore, we aimed to highlight current challenges and extend the repertoire of available methods for the assessment of human γδ T cells in peripheral blood as well as in tissue. By providing a basic framework we intend to contribute to standardization in the field of γδ T cell immunology thereby improving comparability between research centers.

7.1.1 Pitfalls in the characterization of circulating and tissue-resident human γδ T cells

Based on our own experiences and literature research, we recognized the need for standardization in the phenotypic and functional investigation of the circulating, tissue-resident or tumor-infiltrating human γδ T cell compartment. Therefore, we present a compilation of commonly used methods including magnetic cell isolation, flow and mass cytometry and IHC in publication 1. We point out potential challenges and how to overcome these in order to avoid bias in the analysis and the drawn conclusions.

Magnetic cell isolation is routinely used to separate or enrich certain immune cell subsets. The isolation procedure can strongly influence the subsequent experiments as shown by Schilbach et al. reporting an inhibitory effect of Vδ2 T cells on the proliferation of αβ T cells when these cells were positively isolated, while this was not the case for negatively isolated Vδ2 T cells [106]. In general, positive isolation is more straightforward especially when aiming for the isolation of specific γδ T cell subsets and spares the non-targeted cells for subsequent experiments. However, the utilized antibodies lead to TCR crosslinking making this approach only suitable for non-functional analysis like TCR sequencing. When evaluating activation markers, determining cytokine expression or studying cytotoxic or suppressive functions, untouched isolation procedures should be used. The currently available commercial negative isolation kits achieve high purities, yet the composition of the depletion cocktails is not disclosed by the manufacturers. We report that these kits contain anti-CD16 antibodies for depletion of NK cells, though CD16 like many other NK cell markers

is also expressed on γδ T cells, resulting in the loss of this subset. As a substitution, we suggest the use of anti-Nkp30/46 antibodies since these natural cytotoxicity receptors are constitutively expressed on resting NK cells [107], while peripheral γδ T cells from healthy donors express only very low levels. Nevertheless, expression of these receptors can be induced upon long-term activation in culture [74, 108, 109], elevated in the context of different diseases [88, 110] and has been reported on tissue-resident γδ T cells [79]. Hence, there is still a need for the identification of NK cell-exclusive markers or marker combinations in order to optimize the negative isolation of γδ T cells.

Most immunological studies using flow or mass cytometry and the majority of Optimized Multicolor Immunofluorescence Panels (OMIPs), with the exception of a few [111-113], either neglect or examine γδ T cells as a whole population, but do not distinguish subsets. However, γδ T cells are a heterogeneous population and it is important to differentiate between the two major subsets, namely the innate-like Vγ9Vδ2 and the adaptive-like Vδ1 T cells. As previously reported in the OMIP-20 [112], there are pitfalls when combining antibodies for the phenotypic identification of γδ T cell subsets likely caused by steric hindrance due to the close spatial proximity of the recognized epitopes. Combination of the Vδ2 antibody clone B6 with different pan-γδTCR antibodies showed that several pan-γδTCR clones were unable to recognize the whole Vδ2 subset unless an indirect staining approach was utilized. In addition to that, clone B6 most likely recognizes not all Vδ2 T cells, but only Vγ9Vδ2 T cells [33]. Furthermore, staining of CD3 is known to interfere with the binding of the pan-γδTCR antibody clone B1. We show that the more recently released antibody clones overcome these challenges. Yet, the other clones are still commercially available and have been and continue to be used in potentially problematic combinations [114, 115] as previously addressed in a comment [116] and by us in a letter to the editor (Publication 2). Moreover, one needs to be aware that certain γ and δ chains can also be expressed by αβ T cells [31, 117]. In these cases and when studying stimulated samples or tumor-infiltrating lymphocytes, it is recommended to include a pan-γδTCR antibody to unambiguously identify γδ T cells. By utilizing secondary detection of the γδTCR via biotin and streptavidin signal amplification and thereby a higher stain index can be achieved.

The need for standardization is exemplified by reported discrepancies regarding the composition of the peripheral blood γδ T cell population in melanoma patients determined by flow cytometric analyses. In non-metastatic melanoma, a reduction of γδ T cells due to lower numbers of Vδ2 T cells [89, 90] as well as an increase in γδ T cells due to an accumulation of $CD28^-$ γδ T cells [92] and unchanged levels of γδ T cells also in stage III and IV patients [91, 93] have been described. These inconsistencies might be due to differences in patient

characteristics, but the interplay between different clones from different manufacturers in a multicolor panel might as well play a role.

Complementing flow cytometry, IHC provides spatial information and enables assessment of the abundance and localization of tissue- or tumor-infiltrating γδ T cells. Since the pan-γδTCR antibody clone γ3.20 is no longer available, clone H-41 is presently used for the detection of γδ T cells in formaldehyde-fixed paraffin-embedded tissue (FFPE) tissue [118] and has meanwhile been validated in a variety of tissues [119]. A more detailed characterization can be achieved by staining for Vγ9 (clone 7A5) or Vγ2,3,4 (clone 23D12), however, there is currently a lack of antibodies enabling the detection of Vδ1 and Vδ2 T cells in FFPE tissue. For fresh-frozen tissue fixed with acetone, a comprehensive γδ T cell panel has been published [120], yet fresh-frozen tissue is often not available, while FFPE tissue is routinely prepared in most pathology departments. In general, IHC is limited to the analysis of a single section thereby not capturing tissue or tumor heterogeneity and most commonly serial sections are used instead of higher-order multicolor IHC resulting in a certain inaccuracy when determining proportions of T cell subsets. This aspect is addressed by the development of a high-dimensional imaging approach described in publication 4.

7.1.2 Integrin activation enables rapid detection of functional Vδ1$^+$ and Vδ2$^+$ γδ T cells

Assessing T cells and their functionality is important to track alterations and response dynamics in patients, especially in the context of monitoring and improving immunotherapy. Commonly used techniques based on cytokine expression include ELISpot, though lacking information on the phenotype, and intracellular cytokine staining (ICS) combined with extracellular staining [121]. The latter requires the use of protein trafficking inhibitors and permeabilization and fixation of cells prior to intracellular staining. Clustering and conformational change of Lymphocyte function-associated antigen 1 (LFA-1) upon TCR-mediated stimulation is an early marker of activated T cells and can be detected by flow cytometry using a monoclonal anti-LFA-1 antibody clone m24 or ICAM-1 multimers [122, 123]. During this inside-out signaling process LFA-1 changes from a bent structure with low ligand affinity to an extended open high affinity conformation [124]. Since no de-novo expression is required, this process occurs rapidly thereby enabling an earlier detection of T cell activation compared to cytokines. The practicability of clone m24 staining has been shown for αβ T cells [122], here we aimed to transfer this assay to γδ T cells.

In publication 3, we demonstrate the suitability of clone m24 staining for the detection of functional Vδ1 and Vδ2 T cells and that this staining coincides with and extends beyond cytokine expression determined by ICS. Stimulation with PMA/Ionomycin, γδTCR-directed antibodies, phosphoantigens as well as co-culture with a bisphosphonate-treated melanoma

cell line resulted in detectable activation, though with different stimuli-dependent kinetics. This enables a more rapid assessment of γδ T cell functionality and since there is no requirement for fixation it allows sorting of viable, activated cells. However, when immediate acquisition is not possible or when acquiring a larger number of samples, fixation is recommended. A limitation of this method is the comparatively high background expression, especially on Vδ1 T cells, of the high-affinity conformation of LFA-1 compared to αβ T cells and in contrast to a very low background in ICS. Therefore, it is recommended to combine clone m24 staining with other early activation markers as shown for CD4 T cells [122]. Moreover, different cytokines or cytokine combinations are expressed in the context of different diseases and T cell subsets or by peripheral compared to tumor-infiltrating T cells which is not captured by this assay. Besides the γδTCR, γδ T cells carry NK cell receptors like NKG2D and Nkp30, Nkp44 and Nkp46 can be expressed upon activation. Further experiments are warranted to investigate clone m24 staining in response to activation of these receptors. For NK cells it has been shown that stimulation via cross-linking of NKG2D, Nkp30 and NKp46 resulted in a very weak activation of LFA-1. Yet, triggering of CD16, which is also expressed on γδ T cells, leads to strong LFA-1 activation [125].

Taken together, we show that staining of activated LFA-1 with the m24 monoclonal antibody is feasible for rapidly detecting functional Vδ1 and Vδ2 T cells. This enables high-throughput functional analyses of peripheral blood, tissue-resident or tumor-infiltrating γδ T cells without requiring protein trafficking inhibitors or intracellular staining.

7.1.3 High-dimensional in situ proteomics imaging to assess γδ T cells in spatial biology

Standard IHC based on chromogenic or fluorescent detection is limited in the number of markers that can be investigated in one tissue section thereby hampering a detailed characterization of the tumor or tissue microenvironment. In publication 4, we describe a high-dimensional imaging approach allowing us to define γδ T cell subsets and their phenotype as well as to generate information about localization, spatial organization and surrounding cells in fresh-frozen paraformaldehyde (PFA) fixed tissue. This method is based on an iterative cyclic procedure of staining, imaging and signal erasure by photobleaching or enzymatic digestion. Moreover, we combined this approach with bioinformatics analysis to study the environment of γδ T cells in human colon and colorectal cancer tissue. In addition to that we discuss current challenges and limitations.

A variety of commercially available γδTCR-specific antibodies were screened for their performance and a panel of four antibodies was selected for the identification of innate-like Vγ9Vδ2 and adaptive-like Vδ1 T cells. Satisfactory staining of this selection was shown in

different malignant and non-malignant tissues including adenoid, colon and colorectal cancer as well as pancreatic cancer and cholangiocarcinoma. Next, the γδTCR-specific antibodies were incorporated into a high-dimensional panel comprising 55 additional markers for a detailed phenotypic investigation and assessment of other immune cells, epithelial cells, myocytes, vasculature and extracellular matrix. This panel was utilized for a proof-of-principle study examining colorectal cancer and paired healthy tissue to identify γδ T cells and in-depth characterize their neighborhood using unbiased bioinformatics analysis. Based on marker expression profiles, cell types were assigned to the obtained clusters. Vδ1 T cells mainly displayed a late differentiated phenotype, while Vγ9Vδ2 T cells exhibited a more heterogeneous phenotypic profile. Neighborhood analysis showed the proximity of γδ T cells to tumor cells, B cells and myeloid cells in accordance with their pleiotropic functions including involvement in cancer immunity and T helper functionality [67].

Since there is only a limited number of commercially available antibodies recognizing the Vδ1 TCR, it is to our knowledge currently not possible to identify this subset in FFPE tissue and there is still room for improvement of the staining quality in our panel. However, high-dimensional imaging offers the advantage of looking at co-expression, in this case of the markers CD45, CD3 and pan-γδTCR facilitating the identification of Vδ1 T cells. Similar to what has been earlier described for multicolor flow cytometry, one might run into issues due to sterical hindrance in high dimensional IHC when using classical fluorescently labeled hybridoma antibodies. A solution for this can be the utilization of digestible antibodies, though currently the available repertoire is limited [126]. In addition to that, enzymatic digestion is faster than photobleaching especially for larger regions of interest (ROIs) thus accelerating the procedure. Repeatedly an overlap between T and B cell markers e.g. between CD3 or CD4 and CD20 or IgD that are considered exclusive was observed. $CD20^+$ T cells and the appearance of CD3 on the surface of B cells have been described occasionally. The respective surface molecules are likely acquired by the transfer of plasma membrane segments via trogocytosis since expression was not observed on the RNA level [127-129]. Further markers, preferentially intracellular proteins like the transcription factors TOX and TCF-1 that are not subjected to trogocytosis, need to be incorporated into the panel to unambiguously identify cells belonging to either the B or T cell lineage. While the majority of antibodies showed a good signal-to-noise ratio on tonsil or adenoid tissue, this was not the case for colon tissue probably due to tissue-type-dependent antigen accessibility and epitope shielding. This especially affected CD4, CD20 and several myeloid markers. Therefore, we are currently evaluating alternative fixation protocols including a periodate-lysine-paraformaldehyde fixative, an acetone or methanol incubation step before PFA fixation and lower percentages of PFA to reduce the extent of cross-linking. Furthermore, an indirect

staining approach might amplify the signal and allow prolonged incubation times outside of the automated imaging system.

Besides the above-discussed challenges in IHC, tissue and staining quality is of great importance in the context of high-dimensional imaging combined with computational analysis to avoid artefactual marker expression resulting in incorrect cell type annotation. Hence, a careful panel design taking bleed-over between fluorophores into consideration and diligent experimental execution minimizing the time between surgery, tissue dissection and freezing as well as tissue folds and antibody aggregates are warranted.

The here employed MACSima technology requires the expert-driven selection of ROIs in contrast to the PhenoCycler, formerly known as CODEX, utilizing a slide scanner. The latter is based on antibody-oligonucleotide conjugates and complementary fluorescently labeled DNA probes enabling the detection of up to 60 markers [130], while staining of a single specimen with more than 300 antibodies has been reported for the MACSima [126]. Apart from these fluorescent-based technologies, there are two commercially available mass spectrometry-based systems offering multiparametric tissue imaging at single-cell resolution. Both, the Multiplexed Ion Beam Imaging (MIBI) scope system and the Hyperion imaging mass cytometry instrument allow the detection of about 40 markers, though since the latter utilizes laser tissue ablation the specimen cannot be further used [131].

Combination of these high-dimensional imaging technologies with bioinformatics analysis and the respective clinical data offers great potential in translational research and the field of immuno-oncology and may guide the development of immunotherapies e.g. by identifying new solid tumor targets for cellular therapy [126].

7.1.4 Conclusion and outlook

γδ T cell subsets might be lost during magnetic cell isolation procedures or remain undetected in flow or mass cytometry experiments depending on which antibodies are used and combined and this likely extends to IHC. By highlighting these issues and contributing to the repertoire of available assays we hope to achieve a higher comparability in the field.

Beyond the discussed methods, careful experimental design is also important when studying cytotoxic activity. Due to the low abundance of γδ T cells, this often requires prior expansion and can hardly be studied ex vivo. Yet, expansion protocols lead to bias by inducing activation and promoting the expansion of certain subsets [74, 78] and the addition of stimuli like IL-18 can result in enhanced cytokine production [132]. Furthermore, different clones might exhibit variable expansion capacity depending on the utilized stimuli and culture conditions, though for Vδ2 T cells it has been shown that the TCR repertoire composition remains rather stable after phosphoantigen stimulation [133].

Caution also needs to be taken on the computational side as exemplified by gene expression analysis via the CIBERSORT method identifying intratumoral γδ T cells as the most significant favorable prognostic immune population across a variety of cancers [134]. Applying this algorithm to purified immune populations revealed that CIBERSORT misclassifies most γδ T cells as NK cells, CD4 or CD8 T cells and vice versa [135] questioning the reported association with favorable survival outcome. An optimized version LM7, trained on Vγ9Vδ2 T cells, correctly classifies the majority of Vγ9Vδ2 T cells, but detection rates for mixed populations containing Vδ1, Vδ2 and Vδ3 T cells are low [135].

Further approaches towards standardizations are warranted to elucidate the conflicting results that have been reported not only in melanoma, as discussed above, but also in colon and breast cancer. Tumor-infiltrating γδ T cells have been described as the major source of IL-17 in colon cancer and were associated with tumor stage and invasiveness [136]. However, another study demonstrated nearly no IL-17 production by γδ T cells in colon cancer patients. Furthermore, a higher abundance of tumor-infiltrating γδ T cells was linked to longer disease-free survival [137]. Yet, CIBERSORT-LM7 was used in this study to determine the relative fractions of infiltrating leukocytes and as earlier mentioned this approach is not suitable for detecting non-Vγ9Vδ2 T cells. In a cohort of breast cancer patients with different tumor stages and variable ER and HER status high numbers of intratumoral γδ T cells, determined by IHC, correlated with advanced tumor stage, poor OS and relapse-free survival [138]. In contrast to that, quantitative sequencing of DNA extracted from FFPE tissue indicated no correlation of total γδ T cells with survival, but a higher representation of Vδ1 T cells correlated with longer PFS and OS in triple-negative breast cancer [139].

Besides experimental deviations, these opposing results might be explained by differences in patient characteristics, treatment regimen or sample collection and processing. This stresses the importance of reporting this information as well as the experimental procedure in detail in order to improve comparability.

7.2 The role of γδ T cells in melanoma in the context of anti-PD-1 therapy

Immune therapy utilizing checkpoint inhibitors targeting CTLA-4 or PD-1 has revolutionized melanoma treatment, yet prediction of clinical response remains a challenge. Furthermore, patients with distant organ metastases still have a poor prognosis, stressing the importance of unraveling the underlying mechanisms and involved immune populations [9, 10]. PD-1 blockade has been shown to reinvigorate exhausted CD8 T cells [25], yet PD-1 is expressed by a variety of immune populations including γδ T cells [140]. These unconventional T cells are of growing interest due to their involvement in the anti-tumor immune response in multiple cancer entities and their implications in orchestrating immunity [67, 95]. In ipilimumab-treated melanoma patients high frequencies of peripheral Vδ1 T cells were associated with poor OS and the dominance of a late-differentiated phenotype [94]. Under anti-PD-1 therapy intratumoral γδ T cell frequencies increased in DNA mismatch repair-deficient cancers with HLA class I defects**.** Moreover, these tumor-infiltrating Vδ1 and Vδ3 T cells were able to recognize and display cytotoxic activity against cancer cells, suggesting a contribution to ICB responsiveness [141].

In publication 5, we investigated the phenotype, functionality, TCR repertoire and alterations therein in late-stage melanoma patients as well as immunotherapy-induced changes. This enables us to gain insight into potential impairments of γδ T cells in melanoma as well as into the capability of ICB to reconstitute these. In addition to that we assessed paired tumor and blood samples studying the interrelationship between circulating and tumor-infiltrating γδ T cells to elucidate their role and clinical relevance in melanoma in the context of anti-PD-1 therapy and with regard to utilization for novel therapeutic approaches.

7.2.1 Vδ1 T cells are associated with survival and show phenotypic alterations

PD-1 expression has been described in healthy donors as well as on peripheral blood and tumor-infiltrating Vδ1 T cells in various solid malignancies [140, 142, 143]. In advanced melanoma, we show that around 20% of peripheral Vδ1 T cells carry the PD-1 receptor on the cell surface, levels comparable to healthy donors. An indirect staining approach [144] enabled us to detect therapeutic antibodies bound to PD-1 on Vδ1 T cells, confirming the direct targeting of these unconventional T cells. Furthermore, we report an early decline in the proportion of PD-1 expressing Vδ1 T cells under therapy indicating modulation of this subset by PD-1 blockade.

Utilizing mass cytometry the phenotypic profile of γδ T cells was comprehensively determined in a small cohort of melanoma patients before treatment initiation. Similar to what has been observed in patients receiving ipilimumab [94], patients with above-median frequencies of Vδ1 T cells amongst all T cells ($Vδ1^{high}$) had significantly shorter OS compared to those with low frequencies ($Vδ1^{low}$). Moreover, we noted major differences in the

phenotypic marker distribution. The Vδ1^{high} group was characterized by the dominance of a late-differentiated phenotype and upregulation of NK cell-associated markers. Two independent larger cohorts were explored by flow cytometry to validate the discovered associations. Cohort 1 encompassed 91 patients treated with anti-PD-1 antibodies, while two-thirds of the patients in cohort 2, comprising 70 individuals, received ipilimumab + nivolumab combination therapy. Applying the afore-determined cutoff, confirmed the association between high Vδ1 frequency and poor OS. Moreover, the Vδ1^{high} group displayed an elevated frequency of T_{EMRA}-like and CD57^{+} cells. Expression of CD57 on Vδ1 T cells is linked to shortened telomeres and diminished proliferative capacity implying proliferative senescence [145] as well as to expression of granzymes and perforin [146]. Functional analyses revealed a reduction of the proliferative potential in patients, though cytokine expression was similar to healthy individuals and did not differ between the two patient groups.

Anti-PD-1 therapy is known to reinvigorate exhausted CD8 T cells, though the mode of action is likely broader involving immunomodulation of the peripheral blood, lymphoid and tumor compartment [25]. For example, the loss of β2 microglobulin (B2M), which is essential for the assembly of functional HLA class I complexes, has been linked to resistance to immune checkpoint therapy [147]. However, patients deficient for or carrying mutant B2M still obtain clinical benefit from anti-PD-(L)1 therapy [148], suggesting the contribution of other immune cell subsets apart from CD8 T cells to the anti-tumor response. Chronic stimulation can result in exhaustion of T cells, a dynamic process during which progenitor-exhausted cells with limited cytotoxicity and intermediate PD-1 expression differentiate into short-lived terminally exhausted cells marked by high cytotoxic activity and expression of multiple inhibitory receptors [24, 25, 149]. The latter subset is considered unresponsive to PD-1 blockade [24] and prolonged survival of melanoma patients with a higher proportion of progenitor-exhausted CD8 T cells infiltrating the tumor prior to combination therapy has been reported [30]. We observed no differences in PD-1 expression between the Vδ1^{high} and Vδ1^{low} group by flow cytometry and in-depth mass cytometric analyses revealed no cluster corresponding to terminally exhausted Vδ1 T cells or indicating enrichment of such cells in the Vδ1^{high} group. Therefore, the extent of T cell exhaustion is likely not different between the two patient groups.

Another crucial state of T cell dysfunction is senescence, characterized by shortened telomeres, a diminished proliferative potential and downregulation of CD28 [26, 150]. High frequencies of senescent T cells are linked to poor survival in various solid malignancies and therapy settings including ICB [151, 152]. The co-stimulatory receptor CD28 has been described as the primary target of PD-1-mediated T cell suppression [153] and the majority

of CD8 T cells proliferating under PD-1 blockade express CD28 [154]. Yet, other reports suggest that CD28 is not required for response to anti-PD-1 therapy, but serves as a marker of responsiveness [155]. Patients of the Vδ1^{high} group showed an enrichment of features associated with senescence for example a T_{EMRA}-like phenotype, loss of CD28, high levels of CD57 and expression of NK cell-related markers like CD56, NKG2A and CD161. Since these cells are presumably unresponsive to anti-PD-1 therapy, a dominance of this late differentiated senescent-like phenotype might be disadvantageous in the studied setting.
Under therapy, we noted no distinct changes in the differentiation signature, cytokine expression or proliferation. However, we observed a decline in the frequency of CD57^{+} cells and an increase in TRDV1 repertoire diversity, indicating a polyclonal expansion of CD57^{-} cells. Importantly, the change in clonal diversity of the TRDV1 repertoire was only significant in the Vδ1^{low} group, which would be consistent with a higher number of therapy-responsive cells in this group.

IHC analysis of pre-therapy metastases confirmed the presence of intratumoral γδ T cells in three-quarters of patients, albeit at low abundance. This is in line with other studies demonstrating scarce infiltration or absence of γδ T cells in advanced stages and metastases [85, 86]. Comparison of paired tumor and peripheral blood samples showed an overlap of TRD clonotypes and intermediate to high repertoire similarity, supporting trafficking between the periphery and tumor site. The TCR repertoire of Vδ1 T cells is considered private [41], concordantly no tumor-infiltrating TRDV1 clonotypes were shared among the eight examined patients. Due to the limited number of available tumor samples, we had to refer to a dataset from the Cancer Genome Atlas (TCGA) Skin Cutaneous Melanoma (SKCM) project for survival analysis. In contrast to our results in peripheral blood, above median TRDV1 expression in the tumor was associated with prolonged OS, yet the therapy setting is not specified limiting comparability to our data. In a previous study infiltration of Vδ1 T cells in choroidal melanomas correlated positively with survival [87], yet uveal and cutaneous melanoma display a distinct biology and differ in response to treatment [156]. Another study showed that melanoma patients with a higher proportion of intratumoral total γδ T cells experienced longer OS, though mainly metastatic lymph nodes were studied [88], which were excluded from our analyses. The ImmuCellAI algorithm applied to a gene expression dataset of melanoma patients undergoing anti-PD-1 therapy data revealed an increase in infiltrating γδ T cells under therapy as well as a higher abundance on treatment in responders [157]. This endorses the presence of ICB-responsive γδ T cells and their contribution to anti-tumor immunity in melanoma. In non–small cell lung cancer a higher abundance of tumor-infiltrating effector memory Vδ1 T cells or tissue-resident memory Vδ1 T cells in non-tumor lung was linked to prolonged relapse-free survival [158]. This study also

investigated a public dataset, the TCGA lung adenocarcinoma and lung squamous cell carcinoma project, and likewise reported favorable OS of patients with higher than median TRDV1 expression. Furthermore, re-analysis of gene expression data originating from the INSPIRE trial of pembrolizumab, which examined alterations of the immune landscape in various advanced solid cancers including melanoma [159], demonstrated that above-median TRDV1 expression was associated with prolonged OS [158] further supporting our observations. Flow cytometry analysis of paired tumor and peripheral blood samples revealed significantly decreased percentages of $CD57^+$ Vδ1 T cells in the tumor, indicating a lower prevalence of the late-differentiated senescent-like phenotype at the tumor site. Patients in which the peripheral Vδ1 T cell compartment is dominated by this presumably anti-PD-1 unresponsive phenotype might therefore have poorer chances of eliciting a sufficient anti-tumor response in this therapy setting.

7.2.2 Vδ2 T cells play a minor role

Compared to the Vδ1 subset, a lower percentage of Vδ2 T cells expressed PD-1, yet proportions were likewise comparable to healthy individuals. Similar to Vδ1 T cells we observed a decrease of PD-1 expressing cells under therapy, indicating manipulation of this subset. However, neither mass nor flow cytometric analysis revealed an association of Vδ2 T cell frequency or phenotype with clinical outcome. The T cell differentiation profile was not examined since the Vγ9Vδ2 population, which represents the vast majority of Vδ2 T cells, acts rather innate-like and the expression of characteristic markers likely has different implications [160]. This is subject of an ongoing controversy [161]. On the one hand, the expression pattern of homing receptors, tissue distribution and lineage differentiation in long-term culture resemble the behavior of αβ T cells [162]. On the other hand, Vγ9Vδ2 T cells are characterized by polyclonal expansions [42], a rather stable distribution of phenotypic profiles [43] and a distinct transcriptional program [40]. Furthermore, the lack of alterations in composition and functionality with age suggests a divergent trajectory during aging [145, 163], implying altogether a different biology underlying Vδ1 and Vδ2 T cells. Despite these differences, expression of CD57 seems to have similar functional implications and is linked to diminished proliferation [145] and expression of granzymes and perforin [146]. Levels of CD57 expressing Vδ2 T cells were higher in patients than healthy donors and the proliferation index determined by dye-dilution after stimulation with the bisphosphonate zoledronate or an anti-TCRγδ antibody was reduced. Moreover, patients' Vδ2 T cells expressed lower levels of cytokines, demonstrating an altered phenotype and decreased functionality in advanced melanoma. Similar observations have been made by Petrini et al. reporting an elevated percentage of $CD57^+$ and diminished cytotoxicity of zoledronate expanded γδ T cells in melanoma patients. However, this study did not distinguish between

the Vδ1 and Vδ2 subset [91]. Under therapy, we observed no changes in expression of CD57 and cytokines, proliferative capacity or composition of the TRDV2 repertoire, questioning modulation of this subset by PD-1 blockade.

Examination of the TDR repertoire in paired samples of peripheral blood mononuclear cells and TILs revealed the dominance of TRDV2 sequences in most of the eight studied patients. Clonotypes overlapped between tumor and periphery, implying ongoing exchange between these compartments. Similar to what has been reported in breast cancer, we detected several shared Vδ2 clonotypes within TILs, while there were no public TRDV1 sequences [139]. The most shared clonotype, observed in five patients, corresponded to the public CDR3 sequence “CACDTLGDTDKLIF“ that has been repeatedly described by others [100, 164, 165]. As for Vδ1 T cells, frequencies of $CD57^+$ Vδ2 T cells were lower in the tumor compared to the paired blood sample, indicating a higher proliferative capacity of the intratumoral Vδ2 population.

Altogether our data suggest only a minor role for Vδ2 T cells with respect to the anti-tumor response in advanced melanoma at least in the current immunotherapy setting. A study from de Vries et al. investigating γδ T cells in colon cancer patients receiving immune checkpoint blockade came to similar conclusions [141]. Furthermore, Vδ1 T cells might be the more potent cytotoxic effectors compared to their Vδ2 counterpart [166, 167].

7.2.3 Conclusion and outlook

We demonstrate a robust association between high frequencies of peripheral Vδ1 T cells before the start of PD-1 blockade and poor OS of metastatic melanoma patients. This is furthermore linked to the high prevalence of a late-differentiated senescent-like phenotype, probably marking these Vδ1 T cells as unresponsive to therapy. Yet, in patients with low Vδ1 frequencies and superior OS ICB was able to induce a polyclonal expansion, indicating the presence of a subset of therapy-responsive Vδ1 T cells. Senescent and exhausted cells are restrained by distinct pathways [26], so anti-PD-1 therapy is likely insufficient to elicit an effective anti-tumor immune response in patients dominated by the senescent-like phenotype. At the tumor site, this phenotype represents a lower fraction of the Vδ1 compartment compared to the periphery and in contrast to peripheral blood, a higher abundance of tumor-infiltrating Vδ1 T cells is associated with favorable OS. Taken together our study supports the ongoing endeavors leveraging the potential of Vδ1 T cells for novel approaches in cancer immunotherapy.

Defining exhaustion or senescence in T cells is challenging since there are currently no mutually exclusive phenotypic markers or marker combinations [150]. In addition to that it

remains to be explored to which extent this conception can be transferred to the unconventional population of γδ T cells. In this context and with regard to therapeutic targeting, a thorough examination of the functional capacity of late-differentiated $CD57^+$ Vδ1 T cells would be important. This investigation can be facilitated by employing the integrin-based activation assay, among other techniques. Yet, growing evidence suggests an adaptive differentiation program and clonal selection in Vδ1 T cells implying similarity to CD8 T cells, whereas the Vδ2 subset displays a rather innate-like behavior [33, 40, 41].

Limited availability of tumor samples impeded the exploration of correlations between tumor-infiltrating γδ T cells and clinical data and the TCGA dataset did not represent the immunotherapy setting. Thus, further studies should examine a larger patient cohort and ideally pre- and post-treatment samples. Furthermore, in-depth analysis of the phenotype and spatial organization of γδ T cells in the tumor, for example via the above-described high-dimensional imaging approach, will generate a more detailed picture of the role they play in cancer immunosurveillance and concerning potential interaction partners. Sample availability also restricted comparison between patients receiving monotherapy or combination therapy. In CD8 T cells mostly additive effects were observed in the context of combination therapy, though there were multiple distinct cellular responses and terminally differentiated effector cells expanded only in this setting [168]. Therefore, studying unique and additive modulations in γδ T cells would be of great interest. Beyond that, genome-wide CRISPR libraries might advance the identification of ligands activating different γδTCRs in the context of malignant transformation and thereby shed light on the discrimination between stress and homeostasis [46].

Tumor recognition independent of antigen presentation by HLA, which might be downregulated or defective in malignancies, and an intrinsic low risk of graft-versus-host disease makes γδ T cells attractive effectors of cancer immunotherapy. Due to huge interspecies differences and the lack of conservation of the TRG and TRD locus [31], data is not easily transferable between mice and humans. There is neither an orthologue of the phosphoantigen reactive Vγ9Vδ2 subset in mice nor an equivalent of dendritic epidermal γδ T cells (DETC) in humans [39]. Furthermore, mouse γδ T cells can be categorized by functionality into the two major subsets of $CD27^+$ IFNγ-producing and $CD27^-$ IL-17-producing cells [169]. This is not applicable to human γδ T cells, in general production of IL-17 by γδ T cells is rarely observed in humans [170] and whether pro-tumor functions are IL-17-mediated remains controversial [80]. Altogether this hampers the translation of findings and complicates the use of in-vivo models.

Previous in-human studies based on in-vivo bisphosphonate stimulation or adoptive transfer of expanded Vγ9Vδ2 T cells demonstrated a good safety profile, yet clinical responses were

variable and infrequent [97, 171]. In line with that, Vδ2 T cells played a minor role in the present study. Recently, the focus of γδ T cell immunotherapy has shifted from the innate-like Vγ9Vδ2 subset to the adaptive-like Vδ1 T cells. A direction supported by our data demonstrating the association of the latter with clinical outcome. Their tissue-resident nature might allow more efficient trafficking to and infiltration of the tumor as well as persistence in the TME. Polyclonal Vδ1 T cell lines derived from melanoma-infiltrating cells were able to mount cytotoxic responses against a melanoma cell line [86]. Furthermore, a melanoma xenograft SCID mouse model demonstrated the ability of Vδ1 T cells to home to the tumor site and inhibit tumor growth [172]. A growing number of companies and several ongoing clinical trials explore targeting of the Vδ1 subset in solid cancers. Besides antibody- and CAR-based strategies, allogenic or even off-the-shelf adoptive transfer approaches are under development [97]. In this context, the phenotypic composition of the expanded cellular products should be considered, since high percentages of T_{EMRA} of CD57-expressing cells might limit efficacy. For example, the Delta One T (DOT) cell expansion protocol results in a product containing mainly $CD27^+$ cells [78], indicating a favorable profile. Moreover, further investigation of the mechanisms underlying T cell senescence especially with regard to γδ T cells is warranted and might enable reversal or prevention of this dysfunctional state.

References

1. Arnold, M., et al., *Global Burden of Cutaneous Melanoma in 2020 and Projections to 2040.* JAMA Dermatol., 2022. **158**(5): p. 495-503.
2. Gershenwald, J.E., et al., *Melanoma staging: Evidence-based changes in the American Joint Committee on Cancer eighth edition cancer staging manual.* CA Cancer J. Clin., 2017. **67**(6): p. 472-492.
3. Tsao, H., M.B. Atkins, and A.J. Sober, *Management of cutaneous melanoma.* N. Engl. J. Med., 2004. **351**(10): p. 998-1012.
4. Larkin, J., et al., *Five-Year Survival with Combined Nivolumab and Ipilimumab in Advanced Melanoma.* N Engl J Med, 2019. **381**(16): p. 1535-1546.
5. Alexandrov, L.B., et al., *Signatures of mutational processes in human cancer.* Nature, 2013. **500**(7463): p. 415-+.
6. Pleasance, E.D., et al., *A comprehensive catalogue of somatic mutations from a human cancer genome.* Nature, 2010. **463**(7278): p. 191-6.
7. Switzer, B., et al., *Managing Metastatic Melanoma in 2022: A Clinical Review.* Jco Oncology Practice, 2022. **18**(5): p. 335-+.
8. Hodi, F.S., et al., *Improved survival with ipilimumab in patients with metastatic melanoma.* N Engl J Med, 2010. **363**(8): p. 711-23.
9. Huang, A.C. and R. Zappasodi, *A decade of checkpoint blockade immunotherapy in melanoma: understanding the molecular basis for immune sensitivity and resistance.* Nat. Immunol., 2022. **23**(5): p. 660-670.
10. Wolchok, J.D., et al., *Long-Term Outcomes With Nivolumab Plus Ipilimumab or Nivolumab Alone Versus Ipilimumab in Patients With Advanced Melanoma.* J Clin Oncol, 2022. **40**(2): p. 127-137.
11. Garbe, C., et al., *European consensus-based interdisciplinary guideline for melanoma. Part 2: Treatment - Update 2022.* European Journal of Cancer, 2022. **170**: p. 256-284.
12. De Velasco, G., et al., *Comprehensive Meta-analysis of Key Immune-Related Adverse Events from CTLA-4 and PD-1/PD-L1 Inhibitors in Cancer Patients.* Cancer Immunol. Res., 2017. **5**(4): p. 312-318.
13. Vesely, M.D., T.X. Zhang, and L.P. Chen, *Resistance Mechanisms to Anti-PD Cancer Immunotherapy.* Annu. Rev. Immunol., 2022. **40**: p. 45-74.
14. Jenkins, R.W. and D.E. Fisher, *Treatment of Advanced Melanoma in 2020 and Beyond.* Journal of Investigative Dermatology, 2021. **141**(1): p. 23-31.
15. Archilla-Ortega, A., et al., *Blockade of novel immune checkpoints and new therapeutic combinations to boost antitumor immunity.* J. Exp. Clin. Cancer Res., 2022. **41**(1): p. 62.
16. Marin-Acevedo, J.A., E.O. Kimbrough, and Y. Lou, *Next generation of immune checkpoint inhibitors and beyond.* J. Hematol. Oncol., 2021. **14**(1): p. 45.
17. Tawbi, H.A., et al., *Relatlimab and Nivolumab versus Nivolumab in Untreated Advanced Melanoma.* N. Engl. J. Med., 2022. **386**(1): p. 24-34.
18. Mutz-Rabl, C.G., P. Koelblinger, and L. Koch, *Immunotherapy for metastatic melanoma-from little benefit to first-line treatment.* Memo-Magazine of European Medical Oncology, 2023. **16**(2): p. 108-112.
19. Schachter, J., et al., *Pembrolizumab versus ipilimumab for advanced melanoma: final overall survival results of a multicentre, randomised, open-label phase 3 study (KEYNOTE-006).* Lancet, 2017. **390**(10105): p. 1853-1862.
20. Larkin, J., et al., *Combined Nivolumab and Ipilimumab or Monotherapy in Untreated Melanoma.* N Engl J Med, 2015. **373**(1): p. 23-34.
21. Francisco, L.M., P.T. Sage, and A.H. Sharpe, *The PD-1 pathway in tolerance and autoimmunity.* Immunol. Rev., 2010. **236**: p. 219-242.
22. Keir, M.E., et al., *PD-1 and its ligands in tolerance and immunity.* Annual Review of Immunology, 2008. **26**: p. 677-704.
23. McLane, L.M., M.S. Abdel-Hakeem, and E.J. Wherry, *CD8 T Cell Exhaustion During Chronic Viral Infection and Cancer.* Annu. Rev. Immunol., 2019. **37**: p. 457-495.
24. Jiang, W.Q., et al., *Exhausted CD8+T Cells in the Tumor Immune Microenvironment: New Pathways to Therapy.* Front. Immunol., 2021. **11**.
25. Budimir, N., et al., *Reversing T-cell Exhaustion in Cancer: Lessons Learned from PD-1/PD-L1 Immune Checkpoint Blockade.* Cancer Immunol. Res., 2022. **10**(2): p. 146-153.
26. Zhao, Y.J., Q.X. Shao, and G.Y. Peng, *Exhaustion and senescence: two crucial dysfunctional states of T cells in the tumor microenvironment.* Cellular & Molecular Immunology, 2020. **17**(1): p. 27-35.

27. Milleron, R.S. and S.B. Bratton, *Heat shock induces apoptosis independently of any known initiator caspase-activating complex.* J. Biol. Chem., 2006. **281**(25): p. 16991-17000.
28. Blackburn, S.D., et al., *Selective expansion of a subset of exhausted CD8 T cells by alpha PD-L1 blockade.* Proc. Natl. Acad. Sci. U.S.A., 2008. **105**(39): p. 15016-15021.
29. Huang, A.C., et al., *A single dose of neoadjuvant PD-1 blockade predicts clinical outcomes in resectable melanoma.* Nat. Med., 2019. **25**(3): p. 454-461.
30. Miller, B.C., et al., *Subsets of exhausted CD8(+) T cells differentially mediate tumor control and respond to checkpoint blockade.* Nat. Immunol., 2019. **20**(3): p. 326-336.
31. Hayday, A.C., *gamma delta cells: A right time and a right place for a conserved third way of protection.* Annu. Rev. Immunol., 2000. **18**: p. 975-1026.
32. Boehme, L., J. Roels, and T. Taghon, *Development of gamma delta T cells in the thymus - A human perspective.* Semin. Immunol. , 2022. **61**.
33. Davey, M.S., et al., *The human Vdelta2(+) T-cell compartment comprises distinct innate-like Vgamma9(+) and adaptive Vgamma9(-) subsets.* Nat Commun, 2018. **9**(1): p. 1760.
34. Davey, M.S., et al., *Clonal selection in the human Vdelta1 T cell repertoire indicates gammadelta TCR-dependent adaptive immune surveillance.* Nat. Commun., 2017. **8**: p. 14760.
35. Deusch, K., et al., *A Major Fraction of Human Intraepithelial Lymphocytes Simultaneously Expresses the Gamma/Delta T-Cell Receptor, the Cd8 Accessory Molecule and Preferentially Uses the V-Delta-1 Gene Segment.* Eur. J. Immunol., 1991. **21**(4): p. 1053-1059.
36. Ravens, S., et al., *Human gammadelta T cells are quickly reconstituted after stem-cell transplantation and show adaptive clonal expansion in response to viral infection.* Nat Immunol, 2017. **18**(4): p. 393-401.
37. McVay, L.D. and S.R. Carding, *Extrathymic origin of human gamma delta T cells during fetal development.* J. Immunol., 1996. **157**(7): p. 2873-2882.
38. McVay, L.D., et al., *The generation of human gammadelta T cell repertoires during fetal development.* J. Immunol., 1998. **160**(12): p. 5851-60.
39. Sanchez, G.S., et al., *Surfing on the waves of the human gamma delta T cell ontogenic sea.* Immunol. Rev., 2023.
40. McMurray, J.L., et al., *Transcriptional profiling of human Vdelta1 T cells reveals a pathogen-driven adaptive differentiation program.* Cell Rep., 2022. **39**(8): p. 110858.
41. Davey, M.S., et al., *Clonal selection in the human Vdelta1 T cell repertoire indicates gammadelta TCR-dependent adaptive immune surveillance.* Nat Commun, 2017. **8**: p. 14760.
42. Ravens, S., et al., *Microbial exposure drives polyclonal expansion of innate gammadelta T cells immediately after birth.* Proc Natl Acad Sci U S A, 2020. **117**(31): p. 18649-18660.
43. Ryan, P.L., et al., *Heterogeneous yet stable V delta 2((+)) T-cell profiles define distinct cytotoxic effector potentials in healthy human individuals.* Proc. Natl. Acad. Sci. U.S.A., 2016. **113**(50): p. 14378-14383.
44. Angelini, D.F., et al., *Fc gamma RIII discriminates between 2 subsets of V gamma 9V delta 2 effector cells with different responses and activation pathways.* Blood, 2004. **104**(6): p. 1801-1807.
45. Benveniste, P.M., et al., *Generation and molecular recognition of melanoma-associated antigen-specific human gammadelta T cells.* Sci. Immunol., 2018. **3**(30).
46. Deseke, M. and I. Prinz, *Ligand recognition by the gammadelta TCR and discrimination between homeostasis and stress conditions.* Cell. Mol. Immunol., 2020.
47. Gober, H.J., et al., *Human T cell receptor gammadelta cells recognize endogenous mevalonate metabolites in tumor cells.* J. Exp. Med., 2003. **197**(2): p. 163-8.
48. Wang, H., et al., *Indirect Stimulation of Human V gamma 2V delta 2 T Cells through Alterations in Isoprenoid Metabolism.* J. Immunol., 2011. **187**(10): p. 5099-5113.
49. Eberl, M., et al., *Microbial isoprenoid biosynthesis and human gammadelta T cell activation.* FEBS Lett., 2003. **544**(1-3): p. 4-10.
50. Herrmann, T. and M.M. Karunakaran, *Butyrophilins: gamma delta T Cell Receptor Ligands, Immunomodulators and More.* Front. Immunol., 2022. **13**.
51. Karunakaran, M.M., et al., *Butyrophilin-2A1 Directly Binds Germline-Encoded Regions of the Vgamma9Vdelta2 TCR and Is Essential for Phosphoantigen Sensing.* Immunity, 2020. **52**(3): p. 487-498 e6.
52. Rigau, M., et al., *Butyrophilin 2A1 is essential for phosphoantigen reactivity by gammadelta T cells.* Science, 2020. **367**(6478).
53. Grunder, C., et al., *gamma9 and delta2CDR3 domains regulate functional avidity of T cells harboring gamma9delta2TCRs.* Blood, 2012. **120**(26): p. 5153-62.

54. Deseke, M., et al., *A CMV-induced adaptive human Vdelta1+ gammadelta T cell clone recognizes HLA-DR.* J. Exp. Med., 2022. **219**(9).
55. Wegrecki, M., et al., *Atypical sideways recognition of CD1a by autoreactive gammadelta T cell receptors.* Nat. Commun., 2022. **13**(1): p. 3872.
56. Reijneveld, J.F., et al., *Human gamma delta T cells recognize CD1b by two distinct mechanisms.* Proceedings of the National Academy of Sciences of the United States of America, 2020. **117**(37): p. 22944-22952.
57. Roy, S., et al., *Molecular Analysis of Lipid-Reactive Vdelta1 gammadelta T Cells Identified by CD1c Tetramers.* J. Immunol., 2016. **196**(4): p. 1933-42.
58. Uldrich, A.P., et al., *CD1d-lipid antigen recognition by the gamma delta TCR.* Nat. Immunol., 2013. **14**(11): p. 1137-U125.
59. Le Nours, J., et al., *A class of gammadelta T cell receptors recognize the underside of the antigen-presenting molecule MR1.* Science, 2019. **366**(6472): p. 1522-1527.
60. Xu, B., et al., *Crystal structure of gamma delta T-cell receptor specific for the human MHC class I homolog MICA.* Proc. Natl. Acad. Sci. U.S.A., 2011. **108**(6): p. 2414-2419.
61. Zeng, X., et al., *Gammadelta T cells recognize a microbial encoded B cell antigen to initiate a rapid antigen-specific interleukin-17 response.* Immunity, 2012. **37**(3): p. 524-34.
62. Marlin, R., et al., *Sensing of cell stress by human gamma delta TCR-dependent recognition of annexin A2.* Proc. Natl. Acad. Sci. U.S.A., 2017. **114**(12): p. 3163-3168.
63. Dai, Y.M., et al., *Ectopically Expressed Human Tumor Biomarker MutS Homologue 2 Is a Novel Endogenous Ligand That Is Recognized by Human gamma delta T Cells to Induce Innate Anti-tumor/Virus Immunity.* J. Biol. Chem., 2012. **287**(20): p. 16812-16819.
64. Willcox, C.R., et al., *Butyrophilin-like 3 Directly Binds a Human Vgamma4(+) T Cell Receptor Using a Modality Distinct from Clonally-Restricted Antigen.* Immunity, 2019. **51**(5): p. 813-825 e4.
65. Melandri, D., et al., *The gamma delta TCR combines innate immunity with adaptive immunity by utilizing spatially distinct regions for agonist selection and antigen responsiveness.* Nature Immunology, 2018. **19**(12): p. 1352-+.
66. Lo Presti, E., et al., *Deciphering human gammadelta T cell response in cancer: Lessons from tumor-infiltrating gammadelta T cells.* Immunol Rev, 2020.
67. Silva-Santos, B., S. Mensurado, and S.B. Coffelt, *gammadelta T cells: pleiotropic immune effectors with therapeutic potential in cancer.* Nat. Rev. Cancer, 2019. **19**(7): p. 392-404.
68. Altvater, B., et al., *Activated human gammadelta T cells induce peptide-specific CD8+ T-cell responses to tumor-associated self-antigens.* Cancer Immunol. Immunother., 2012. **61**(3): p. 385-96.
69. Brandes, M., K. Willimann, and B. Moser, *Professional antigen-presentation function by human gamma delta T cells.* Science, 2005. **309**(5732): p. 264-268.
70. Rampoldi, F., L. Ullrich, and I. Prinz, *Revisiting the Interaction of gamma delta T-Cells and B-Cells.* Cells, 2020. **9**(3): p. 743.
71. Bansal, R.R., et al., *IL-21 enhances the potential of human gamma delta T cells to provide B-cell help.* Eur. J. Immunol., 2012. **42**(1): p. 110-119.
72. Zhao, Y., C. Niu, and J. Cui, *Gamma-delta (gammadelta) T cells: friend or foe in cancer development?* J. Transl. Med., 2018. **16**(1): p. 3.
73. Maniar, A., et al., *Human gamma delta T lymphocytes induce robust NK cell-mediated antitumor cytotoxicity through CD137 engagement.* Blood, 2010. **116**(10): p. 1726-1733.
74. Almeida, A.R., et al., *Delta One T Cells for Immunotherapy of Chronic Lymphocytic Leukemia: Clinical-Grade Expansion/Differentiation and Preclinical Proof of Concept.* Clin. Cancer Res., 2016. **22**(23): p. 5795-5804.
75. Raulet, D.H., et al., *Regulation of ligands for the NKG2D activating receptor.* Annu. Rev. Immunol., 2013. **31**: p. 413-41.
76. Toutirais, O., et al., *DNAX accessory molecule-1 (CD226) promotes human hepatocellular carcinoma cell lysis by V gamma 9V delta 2 T cells.* Eur. J. Immunol., 2009. **39**(5): p. 1361-1368.
77. Simoes, A.E., B. Di Lorenzo, and B. Silva-Santos, *Molecular Determinants of Target Cell Recognition by Human gamma delta T Cells.* Frontiers in Immunology, 2018. **9**.
78. Di Lorenzo, B., et al., *Broad Cytotoxic Targeting of Acute Myeloid Leukemia by Polyclonal Delta One T Cells.* Cancer Immunol. Res., 2019. **7**(4): p. 552-558.
79. Mikulak, J., et al., *NKp46-expressing human gut-resident intraepithelial Vdelta1 T cell subpopulation exhibits high antitumor activity against colorectal cancer.* JCI Insight, 2019. **4**(24).

80. Mensurado, S. and B. Silva-Santos, *Battle of the gammadelta T cell subsets in the gut.* Trends Cancer, 2022. **8**(11): p. 881-883.
81. Chabab, G., et al., *Identification of a regulatory V delta 1 gamma delta T cell subpopulation expressing CD73 in human breast cancer.* J. Leukoc. Biol., 2020. **107**(6): p. 1057-1067.
82. Peng, G., et al., *Tumor-infiltrating gammadelta T cells suppress T and dendritic cell function via mechanisms controlled by a unique toll-like receptor signaling pathway.* Immunity, 2007. **27**(2): p. 334-48.
83. Wesch, D., C. Peters, and G.M. Siegers, *Human gamma delta T regulatory cells in cancer: fact or fiction?* Front. Immunol., 2014. **5**.
84. Peters, C., et al., *Phenotype and regulation of immunosuppressive Vdelta2-expressing gammadelta T cells.* Cell. Mol. Life Sci., 2014. **71**(10): p. 1943-60.
85. Bachelez, H., et al., *TCR gamma delta bearing T lymphocytes infiltrating human primary cutaneous melanomas.* J. Invest. Dermatol., 1992. **98**(3): p. 369-74.
86. Cordova, A., et al., *Characterization of Human gamma delta T Lymphocytes Infiltrating Primary Malignant Melanomas.* Plos One, 2012. **7**(11).
87. Bialasiewicz, A.A., J.X. Ma, and G. Richard, *alpha/beta and gamma/delta TCR+ lymphocyte infiltration in necrotising choroidal melanomas.* Br. J. Ophthalmol., 1999. **83**(9): p. 1069-1073.
88. Girard, P., et al., *The features of circulating and tumor-infiltrating gammadelta T cells in melanoma patients display critical perturbations with prognostic impact on clinical outcome.* Oncoimmunology, 2019. **8**(8): p. 1601483.
89. Argentati, K., et al., *Reduced number and impaired function of circulating gamma delta T cells in patients with cutaneous primary melanoma.* J. Invest. Dermatol., 2003. **120**(5): p. 829-834.
90. Re, F., et al., *Circulating gammadelta T cells in young/adult and old patients with cutaneous primary melanoma.* Immun. Ageing, 2005. **2**(1): p. 2.
91. Petrini, I., et al., *Impaired function of gamma-delta lymphocytes in melanoma patients.* Eur J Clin Invest, 2011. **41**(11): p. 1186-94.
92. Campillo, J.A., et al., *Increased number of cytotoxic CD3+ CD28- gammadelta T cells in peripheral blood of patients with cutaneous malignant melanoma.* Dermatology (Basel), 2007. **214**(4): p. 283-8.
93. Wistuba-Hamprecht, K., et al., *Phenotypic characterization and prognostic impact of circulating gammadelta and alphabeta T-cells in metastatic malignant melanoma.* Int. J. Cancer, 2016. **138**(3): p. 698-704.
94. Wistuba-Hamprecht, K., et al., *Proportions of blood-borne Vdelta1+ and Vdelta2+ T-cells are associated with overall survival of melanoma patients treated with ipilimumab.* Eur. J. Cancer, 2016. **64**: p. 116-26.
95. Mensurado, S., R. Blanco-Dominguez, and B. Silva-Santos, *The emerging roles of gammadelta T cells in cancer immunotherapy.* Nat. Rev. Clin. Oncol., 2023. **20**(3): p. 178-191.
96. Zlatareva, I. and Y. Wu, *Local gamma delta T cells: translating promise to practice in cancer immunotherapy.* Br. J. Cancer, 2023.
97. Saura-Esteller, J., et al., *Gamma Delta T-Cell Based Cancer Immunotherapy: Past-Present-Future.* Front. Immunol., 2022. **13**.
98. De Gassart, A., et al., *Development of ICT01, a first-in-class, anti-BTN3A antibody for activating Vgamma9Vdelta2 T cell-mediated antitumor immune response.* Sci. Transl. Med., 2021. **13**(616): p. eabj0835.
99. Hoeres, T., et al., *Improving the Efficiency of V gamma 9V delta 2 T Cell Immunotherapy in Cancer.* Front. Immunol., 2018. **9**.
100. Kakimi, K., et al., *Adoptive transfer of zoledronate-expanded autologous V gamma 9V delta 2 T-cells in patients with treatment-refractory non-small-cell lung cancer: a multicenter, open-label, single-arm, phase 2 study.* J. Immunother. Cancer, 2020. **8**(2).
101. Xu, Y., et al., *Allogeneic Vgamma9Vdelta2 T-cell immunotherapy exhibits promising clinical safety and prolongs the survival of patients with late-stage lung or liver cancer.* Cell. Mol. Immunol., 2021. **18**(2): p. 427-439.
102. Amani Makkouk, X.C.Y., Taylor Barca, Anthony Lucas, Mustafa Turkoz, Jonathan T S Wong, Kevin P Nishimoto, Mary M Brodey, Maryam Tabrizizad, Smitha R Y Gundurao, Lu Bai, Arun Bhat, Zili An, Stewart Abbot, Daulet Satpayev, Blake T Aftab and Marissa Herrman, *Off-the-shelf Vδ1 gamma delta T cells engineered with glypican-3 (GPC-3)-specific chimeric antigen receptor (CAR) and soluble IL-15 display robust antitumor efficacy against hepatocellular carcinoma.* 2021.
103. Johanna, I., et al., *Evaluating in vivo efficacy - toxicity profile of TEG001 in humanized mice xenografts against primary human AML disease and healthy hematopoietic cells.* J. Immunother. Cancer, 2019. **7**.

104. Straetemans, T., et al., *GMP-Grade Manufacturing of T Cells Engineered to Express a Defined gamma delta TCR.* Front. Immunol., 2018. **9**.
105. Lamb, L.S., et al., *A combined treatment regimen of MGMT-modified gamma delta T cells and temozolomide chemotherapy is effective against primary high grade gliomas.* Sci. Rep., 2021. **11**(1).
106. Schilbach, K., et al., *Suppressive activity of V delta 2(+) gamma delta T cells on alpha beta T cells is licensed by TCR signaling and correlates with signal strength.* Cancer Immunol. Immunother., 2020. **69**(4): p. 593-610.
107. Barrow, A.D., C.J. Martin, and M. Colonna, *The Natural Cytotoxicity Receptors in Health and Disease.* Front. Immunol., 2019. **10**: p. 909.
108. Correia, D.V., et al., *Differentiation of human peripheral blood Vdelta1+ T cells expressing the natural cytotoxicity receptor NKp30 for recognition of lymphoid leukemia cells.* Blood, 2011. **118**(4): p. 992-1001.
109. Hudspeth, K., et al., *Engagement of NKp30 on V delta 1 T cells induces the production of CCL3, CCL4, and CCL5 and suppresses HIV-1 replication.* Blood, 2012. **119**(17): p. 4013-4016.
110. Li, X.H., et al., *Circulating PD1(+)Vdelta1(+)gammadelta T Cell Predicts Fertility in Endometrial Polyp Patients of Reproductive-Age.* Front. Immunol., 2021. **12**: p. 639221.
111. Mahnke, Y.D., M.H. Beddall, and M. Roederer, *OMIP-019: Quantification of Human gamma delta T-Cells, iNKT-Cells, and Hematopoietic Precursors.* Cytometry A, 2013. **83a**(8): p. 676-678.
112. Wistuba-Hamprecht, K., G. Pawelec, and E. Derhovanessian, *OMIP-020: Phenotypic characterization of human gammadelta T-cells by multicolor flow cytometry.* Cytometry A, 2014. **85**(6): p. 522-4.
113. Barros-Martins, J., et al., *OMIP-084: 28-color full spectrum flow cytometry panel for the comprehensive analysis of human gammadelta T cells.* Cytometry A, 2022.
114. Stervbo, U., et al., *Effects of aging on human leukocytes (part II): immunophenotyping of adaptive immune B and T cell subsets.* Age (Dordr), 2015. **37**(5): p. 93.
115. Bagwell, C.B., et al., *Multi-site reproducibility of a human immunophenotyping assay in whole blood and peripheral blood mononuclear cells preparations using CyTOF technology coupled with Maxpar Pathsetter, an automated data analysis system.* Cytometry B Clin Cytom, 2019.
116. Wistuba-Hamprecht, K. and G. Pawelec, *Characterization of gammadelta T-cells via flow cytometry.* Age (Dordr), 2015. **37**(6): p. 123.
117. Hinz, T., et al., *Cell-surface expression of transrearranged Vgamma-cbeta T-cell receptor chains in healthy donors and in ataxia telangiectasia patients.* Br. J. Haematol., 2000. **109**(1): p. 201-10.
118. Jungbluth, A.A., et al., *Immunohistochemical Detection of gamma/delta T Lymphocytes in Formalin-fixed Paraffin-embedded Tissues.* Appl. Immunohistochem. Mol. Morphol., 2018.
119. Chabab, G., et al., *Diversity of Tumor-Infiltrating, gamma delta T-Cell Abundance in Solid Cancers.* Cells, 2020. **9**(6).
120. Olofsson, K., S. Hellstrom, and M.L. Hammarstrom, *The surface epithelium of recurrent infected palatine tonsils is rich in gammadelta T cells.* Clin. Exp. Immunol., 1998. **111**(1): p. 36-47.
121. Gouttefangeas, C., J. Schuhmacher, and S. Dimitrov, *Adhering to adhesion: assessing integrin conformation to monitor T cells.* Cancer Immunol Immunother, 2019. **68**(11): p. 1855-1863.
122. Schollhorn, A., et al., *Integrin Activation Enables Sensitive Detection of Functional CD4(+) and CD8(+) T Cells: Application to Characterize SARS-CoV-2 Immunity.* Front. Immunol., 2021. **12**: p. 626308.
123. Dimitrov, S., et al., *Activated integrins identify functional antigen-specific CD8(+) T cells within minutes after antigen stimulation.* Proc. Natl. Acad. Sci. U.S.A., 2018. **115**(24): p. E5536-E5545.
124. Hogg, N., I. Patzak, and F. Willenbrock, *The insider's guide to leukocyte integrin signalling and function.* Nat. Rev. Immunol., 2011. **11**(6): p. 416-426.
125. Urlaub, D., et al., *LFA-1 Activation in NK Cells and Their Subsets: Influence of Receptors, Maturation, and Cytokine Stimulation.* J. Immunol., 2017. **198**(5): p. 1944-1951.
126. Kinkhabwala, A., et al., *MACSima imaging cyclic staining (MICS) technology reveals combinatorial target pairs for CAR T cell treatment of solid tumors.* Sci. Rep., 2022. **12**(1): p. 1911.
127. Nagel, A., et al., *CD3-positive B cells: a storage-dependent phenomenon.* PLoS One, 2014. **9**(10): p. e110138.

128. Lee, A.Y.S., *CD20(+) T cells: an emerging T cell subset in human pathology.* Inflamm. Res., 2022. **71**(10-11): p. 1181-1189.
129. Vlaming, M., et al., *CD20 positive CD8 T cells are a unique and transcriptionally-distinct subset of T cells with distinct transmigration properties.* Sci. Rep., 2021. **11**(1): p. 20499.
130. Black, S., et al., *CODEX multiplexed tissue imaging with DNA-conjugated antibodies.* Nature Protocols, 2021. **16**(8): p. 3802-+.
131. Hernandez, S., et al., *Challenges and Opportunities for Immunoprofiling Using a Spatial High-Plex Technology: The NanoString GeoMx (R) Digital Spatial Profiler.* Front. Oncol., 2022. **12**.
132. Li, W., et al., *Effect of IL-18 on Expansion of gamma delta T Cells Stimulated by Zoledronate and IL-2.* J. Immunother., 2010. **33**(3): p. 287-296.
133. Fichtner, A.S., et al., *TCR repertoire analysis reveals phosphoantigen-induced polyclonal proliferation of Vgamma9Vdelta2 T cells in neonates and adults.* J Leukoc Biol, 2020. **107**(6): p. 1023-1032.
134. Gentles, A.J., et al., *The prognostic landscape of genes and infiltrating immune cells across human cancers.* Nature Medicine, 2015. **21**(8): p. 938-945.
135. Tosolini, M., et al., *Assessment of tumor-infiltrating TCRVgamma9Vdelta2 gammadelta lymphocyte abundance by deconvolution of human cancers microarrays.* Oncoimmunology, 2017. **6**(3): p. e1284723.
136. Wu, P., et al., *gammadeltaT17 cells promote the accumulation and expansion of myeloid-derived suppressor cells in human colorectal cancer.* Immunity, 2014. **40**(5): p. 785-800.
137. Meraviglia, S., et al., *Distinctive features of tumor-infiltrating gammadelta T lymphocytes in human colorectal cancer.* Oncoimmunology, 2017. **6**(10): p. e1347742.
138. Ma, C., et al., *Tumor-infiltrating gammadelta T lymphocytes predict clinical outcome in human breast cancer.* J. Immunol., 2012. **189**(10): p. 5029-36.
139. Wu, Y., et al., *An innate-like V delta 1(+) gamma delta T cell compartment in the human breast is associated with remission in triple-negative breast cancer.* Sci. Transl. Med., 2019. **11**(513).
140. Catafal-Tardos, E., M.V. Baglioni, and V. Bekiaris, *Inhibiting the Unconventionals: Importance of Immune Checkpoint Receptors in gamma delta T, MAIT, and NKT Cells.* Cancers, 2021. **13**(18).
141. de Vries, N.L., et al., *gammadelta T cells are effectors of immunotherapy in cancers with HLA class I defects.* Nature, 2023.
142. Weimer, P., et al., *Tissue-Specific Expression of TIGIT, PD-1, TIM-3, and CD39 by gamma delta T Cells in Ovarian Cancer.* Cells, 2022. **11**(6).
143. Li, P., et al., *Androgens in Patients With Luminal B and HER2 Breast Cancer Might Be a Biomarker Promoting Anti-PD-1 Efficacy.* Frontiers in Oncology, 2022. **12**.
144. Zelba, H., et al., *Accurate quantification of T-cells expressing PD-1 in patients on anti-PD-1 immunotherapy.* Cancer Immunol Immunother, 2018.
145. Xu, W., et al., *Mapping of gamma/delta T cells reveals Vdelta2+ T cells resistance to senescence.* EBioMedicine, 2018. **39**: p. 44-58.
146. Chattopadhyay, P.K., et al., *The cytolytic enzymes granyzme A, granzyme B, and perforin: expression patterns, cell distribution, and their relationship to cell maturity and bright CD57 expression.* J. Leukoc. Biol., 2009. **85**(1): p. 88-97.
147. Sade-Feldman, M., et al., *Resistance to checkpoint blockade therapy through inactivation of antigen presentation.* Nat. Commun., 2017. **8**.
148. Middha, S., et al., *Majority of B2M-Mutant and -Deficient Colorectal Carcinomas Achieve Clinical Benefit From Immune Checkpoint Inhibitor Therapy and Are Microsatellite Instability-High.* JCO Precis. Oncol., 2019. **3**.
149. Zhao, Y.J., Q.X. Shao, and G.Y. Peng, *Exhaustion and senescence: two crucial dysfunctional states of T cells in the tumor microenvironment.* Cell. Mol. Immunol., 2020. **17**(1): p. 27-35.
150. Crespo, J., et al., *T cell anergy, exhaustion, senescence, and stemness in the tumor microenvironment.* Curr. Opin. Immunol., 2013. **25**(2): p. 214-21.
151. Zhang, J., et al., *Senescent T cells: a potential biomarker and target for cancer therapy.* EBioMedicine, 2021. **68**.
152. Ferrara, R., et al., *Circulating T-cell Immunosenescence in Patients with Advanced Non-small Cell Lung Cancer Treated with Single-agent PD-1/PD-L1 Inhibitors or Platinum-based Chemotherapy.* Clin. Cancer Res., 2021. **27**(2): p. 492-503.
153. Hui, E.F., et al., *T cell costimulatory receptor CD28 is a primary target for PD-1-mediated inhibition.* Science, 2017. **355**(6332): p. 1428-+.
154. Kamphorst, A.O., et al., *Rescue of exhausted CD8 T cells by PD-1-targeted therapies is CD28-dependent.* Science, 2017. **355**(6332): p. 1423-1427.

155. Kim, K.H., et al., *PD-1 blockade-unresponsive human tumor-infiltrating CD8(+) T cells are marked by loss of CD28 expression and rescued by IL-15.* Cell. Mol. Immunol., 2021. **18**(2): p. 385-397.
156. van der Kooij, M.K., et al., *Uveal Versus Cutaneous Melanoma; Same Origin, Very Distinct Tumor Types.* Cancers 2019. **11**(6).
157. Miao, Y.R., et al., *ImmuCellAI: A Unique Method for Comprehensive T-Cell Subsets Abundance Prediction and its Application in Cancer Immunotherapy.* Adv. Sci., 2020. **7**(7).
158. Wu, Y., et al., *A local human V delta 1 T cell population is associated with survival in nonsmall-cell lung cancer.* Nat. Cancer, 2022. **3**(6): p. 696-+.
159. Cindy Yang, S.Y., et al., *Pan-cancer analysis of longitudinal metastatic tumors reveals genomic alterations and immune landscape dynamics associated with pembrolizumab sensitivity.* Nat. Commun., 2021. **12**(1): p. 5137.
160. Xu, W.L. and A. Larbi, *Markers of T Cell Senescence in Humans.* Int J Mol Sci, 2017. **18**(8): p. 1742.
161. Mikulak, J., F. Dieli, and D. Mavilio, *Are human V delta 2(pos) T cells really resistant to aging and Human Cytomegalovirus infection?* EBioMedicine, 2019. **43**: p. 30-30.
162. Dieli, F., et al., *Differentiation of effector/memory V delta 2 T cells and migratory routes in lymph nodes or inflammatory sites.* J. Exp. Med., 2003. **198**(3): p. 391-397.
163. Tan, C.T., et al., *Vdelta2+ and alpha/ss T cells show divergent trajectories during human aging.* Oncotarget, 2016. **7**(29): p. 44906-44918.
164. Papadopoulou, M., et al., *Fetal public V gamma 9V delta 2 T cells expand and gain potent cytotoxic functions early after birth.* Proceedings of the National Academy of Sciences of the United States of America, 2020. **117**(31): p. 18638-18648.
165. Deng, L.H., et al., *Systematic pattern analyses of V delta 2(+) TCRs reveal that shared "public" V delta 2(+) gamma delta T cell clones are a consequence of rearrangement bias and a higher expansion status (vol 13, 960920, 2022).* Front. Immunol., 2022. **13**.
166. Wu, D., et al., *Ex vivo expanded human circulating Vdelta1 gammadeltaT cells exhibit favorable therapeutic potential for colon cancer.* Oncoimmunology, 2015. **4**(3): p. e992749.
167. Maeurer, M.J., et al., *Human intestinal V delta 1(+) T lymphocytes recognize tumor cells of epithelial origin.* J. Exp. Med., 1996. **183**(4): p. 1681-1696.
168. Wei, S.C., et al., *Combination anti-CTLA-4 plus anti-PD-1 checkpoint blockade utilizes cellular mechanisms partially distinct from monotherapies.* Proc Natl Acad Sci U S A, 2019. **116**(45): p. 22699-22709.
169. Serre, K. and B. Silva-Santos, *Molecular Mechanisms of Differentiation of Murine Pro-Inflammatory gammadelta T Cell Subsets.* Front. Immunol., 2013. **4**: p. 431.
170. O'Brien, R.L. and W.K. Born, *Two functionally distinct subsets of IL-17 producing gammadelta T cells.* Immunol. Rev., 2020. **298**(1): p. 10-24.
171. Sebestyen, Z., et al., *Translating gammadelta (gammadelta) T cells and their receptors into cancer cell therapies.* Nat Rev Drug Discov, 2019.
172. Lozupone, F., et al., *Effect of human natural killer and gamma delta T cells on the growth of human autologous melanoma xenografts in SCID mice.* Cancer Res., 2004. **64**(1): p. 378-385.

Appendix

a) Accepted publications

(1) Pitfalls in the characterization of circulating and tissue-resident human γδ T cells (2020).

(2) Accurate determination of γδ T cells in multi-channel mass and flow cytometry (2020).

(3) Integrin activation enables rapid detection of functional Vδ1^{+} and Vδ2^{+} γδ T cells (2022).

(4) High-dimensional in situ proteomics imaging to assess γδ T cells in spatial biology (2024).

b) Submitted manuscripts

(5) A Vδ1 T cell subset is responsive to PD-1 blockade and associated with survival in melanoma (2024).

Pitfalls in the characterization of circulating and tissue-resident human γδ T cells

Nicola Beucke[1], Daniela Wesch[2], Hans-Heinrich Oberg[2], Christian Peters[2], Jonas Bochem[1], Benjamin Weide[1], Claus Garbe[1], Graham Pawelec[3,4], Susanne Sebens[5], Christoph Röcken[6], Hisayoshi Hashimoto[7], Markus W. Löffler[3,8,9], Paola Nocerino[10], Shahram Kordasti[10], Dieter Kabelitz[2], Karin Schilbach[7], Kilian Wistuba-Hamprecht[1]

[1] Department of Dermatology, University Medical Center, Tübingen, Germany.
[2] Institute of Immunology, Christian-Albrechts University of Kiel, Kiel, Germany.
[3] Interfaculty Institute for Cell Biology, Department of Immunology, University of Tübingen, Tübingen, Germany.
[4] Health Sciences North Research Institute, Sudbury, ON, Canada.
[5] Institute for Experimental Cancer Research, Christian-Albrechts-University of Kiel, Kiel, Germany.
[6] Institute of Pathology, University Hospital Schleswig-Holstein, Kiel, Germany.
[7] Department of Pediatric Hematology and Oncology, University Children's Hospital Tübingen,
Tübingen, Germany.
[8] Department of General, Visceral and Transplant Surgery, University Hospital Tübingen, Tübingen, Germany.
[9] Department of Clinical Pharmacology, University Hospital Tübingen, Tübingen, Germany
[10] Systems Cancer Immunology, Comprehensive Cancer Centre, King's College London, London, UK.

Correspondence: Kilian Wistuba-Hamprecht, Department of Dermatology, University Medical Center, Waldhörnlestraße 22, 72072 Tübingen, Germany.
Email: kilian.wistuba-hamprecht@uni-tuebingen.de

Short running title: Pitfalls in the characterization of γδ T cells

Summary sentence: Overviewing the state-of-the-art and own experiences, highlighting pitfalls with commercially-available reagents for γδ T cell characterization by flow cytometry, CyTOF, magnetic cell isolation or immunohistochemistry.

Keywords: Flow Cytometry, Mass Cytometry, Immunohistochemistry, Magnetic Cell Isolation, Immunomonitoring

Abbreviations

ADCC: Antibody-dependent cellular cytotoxicity
AEC: Aminoethyl-carbazole
APC: Allophycocyanine
BV: Brilliant Violet
CMV: Cytomegalovirus
CyTOF: Mass cytometry
EBV: Epstein-Barr-Virus
EDTA: Ethylenediaminetetraacetic acid
EPCR: Endothelial protein C receptor
Er: Erbium
FITC: Fluorescein isiothiocyanate
Gd: Gadolinium
IHC: Immunohistochemistry
Ir: Iridium
Monoclonal antibody: mAb
PBMC: Peripheral blood mononuclear cell
PBS: Phosphate-buffered saline
PE: Phycoerythrin
PHA-L: Phytohemagglutinin-L
PI: Positive isolation
PMA: Phorbol 12-myristate 13-acetate
Pr: Praseodymium
Sm: Samarium
TCR: T-cell receptor

Abstract

Dissection of the role and function of human γδ T cells and their heterogeneous subsets in cancer, inflammation and auto-immune diseases is a growing and dynamic research field of increasing interest to the scientific community. Therefore, harmonization and standardization of techniques for the characterization of peripheral and tissue-resident γδ T cells is crucial to facilitate comparability between published and emerging research. The application of commercially-available reagents to classify γδ T cells, in particular the combination of multiple antibodies, is not always trouble-free, posing major demands on researchers entering this field. Occasionally, even entire γδ T cell subsets may remain undetected when certain antibodies are combined in flow cytometric analysis with multicolor antibody panels, or might be lost during cell isolation procedures. Here, based on the recent literature and our own experience, we provide an overview of methods commonly employed for the phenotypic and functional characterization of human γδ T cells including advanced polychromatic flow, mass cytometry, immunohistochemistry and magnetic cell isolation. We highlight potential pitfalls and discuss how to circumvent these obstacles.

Introduction

Knowledge of the orchestration of γδ T cells in the ensemble of immunity is still limited, especially in humans. These “unconventional” T cells are a numerically minor population in peripheral blood, representing 1-10% of all T cells and are, unlike αβ T cells, not MHC-restricted [1]. Knowledge of γδ T cell receptor (TCR) ligands is sparse; only a few, structurally diverse molecules such as phosphoantigens, CD1, endothelial protein C receptor (EPCR) and other cell-surface structures have been identified [2], suggesting an immense potential for diversity. The γδ T cell population comprises heterogeneous subsets with various functions including secretion of cytokines such as TNF, IFN-γ and IL-17 [3], cytotoxic activity via the granzyme-perforin axis and antibody-dependent cellular cytotoxicity (ADCC) by CD16 expressing cells [4], antigen-presentation functions [5] and interactions with B cells promoting immunoglobulin class switching [6]. Vδ1 γδ T cells are the predominant T cell subset in some tissues, accounting for around 40% of all intra-epithelial lymphocytes in the large intestine, for example [7]. The Vδ1 TCR repertoire is often private, highly focused on a few clones, and displays features of the adaptive immune system [8]. On the other hand, Vδ2 γδ T cells, which dominate the γδ TCR repertoire in peripheral blood, have a semi-invariant TCR, a diverse public repertoire and mainly behave in an innate-like manner [9]. Due to their pleiotropic roles in immunity and implications in cancer, infectious and auto-immune diseases, γδ T cells are of rapidly growing interest. Transcriptomic analyses have documented that intra-tumoral γδ T cells may represent significant favorable prognostic immune cell populations in several different cancers [10] and Oberg et al. observed large numbers of different γδ T cell subsets infiltrating isolated pancreatic and ovarian tumors *ex vivo* [11, 12, Oberg et al. this volume]. In areas other than cancer, γδ T cells have been shown to contribute to the immune response against CMV [13, 14] and malaria [15], and to be involved in various inflammatory conditions [16]. It is therefore important to harmonize and standardize techniques for the investigation of γδ T cells in order to avoid potential pitfalls when using and combining commercially-available antibodies and comparing results between centers. Here, we aim to provide a basic framework for the phenotypic and functional characterization of peripheral and tissue-resident γδ T cells, including magnetic cell isolation, advanced polychromatic flow cytometry, mass cytometry (CyTOF) and immunohistochemistry (IHC).

Material and Methods

Study participants and sample acquisition

Blood samples were obtained from healthy adult volunteers at the Department of Hematology and Oncology, Children's Hospital, University of Tübingen (Project no. 38/2009BO2, 470/2013BO2, 673/2015BO2, 105/2017BO2 and 880/2017BO2) and from the biobank at the Interfaculty Institute of Cell Biology (IFIZ), Department of immunology, University of Tübingen (Project no. 156/2012BO1 and 633/2019BO2). Tissue samples from patients with EBV-associated Hodgkin's lymphoma (with pathological features assessed according to the WHO classification) and colon carcinoma (staged according to the UICC TNM classification system) were obtained at the University Hospital Schleswig-Holstein, Kiel (D430/09). Written informed consent was obtained from all blood and tissue donors. This study was conducted in accordance with the Declaration of Helsinki and applicable laws and regulations, and has been approved by the respective institutional review boards (Ethics Committees at the University Hospital Schleswig-Holstein in Kiel and at the University Hospital Tübingen).

Magnetic cell isolation

γδ T cells were isolated from fresh peripheral blood mononuclear cells (PBMCs) via magnetic cell isolation using the following commercial kits: i) Immunomagnetic negative selection cell isolation kit: TCRγ/δ+ T Cell Isolation Kit Human (Miltenyi Biotec) or Immunomagnetic negative selection cell isolation kit: EasySep™ Human Gamma/Delta T Cell Isolation Kit (STEMCELL Technologies) or, as we show in Figure 1, customized versions of both kits were used, both omitting anti-CD16 antibodies. Immunomagnetic positive selection was performed with a fluorochrome-labelled Vδ2-specific antibody (clone B6, BD) and for secondary labelling and anti-fluorochrome sorting, either anti-FITC Micro-beads (Miltenyi Biotec) or anti-PE MicroBeads Ultra Pure (Miltenyi Biotec) or an Immunomagnetic positive selection kit EasySep™ PE Positive Selection Kit II (STEMCELL Technologies) were used.

Polychromatic flow cytometry

Phenotypic and functional analysis followed standardized protocols on cryopreserved samples. For immunomonitoring studies, cryopreservation is still the gold standard to minimize bias introduced by batch to batch variance in polychromatic flow cytometry, although the expression pattern of some particular markers may be affected. In brief, peripheral blood was drawn and anticoagulated using EDTA, followed by Ficoll-Hypaque density gradient centrifugation to isolate PBMCs. After washing twice, the cells were cryopreserved in medium with 10% DMSO and 20% FCS in RPMI-1640 and stored at -196^{o}C. Cryopreserved PBMCs were thawed, incubated with an Fc-receptor-blocking reagent (Gammunex, Grifols) and ethidium monoazide (EMA, Biotium) or LIVE/DEAD fixable red

(Thermo Fisher Scientific) to label dead cells. Next, characteristic cell surface antigens of γδ T cells were stained using the following monoclonal antibodies (mAbs) to illustrate various common panel compositions: CD3 Alexa Fluor 700 and CD3 BV510 (both clone UCHT1, Biolegend), pan-γδ TCR Biotin (clone 11F2, Miltenyi Biotec), pan-γδ TCR FITC (clone 11F2, BD), pan-γδ TCR purified and pan-γδ TCR PE (both clone IMMU510, Beckman Coulter), Vδ1 TCR FITC, Vδ1 TCR PerCP-Vio700 and Vδ1 TCR APC (all clone REA173, Miltenyi Biotec), Vδ2 TCR PerCP (clone B6, Biolegend), Vδ2 TCR PE and Vδ2 TCR FITC (both clone 123R3, Miltenyi Biotec), Streptavidin-PE (Biolegend), F(ab')2-Fragment goat anti mouse Pacific Orange (Invitrogen). For characterization of established T cell clones, antibodies against Vγ2/3/4 (clone 23D12) [17], Vγ3/5 (clone 56.3) [18] and pan-αβ TCR FITC (clone IP26, Biolegend) were used. The generation of 56.3^+ T cell clones has been described previously. In brief, 56.3 positive cells were selected by MACS from PBMCs from healthy donors and were cloned at 0.3 cells per well in the presence of irradiated feeder cells, PHA 0.5 µg/mL and IL-2 (50 IU) [18].

For intracellular staining, cryopreserved PBMCs that had been stimulated with PMA (20 ng/ml, Sigma) and Ionomycin (750 ng/ml, Merck) or Zoledronate (5 µM, Hexal) and incubated with Brefeldin A (GolgiPlug, BD), Monensin (GolgiStop, BD) and CD107a Pacific Blue (clone H4A3, Biolegend) for 12h, were fixed and permeabilized using a fixation/permeabilization solution kit (BD) and stained with the following antibodies: IFN-γ PE-Cy7 (clone B27, Biolegend), IL-17A BV711 (clone BL168, Biolegend), TNF-α Alexa Fluor 700 (clone Mab11, Biolegend). Proliferation in response to stimulation with PHA-L (Roche) was tracked by labelling cells with CellTraceViolet (Thermo Fisher Scientific). Optimal results were achieved when seeding $0.2x10^6$ cells in 200 µL medium per well in 96-well U bottom plates (Greiner). Proportional upscaling, e.g. seeding $0.6x10^6$ cells in 600µl medium in a 48-well plate, was possible though not optimal, enabling analysis of donors with low percentages of γδ T cells, patient samples and subpopulations. Panels for functional analysis and for tracking of proliferation are summarized in Table 1. Data were acquired using a three laser LSR II (BD) with FACSDiva software V6.1.3 (BD) and customized filter settings and data analysis was performed with FlowJo V10.5.3 (BD; gating strategy, Supplementary Figure 1).

Mass cytometry

Mass cytometric analysis followed established protocols [19]. In brief, cryopreserved PBMCs were thawed, dead cells were stained with Rhodium 103 and cell surface Fc receptors were blocked. Samples were then incubated with an antibody cocktail for cell surface staining which contained antibodies against CD3 170Er (clone UCTH1, Fluidigm), pan-γδ TCR 152Sm (clone 11F2, Fluidigm), Vδ2 TCR141Pr (clone B6, Biolegend; in house-conjugated, using Fluidigm´s Maxpar antibody labelling kit; catalog no.: 201141B) and Vδ1 TCRFITC (clone TS8.2, Thermo Fisher Scientific) amongst others. Next, an anti-FITC 160Gd antibody

(Fluidigm) was used to stain Vδ1 T cells. After fixation, permeabilization and staining of intracellular antigens, samples were incubated for at least 12 hours in a solution of 4% paraformaldehyde in PBS. Samples were stained in batches with 125Ir on the mornings of the respective days of data acquisition. Each sample was rebuffered in purified water directly before acquisition on a Helios system (Fluidigm) at King´s College London. Data analysis was performed with FlowJo V10.5.3 (BD).

Immunohistochemistry

Immunostaining with mAbs against γδ TCR (clone γ3.20, Thermo Fisher Scientific), Vγ9 TCR (clone 7A5) [20], Vγ2/3/4 TCR (clone 23D12) [17, 18] or mouse IgG1 isotype control (Thermo Fisher) of serial paraffin-embedded tissue sections from patients with EBV-associated Hodgkin's lymphoma was carried out after deparaffinization with the fully automated Bond Max-system using the Bond Polymer Refine Detection Kit (Leica-Menarini). Automated antigen retrieval was performed in in Bond Epitope Retrieval Solution 1 (citrate buffer pH 6.0; Leica-Menarini). Additionally, immunostaining with Vγ2/3/4 TCR (clone 23D12), Vδ1 TCR (clone R3.12, Beckman Coulter) or mouse IgG1 isotype control of cryopreserved sections from patients with colon carcinoma was done after acetone fixation and blockade with 4% bovine serum albumin. As second step, antibody EnVision mouse horseradish peroxidase (DAKO) was used. The substrate reaction was performed using the AEC substrate for peroxidase (DAKO). Finally, sections were stained with hematoxylin and embedded in glycerine gelatine (Merck).

Results and Discussion

Magnetic isolation of γδ T cells and subsets

Isolation of γδ T cells is a critical procedure and the methodology of choice needs to be adapted to the design of each particular experiment. The total γδ T cell compartment can be positively or negatively selected using kits from commercial suppliers (e.g. Miltenyi Biotec and STEMCELL Technologies) (Figure 1A, 1B). In addition to beads directly coupled to a γδ TCR-targeting antibody (Miltenyi Biotec), secondary labelling strategies allow sorting and discriminating γδ T cell subsets. Multi-sort beads facilitate multiple rounds of positive selection because these labels can be removed. Positive isolation (PI) is suitable for separating aminobisphosphonate-expanded γδ T cells or γδ T cells expressing particular Vγ/Vδ elements from PBMCs (Figure 1B), and γδ T cells from intra-tumoral lymphoid compartments, e.g. for TCR sequence analysis, offering the advantage of sparing other (infiltrating) cells for further isolation/analysis. On the other hand, for studies examining cell activation status, receptor signaling, cytokine expression and/or cytotoxicity, γδ T cells should be negatively selected to avoid antibody-cross-linking of the γδ TCR. Although some manufacturers claim that immune cells experience no activation through their PI procedure, γδ T cells do upregulate CD69 after PI [21] and show significant functional bias compared to negatively selected cells from the same donor. The EasySep™ Human Gamma/Delta T Cell Isolation Kit from STEMCELL Technologies removes non-γδ T cells with tetrameric antibody complexes and dextran-coated magnetic particles by retaining them inside a tube using a strong magnetic field. Whereas labelled cells remain attached to the tube wall, the remaining (negatively-selected) cells can be poured into a separate tube. Similarly, Miltenyi Biotec's biotin-conjugated depletion cocktail eliminates non-γδ T cells via a secondary magnetic label that retains them on a "MACS® Column" in a magnetic field. High purities – above 98.5% γδ T cells – are routinely achieved with both methods independent of the initial content of γδ T cells and obtained isolates do not contain any undesired αβ T cells (Fig. 1A). The "untouched" negatively-sorted cells are not activated. The STEMCELL Technologies procedure is faster and yields remain quantitative, even when drastically downscaling initial cell numbers (due to zero dead space volume). Moreover, physiological stressors such as mechanical stress, centrifugal forces, and extensive incubation at unphysiologically low temperatures during labelling and purification are avoided.

Pitfalls that may be encountered, when using either of these negative selection procedures are: i) depleted cells are heavily labelled and can not be used for further downstream applications; ii) depletion cocktails often contain antibodies targeting molecules also expressed by subpopulations of γδ T cells, e.g. CD16, which may severely bias subsequent (functional) studies, such as ADCC or gene expression analyses. We therefore suggest the

use of anti-NKp46 (a lineage marker of NK cells) and anti-NKp30 instead of anti-CD16 for NK-cell elimination during negative γδ T cell isolation. NKp46 and NKp30 are expressed on peripheral NK cells but not on γδ T cells in the peripheral blood. However, it should be noted that long-term activation of γδ T cells induces the expression of NKp46, NKp30 and also of Nkp44 in certain subsets (Supplementary Figure 2) [22]. Until commercial kits that exclude anti-human CD16 mAbs become available customized kits are an option.

When aiming to negatively isolate specific subsets of γδ T cells, a combination of strategies is required. For selecting untouched Vδ2 γδ T cells from PBMCs, Vδ1 and other γδ T cell subsets such as Vδ3 γδ T cells must be removed (via PI) before γδ T cell negative selection yields the Vδ2 T cell subset isolate. Unless an anti-human Vδ3 mAb is available, individuals with high numbers of $Vδ1^{-}Vδ2^{-}$ γδ T cells are not suitable for Vδ2 negative selection (Figure 1C). A potential candidate for this approach might be the monoclonal anti-human T cell receptor Vδ3 antibody (clone P11.5B), which was previously distributed by Gentaur and Coulter. However, at the time of writing, the commercial availability of this antibody, its format and thus its suitability for magnetic cell isolation remain unclear.

Phenotypic and functional analysis via polychromatic flow cytometry

When designing an antibody panel for multicolor flow cytometry a few considerations need to be taken into account, in order to avoid certain γδ T cell subsets remaining undetected, and thus biasing subsequent analysis. Below, we aim to highlight the commonest problems and to provide a framework for the flow cytometric analysis of γδ T cells. Furthermore, we briefly present panels designed for the investigation of phenotypic markers, as well as functional and proliferative properties.

We previously reported that the unconjugated pan-γδ TCR antibody clone 11F2 was the only tested antibody able to detect all γδ T cells when combined with a Vδ2 antibody (B6, IMMU389), while the conjugated forms of the commercially-available clones 11F2, B1/B1.1 do not always stain 100% of the γδ T cell population [23]. Moreover, clone B1/B1.1 is unsuitable for multicolor flow cytometry panels including a CD3 antibody due to interference between these two antibodies [23]. The recently-developed generation of γδ TCR subset-specific antibodies, namely Vδ1 clone REA173 and Vδ2 clone 123R3 in combination with pan-γδ TCR antibodies (11F2, IMMU510) seems to offer a standard for flow cytometric characterization of γδ T cells (Figure 2A), overcoming the above-mentioned issues (Supplementary Figure 3A). We tested directly fluorophore-labelled and secondarily detected pan-γδ TCR antibodies (11F2 and IMMU510) to achieve an optimal balance between a rapid and straightforward staining protocol, low background signal and a high staining index (Figure 2B). Separation of the γδ T cell population via directly-labelled pan-γδ TCR

antibodies (11F2, IMMU510) can be problematic in the detection of Vδ1 T cells with low surface TCR expression levels (Supplementary Figure 3B) as seen in patient samples or in *in vitro* culture systems. Detection of the purified formats of these antibodies via fluorophore-labelled anti-mouse antibodies is generally not preferable due to prolonged staining procedures and high background signals. We identified the biotinylated 11F2 clone as an optimal choice (Figure 2A, 2B), because the biotin/streptavidin detection system combines signal amplification with simultaneously low background, resulting in improved separation of the target population, especially in fixed cells (Supplementary Figure 3C). The prolonged staining protocol (1) pan-γδ TCR, (2) streptavidin conjugate, (3) surface antibody cocktail can be reduced by integration of the streptavidin conjugate into the antibody master mix for extracellular staining. In general, use of PE-conjugates for pan γδ T cell antibodies is recommended, because PE itself is recognized by certain γδ TCRs and thus stains a small percentage of peripheral γδ T cells [24]. This should also be kept in mind when tandem conjugates containing PE (e.g. PE-Cy7, PE-Cy5.5 etc.) are included in the antibody panel. As stated above, the Vδ2 123R3 antibody is, in contrast to clone B6, compatible with fluorophore-conjugated pan-γδ TCR antibodies. Of note, clone B6 might be specific for the Vγ9Vδ2 TCR pairing, because it has been reported that detection of the $Vγ9^{-}Vδ2^{+}$ population is not possible with clone B6, but clone 123R3 can be used as an alternative to also detect the rare population of $Vγ9^{-}Vδ2^{+}$ T cells [9].

On the basis of this framework for detection of γδ T cells, we developed several polychromatic antibody panels: i) a phenotypic γδ T cell panel including markers for differentiation state [23] ii) a panel to monitor functionality of γδ T cells including the degranulation marker CD107a and the cytokines TNF, IFN-γ and IL-17A (Figure 3A) and iii) a panel to track γδ T cell proliferative capacity using CellTraceViolet (Figure 3B). The above-described basic phenotypic markers (pan-γδ TCR, Vδ1 and Vδ2) also worked well after fixation and permeabilization.

Using a combination of available mAbs, flow cytometry is also useful to monitor the entire expressed human Vγ repertoire [18]. Such an analysis is based on antibodies detecting Vγ9 (e.g., clone 7A5) [20], Vγ2/3/4 (clone 23D12) [17, 25], Vγ3/5 (clone 56.3) [18] and Vγ8 (clone R4.5.1) [26, 27]. As an example, the combination of mAb 56.3 and 23D12 unequivocally identifies γδ T cell clones expressing Vγ3 ($56.3^{+}23D12^{+}$) and Vγ5 ($56.3^{+}23D12^{-}$) (Figure 4A, 4B). Moreover, such antibodies are useful for detecting rare αβ T cells with a trans-rearranged TCR [13, 28]. As shown in Figure 4C, the 56.3-positive clone (established by positive selection of 56.3-positive cells from PBMC) stains with a pan-αβ T cell antibody (clone IP26) but not with a pan-γδ antibody (clone 11F2). These cells carry an in-frame Vγ5-Jβ-Cβ trans-rearrangement [18] .

Identification of immune signatures via mass cytometry

A good choice of markers for basic identification of cell populations intended to be divided into numerous subsets is essential for mass cytometric analysis, as currently up to 40 channels can be acquired in parallel and multidimensional, automated data analysis is performed. At the time of writing, the only commercially-available pan γδ T cell antibody suitable for mass cytometry derives from the 11F2 clone. We identified even greater problems in mass cytometry than those we faced in polychromatic flow cytometry when using the 11F2 TCR γδ 152 Sm antibody in combination with custom-made B6 TCR Vδ2 141 Pr and TS8.2 Vδ1 FITC antibodies (detected via an anti-FITC 160 Gd). Large proportions of Vδ1 T cells were stained with the pan-γδ TCR antibody, but none or only a fraction of the Vδ2 T cells (Figure 2C). Steric hindrance caused by close proximity of the recognized epitopes and size and nature of the antibody tags might account for these observations. Further testing of the combinations of Vδ1 REA173 and Vδ2 123R3 with the pan-γδ 11F2 antibodies that achieved good resolution in polychromatic flow cytometry is also warranted in mass cytometry.

Immunohistochemical detection of tissue-associated γδ T cells

IHC-based tissue analysis enables tissue-infiltrating (γδ) T cell subsets to be analyzed in the context of their native surroundings, thereby providing a complementary approach to the above-discussed flow cytometry experiments. In the cancer setting, monitoring the abundance of tumor-infiltrating γδ T cells and the localization of distinct γδ T cell subsets can provide a more comprehensive assessment of the tumor status [11]. The best choice for analysis of the γδ TCR expression was the anti-TCR γ clone γ3.20. As we previously reported, IHC staining of consecutive paraffin-embedded sections of pancreatic ductal adenocarcinoma tissue revealed that a large proportion of the $CD3^+CD8^+$ T cells in the ductal epithelium were γδ T cells [11, 12]. Unfortunately the clone γ3.20 is no longer available, but Jungbluth et al. recently reported that the TCR δ antibody clone H-41 (SC-100289, Santa Cruz) is an alternative for the detection of γδ T cells in paraffin-embedded tissue [29]. To visualize the distribution of different γδ T cell-subsets, serial tissue sections were stained with our in-house Vγ9 and Vγ2/3/4 antibodies. Analysis of sections from patients with EBV-associated Hodgkin's lymphoma showed that most of the γδ T cells from these patients expressed Vγ9, whereas γδ T cells expressing Vγ2, 3 or 4 were nearly absent (Figure 5A). Furthermore, staining of cryosections obtained from patients with colon adenocarcinoma using the Vδ1 and Vγ2/3/4 antibodies revealed that these γδ T cells are enriched in respective malignancies, as shown for one representative patient (Figure 5B). This indicates that the Vγ2/3/4 clone 23D12 is also suitable for staining cryosections.

Concluding remarks

The variety of available reagents for the characterization of γδ T cells is, as the research field itself, dynamic and growing, but currently still very limited. Here, we outlined a framework for the phenotypic and functional characterization of human γδ T cells based on currently available reagents. We are certainly aware that the above-described antibodies and antibody combinations still have room for improvement. On the part of the manufacturers, a broader spectrum of fluorophore-antibody conjugates, preferably of smaller size to minimize potential steric hindrance problems, would be appreciated. One must also be aware that rare αβ T cells harbor a TCR trans-rearrangement and thus may express a Vγ rather than a Vβ element. Such αβ T cells stain with anti-Vγ antibodies as shown here for Vγ5, and this has been reported previously also for Vγ4 and Vγ9 [25, 28]. When characterizing γδ T cells in tissue samples the following issues should be taken into account. First, one should carefully select the enzymes used for tissue dissociation in order to avoid the loss of certain cell surface markers. Besides that, sample size and in some cases the low abundance of γδ T cells may be limiting factors. For γδ T cell immunomonitoring within tumor-infiltrating lymphocytes or tumor-ascites lymphocytes by flow cytometry, the additional use of an anti-CD45 mAb in a multicolor panel is recommended for precise analysis of the different γδ and αβ T cell subsets surrounded by many other tumor-associated immune cells and tumor cells (Oberg et al. this volume). Furthermore, the development of antibodies suitable for staining paraffin-embedded tissue sections, and antibodies compatible with the fluorescence microscopy-based MACSima imaging system or the mass cytometry-based Hyperion imaging system could take γδ T cell research to a new level, supporting the various promising attempts to exploit these remarkable cells for treating infectious and non-infectious diseases as well as malignancies.

Authorship

Conceptualization: NB, DW, HO, GP, SK, KS, KWH
Investigation: NB, DW, HO, JB, BW, CG, SS, CR, HH, CP, PN, SK, KS, KWH
Data curation - formal analysis: NB, DW, HO, JB, SS, CR, HH, PN, SK, KS, KWH
Writing - original draft: NB, DW, KS, KWH
Writing - review, editing, and revision: NB, DW, HO, GP, MWL, SK, DK, KS, KWH

Acknowledgments

The authors gratefully thank Janine Spreuer for technical help and Sandra Kröger for her support in staining the tissues of patients with EBV-associated Hodgkin's lymphoma. HH was supported by a grant from the Stefan-Morsch Foundation and KS was supported by a grant from the Jürgen Manchot Foundation. KWH received funding from the DFG (WI 5021-21 – FOR2799), the Klaus Tschira Foundation (00.316.2017) and the Medical Faculty of the University of Tübingen (2509-0-0). DW obtained funding from the DFG (WE 3559/6-1 – FOR2799), DK obtained funding from the DFG (Ka 502/19-1).

Conflict of Interest Disclosure

DK is a member of scientific advisory boards of Incysus, Imcheck, Lava Therapeutics, and Qu Biologics.GP has received research support from Immatics Biotechnologies GmbH, speaker's honoraria from Celgene, Pfizer, Sanofi, 4D-Pharma, Clasado, and Seqirus and is a Consultant to Repair Biotechnologies, Inc. KWH received commercial research grants from Catalym GmbH and travel support from SITC (Society for Immunotherapy of Cancer). MWL is an inventor of patents owned by Immatics Biotechnologies GmbH. No potential conflicts of interest were disclosed by the other authors.

References

1. Chien, Y. H., Jores, R., Crowley, M. P. 1996 Recognition by gamma/delta T cells. Annual Review of Immunology 14, 511-532.
2. Vantourout, P. and Hayday, A. 2013 Six-of-the-best: unique contributions of gammadelta T cells to immunology. Nat Rev Immunol 13, 88-100.
3. Ramstead, A. G. and Jutila, M. A. 2012 Complex Role of gamma delta T-Cell-Derived Cytokines and Growth Factors in Cancer. J Interf Cytok Res 32, 563-569.
4. Couzi, L., Pitard, V., Sicard, X., Garrigue, I., Hawchar, O., Merville, P., Moreau, J. F., Dechanet-Merville, J. 2012 Antibody-dependent anti-cytomegalovirus activity of human gamma delta T cells expressing CD16 (Fc gamma RIIIa). Blood 119, 1418-1427.
5. Brandes, M., Willimann, K., Moser, B. 2005 Professional antigen-presentation function by human gamma delta T cells. Science 309, 264-268.
6. Wen, L., Pao, W., Wong, F. S., Peng, Q. S., Craft, J., Zheng, B., Kelsoe, G., Dianda, L., Owen, M. J., Hayday, A. C. 1996 Germinal center formation, immunoglobulin class switching, and autoantibody production driven by "Non alpha/beta" T cells. J Exp Med 183, 2271-2282.
7. Deusch, K., Luling, F., Reich, K., Classen, M., Wagner, H., Pfeffer, K. 1991 A Major Fraction of Human Intraepithelial Lymphocytes Simultaneously Expresses the Gamma/Delta T-Cell Receptor, the Cd8 Accessory Molecule and Preferentially Uses the V-Delta-1 Gene Segment. European Journal of Immunology 21, 1053-1059.
8. Davey, M. S., Willcox, C. R., Joyce, S. P., Ladell, K., Kasatskaya, S. A., McLaren, J. E., Hunter, S., Salim, M., Mohammed, F., Price, D. A., Chudakov, D. M., Willcox, B. E. 2017 Clonal selection in the human Vdelta1 T cell repertoire indicates gammadelta TCR-dependent adaptive immune surveillance. Nat Commun 8, 14760.
9. Davey, M. S., Willcox, C. R., Hunter, S., Kasatskaya, S. A., Remmerswaal, E. B. M., Salim, M., Mohammed, F., Bemelman, F. J., Chudakov, D. M., Oo, Y. H., Willcox, B. E. 2018 The human Vdelta2(+) T-cell compartment comprises distinct innate-like Vgamma9(+) and adaptive Vgamma9(-) subsets. Nat Commun 9, 1760.
10. Gentles, A. J., Newman, A. M., Liu, C. L., Bratman, S. V., Feng, W. G., Kim, D., Nair, V. S., Xu, Y., Khuong, A., Hoang, C. D., Diehn, M., West, R. B., Plevritis, S. K., Alizadeh, A. A. 2015 The prognostic landscape of genes and infiltrating immune cells across human cancers. Nat Med 21, 938-945.
11. Oberg, H. H., Grage-Griebenow, E., Adam-Klages, S., Jerg, E., Peipp, M., Kellner, C., Petrick, D., Gonnermann, D., Freitag-Wolf, S., Rocken, C., Sebens, T., Vogel, I., Becker, T., Ebsen, M., Kabelitz, D., Wesch, D., Sebens, S. 2016 Monitoring and functional characterization of the lymphocytic compartment in pancreatic ductal adenocarcinoma patients. Pancreatology 16, 1069-1079.
12. Oberg, H. H., Peipp, M., Kellner, C., Sebens, S., Krause, S., Petrick, D., Adam-Klages, S., Rocken, C., Becker, T., Vogel, I., Weisner, D., Freitag-Wolf, S., Gramatzki, M., Kabelitz, D., Wesch, D. 2014 Novel bispecific antibodies increase gammadelta T-cell cytotoxicity against pancreatic cancer cells. Cancer Res 74, 1349-60.
13. Dechanet, J., Merville, P., Lim, A., Retiere, C., Pitard, V., Lafarge, X., Michelson, S., Meric, C., Hallet, M. M., Kourilsky, P., Potaux, L., Bonneville, M., Moreau, J. F. 1999 Implication of gammadelta T cells in the human immune response to cytomegalovirus. J Clin Invest 103, 1437-49.
14. Halary, F., Pitard, V., Dlubek, D., Krzysiek, R., de la Salle, H., Merville, P., Dromer, C., Emilie, D., Moreau, J. F., Dechanet-Merville, J. 2005 Shared reactivity of V delta 2(neg) gamma delta T cells against cytomegalovirus-infected cells and tumor intestinal epithelial cells. J Exp Med 201, 1567-1578.
15. Mordmuller, B., Surat, G., Lagler, H., Chakravarty, S., Ishizuka, A. S., Lalremruata, A., Gmeiner, M., Campo, J. J., Esen, M., Ruben, A. J., Held, J., Calle, C. L., Mengue, J. B., Gebru, T., Ibanez, J., Sulyok, M., James, E. R., Billingsley, P. F., Kc, N., Manoj, A., Murshedkar, T., Gunasekera, A., Appen, A. G. E., Li, T., Stafford, R. E., Li, M. L., Felgner, P. L., Seder, R. A., Richie, T. L., Sim, B. K. L., Hoffman, S. L., Kremsner, P. G. 2017 Sterile protection against human malaria by chemoattenuated PfSPZ vaccine. Nature 542, 445-+.
16. Lawand, M., Dechanet-Merville, J., Dieu-Nosjean, M. C. 2017 Key Features of Gamma-Delta T-Cell Subsets in Human Diseases and Their Immunotherapeutic Implications. Front Immunol 8, 761.
17. Kabelitz, D., Ackermann, T., Hinz, T., Davodeau, F., Band, H., Bonneville, M., Janssen, O., Arden, B., Schondelmaier, S. 1994 New monoclonal antibody (23D12) recognizing three

different V gamma elements of the human gamma delta T cell receptor. 23D12+ cells comprise a major subpopulation of gamma delta T cells in postnatal thymus. J Immunol 152, 3128-36.
18. Hinz, T., Wesch, D., Halary, F., Marx, S., Choudhary, A., Arden, B., Janssen, O., Bonneville, M., Kabelitz, D. 1997 Identification of the complete expressed human TCR V gamma repertoire by flow cytometry. Int Immunol 9, 1065-1072.
19. Kordasti, S., Costantini, B., Seidl, T., Perez Abellan, P., Martinez Llordella, M., McLornan, D., Diggins, K. E., Kulasekararaj, A., Benfatto, C., Feng, X., Smith, A., Mian, S. A., Melchiotti, R., de Rinaldis, E., Ellis, R., Petrov, N., Povoleri, G. A., Chung, S. S., Thomas, N. S., Farzaneh, F., Irish, J. M., Heck, S., Young, N. S., Marsh, J. C., Mufti, G. J. 2016 Deep phenotyping of Tregs identifies an immune signature for idiopathic aplastic anemia and predicts response to treatment. Blood 128, 1193-205.
20. Janssen, O., Wesselborg, S., Hecklostreicher, B., Pechhold, K., Bender, A., Schondelmaier, S., Moldenhauer, G., Kabelitz, D. 1991 T-Cell Receptor Cd3-Signaling Induces Death by Apoptosis in Human T-Cell Receptor Gamma-Delta+T-Cells. Journal of Immunology 146, 35-39.
21. Wesch, D., Beetz, S., Oberg, H. H., Marget, M., Krengel, K., Kabelitz, D. 2006 Direct costimulatory effect of TLR3 ligand poly(I : C) on human gamma delta T lymphocytes. Journal of Immunology 176, 1348-1354.
22. Correia, D. V., Fogli, M., Hudspeth, K., da Silva, M. G., Mavilio, D., Silva-Santos, B. 2011 Differentiation of human peripheral blood Vdelta1+ T cells expressing the natural cytotoxicity receptor NKp30 for recognition of lymphoid leukemia cells. Blood 118, 992-1001.
23. Wistuba-Hamprecht, K., Pawelec, G., Derhovanessian, E. 2014 OMIP-020: Phenotypic characterization of human gammadelta T-cells by multicolor flow cytometry. Cytometry A 85, 522-4.
24. Zeng, X., Wei, Y. L., Huang, J., Newell, E. W., Yu, H., Kidd, B. A., Kuhns, M. S., Waters, R. W., Davis, M. M., Weaver, C. T., Chien, Y. H. 2012 Gammadelta T cells recognize a microbial encoded B cell antigen to initiate a rapid antigen-specific interleukin-17 response. Immunity 37, 524-34.
25. Davodeau, F., Peyrat, M. A., Gaschet, J., Hallet, M. M., Triebel, F., Vie, H., Kabelitz, D., Bonneville, M. 1994 Surface Expression of Functional T-Cell Receptor Chains Formed by Interlocus Recombination on Human T-Lymphocytes. J Exp Med 180, 1685-1691.
26. Soderstrom, K., Bucht, A., Halapi, E., Lundqvist, C., Gronberg, A., Nilsson, E., Orsini, D. L. M., Vandewal, Y., Koning, F., Hammarstrom, M. L., Kiessling, R. 1994 High Expression of V-Gamma-8 Is a Shared Feature of Human Gamma-Delta T-Cells in the Epithelium of the Gut and in the Inflamed Synovial Tissue. Journal of Immunology 152, 6017-6027.
27. Wesch, D., Hinz, T., Kabelitz, D. 1998 Analysis of the TCR V gamma repertoire in healthy donors and HIV-1-infected individuals. Int Immunol 10, 1067-1075.
28. Hinz, T., Allam, A., Wesch, D., Schindler, D., Kabelitz, D. 2000 Cell-surface expression of transrearranged Vgamma-cbeta T-cell receptor chains in healthy donors and in ataxia telangiectasia patients. Br J Haematol 109, 201-10.
29. Jungbluth, A. A., Frosina, D., Fayad, M., Pulitzer, M. P., Dogan, A., Busam, K. J., Imai, N., Gnjatic, S. 2018 Immunohistochemical Detection of gamma/delta T Lymphocytes in Formalin-fixed Paraffin-embedded Tissues. Appl Immunohistochem Mol Morphol.

Figures

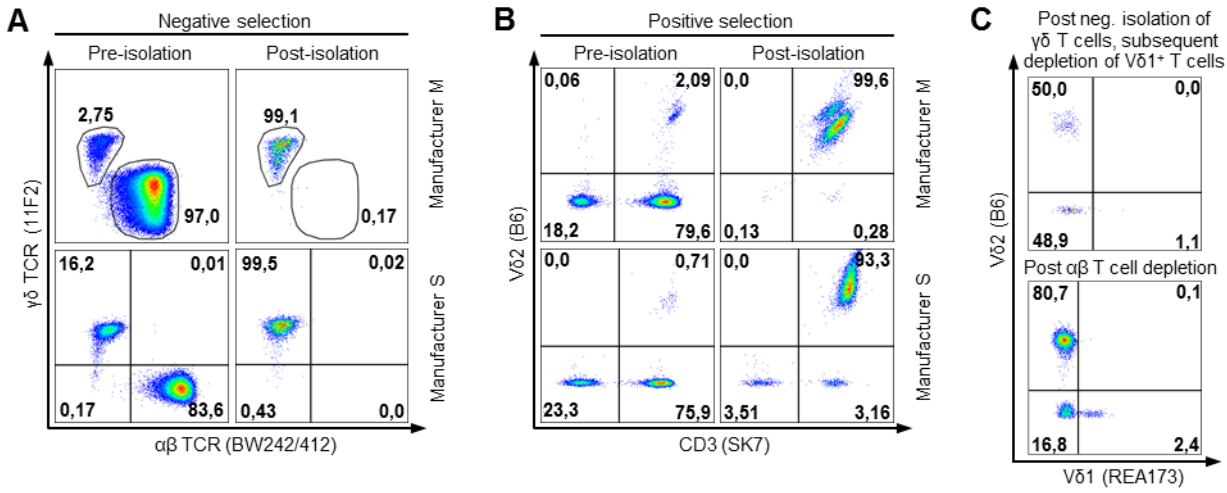

Figure 1: Magnetic isolation of γδ T cells from PBMCs (A) Representative FACS plots showing the CD3 compartment pre and post isolation of untouched γδ T cell preparations. Presented data reflect the reproducibly high purities that are achieved using kits from either Miltenyi Biotec (Manufacturer M) or STEMCELL Technologies (Manufacturer S). Viability is reproducibly above 99%. **(B)** Representative FACS plots of cell isolates gained with positive selection strategy using kits from Miltenyi Biotec or STEMCELL Technologies. Shown are target cells in the $CD3^+$ gate. Viability is reproducibly above 98%. **(C)** $Vδ1^-Vδ2^-$ cell fractions from two healthy adult donors are presented (gated on $CD3^+$ T cells, no contaminating αβ T cells are present). Without the availability of an anti-human Vδ3 antibody these donors cannot be used for the isolation of negatively selected pure Vδ2 γδ T cells.

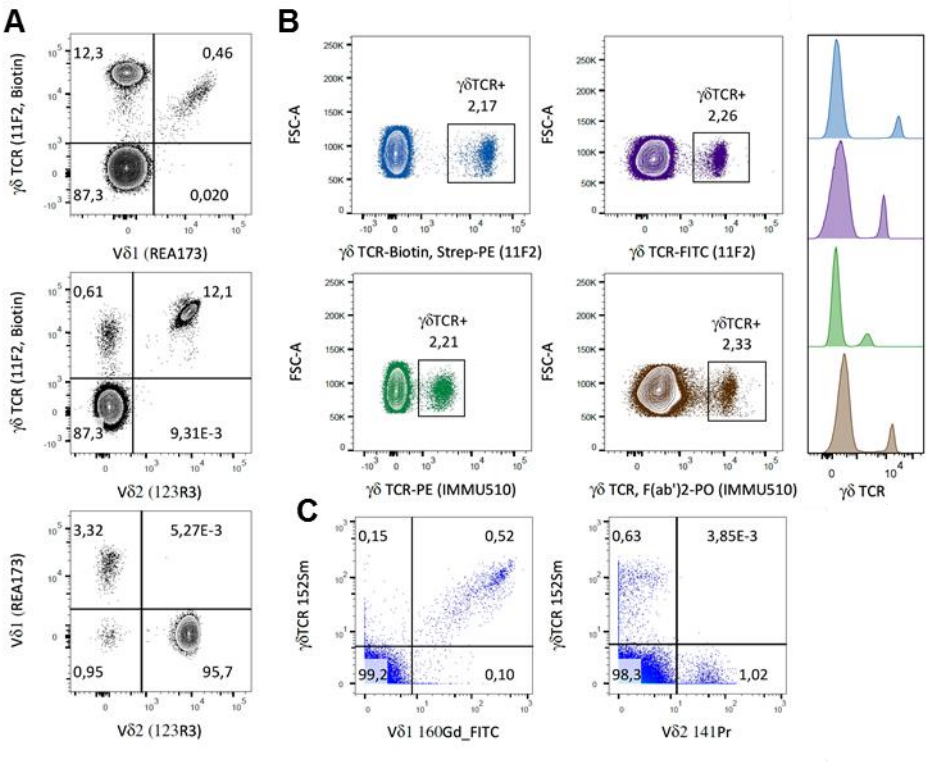

Figure 2: Phenotypic characterization of γδ T cells via flow cytometry and CyTOF (A) Phenotypic characterization of the Vδ1 and Vδ2 sub-populations via flow cytometry. Gating on peripheral, viable, $CD3^+$, lymphocytes showed that the γδ TCR antibody (clone 11F2) recognized all $Vδ1^+$ (clone REA173) and $Vδ2^+$ (clone 123R3) cells. Sufficient separation of the sub-populations, gated on γδ TCR^+ T cells, was achieved. **(B)** Direct and indirect staining of the γδ TCR with the clones 11F2 and IMMU510. The best separation with the lowest background signal in flow cytometry was achieved with the biotinylated 11F2 clone. The population was gated on viable, $CD3^+$ lymphocytes. **(C)** Characterization of γδ T cell sub-populations by CyTOF in a fixed and permeabilized representative sample. Both plots display the same population that was gated on viable, $CD45^+$, $CD14^-$, $CD33^-$, $CD20^-$, $CD3^+$ T cells. γδ TCR (clone 11F2; Sm152) stained the vast majority of the indirectly stained $Vδ1^+$ (clone TS8.2 FITC a Gd160), but none of the $Vδ2^+$ (clone B6 ; Pr141) γδ T cells.

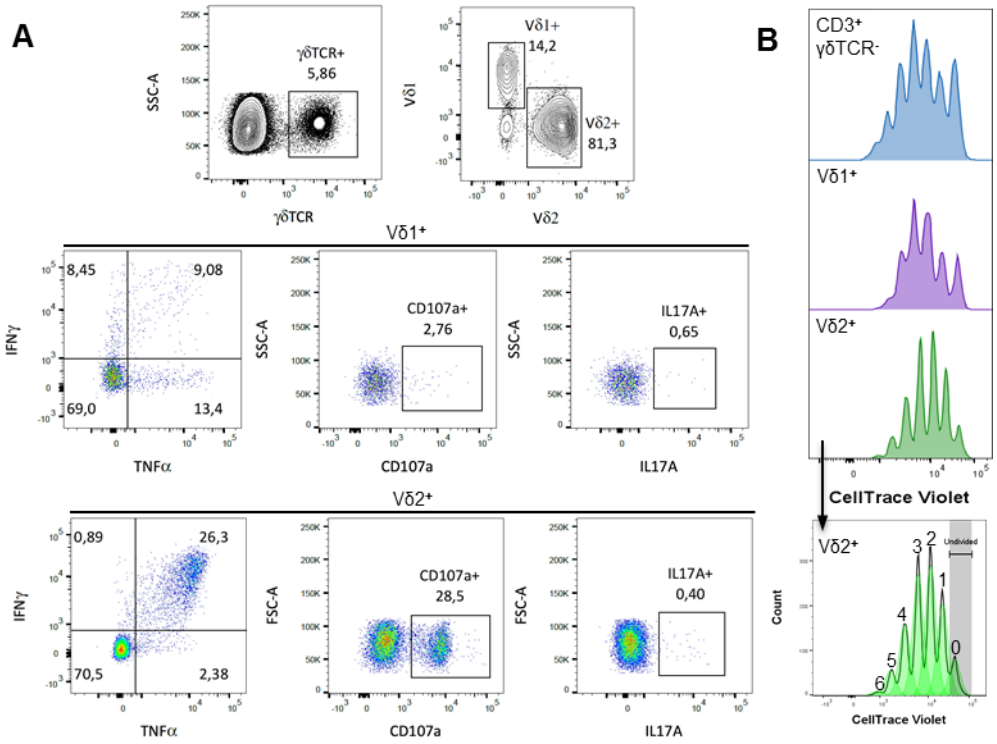

Figure 3: Functional characterization of γδ T cells via flow cytometry. (A) Analysis of cytokine expression in fixed PBMC samples after stimulation with Zoledronate ($Vδ2^+$) or PMA/Ionomycin ($Vδ1^+$). $Vδ1^+$ and $Vδ2^+$ cells were gated on viable, $CD3^+$, γδ TCR^+ lymphocytes. **(B)** Proliferation of $CD3^+γδTCR^-$, $Vδ1^+$ and $Vδ2^+$ T cells after stimulation with PHA-L was tracked on the basis of dye dilution using CellTrace Violet. γδ T cell subpopulations were gated on viable, $CD3^+$, γδ TCR^+ lymphocytes. The proliferation modeling tool included in the FlowJo software enabled a more in-depth analysis of the proliferative properties.

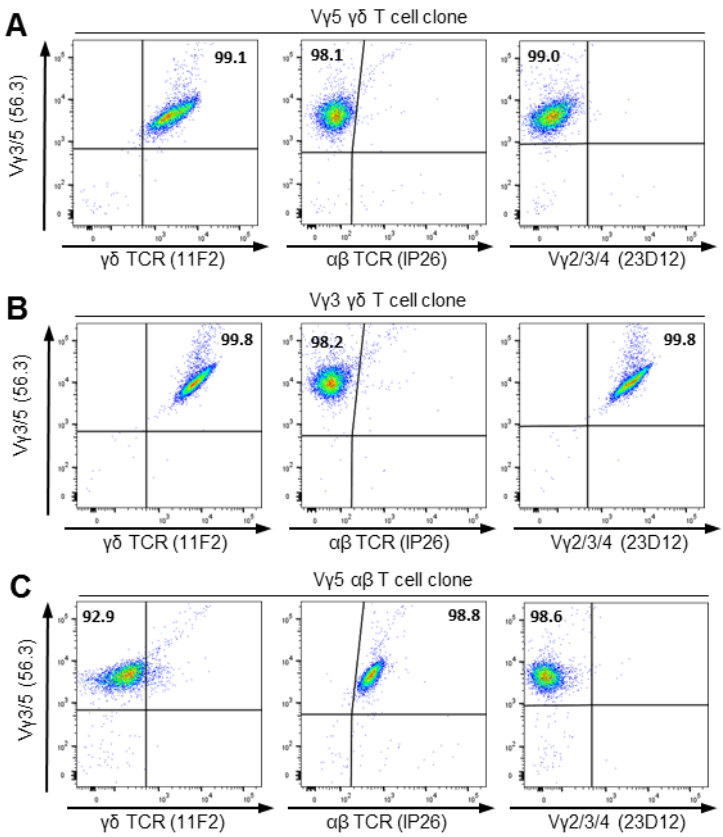

Figure 4: Identification of Vγ3 and Vγ5 γδ and αβ T cell clones. Viable cells were discriminated by gating on lymphocytes (FSC vs. SSC) and by near infra-red live/dead-staining. γδ and αβ T cell clones stained by mAb Vγ3/5 (clone 56.3) were co-labeled with the mAbs recognizing the αβ TCR (clone IP26), γδ TCR (clone 11F2), Vγ2/3/4 (clone 23D12). (**A)** Vγ5 γδ clone (IP26^{-},11F2^{+},56.3^{+},23D12^{-}) (**B)** Vγ3 γδ clone (IP26,11F2^{+},56.3^{+},23D12^{+}); (**C)** Vγ5 αβ clone (IP26^{+},11F2^{-},56.3^{+},23D12^{-}).

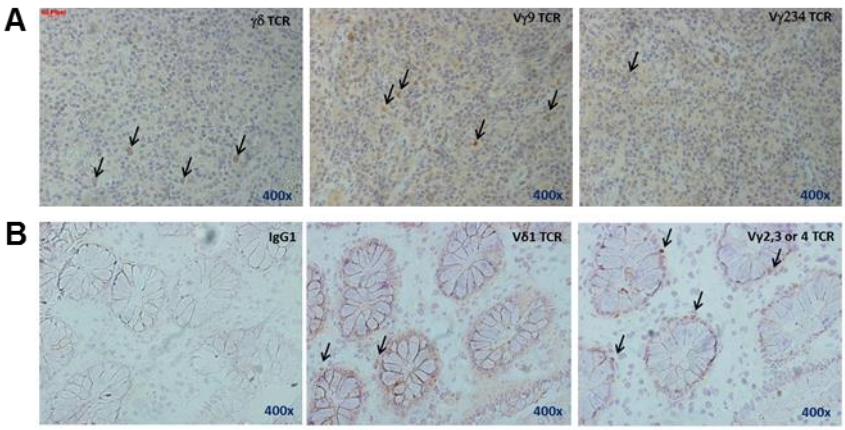

Figure 5: Distribution of different T cell subsets in EBV-associated Hodgkin´s lymphoma tissues and colon adenocarcinoma tissue. **(A)** Serial paraffin-embedded tissue sections from patients with EBV-associated Hodgkin´s lymphoma were stained with γδ TCR (clone γ3.20), Vγ9 (clone 7A5), Vγ2/3/4 (clone 23D12) mAbs as indicated in one representative donor. **(B)** Serial cryosections obtained from colon adenocarcinoma patients were stained with IgG control, Vδ1 (clone R3.12), Vγ2/3/4 (clone 23D12) mAbs as indicated in one representative patient. IHC staining was performed as described in the Materials and Methods section.

Table 1: Monoclonal antibody panels for the functional characterization and for tracking the proliferation of γδ T cells via flow cytometry

	Fluorophore	Clone
Functional characterization		
Dead cells	Fixable red	
CD3	BV510	UCHT1
γδ TCR	Biotin + Streptavidin-PE	11F2
Vδ1	PerCP-Vio700	REA173
Vδ2	FITC	123R3
IFN-γ	PE-Cy7	B27
TNF-α	Alexa Fluor 700	Mab11
IL17A	BV711	BL168
CD107a	Pacific Blue	H4A3
Tracking of proliferation		
Dead cells	Fixable red	
CD3	Alexa Fluor 700	UCHT1
γδ TCR	Biotin + Streptavidin-PE	11F2
Vδ1	APC	REA173
Vδ2	FITC	123R3

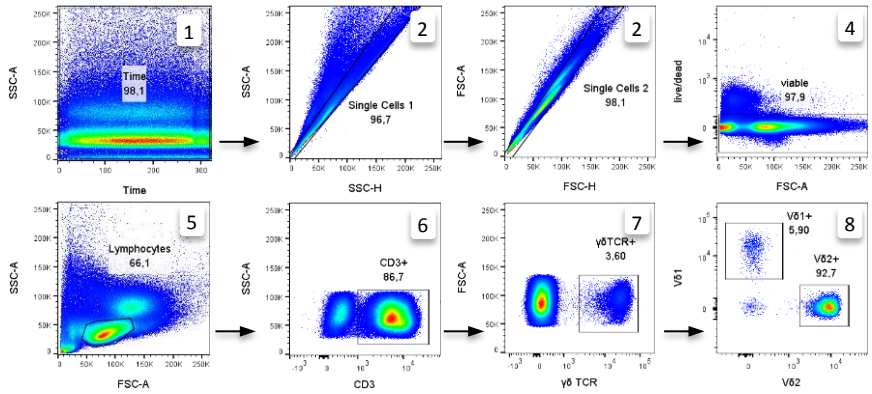

Supplementary Figure 1. Gating strategy for flow cytometric characterization of γδ T cells. In order to avoid cross-contamination between sequentially measured samples and to monitor potentially occurring fluctuation in the pressure system of the flow cytometer, gating started with a time gate (1) followed by singlet gating (2 and 3). Dead cells were excluded by a viable gate (4), followed by lymphocyte gating (5). Next, a gate on the CD3⁺ population (6) was set. Finally, *γδ TCR⁺ cells (7) are discriminated into Vδ1⁺ and Vδ2⁺ subpopulations (8).*

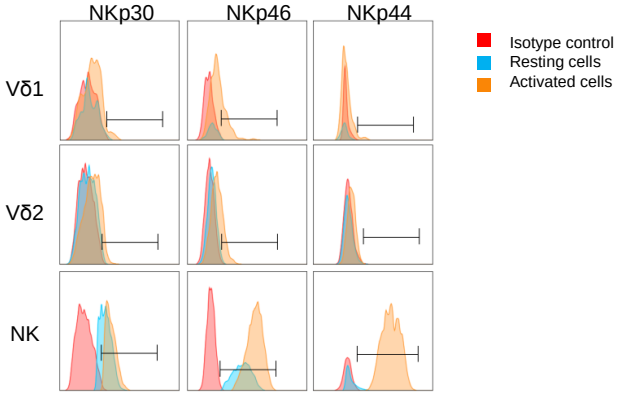

Supplementary Figure 2: Expression of NKp on resting and activated γδ T cells and NK cells. Freshly isolated PBMCs were analyzed for the expression of NKp either *ex vivo* or after incubation for 96h with an immobilized pan-γδ TCR antibody (IMMU510, 1µg/ml) in combination with IL-2 (50U/ml), IL-12 (10ng/ml) and IL-18 (10ng/ml) in complete RPMI. Cells were harvested and NKp30, NKp46 and NKp44 expression was separately analyzed by flow cytometry on Vδ1⁺ cells, Vδ2⁺ cells and NK cells.

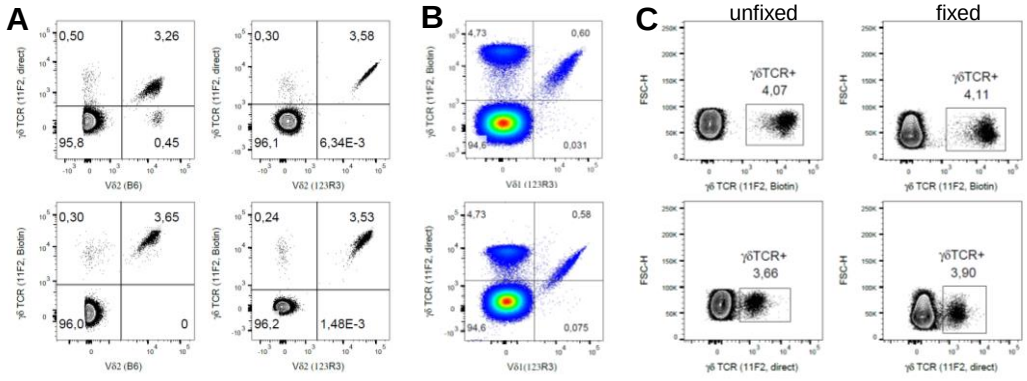

Supplementary Figure 3: Pitfalls in the phenotypic characterization of γδ T cells (A) Comparison of directly fluorophore-labelled and secondarily detected pan-γδ TCR antibodies (clone 11F2) in combination with different Vδ2 antibodies**.** When combining a directly-labelled pan-γδ TCR antibody (FITC) with Vδ2 clone B6 (PerCP), some Vδ2⁺ cells are not stained by the pan-γδ TCR antibody. To overcome this problem, a secondarily detected pan-γδ TCR antibody (Strep-PE) or Vδ2 clone 123R3 (FITC) can be used. **(B)** Low surface expression levels of the γδ TCR on Vδ1⁺ T cells. Improved separation of γδ T cells via secondarily detected pan-γδ TCR (Strep-PE) antibodies compared to directly-labelled antibodies (FITC) facilitates detection of Vδ1⁺ cells with low expression levels of the γδ TCR **(C)** Improved separation via secondarily detected pan-γδ TCR antibodies (clone 11F2) in fixed and unfixed samples**.** Usage of a secondarily detected pan-γδ TCR antibody (Strep-PE) leads to an improvement of separation between the positive and negative population compared to a directly fluorophore-labelled antibody (FITC). The improved separation is maintained after fixation of cells.

Accurate determination of γδ T cells in multi-channel mass and flow cytometry

Nicola Beucke[1], Kilian Wistuba-Hamprecht[1]*

[1]Division of Dermatooncology, Department of Dermatology, University Medical Center, Tübingen, Germany

*Correspondence Kilian Wistuba-Hamprecht, Division of Dermatooncology, Department of Dermatology, University Medical Center, Tübingen, Germany.
Email: kilian.wistuba-hamprecht@uni-tuebingen.de

This is the accepted version of the following letter to the editor: Beucke N, Wistuba-Hamprecht K. Accurate determination of γδ T cells in multi-channel mass and flow cytometry. Cytometry B Clin Cytom. 2021 May;100(3):288-289, which has been published in final form at doi: 10.1002/cyto.b.21885.

Dear Editor, γδ T cells are often neglected in T cell immunomonitoring studies, but their unique properties, bridging innate and adaptive immunity, are attracting growing interest in different research fields like cancer, auto-immunity, and inflammation. Recently, Bagwell et al. evaluated the reproducibility of deep immunophenotyping by mass cytometry in combination with an automated data analysis system in a multi-site study (Bagwell et al., 2019). The 30-marker panel used in that study allowed the identification of 37 immune populations including several subsets of T cells, B cells, NK cells, monocytes, and dendritic cells. Because there remain a number of unoccupied (heavy metal) channels, even more markers can be added to study additional subpopulations. This last stage in the process of validation for the development of a commercially available kit shows that this system consisting of a dry antibody cocktail and automated data analysis achieves a high reproducibility across research centers, an important step toward the urgently needed standardization of mass and flow cytometry. Careful selection of antibodies and an accurate validation of the proposed subsequent automated data analysis tool is essential—in particular when the aim is to commercialize such an approach. In the context of the proposal by Bagwell et al., we believe that optimization of the proposed antibody panel by substituting the pan-γδ T cell receptor (TCR) antibody deriving from the clone "B1" with a different clone, for example, "11F2," is essential. "B1-antibodies" may not be able to identify the entirety of the γδ T cell population when used in combination with a CD3 antibody, probably due to close proximity of the recognized epitopes causing steric hindrance (BD datasheet "clone

B1", Wistuba-Hamprecht, Pawelec, & Derhovanessian, 2014; Beucke et al., 2020). Another advantage of "11F2-antibodies" is that they are known to work well in combination with additional TCR γδ antibodies such as those specific for Vδ1 (clone REA173) or Vδ2 (clone 123R3). Furthermore, the data analysis approach might be improved by examining the known surface marker expression patterns of γδ T cells: usually, the majority of γδ T cells does not express CD4 or CD8, but between 5 and 30% of γδ T cells do express CD8 and a small percentage expresses CD4 (Andreu-Ballester et al., 2012; Garcillan et al., 2015; Hayday, 2000; Wistuba-Hamprecht, Haehnel, Janssen, Demuth, & Pawelec, 2015; Ziegler et al., 2014). The model of Bagwell and colleagues classifies γδ T cells as CD8-negative or -dim and CD4-negative, so depending on the individual a considerable proportion of γδ T cells might be missed. We feel that the readers and potential users of the proposed antibody panel and analysis approach of Bagwell et al. should be aware of these potential limitations.

Conflict of Interest: The authors declare no potential conflict of interest.

References

Andreu-Ballester, J. C., Garcia-Ballesteros, C., Benet-Campos, C., Amigo, V., Almela-Quilis, A., Mayans, J., & Ballester, F. (2012). Values for alpha beta and gamma delta T-lymphocytes and CD4+, CD8+, and CD56+ subsets in healthy adult subjects: Assessment by age and gender. Cytometry Part B, Clinical Cytometry, 82b, 238–244.

Bagwell, C. B., Hunsberger, B., Hill, B., Herbert, D., Bray, C., Selvanantham, T., et al. (2019). Multi-site reproducibility of a human immunophenotyping assay in whole blood and peripheral blood mononuclear cells preparations using CyTOF technology coupled with Maxpar Pathsetter, an automated data analysis system. Cytometry Part B, Clinical Cytometry, 98, 146–160.

Beucke, N., Wesch, D., Oberg, H. H., Peters, C., Bochem, J., Weide, B., et al. (2020). Pitfalls in the characterization of circulating and tissue-resident human gammadelta T cells. Journal of Leukocyte Biology.

Garcillan, B., Marin, A. V. M., Jimenez-Reinoso, A., Briones, A. C., MunozRuiz, M., Garcia-Leon, M. J., et al. (2015). Gamma delta T lymphocytes in the diagnosis of human T cell receptor immunodeficiencies. Frontiers in Immunology, 6, 20.

Hayday, A. C. (2000). Gamma delta cells: A right time and a right place for a conserved third way of protection. Annual Review of Immunology, 18, 975–1026.

Wistuba-Hamprecht, K., Pawelec, G., & Derhovanessian, E. (2014). OMIP020: Phenotypic characterization of human gamma delta T-cells by multicolor flow cytometry. Cytometry. Part A, 85, 522–524.

Wistuba-Hamprecht, K., Haehnel, K., Janssen, N., Demuth, I., & Pawelec, G. (2015). Peripheral blood T-cell signatures from highresolution immune phenotyping of gamma delta and alpha beta Tcells in younger and older subjects in the Berlin aging study II. Immunity & Ageing, 12,25

Ziegler, H., Welker, C., Sterk, M., Hearer, J., Rammensee, H. G., Handgretinger, R., & Schilbach, K. (2014). Human peripheral CD4(+) V delta 1(+) gamma delta T cells can develop into alpha beta T cells. Frontiers in Immunology, 5,1–23.

Integrin activation enables rapid detection of functional Vδ1+ and Vδ2+ γδ T cells

Nicola Herold[1]*, Anna Schöllhorn[2], Adrian Feile[1], Andrea Gaißler[1], Anne Mohrholz[1], Graham Pawelec[2,3], Markus W. Löffler[2,4,5,6,7], Stoyan Dimitrov[8], Cécile Gouttefangeas[2,6,7], Kilian Wistuba-Hamprecht[1,2,6,9]*

[1] Department of Dermatology, University Hospital Tübingen, Tübingen, Germany.
[2] Department of Immunology, Institute for Cell Biology, University of Tübingen, Tübingen, Germany .
[3] Health Sciences North Research Institute, Sudbury, Ontario, Canada.
[4] Department of General, Visceral and Transplant Surgery, University Hospital Tübingen, Tübingen, Germany.
[5] Department of Clinical Pharmacology, University Hospital Tübingen, Tübingen, Germany.
[6] German Cancer Consortium (DKTK) and German Cancer Research Center (DKFZ) partner site Tübingen, Tübingen, Germany.
[7] Cluster of Excellence iFIT (EXC2180) "Image-Guided and Functionally Instructed Tumor Therapies", University of Tübingen, Tübingen, Germany.
[8] Institute of Medical Psychology and Behavioral Neurobiology, University of Tübingen, Tübingen, Germany.
[9] Section for Clinical Bioinformatics, Department of Internal Medicine I, University Hospital Tübingen, Tübingen, Germany.

*Correspondence:
Nicola Herold: Otfried-Müller-Straße 10, 72076 Tübingen; Nicola.Beucke@med.uni-tuebingen.de
Kilian Wistuba-Hamprecht: Otfried-Müller-Straße 10, 72076 Tübingen; kilian.wistuba-hamprecht@uni-tuebingen.de

This is the peer reviewed version of the following article: Herold N, Schöllhorn A, Feile A et al. Integrin activation enables rapid detection of functional Vδ1+ and Vδ2+ γδ T cells. Eur J Immunol. 2022 May;52(5):730-736, which has been published in final form at doi: 10.1002/eji.202149682.

Keywords: γδ T cells, integrin activation, LFA-1, Immunomonitoring, flow cytometry

Abbreviations: LFA-1: lymphocyte function-associated antigen-1; **mAb**: monoclonal antibody; **TCR**: T cell receptor; **ICAM-1**: intercellular adhesion molecule 1; **HMBPP**: 4-hydroxy-3-methylbut-2-enyl pyrophosphate; **PBMCs**: Peripheral blood mononuclear cells; **PMA**: phorbol 12-myristate 13-acetate; **PBS**: phosphate-buffered saline; **EMRA**: effector memory cells re-expressing CD45RA

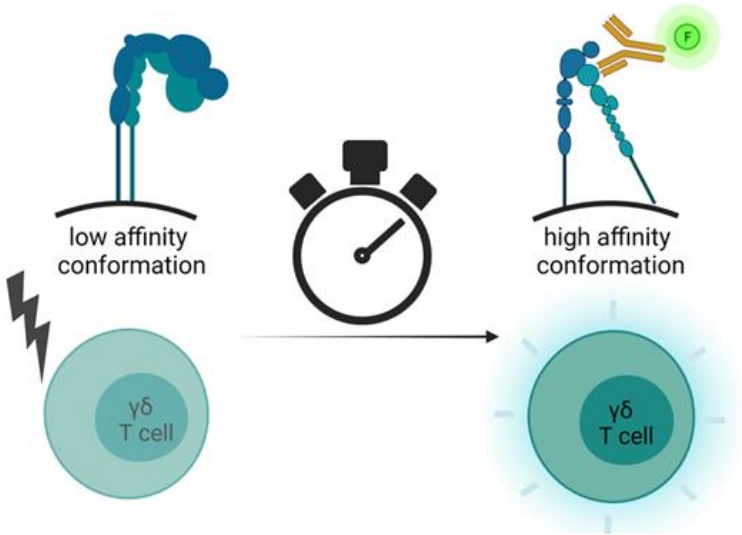

The rapid conformational change of LFA-1 from the low to the high affinity conformation upon T cell activation allows the flow cytometric detection of functional γδ T cells as early as 10 min after stimulation.

Abstract

Conformational change of the β2 integrin lymphocyte function-associated antigen 1 (LFA-1) is an early marker of T cell activation. A protocol using the monoclonal antibody (mAb) clone m24 recognizing the active, extended high-affinity conformation has been previously described for the assessment of functional CD4+ and CD8+ T cells in response to MHC-peptide stimulation. We investigated the applicability of the m24 mAb to detect the activation of γδ T cells in response to different soluble and immobilized stimuli. m24 mAb staining was associated with the expression of cytokines and was detectable as early as 10 min after stimulation, but with different kinetics depending on the nature of the stimulus. Hence, we conclude that this assay is suitable for the detection of functional γδ T cells and allows the assessment of activation more rapidly than alternative methods such as cytokine detection. Intracellular staining, protein trafficking inhibitors or prior knowledge of the stimulating moiety recognized are no longer required for monitoring γδ T cell activation.

Introduction

Conformational change of the lymphocyte function-associated antigen-1 (LFA-1) upon T cell receptor (TCR) engagement can be utilized as an early activation marker to assess T cell functionality (1-3). The β2 integrin LFA-1 is a heterodimeric, membrane-bound receptor constitutively expressed on the cell surface of all mature T cells (4). It is involved in a wide range of T cell functions including cell adhesion and migration, formation of the immunological synapse, cytokine production, proliferation and differentiation (4, 5). TCR-mediated stimulation leads to rapid clustering of integrins and to a conformational change from a bent, low-affinity form to an extended open high-affinity conformation (Figure 1a) (6). This inside-out signaling process does not require de-novo expression of new molecules, thereby allowing an immediate detection of functional T cells. The active, high-affinity state of LFA-1 can be specifically detected via the monoclonal antibody (mAb) clone m24 (2) or using multimers of the LFA-1 ligand intercellular adhesion molecule 1 (ICAM-1) (1). The m24 epitope has been described as a reporter of integrin activation and expression of this epitope corresponds to ligand binding activity (7, 8). While ICAM-1 multimers are suitable for detecting antigen-specific CD8+ T cells, combination of the m24 mAb with EDTA treatment to disrupt cell aggregates of antigen-specific CD4+ T cells enables simultaneous assessment of CD4+ and CD8+ T cell activation in whole blood and cryopreserved samples (2).

Here we aimed to determine whether this assay initially developed for “classical” αβ T cells would also be suitable for assessing activation of the “unconventional” γδ T cell population. γδ T cells represent a minor population of 1-10% of all T cells in the peripheral blood of healthy adults, and may also be present in tissues and tumor infiltrates (9). These non-MHC-restricted T cells comprise several subsets with diverse functionalities ranging from cytotoxic activity to antigen presentation and interaction with B cells (10). The human peripheral γδ T cell compartment consists of the numerically predominant innate-like Vγ9+Vδ2+ cells (11), adaptive-like Vδ1+ cells (12) and several other minor Vδ2−Vδ1− subsets. Vγ9+Vδ2+ γδ T cells sense phosphoantigens such as 4-hydroxy-3-methylbut-2-enyl pyrophosphate (HMBPP) or isopentenyl pyrophosphate via interaction with butyrophilins involving germline-encoded regions of the Vγ9 chain (13, 14). An accumulation of such phosphoantigens can be induced by treatment with aminobisphosphonates, e.g. zoledronate, which inhibit the enzyme farnesyl pyrophosphate synthase of the mevalonate pathway. Knowledge of the ligands recognized by the Vδ1 TCR and the underlying mechanisms of antigen recognition is still sparse. Among the identified antigens are MHC-like molecules, the endothelial protein C receptor, as well as stress-induced antigens (15). Little is known about the expression and role of integrins on γδ T cells. However, integrin

expression differs between Vδ1+ and Vδ2+ γδ T cells, possibly accounting for differences in tissue localization of these two major subsets (16). LFA-1 has been reported to be involved in adhesion, migration and cytotoxicity (16, 17). In comparison to αβ T cells, γδ T cells show an increased adhesiveness that is associated with higher LFA-1 levels (18), but the expression of LFA-1 on Vδ1+ and Vδ2+ γδ T cells is similar (18).

The present work demonstrates the feasibility of the m24 mAb-based assay for the detection of functional γδ T cells, analogous to its utilization for αβ T cells. Integrin activation can be detected as early as 10 min after stimulation, with the exact kinetics depending on the nature of the stimulus. Furthermore, we confirm that m24 mAb staining identifies functional γδ T cells at all stages of differentiation, especially late-differentiated or CD57+ γδ T cells.

Results and Discussion

m24 mAb staining identifies functional γδ T cells

In order to assess whether staining for activated LFA-1 is a marker for γδ T cell functionality, we examined cytokine production by Vδ1+ and Vδ2+ γδ T cells as well as by non-γδ T cells in response to stimulation with PMA/ionomycin (Figure 1b). After 4 h of stimulation virtually all Vδ2+ γδ T cells and most Vδ1+ γδ T cells and non-γδ T cells were stained by the m24 mAb. However, while the majority of Vδ2+ γδ T cells expressed IFN-γ or TNF, only a fraction of Vδ1+ and non-γδ T cells did. Expression of IFN-γ and TNF was largely confined to m24+ cells and especially cells with bright m24 mAb signals co-stained for cytokines, similar to observations in CD8+ T cells using ICAM-1 multimers (1). To assess the induction of cytotoxic activity and m24 expression on γδ T cells in the presence of a natural interaction partner (13, 14), we performed an *ex vivo* short-term co-culture of PBMCs with a melanoma cell line that was either pre-treated with zoledronate or not. Higher proportions of m24+ Vδ2+ γδ T cells and of apoptotic or dead melanoma cells were found in the presence of zoledronate compared to the untreated control (Supplementary Figure 2).

This demonstrates the feasibility of flow cytometric detection of activated LFA-1 using the m24 mAb for assessing not only classical T cells (2), but also functional Vδ1+ and Vδ2+ (Figure 1b) as well as Vδ1−Vδ2− γδ T cells (Supplementary Figure 3a). Moreover, γδ T cells showed a higher m24 mAb staining intensity compared to non-γδ T cells, which could be related to their higher levels of total LFA-1 (18) and/or increased clustering/affinity of LFA-1. Because this assay is based on the detection of a cell surface marker, there is no need for Golgi inhibitors,

permeabilization and intracellular staining, enabling a more straightforward, convenient and rapid staining protocol.

Kinetics of integrin activation depend on the nature of the stimulus

Time course experiments were performed to determine the kinetics of LFA-1 activation in γδ T cells in response to the soluble stimuli PMA/ionomycin and HMBPP or immobilized mAbs directed against the γδ TCR (IMMU510) or the Vδ1 TCR (R9.12) together with soluble CD28 and IL-2. Rested PBMCs were stimulated at different time points so that all samples could be processed together at the end of the experiment. An increase in the percentage of m24+ cells was generally observed 10 min after exposure to the stimulus, but the kinetics of LFA-1 expression differed greatly thereafter (Figure 2). While 10 min of stimulation with PMA/ionomycin were sufficient to reach a high percentage of m24+ cells, an increase in staining intensity over time was observed for γδ as well as CD4+ and CD8+ T cells (Figure 2, Supplementary Figure 3b, Supplementary Figure 4). The response of Vδ2+ γδ T cells to HMBPP increased rapidly in the first 60 min approaching a plateau at 2 h (Figure 2c, 2d). Integrin activation in response to stimulation with immobilized antibodies was overall lower, showed higher donor variability and the m24 mAb staining was comparatively dim (Figure 2). The maximum may not have been reached at 4 h, but longer stimulation times were not feasible due to downregulation of the TCR impairing flow cytometric staining. m24 mAb staining of the unstimulated sample increased slightly over time and γδ T cells in general showed a higher background staining than CD4+ and CD8+ T cells (Supplementary Figure 5). Differences in the kinetics were to be expected due to the diversity of the applied stimuli and are in line with the results from Dimitrov et al. observing different kinetics in response to different peptides and peptide pools (1). Taken together, these results document that the functionality of γδ T cells in response to different soluble or immobilized stimuli can be readily assessed by m24 mAb staining, though the optimal stimulation time depends on the type of stimulus and mode of presentation and needs individual adjustment depending on the research question. The expression of surface proteins such as CD69, CD137 or CD154 (intra- or extracellular) and the production of cytokines are frequently used as markers for T cell activation, allowing the detection of activated γδ T cells after 2-6 h at the earliest (19-22). Because this assay is based on the conformational change of the β2 integrin LFA-1 on the cell surface, T cell activation can be assessed more rapidly. However, when studying rare populations a combination of m24 mAb staining with other markers at appropriate time points could increase sensitivity (2). Furthermore, the commonly used peptide-MHC (p-MHC) multimer staining is, with some rare exceptions (23), not applicable to γδ T cells

due to the lack of p-MHC restriction and the requirement for prior knowledge about the recognized epitopes. The m24 mAb assay therefore provides an elegant tool for straightforward flow cytometric assessment of activated or even antigen-specific γδ T cells, circumventing these limitations.

m24 mAb detects LFA-1 activation across all differentiation stages

Phenotypic markers were assessed in order to characterize Vδ1+ and Vδ2+ γδ T cells stained by the m24 mAb after 2 h stimulation with the γδ TCR mAb IMMU510. Staining of CD27, CD28 and CD45RA showed that the Vδ1 compartment of three different donors was dominated by effector memory cells re-expressing CD45RA (EMRA). Vδ1+ γδ T cells were divided into putatively naïve (CD27+CD28+CD45RA+), pooled memory (CD27+CD28+CD45RA−, CD27+CD28−, CD27−CD28+ and CD27−CD27−CD45RA−) and EMRA (CD27−CD28−CD45RA+) stages. LFA-1 activation using the m24 mAb was detected across all these differentiation stages. However, less naïve and more EMRA Vδ1+ γδ T cells were observed in the m24+ fraction (Figure 3a, Supplementary Figure 6). While Vδ1+ γδ T cells seem to follow the αβ memory differentiation model, this model most likely does not apply to the innate-like Vγ9Vδ2 subset (24, 25). Therefore, Vδ2+ γδ T cells were excluded from memory subset analysis. Staining for CD57, a potential marker of replicative senescence, revealed a significantly higher percentage ($p = 0.031$ for both subsets) of CD57+ cells in the m24+ fraction compared to the m24− fraction of Vδ1+ and Vδ2+ γδ T cells (Figure 3b). No significant association between m24 mAb staining and PD-1 expression, characteristic of a dysfunctional phenotype when continuously expressed or for T cell activation when transiently expressed (26), was observed (Supplementary Figure 7). These findings are in accordance with the results from Dimitrov et al. demonstrating detection of antigen-specific CD8+ T cells of various stages of differentiation. They observed lower percentages of naïve or early-differentiated and a higher proportion of CD8+ T cells with an intermediate or late phenotype in the ICAM-1 multimer-positive fraction in response to staphylococcus enterotoxin B or peptide stimulation (1).

Concluding Remarks

Taken together, we conclude that the m24 mAb assay detecting activated LFA-1 is suitable for the rapid assessment of functional Vδ1+ and Vδ2+ γδ T cells. This assay should emerge as a valuable tool for addressing various research questions, including high-throughput analyses of functional peripheral blood or tissue-resident γδ T cell subsets in cancer or vaccination immunomonitoring studies or for screening approaches to identify novel γδ T cell ligands.

Materials and Methods

Subjects and Samples

Peripheral blood mononuclear cells (PBMCs) were isolated by density gradient centrifugation (FicoLite®-H, LINARIS) using EDTA-anticoagulated blood from seven healthy donors (aged 25-56; 3 females and 4 males). After washing three times with Hanks′ Balanced Salt solution (Sigma-Aldrich), isolated PBMCs were cryopreserved in RPMI-1640 (Sigma-Aldrich) with 10% dimethyl sulfoxide (SERVA) and 20% fetal bovine serum (Thermo Fisher Scientific) and stored in liquid nitrogen. This study was conducted in accordance with the Declaration of Helsinki and applicable laws and regulations, has been approved by the Ethics Committees of the University of Tübingen (Project 633/2019BO2) and written informed consent was obtained from all participants.

T cell Activation

Cryopreserved PBMCs were thawed, washed twice with RPMI-1640 containing 25 U/ml Pierce™ Universal Nuclease for Cell Lysis (Thermo Fisher Scientific) and rested overnight in cell culture tubes in CTS™ OpTmizer™ T Cell Expansion Serum-Free medium (Thermo Fisher Scientific) supplemented with 2 mM L-Glutamine (Thermo Fisher Scientific) and 100 U/ml penicillin/100 µg/ml streptomycin (Sigma-Aldrich). Rested PBMCs were washed, 1 x 10^6 (or 3 x 10^6 for analysis of T cell differentiation) cells were seeded into wells of a 96-well plate (F bottom) and stimulated for 10-240 min at 37°C with 1) 20 ng/ml phorbol 12-myristate 13-acetate (PMA) (Sigma-Aldrich) and 750 ng/ml ionomycin (Merck), 2) 10 µM HMBPP (Sigma-Aldrich), 3) 1.5 µg/ml γδ TCR antibody (IMMU510, Beckman Coulter) or 1 µg/ml Vδ1 TCR antibody (R9.12, Beckman Coulter), both coated onto the plates together with 0.75 µg/ml CD28 or 5 µl/well CD28 APC (CD28.2, BD Biosciences) and 100 U/ml IL-2 (Proleukin S, Novartis). Plates were briefly centrifuged to settle cells down. When assessing intracellular cytokines, PBMCs were stimulated in the presence of 1 µl/ml brefeldin A (GolgiPlug, BD Biosciences) and 0.67 µl/ml monensin (GolgiStop, BD Biosciences).

m24 Staining and Flow Cytometry

The staining procedure was performed at room temperature. Stimulated PBMCs were transferred to a 96-well plate (U bottom) and stained with Zombie Violet (BioLegend) and anti-LFA-1 PE mAb (m24, BioLegend) for 15 min. Next, EDTA (SERVA) was added to a final concentration of 4 mM together with antibodies for staining surface markers and incubated for 15 min with CD3 BV510 (UCHT1), CD4 PE-Cy7 (OKT4), CD27 BV605 (O323), CD45RA Alexa

Fluor® 700 (HI100) and PD-1 BV711 (EH12.2H7) or the corresponding BV711 isotype control (all from BioLegend), CD8 APC-H7 (SK1), CD57 PE-CF594 (NK-1), γδ TCR BV711 or APC-R700 (11F2) (all from BD Biosciences), Vδ1 TCR FITC (REA173), Vδ2 TCR APC (123R3) (all from Miltenyi). Samples were centrifuged and the pellet was resuspended in 100 µl phosphate-buffered saline (PBS) before addition of 100 µl 2% formaldehyde (Polysciences) in PBS. Cells were fixed for 10 min. After centrifugation, samples were washed once with PBS, resuspended in PBS and acquired immediately on the flow cytometer.
For intracellular cytokine staining, fixed cells were permeabilized for 15 min using the eBioscience™ Permeabilization Buffer (Thermo Fisher Scientific) and stained for 30 min with IFN-γ PE-Cy7 (B27) and TNF Alexa Fluor® 700 (Mab11) from BioLegend. Samples were washed twice with permeabilization buffer, resuspended in PBS and analyzed immediately.

Data were acquired using a 3 laser LSR-II flow cytometer (BD Biosciences) with customized filter settings running on FACSDiva software V6.1.3 (BD Biosciences). Maximal events were collected for all samples. Single color controls were used for automatic compensation.

Data Analysis

Data analysis was performed using FlowJo V10.5.3 (BD Biosciences) following the gating strategy displayed in Supplementary Figure 1. Prism V5.04 (Graph Pad) was used for statistical analysis. Expression of differentiation markers by the m24+ and m24− populations was compared using the Wilcoxon matched-pairs signed rank test. P-Values <0.05 were considered to be statistically significant.

Data availability statement

The data supporting the findings of this study are available from the corresponding author upon reasonable request.

Author contributions

Conceptualization: NB, MWL, SD, CG, KWH

Formal Analysis: NB, KWH

Funding acquisition: KWH

Investigation: NB, AS, AF, AG, AM, SD, CG, KWH

Writing – Original Draft Preparation: NB, KWH

Writing – Review & Editing: NB, AS, AF, AM, GP, MWL, SD, CG, KWH

Acknowledgments

AS and CG are supported by the Deutsche Forschungsgemeinschaft (DFG) (CRC 1399). CG and MWL acknowledge funding by the DFG under Germany's Excellence Strategy (EXC 2180 – 390900677; Cluster of Excellence iFIT "Image-Guided and Functionally Instructed Tumor Therapies", University of Tübingen, Germany. KWH received funding from the DFG (WI 5021-21 – FOR2799) and the Medical Faculty of the University of Tübingen (2509-0-0). We thank all voluntary blood donors for their support and participation in this study. The graphical abstract was created with BioRender.com

Conflict of interest disclosure

The authors declare no conflict of interest.

References

1. Dimitrov S, Gouttefangeas C, Besedovsky L, Jensen ATR, Chandran PA, Rusch E, Businger R, Schindler M, Lange T, Born J, Rammensee HG. 2018. Activated integrins identify functional antigen-specific CD8(+) T cells within minutes after antigen stimulation. *Proc. Natl. Acad. Sci. U.S.A.* 115: E5536-E45
2. Schollhorn A, Schuhmacher J, Besedovsky L, Fendel R, Jensen ATR, Stevanovic S, Lange T, Rammensee HG, Born J, Gouttefangeas C, Dimitrov S. 2021. Integrin Activation Enables Sensitive Detection of Functional CD4(+) and CD8(+) T Cells: Application to Characterize SARS-CoV-2 Immunity. *Front. Immunol.* 12: 626308
3. Gouttefangeas C, Schuhmacher J, Dimitrov S. 2019. Adhering to adhesion: assessing integrin conformation to monitor T cells. *Cancer Immunol Immunother* 68: 1855-63
4. Walling BL, Kim M. 2018. LFA-1 in T Cell Migration and Differentiation. *Front. Immunol.* 9: 952
5. Verma NK, Kelleher D. 2017. Not Just an Adhesion Molecule: LFA-1 Contact Tunes the T Lymphocyte Program. *J. Immunol.* 199: 1213-21
6. Hogg N, Patzak I, Willenbrock F. 2011. The insider's guide to leukocyte integrin signalling and function. *Nat. Rev. Immunol.* 11: 416-26
7. Dransfield I, Hogg N. 1989. Regulated expression of Mg2+ binding epitope on leukocyte integrin alpha subunits. *EMBO J.* 8: 3759-65
8. Dransfield I, Cabanas C, Craig A, Hogg N. 1992. Divalent cation regulation of the function of the leukocyte integrin LFA-1. *J. Cell Biol.* 116: 219-26
9. Beucke N, Wesch D, Oberg HH, Peters C, Bochem J, Weide B, Garbe C, Pawelec G, Sebens S, Rocken C, Hashimoto H, Loffler MW, Nocerino P, Kordasti S, Kabelitz D, Schilbach K, Wistuba-Hamprecht K. 2020. Pitfalls in the characterization of circulating and tissue-resident human gammadelta T cells. *J. Leukoc. Biol.*
10. Vantourout P, Hayday A. 2013. Six-of-the-best: unique contributions of gammadelta T cells to immunology. *Nat Rev Immunol* 13: 88-100
11. Davey MS, Willcox CR, Hunter S, Kasatskaya SA, Remmerswaal EBM, Salim M, Mohammed F, Bemelman FJ, Chudakov DM, Oo YH, Willcox BE. 2018. The human Vdelta2(+) T-cell compartment comprises distinct innate-like Vgamma9(+) and adaptive Vgamma9(-) subsets. *Nat Commun* 9: 1760
12. Davey MS, Willcox CR, Joyce SP, Ladell K, Kasatskaya SA, McLaren JE, Hunter S, Salim M, Mohammed F, Price DA, Chudakov DM, Willcox BE. 2017. Clonal selection in the human Vdelta1 T cell repertoire indicates gammadelta TCR-dependent adaptive immune surveillance. *Nat Commun* 8: 14760
13. Karunakaran MM, Willcox CR, Salim M, Paletta D, Fichtner AS, Noll A, Starick L, Nohren A, Begley CR, Berwick KA, Chaleil RAG, Pitard V, Dechanet-Merville J, Bates PA, Kimmel B, Knowles TJ, Kunzmann V, Walter L, Jeeves M, Mohammed F, Willcox BE, Herrmann T. 2020. Butyrophilin-2A1 Directly Binds Germline-Encoded Regions of the Vgamma9Vdelta2 TCR and Is Essential for Phosphoantigen Sensing. *Immunity* 52: 487-98 e6
14. Rigau M, Ostrouska S, Fulford TS, Johnson DN, Woods K, Ruan Z, McWilliam HEG, Hudson C, Tutuka C, Wheatley AK, Kent SJ, Villadangos JA, Pal B, Kurts C, Simmonds J, Pelzing M, Nash AD, Hammet A, Verhagen AM, Vairo G, Maraskovsky E, Panousis C, Gherardin NA, Cebon J, Godfrey DI, Behren A, Uldrich AP. 2020. Butyrophilin 2A1 is essential for phosphoantigen reactivity by gammadelta T cells. *Science* 367
15. Deseke M, Prinz I. 2020. Ligand recognition by the gammadelta TCR and discrimination between homeostasis and stress conditions. *Cell. Mol. Immunol.*
16. Siegers GM. 2018. Integral Roles for Integrins in gammadelta T Cell Function. *Front Immunol* 9: 521

17. Wang P, Malkovsky M. 2000. Different roles of the CD2 and LFA-1 T-cell co-receptors for regulating cytotoxic, proliferative, and cytokine responses of human V gamma 9/V delta 2 T cells. *Mol. Med.* 6: 196-207
18. Nakajima S, Roswit WT, Look DC, Holtzman MJ. 1995. A Hierarchy for Integrin Expression and Adhesiveness among T-Cell Subsets That Is Linked to Tcr Gene Usage and Emphasizes V-Delta-1(+) Gamma-Delta T-Cell Adherence and Tissue Retention. *J. Immunol.* 155: 1117-31
19. Pei YJ, Wen K, Xiang Z, Huang CY, Wang XW, Mu XF, Wen LY, Liu YP, Tu WW. 2020. CD137 costimulation enhances the antiviral activity of V gamma 9V delta 2-T cells against influenza virus. *Signal Transduct Target Ther* 5
20. Kunzmann V, Bauer E, Feurle J, Weissinger F, Tony HP, Wilhelm M. 2000. Stimulation of gammadelta T cells by aminobisphosphonates and induction of antiplasma cell activity in multiple myeloma. *Blood* 96: 384-92
21. Dessarth B, Thedrez A, Latouche JB, Cabillic F, Drouet A, Daniel P, de la Pintiere CT, Catros V, Toutiraisx O. 2013. CRTAM Receptor Engagement by Necl-2 on Tumor Cells Triggers Cell Death of Activated V gamma 9V delta 2 T Cells. *J. Immunol.* 190: 4868-76
22. Horner AA, Jabara H, Ramesh N, Geha RS. 1995. gamma/delta T lymphocytes express CD40 ligand and induce isotype switching in B lymphocytes. *J. Exp. Med.* 181: 1239-44
23. Benveniste PM, Roy S, Nakatsugawa M, Chen ELY, Nguyen L, Millar DG, Ohashi PS, Hirano N, Adams EJ, Zuniga-Pflucker JC. 2018. Generation and molecular recognition of melanoma-associated antigen-specific human gammadelta T cells. *Sci. Immunol.* 3
24. Xu W, Monaco G, Wong EH, Tan WLW, Kared H, Simoni Y, Tan SW, How WZY, Tan CTY, Lee BTK, Carbajo D, K GS, Low ICH, Mok EWH, Foo S, Lum J, Tey HL, Tan WP, Poidinger M, Newell E, Ng TP, Foo R, Akbar AN, Fulop T, Larbi A. 2019. Mapping of gamma/delta T cells reveals Vdelta2+ T cells resistance to senescence. *EBioMedicine* 39: 44-58
25. Xu WL, Larbi A. 2017. Markers of T Cell Senescence in Humans. *Int J Mol Sci* 18: 1742
26. Jubel JM, Barbati ZR, Burger C, Wirtz DC, Schildberg FA. 2020. The Role of PD-1 in Acute and Chronic Infection. *Front. Immunol.* 11: 487

Figures

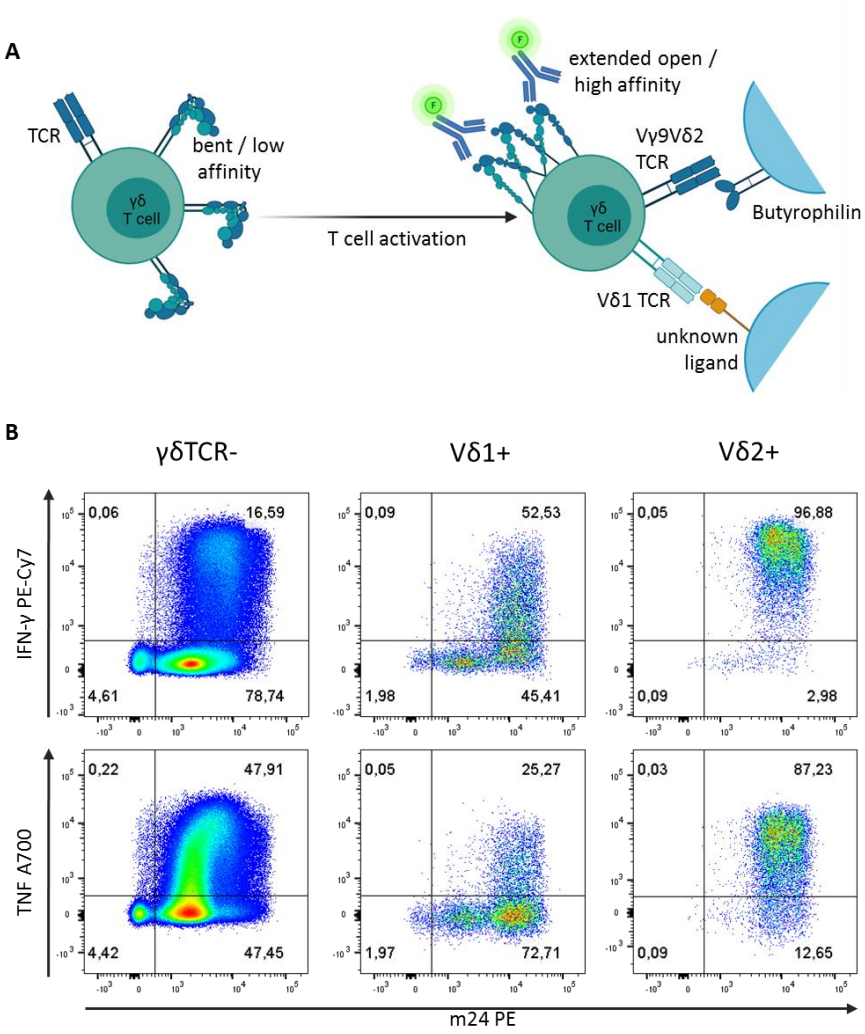

Figure 1: Integrin activation allows assessment of functional γδ T cells. (a) Upon T cell activation, a conformational change of the β2 integrin LFA-1 occurs. The high-affinity conformation of LFA-1 can be specifically detected by the mAb clone m24. Ligands of the γδ TCR are largely unknown. Figure 1(a) was created with BioRender.com. **(b)** Cytokine expression in m24+ γδ T cells and non-γδ T cells. Rested PBMCs were stimulated for 4 h with PMA/ionomycin. Pseudocolor plots show expression of activated LFA-1 detected by the m24 mAb, IFN-γ and TNF in γδTCR−, γδTCR+Vδ1+ and γδTCR+Vδ2+ CD3+ T cells. Numbers indicate frequencies among the respective T cell subset. For each γδ T cell subset one representative donor out of three is shown.

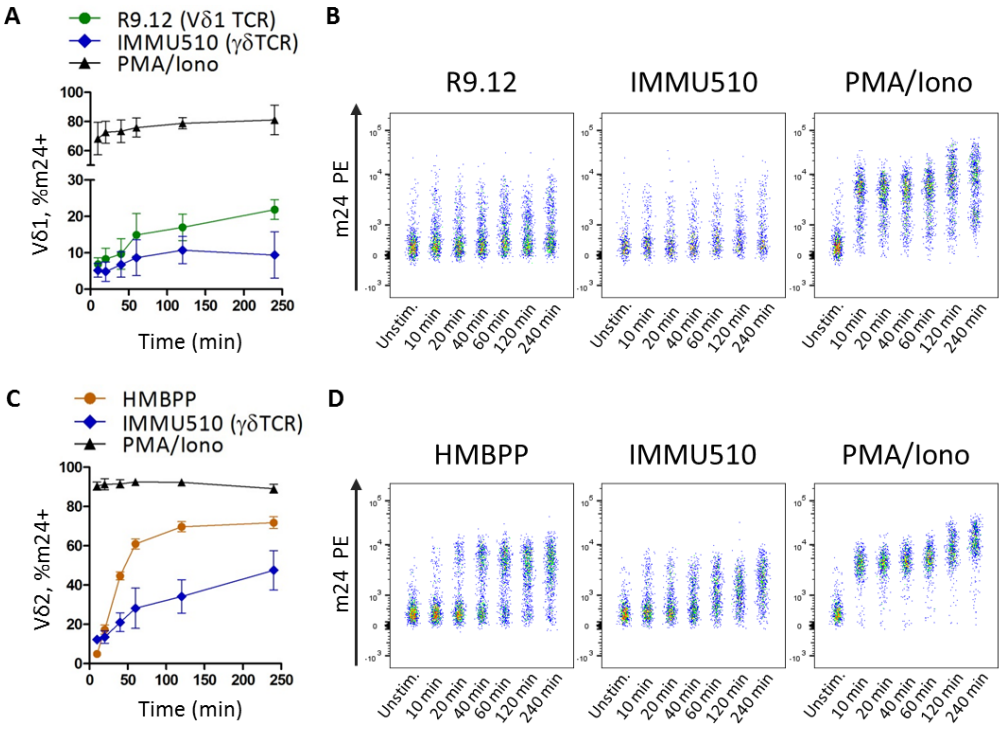

Figure 2: Time course of activated LFA-1 detected with m24 mAb staining. Rested PBMCs were stimulated for 10-240 min with PMA/ionomycin, HMBPP, or immobilized mAbs against the γδ TCR (clone IMMU510) or the Vδ1 TCR (clone R9.12) (both combined with a soluble anti-CD28 mAb and IL-2). **(a/c)** Percentage of m24+ cells among Vδ1+ **(a)** or Vδ2+ **(c)** γδ T cells obtained from three donors are shown (mean +/− SEM). Background from the corresponding unstimulated sample was subtracted. **(b/d)** Concatenated pseudocolor plots depict m24 mAb staining of Vδ1+ **(b)** and Vδ2+ **(d)** γδ T cells after 10, 20, 40, 60, 120 and 240 min of stimulation. The unstim. sample illustrates the background at the first timepoint. One representative donor out of three is shown.

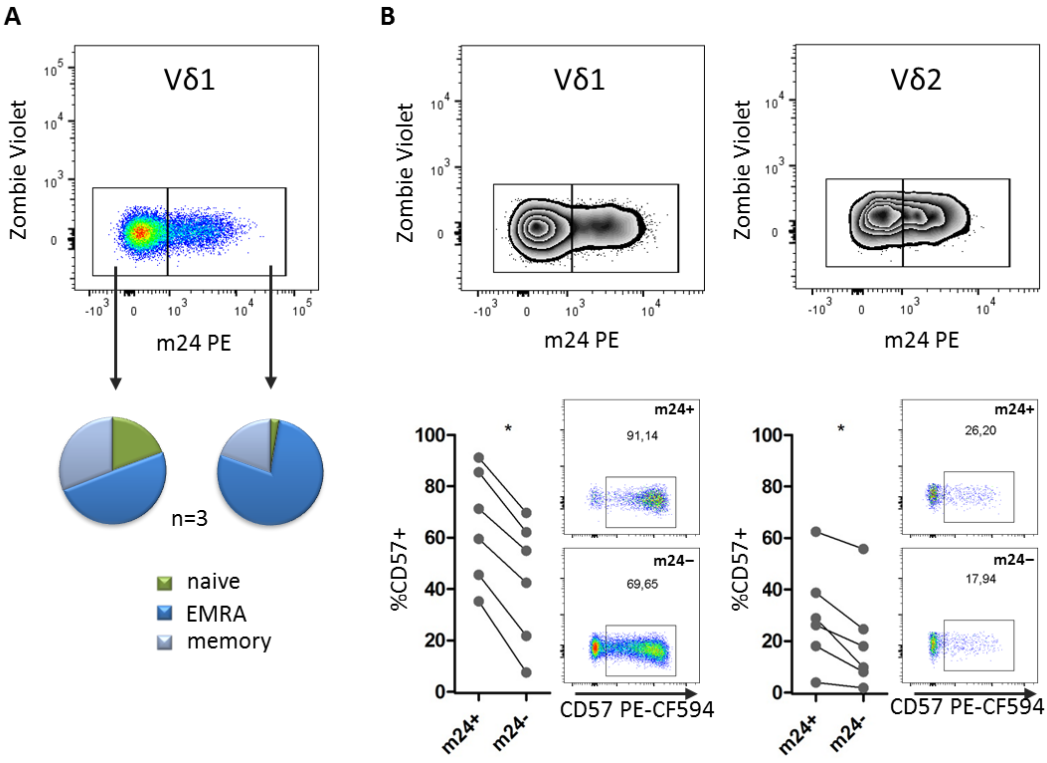

Figure 3: Expression of differentiation markers on γδ T cells with regard to LFA-1 activation. Rested PBMCs were stimulated for 2 h with the γδTCR mAb IMMU510 together with CD28 and IL-2. **(a)** The m24+ and m24− fractions of Vδ1+ γδ T cells were divided into naïve, memory and EMRA cells based on the expression of the differentiation markers CD27, CD28 and CD45RA. Pie charts represent the mean percentage of these subsets among three donors. **(b)** CD57 expression in the m24+ and m24− fractions of Vδ1+ and Vδ2+ γδ T cells was assessed in six donors. Pseudocolor and zebra plots show one representative donor. Statistical evaluation was performed using the Wilcoxon matched-pairs signed rank test. * $P < 0.05$.

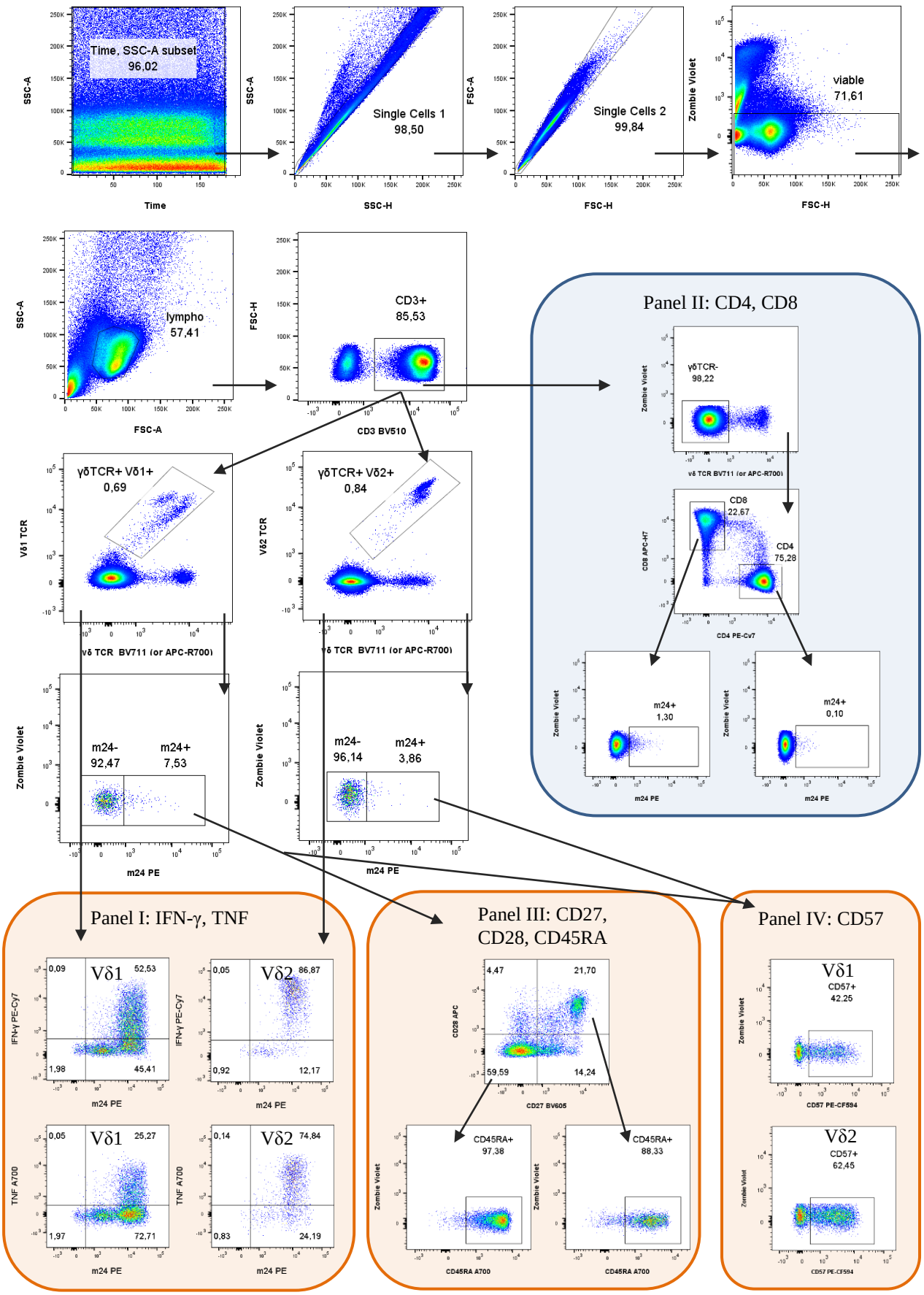

Supplementary Figure 1

Gating strategy. Data from one representative subject illustrates the general gating strategy. Different subjects are shown for the different panels.

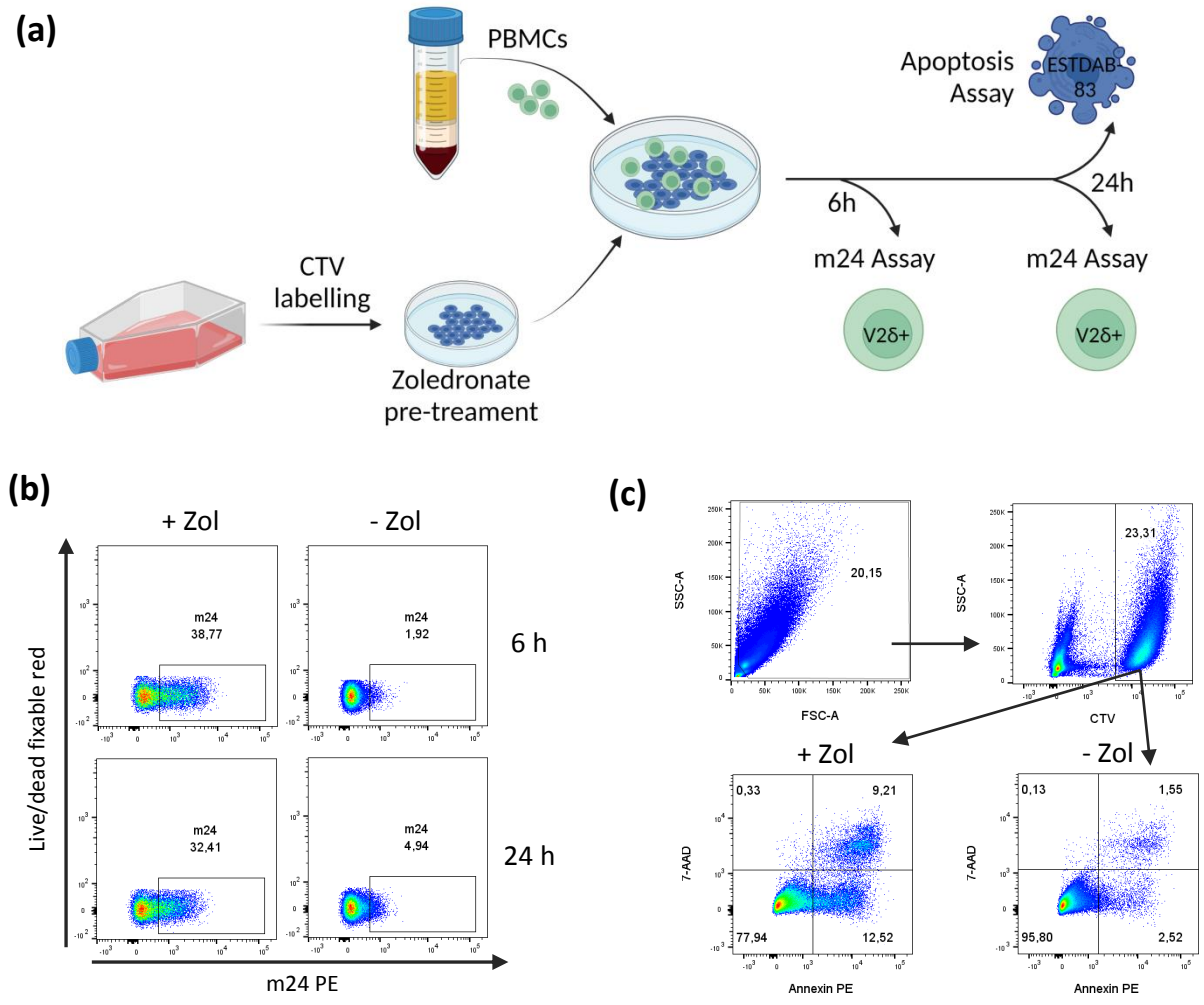

Supplementary Figure 2

(a) The melanoma cell line ESTDAB-83 was labelled with CellTrace Violet and incubated with 5 µM zoledronate overnight. ESTDAB-83 cells and PBMCs were co-cultured for 6 h or 24 h. Activation of T cells was assessed using the m24 mAb assay. Cell death and apoptosis were detected using the PE Annexin V Apoptosis Detection Kit I from BD. **(b)** Pseudocolor plots depict the percentage of m24+ Vδ2+ γδ T cells in zoledronate-treated and untreated samples after 6 h and 24 h of co-culture. **(c)** Debris and small cells were excluded, next ESTDAB-83 cells were identified based on CellTrace Violet staining. The percentage of dead (7-AAD+Annexin+) and apoptotic (7-AAD-Annexin+) cells in the zoledronate-treated sample compared to the untreated sample was examined after 24 h of co-culture. Supplementary Figure 2a was created with BioRender.com.

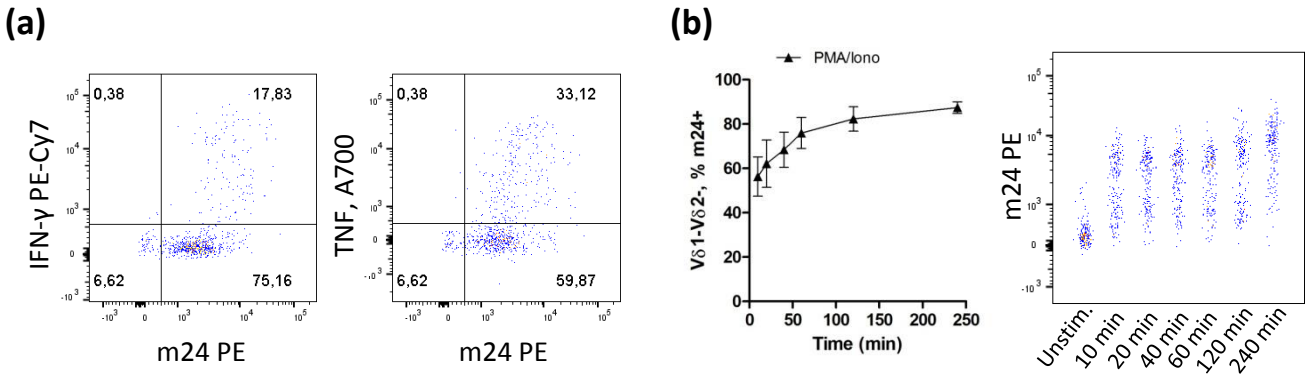

Supplementary Figure 3

Expression of activated LFA-1 on Vδ1−Vδ2− γδ T cells. **(a)** Cytokine Expression of m24+ Vδ1−Vδ2− γδ T cells. Rested PBMCs were stimulated for 4 h with PMA/ionomycin. Pseudocolor plots show expression of m24, IFN-γ and TNF. Numbers indicate frequencies amongst Vδ1−Vδ2− γδ T cells. **(b)** Time course of activated LFA-1 staining in response to stimulation with PMA/ionomycin. Graph plot illustrates results from three different donors (mean +/− SEM). Background from the corresponding unstimulated sample was subtracted. Concatenated pseudocolor plot depicts m24 mAb staining of one representative donor after 10, 20, 40, 60, 120 and 240 min of stimulation.

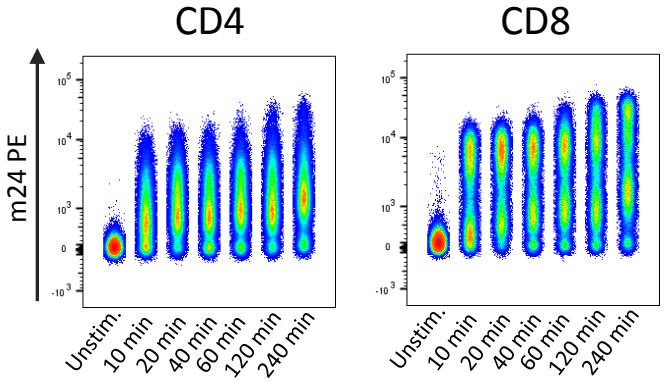

Supplementary Figure 4

Time course of activated LFA-1 staining of CD4+ and CD8+ T cells in response to stimulation with PMA/ionomycin. Concatenated pseudocolor plots depict m24 mAb staining of CD4+ or CD8+ T cells after 10, 20, 40, 60, 120 and 240 min of stimulation. One representative donor is shown.

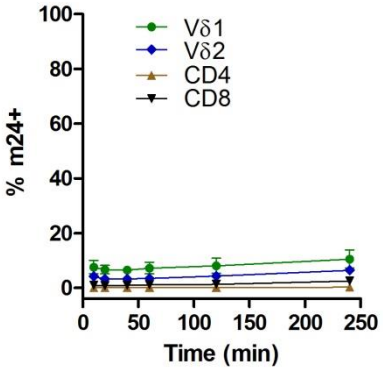

Supplementary Figure 5

Time course of m24 mAb staining of the unstimulated sample. Results for Vδ1+ and Vδ2+ γδ T cells, and CD4+ and CD8+ T cells from three different donors (mean +/− SEM) after 10, 20, 40, 60, 120 and 240 min are shown.

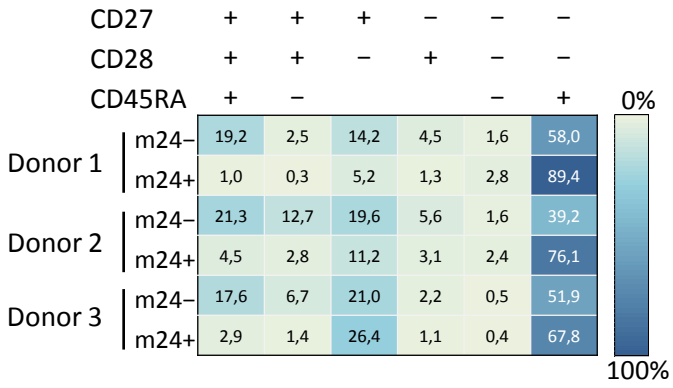

Supplementary Figure 6
Expression of differentiation markers on Vδ1+ γδ T cells with regard to LFA-1 activation. Rested PBMCs were stimulated for 2 h with the γδTCR mAb IMMU510. Columns represent the differentiation phenotypes based on the combined expression of CD27, CD28 and CD45RA. Frequencies of the respective phenotypes are color coded. The m24− and m24+ subset of three donors is shown.

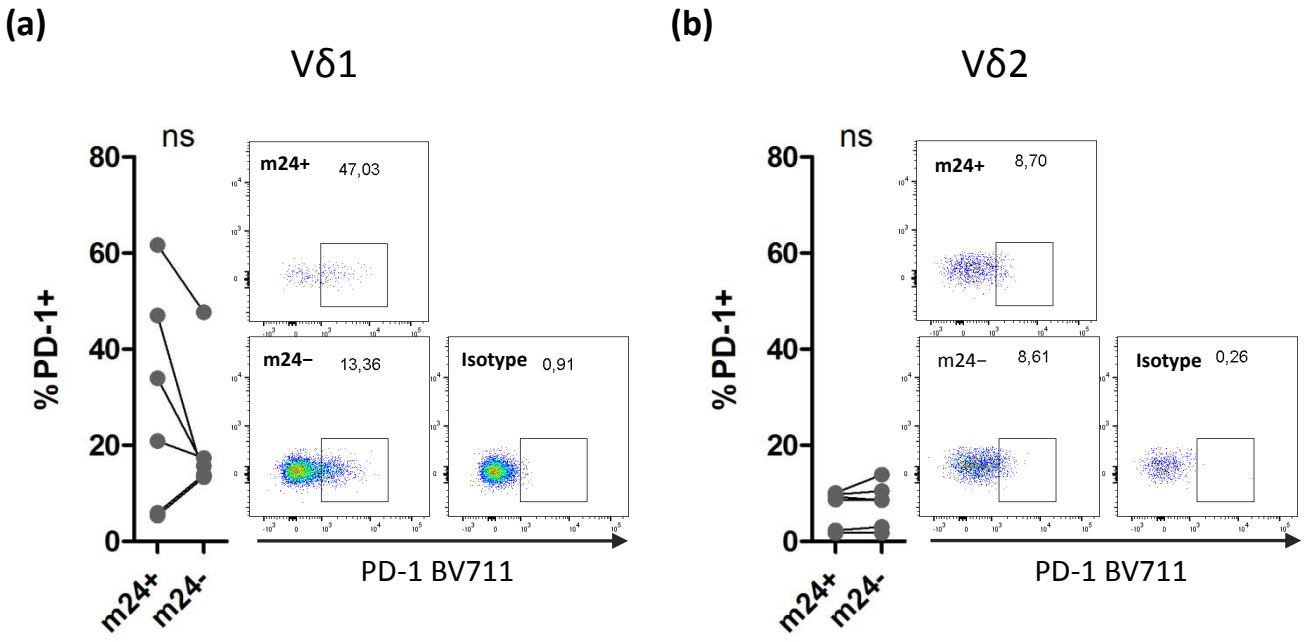

Supplementary Figure 7
Expression of PD-1 on γδ T cells with regard to LFA-1 activation. Rested PBMCs were stimulated for 2 h with the γδTCR mAb IMMU510. PD-1 expression in the m24+ and m24− fraction of Vδ1+ **(a)** and Vδ2+ **(b)** γδ T cells was assessed in six donors. Pseudocolor plots show one representative donor. Statistical evaluation was performed using the Wilcoxon matched-pairs signed rank test. ns, not significant.

High-dimensional *in situ* proteomics imaging to assess γδ T cells in spatial biology

Nicola Herold[1,2], Matthias Bruhns[1,2,3,4], Sepideh Babaei[1,2,3,4], Janine Spreuer[1,2], Arianna Castagna[5], Can Yurttas[5], Sophia Scheuermann[6,7], Christian Seitz[6,7], Benjamin Ruf[1,2,7], Alfred Königsrainer[5], Philipp Jurmeister[8,9], Markus W. Löffler[5,7,10,11,12]*, Manfred Claassen[1,2,3,4]*, Kilian Wistuba-Hamprecht[1,2,10,12]*
*shared authorship

1. Department of Internal Medicine I, University Hospital Tübingen, Eberhard Karls University of Tübingen, Tübingen, Germany
2. M3 Research Center for Malignome, Metabolome and Microbiome, Faculty of Medicine University Tübingen; Tübingen, Germany
3. Department of Computer Science, Eberhard Karls University of Tübingen, Tübingen, Germany
4. Institute of Biomedical Informatics, University Hospital Tübingen, Eberhard Karls University of Tübingen, Tübingen, Germany
5. Department of General, Visceral and Transplant Surgery, University Hospital Tübingen, Tübingen, Germany
6. Department of Pediatric Hematology and Oncology, University Hospital Tübingen, Tübingen, Germany
7. Cluster of Excellence iFIT (EXC 2180) "Image-Guided and Functionally Instructed Tumor Therapies" Tübingen, Germany
8. Institute of Pathology, Ludwig Maximilians University Hospital Munich, Munich, Germany
9. German Cancer Consortium (DKTK), Partner Site Munich, and German Cancer Research Center (DKFZ), Heidelberg, Germany
10. Department of Immunology, Interfaculty Institute for Cell Biology, Eberhard Karls University Tübingen, Tübingen, Germany
11. Institute for Clinical and Experimental Transfusion Medicine, Medical Faculty of Tübingen, University Hospital Tübingen, Tübingen, Germany
12. German Cancer Consortium (DKTK), Partner Site Tübingen, and German Cancer Research Center (DKFZ), Heidelberg, Germany

This is a pre-copyedited, author-produced version of an article accepted for publication in the Journal of Leukocyte Biology following peer review. The version of record: Nicola Herold, Matthias Bruhns, Sepideh Babaei, Janine Spreuer, Arianna Castagna, Can Yurttas, Sophia Scheuermann, Christian Seitz, Benjamin Ruf, Alfred Königsrainer, Philipp Jurmeister, Markus W Löffler, Manfred Claassen, Kilian Wistuba-Hamprecht, High-dimensional in situ proteomics imaging to assess γδ T cells in spatial biology, Journal of Leukocyte Biology, 2024, is available online at: https://doi.org/10.1093/jleuko/qiad167.

Short running title: Multiplexed imaging of γδ T cell microenvironment

Key words: Techniques: Proteomics, General: Cancer, General: Adaptive Immunity, Cells: T Lymphocytes, General: Oncology

Corresponding author:
Kilian Wistuba-Hamprecht
Section for Clinical Bioinformatics
First Department of Internal Medicine
University Hospital Tübingen
72072 Tübingen, Germany
Mail: kilian.wistuba-hamprecht@uni-tuebingen.de

Abstract

This study presents a high-dimensional immunohistochemistry approach to assess human γδ T cell subsets in their native tissue microenvironments at spatial resolution, a hitherto unmet scientific goal due to the lack of established antibodies and required technology. We report an integrated approach based on multiplexed imaging and bioinformatic analysis to identify γδ T cells, characterize their phenotypes, and analyze the composition of their microenvironment. Twenty-eight γδ T cell microenvironments were identified in tissue samples from fresh frozen human colon and colorectal cancer where interaction partners of the immune system but also cancer cells were discovered in close proximity to γδ T cells, visualizing their potential contributions to cancer immunosurveillance.

While this proof-of-principle study demonstrates the potential of this cutting-edge technology to assess γδ T cell heterogeneity and to investigate their microenvironment, future comprehensive studies are warranted to associate phenotypes and microenvironment profiles with features such as relevant clinical characteristics.

Introduction

Unraveling the largely unknown functions and the spatial organization and coordination of the heterogeneous human γδ T cell subsets within their natural surroundings - the tissue microenvironment - remains an unmet scientific goal so far (1).

We addressed this challenge already at the FOR2799 meeting in Erlangen 2019 and identified the lack of available γδ T cell receptor (TCR)-specific antibodies, enabling immunohistochemistry (IHC) in formalin fixed paraffin embedded (FFPE) tissues, as a major bottleneck hindering the progress in this context (2). After the pan γδ TCR clone g3.20 was lost, Jungbluth et al. showed that clone H-41 can also be used to stain FFPE tissue sections (3). The latter has meanwhile become the accepted standard in the field for detecting γδ T cells in one dimensional IHC analyses (4). Analyses of γδ T cell subsets can be performed using antibodies specific for Vγ9 and/or Vγ2/3/4 – usually paired with Vδ2 negative TCRs – in FFPE tissue as for example Kabelitz and Wesch et al. have documented (5-7). Multiparametric investigations of γδ T cells are currently limited to fluorescence-based IHC, as for example recently described by Da Gama Duarte et al., who applied a pan γδ TCR-specific antibody, combined with six additional markers on a single FFPE tissue slide to investigate these unconventional T cells in the context of their surrounding tissue structures (8). However, when aiming for in-depth characterization of the γδ T cell tissue microenvironment (TiME) at cellular level, dozens of additional markers are required to cover characteristics of epithelial and endothelial cells, blood and lymphatic vessels, extracellular matrix components and tissue resident or infiltrating immune cells, as well as their functionally diverse subsets. In addition, for a satisfactory characterization of γδ T cell subsets, specific antibodies against CD45, CD3, pan-γδ TCR should be considered, followed by a separation of this heterogeneous population by the selected TCR γδ chains Vδ1, Vδ2 and Vγ9 to cover the major subsets. Such an endeavor is only feasible using a high-dimensional imaging approach as presented here but currently remains restricted to analyses of fresh frozen tissues, due to the lack of established antibodies. Furthermore, the here presented approach is complemented by suitable image pre-processing and unbiased bioinformatic analysis.

Methods

Patients and Tissues

Fresh frozen tissue samples from patients were obtained in the context of elective surgery performed at the Department of General, Visceral and Transplant Surgery at the University Hospital Tübingen. Respective tissue samples comprised both tissues with malignant

features as well as adjacent benign tissues, which were considered irrelevant for diagnostic purposes by the concerned pathologist.

Fresh tissue samples were transferred to the laboratory in RPMI-1640 medium (Sigma), washed with PBS (Sigma) and dissected into suitable pieces for later use of MACSwell Four Imaging Frames (Miltenyi). Respective tissue pieces were embedded in Tissue-Tek Cryomolds (Sakura) using tissue freezing medium (Leica). The latter were transferred into an aluminum pan containing pre-cooled 99% ethanol, which was then positioned closely above the surface of liquid nitrogen for controlled freezing of the tissue sample. Samples were stored at -80 °C until usage.

All patients included in this study gave their written informed consent for biobanking and use of biomaterials as well as clinical data for scientific evaluation. This project was approved by the local institutional review board at the University Hospital Tübingen (Project Numbers 508/2016BO1 and 280/2022BO2) and conforms with the principles of the Declaration of Helsinki and local laws and regulations.

High dimensional *in situ* proteomics imaging

Frozen tissue samples were cryo-sectioned in 5 µm thick slices (Leica cryocut CM3050S, Leica, Nussloch, Germany) as previously described (9). The glass slides (SuperFrost Plus, Langenbrinck), each containing 4 sections (two from tumor tissue and two from adjacent benign tissue), were dried at room temperature and then stored at -80 °C until further preparation. Serial sections were prepared for each sample, which were used i) for H&E staining for pathohistological evaluation and assignment of regions of interest (ROIs) and ii) for high dimensional *in situ* proteomics imaging. A NanoZoomer 2.0-HT digital slide scanner (Hamamatsu) was used to scan the H&E-stained tissues, followed by digital annotation of the ROIs via NDP.view 2 (Hamamatsu) by a pathologist. For the preparation of the high dimensional *in situ* proteomics imaging, the tissue-bearing glass slides were taken out of the freezer and immediately placed in MACSwell Four Imaging Frames (Miltenyi). Next, samples were fixed using 4% paraformaldehyde solution for 10 minutes at room temperature, followed by two washing steps using MACSima running buffer (Miltenyi). Before the start of the MACSima Imaging Staining (MICS) runs, each sample was pre-stained using a final concentration of 1 µg/mL of the nuclear stain 4',6-diamidino-2-phenylindole (DAPI) (Miltenyi) for 10 minutes at room temperature in the dark, followed by three washing steps using MACSima running buffer (Miltenyi).

The prepared tissue samples and a 96 well plate containing master mixes of a maximum of 3 antibodies in previously determined concentrations were placed in the MACSima device V1.5.0 for fully automated imaging. An Fcγ receptor blocking agent (Miltenyi) was used in the antibody master mixes of all cycles in which hybridoma antibodies were used to reduce

unspecific binding. The ROIs annotated on scans of H&E-stained serial sections were manually transferred to the DAPI overview scan of the tissue samples generated by the MACSima. Then the fully automated MICS run was started. In brief, first a background/autofluorescence image was recorded per channel (FITC, APC & PE), followed by photobleaching and acquisition of a bleached background image. Next, the first staining was performed using the first master mix from the 96 well plate. This staining was imaged, followed by a bleaching step to remove the signal of the previously used fluorochrome-conjugated antibodies. After bleaching, another image was acquired to determine the remaining background signal before the next staining cycle was started. Since DAPI is used during data processing to register the acquired images, every 4th cycle was used to re-stain with a 0.05 µg/mL DAPI solution.

Raw data processing and image generation

For analyses of the performed MACSima measurements of a single, 5 µm thick tissue section per sample, the raw image files were pre-processed using MACSiQ software V1.1.0 (Miltenyi). The individually recorded "field of views" were stitched together to form the imaged ROI, the individual images of the different cycles were registered, the background signal remaining after each bleach cycle was subtracted from the following cycle and the chromatic shift was corrected. The staining quality was then assessed per sample for artifacts and implausible patterns within the MACSiQ software. For examination of the identified γδ T cells circular neighborhoods with a diameter of 600 px (equals 0.1278 mm; supplementary Figure 1) were assigned manually and cell segmentation was performed based on the DAPI staining as well as on those of TCR Vδ1, TCR Vδ2, CD3, CD45, CD326, Vimentin, Cytokeratin and HLA-A/B/C. Next, grayscale values of all markers for each identified cell were exported for subsequent bioinformatic analysis.

All visualizations of the IHC images shown in this manuscript were generated with the MACSiQ software.

Cell type annotation and visualization

We applied the single-cell analysis framework Scanpy (version 1.9.3.) (10) to analyze the segmented cells. We used the functions' default settings, unless stated differently. First, we applied the log(x+1) transformation for variance stabilization. In the following, we scaled the data to have a mean of zero and a variance of one. Principal components were calculated (n_comps=30), and we used the Harmony batch effect correction (11) on these components. We clustered the resulting data using the Leiden algorithm (12) with different resolution settings for cell type annotation. Additionally, for each clustering, we calculated differently

expressed markers (method=wilcoxon, use_raw=True) on the unscaled marker expression. Based on manual inspection of both median expressions per cluster and differently expressed markers, we selected resolution=1.7 for cluster annotation. We generated the clustermaps using the Seaborn library (version 0.12.2) (13) with method='average' and metric='correlation'. The scaling for all protein expression clustermaps was derived from the range of expression shown in supplementary Figure 2.

Single cell RNA expression analyses

To validate our γδ T phenotypes identified by MACSima staining and for further in-depth analysis, we have considered single-cell sequencing (scRNAseq) data. This approach allows us to investigate expression levels of the corresponding genes matching our proteomic profiling. For this purpose, we have re-analyzed three independent, publicly available scRNA-seq datasets across different disease entities. The first dataset, published by Ruf et al. (14), comprises of CD45+ sorted cells from a study in hepatocellular carcinomas (HCC). The other two datasets consist of sorted γδ T cells from studies in colorectal cancer (CRC) published by Harmon et al. and de Vries et al. (15, 16), respectively.

To detect γδ T cells from the HCC dataset, we applied filters for Vδ1+ and Vγ 9+/Vδ2+ cells. Since the other datasets were already sorted for γδ T cells, no additional filtering was necessary. For quality control purposes, we took the following steps: cells with less than 200 measured genes were removed, genes that were present in less than 3 cells were removed, cells in which the percentage of counts in mitochondrial genes was above 15% were removed, gene counts were normalized to 10,000, and finally, log1p-transformation was applied for variance stabilization. All scRNAseq analysis was conducted using Scanpy 1.9.3 (10).

Results and Discussion

Here, we aimed at the identification and establishment of TCR γδ-specific antibody clones in a high-dimensional *in situ* proteomics imaging approach enabling the future elucidation of the multifactorial roles that γδ T cells might play in tissues. To achieve this goal, we selected 4 out of 17 tested commercially available TCR γδ-specific antibody clones and implemented them in our imaging pipeline to (i) identify γδ T cells in their tissue context, (ii) characterize the same tissue context in-depth and (iii) initiate development of computational methodology to characterize their cell type composition.

Visualization of tissue infiltrating γδ T cells

We suggest four selected commercially available antibodies that can be used in human fresh frozen tissue sections to identify γδ T cells for subclassification into the major TCR Vδ1+ and TCR Vγ9+Vδ2+ subsets to enable high-dimensional investigations of these cells in their spatial neighborhood. Therefore, we first tested 7 pan-γδ TCR antibodies (clones B1, B1.1, IMMU510, TS8.2, 11F2, 5A6E91 and TS-1) and identified that clones B1 and B1.1 revealed an unspecific staining pattern of tissue structures in addition to the γδ TCR. A low signal to noise ratio was achieved using the clones 11F2, REA591 and IMMU510 and sequential staining experiments using the TS-1 clone after a Vγ9 antibody revealed only staining of γδ T cells not carrying the Vγ9 chain in their TCR, potentially caused by steric hinderances. We have previously described such limited access to epitopes in the γδ TCR complex when using multiple TCR chain-specific antibodies in flow cytometric experiments (2, 17, 18). Clone 5A6.E9 performed best in our hands for use in high-dimensional *in situ* proteomics imaging, even though it also showed some non-specific staining artifacts, but these were well distinguishable from specifically stained cells (Figure 1 A).

Due to different functionalities and heterogeneity of the γδ T cell compartment, a distinction must be made between the more innate-like TCR Vγ9+Vδ2+ and the more adaptive-like TCR non-Vγ9Vδ2 γδ T cells (19). For the identification of TCR Vδ2+ cells we tested 4 antibody clones (IMMU389, 123R3, REA771 and B6), all of which showed good staining patterns. Clone B6 only binds TCR Vγ9+Vδ2+ cells (20) and was therefore excluded from our analyses. Clone 123R3 revealed slightly dimmer signals as IMMU389 and REA771, which performed best in our hands (Figure 1 B). Combined detection of the Vδ2 and Vγ9 chains allow for the identification of γδ T cell subsets described as expressing semi-invariant TCR repertoires (20), classically considered innate-like and stress-reactive (via the butyrophilin A (BTNA) axis) (21, 22). To this end, we tested 4 antibody clones recognizing TCR Vγ9 (7A5, IMMU360, B3, REA470) and identified 7A5 as unsuitable for IHC using fresh frozen tissues. Clone REA470 revealed a low signal to noise ratio compared to IMMU360 and B3 that performed best in our hands (Figure 1 C).

The major subset of TCR non-Vγ9Vδ2 adaptive-like γδ T cells is usually TCR Vδ1+, and difficult to identify when using the 3 commercially available clones tested here (REA173, TS8.2 and R9.12). Clone REA173 revealed no signal at all, R9.12 was indirectly detected via a secondary anti IgG Fc antibody and showed only a weak signal, while TS8.2 performed best. Nevertheless, this clone also shows unspecific staining patterns and background noise, which could be satisfactorily separated from the specific staining in our high-dimensional analysis approach (Figure 1 D). Pairing of the Vδ1 with the Vγ9 chain has been previously described (23, 24) and can also be visualized (Supplementary Figure 3).

Taken together, for our high-dimensional *in situ* proteomics imaging approach we use clone 5A6.E9 as a TCR γδ-pan marker, clone REA771 to identify TCR Vδ2+, clone B3 to mark TCR Vγ9+ and clone TS8.2 to stain TCR Vδ1+ γδ T cells. These antibodies were successfully used to detect γδ T cell subsets in tissue sections from fresh frozen adenoid and colon samples, as well as from CRC and pancreatic cancer, cholangiocarcinoma, and metastatic cancers (intrahepatic tumors and lymph node metastases from HCC and cholangiocarcinoma as well as liver metastases from a jejunal neuroendocrine tumor) (data not shown).

Determination of the γδ T cell tissue microenvironment via *in situ* proteomics imaging

Next, we aimed at the establishment of γδ TCR-specific antibodies in a high-dimensional *in situ* proteomics imaging workflow, using Miltenyis' MACSima platform. Therefore, we combined the identified γδ TCR antibodies with a high-dimensional marker panel allowing us to visualize the extracellular matrix, epithelial and endothelial cells, myocytes, lymphoid tissues and vasculature, but also key lineage markers for major immune cells as well as markers for differentiation, activation and senescence in a single tissue section. The antibody panel presented here includes 54 markers and was established on healthy human adenoid and colon tissue as well as on malignant tissue (CRC) (Figure 2). We aim to apply this panel in future comprehensive investigations of the TiME and respective immune cell infiltrates, with a special focus on cancer immunosurveillance. All markers used here were identified based on our own preliminary work (2, 17, 18, 25), as well as literature search and exchange with colleagues. In addition, most of the antibody clones used here have recently been validated for the MACSima platform and published (26), so that a *de novo* establishment of these markers was not required. Nevertheless, and to the best of our knowledge, these and all other markers were subjected to strict quality control measures, which took into account cell morphology and distribution patterns of the respective signal within an individual cell, as well as the signal distribution patterns and intensity in the entire examined region of interest (ROI), for example using databases like the human protein atlas as a reference (www.proteinatlas.org).

Challenges and pitfalls of high-dimensional *in situ* proteomics imaging

Limitations of fluorescence-based IHC can also be found in the here applied MICS technology. For example, the quality of sample preparation, e.g., the thickness of tissue sections or the wrinkle- and fold-free mounting onto the glass slide are important aspects when evaluating the individual cell phenotypes and the tissue morphology. Membrane

artifacts of cells whose nucleus may be located above or below the plane of the investigated section may cause confusing signals that could be incorrectly attributed to neighboring cells. Background signal, caused by e.g. unspecific binding of antibodies to cell surface proteins or other tissue structures, requires careful inspection of the acquired signal intensities and distributions. An example of counterintuitively overlapping signals of IgD- and CD3-specific antibodies in B and T cell dense tissue regions, illustrated in supplementary Figure 4, underlines the need for the incorporation of further lineage-specific markers to assign each individual cell to its correct compartment. However, CD20+ T cells and CD3+ B cells have been described occasionally. This might be explained by the transfer of plasma membrane segments via trogocytosis, as no correlating gene expression profile could be associated (27-29). Assessment of transcription factor expression like the T cell-specific TOX and TCF-1 and the B cell-specific PAX-5, that are not subjected to trogocytosis, might be useful to unambiguously identify cells belonging to either of the two lineages. However, the surface marker expression of these cells might still be considered with caution as we currently cannot confidently identify whether they derive from the transcription machinery of the "expressing" or from a neighboring cell.

Although, this might not pose a major problem in low-dimensional analyzes since visual inspection is possible for a low number of markers and easily reveals artifactual marker combinations on the basis of the spatial signal distribution, it is a challenge in automated, unbiased signal analyzes. These typically do not account for spatial distribution signal patterns related to unspecific binding, and therefore result in cell type definitions with artifactual marker combinations.

Future automatic analysis approaches might include modules accounting for spatial signal patterns characteristic for eliminating technical artifacts.

However, problems shared between fluorescence-based IHC and MICS technology are for example the aggregation of antibodies that can cause random and unspecific signals on the tissue section or in the worst case may stain non-specific tissue structures. Tissue-specific shielding of antibody binding to certain proteins was unfortunately also observed by us in human colon tissue for the fluorophore-tagged lineage markers CD4 or CD20 that performed well in other tissues but did not in colon tissue, thus indicating the need for adaptation of high-dimensional antibody panels for *in situ* proteomics imaging to the individual application.

In addition to that, for the MICS technology, the sequence of antibodies in the staining cycles, potential issues with epitope competition of defined antibodies within protein complexes, repeated re-staining of the nuclei needed for image registration, APC photostability, a bleed-over between PE and FITC and acquisition bleaching of FITC during the sequential imaging of the field of views of an ROI must also be taken into account when designing the sequential imaging process.

Another pitfall in the automated analysis of high-dimensional IHC data is the evaluation of tissue structures that extend beyond a single cell. Here, the evaluation of the signal intensities of the individual markers per cell reaches its technical limits. Such an example is shown in Supplementary Figure 5, which illustrates immune cells that, after cell segmentation, seem to carry markers such as actin or desmin, which are often used to identify muscle tissue. Thus, these cells should be considered as muscle adjacent. However, this is only a very limited aspect of assessing muscular structures which, comparable to extracellular matrix (supplementary Figure 6), should not merely be assessed based on cell segmentation.

The combination of single cell analyses with overarching cellular structures (i.e., compounds of the extracellular matrix) in the tissue context, based on spatial location and cell-specific marker expression in combination with signal intensity maps for the latter markers, could represent an approach to include hitherto often unused morphological information in automated and unbiased high-dimensional spatial analyses of tissues in the future.

Analyses of *in situ* proteomics imaging enable in-depth characterization of the γδ T cell tissue microenvironment

Subsequently, we describe our efforts at deriving the cell type composition of the tissue microenvironment of γδ T cells on the basis of the multiplexed imaging data. To illustrate our high-dimensional analysis pipeline described here, we present exemplary analyses of 28 γδ TiMEs (circular neighborhoods of γδ T cells) originating from three benign colon tissue samples, two CRC invasion fronts and one CRC immune infiltrate obtained from 4 CRC patients altogether. Resulting marker expression profiles were used to assign cell types to each cell. For this, we performed Louvain clustering on the profiles (Figure 3 A) and assigned cell types to cell clusters according to the expression of markers characteristic for the respective cell type. We observed a mixed B/T cell cluster as well as two mixed tumor & normal epithelial cells (NEC) clusters. Such clusters can contain different cell types with similar expression profiles and might be separated by further subclustering. However, in our case increasing the number of clusters did not lead to a separation. The mixed B/T cell cluster is likely caused by the overlapping signal of CD3 and IgD described above, impeding an unambiguous cell type identification. The lack of an exclusive CRC-specific marker and a shared protein expression profile between malignant and normal cells of some other markers investigated, resulted in the identification mixed tumor & NEC clusters by our approach.

Next, we evaluated the frequency of each cell type in the spatial proximity of the identified 11 TCR Vδ1+ γδ T cell and 17 TCR Vγ9+Vδ2+ γδ T cell neighborhoods, i.e., TiMEs (Figure 3 B & C). In accordance with the known involvement of γδ T cells in cancer immunosurveillance

(19, 30-32), we found, tumor cells in the close neighborhood of both compartments, as expected (Figure 4). Despite the visualization of tissue resident γδ T cells, the proximity of some γδ T cells to endothelial cells could indicate the exchange of certain clones between the periphery into the studied TiMEs, as supported for example by others (33, 34) and our previous work (Herold et al. manuscript in preparation). The neighborhood of B cells and plasma cells are in line with known T helper functions of γδ T cells (35). Further of interest is the identified proximity of myeloid cells that could induce both pro- and anti-tumor functions. In addition to the spatial resolution of the γδ T cell TiMEs, we also determined the phenotypic signature of all investigated γδ T cells. Overall, γδ T cells were low-abundant (Supplementary Figure 7) and we observed mostly effector or later stage differentiated phenotypes of TCR Vδ1+ and more heterogenous profiles of TCR Vγ9+Vδ2+ γδ T cells (Figure 4, Figure 5 A). The observed protein expression patterns are in line with those of tissue invasive γδ T cells identified by scRNA sequencing in a HCC cohort (dbGaP; accession number: phs003279.v1.p1; (14)) and two public available CRC datasets (GSM6415701 (15) and GSE216534 (16) (Figure 5 B, C and D, respectively), validating the identified in-depth phenotypic signatures.

Since this study is based on a rather limited sample set yielding limited exemplary environments, more comprehensive studies are warranted in the future for their characterization in greater detail as well as many more aspects of γδ T cells in cancer immunosurveillance and with statistical rigor. Such an approach may also allow associations with clinical features, including survival outcome, as for example recently developed by us (36). Further, the implementation of such high-dimensional imaging studies will benefit from the development of standards for image pre-processing and bioinformatic analysis, and thereby not only boost the study of γδ T cells in their tissue environment and disease context but also the assessment of other immune cell types.

References

1. Ruf, B., T. F. Greten, and F. Korangy. 2023. Innate lymphoid cells and innate-like T cells in cancer - at the crossroads of innate and adaptive immunity. *Nature reviews. Cancer* 23:351-371.
2. Beucke, N., D. Wesch, H. H. Oberg, C. Peters, J. Bochem, B. Weide, C. Garbe, G. Pawelec, S. Sebens, C. Rocken, H. Hashimoto, M. W. Loffler, P. Nocerino, S. Kordasti, D. Kabelitz, K. Schilbach, and K. Wistuba-Hamprecht. 2020. Pitfalls in the characterization of circulating and tissue-resident human gammadelta T cells. *Journal of leukocyte biology* 107:1097-1105.
3. Jungbluth, A. A., D. Frosina, M. Fayad, M. P. Pulitzer, A. Dogan, K. J. Busam, N. Imai, and S. Gnjatic. 2019. Immunohistochemical Detection of gamma/delta T Lymphocytes in Formalin-fixed Paraffin-embedded Tissues. *Appl Immunohistochem Mol Morphol* 27:581-583.
4. Chabab, G., F. Boissiere-Michot, C. Mollevi, J. Ramos, E. Lopez-Crapez, P. E. Colombo, W. Jacot, N. Bonnefoy, and V. Lafont. 2020. Diversity of Tumor-Infiltrating, gammadelta T-Cell Abundance in Solid Cancers. *Cells* 9.
5. Janssen, O., S. Wesselborg, B. Heckl-Ostreicher, K. Pechhold, A. Bender, S. Schondelmaier, G. Moldenhauer, and D. Kabelitz. 1991. T cell receptor/CD3-signaling induces death by apoptosis in human T cell receptor gamma delta + T cells. *Journal of immunology* 146:35-39.
6. Kabelitz, D., T. Ackermann, T. Hinz, F. Davodeau, H. Band, M. Bonneville, O. Janssen, B. Arden, and S. Schondelmaier. 1994. New monoclonal antibody (23D12) recognizing three different V gamma elements of the human gamma delta T cell receptor. 23D12+ cells comprise a major subpopulation of gamma delta T cells in postnatal thymus. *Journal of immunology* 152:3128-3136.
7. Hinz, T., D. Wesch, F. Halary, S. Marx, A. Choudhary, B. Arden, O. Janssen, M. Bonneville, and D. Kabelitz. 1997. Identification of the complete expressed human TCR V gamma repertoire by flow cytometry. *International immunology* 9:1065-1072.
8. Da Gama Duarte, J., L. T. Quigley, E. Tavancheh, S. Ostrouska, and A. Behren. 2022. A multispectral immunohistochemistry panel to investigate γδ T cells and butyrophilin molecules in the tumour microenvironment. *Exploration of Immunology*:383-392.
9. Castagna, A., A. J. Zander, I. Sautkin, M. Schneider, R. Shegokar, A. Konigsrainer, and M. A. Reymond. 2021. Enhanced intraperitoneal delivery of charged, aerosolized curcumin nanoparticles by electrostatic precipitation. *Nanomedicine (Lond)* 16:109-120.
10. Wolf, F. A., P. Angerer, and F. J. Theis. 2018. SCANPY: large-scale single-cell gene expression data analysis. *Genome Biol* 19:15.
11. Korsunsky, I., N. Millard, J. Fan, K. Slowikowski, F. Zhang, K. Wei, Y. Baglaenko, M. Brenner, P. R. Loh, and S. Raychaudhuri. 2019. Fast, sensitive and accurate integration of single-cell data with Harmony. *Nature methods* 16:1289-1296.
12. Traag, V. A., L. Waltman, and N. J. van Eck. 2019. From Louvain to Leiden: guaranteeing well-connected communities. *Sci Rep* 9:5233.
13. Waskom, M. L. 2021. seaborn: statistical data visualization. *The Journal of Open Sourvce Software* 6.
14. Ruf, B., M. Bruhns, S. Babaei, N. Kedei, L. Ma, M. Revsine, M. R. Benmebarek, C. Ma, B. Heinrich, V. Subramanyam, J. Qi, S. Wabitsch, B. L. Green, K. C. Bauer, Y. Myojin, L. T. Greten, J. D. McCallen, P. Huang, R. Trehan, X. Wang, A. Nur, D. Q. Murphy Soika, M. Pouzolles, C. N. Evans, R. Chari, D. E. Kleiner, W. Telford, K. Dadkhah, A. Ruchinskas, M. K. Stovroff, J. Kang, K. Oza, M. Ruchirawat, A. Kroemer, X. W. Wang, M. Claassen, F. Korangy, and T. F. Greten. 2023. Tumor-associated macrophages trigger MAIT cell dysfunction at the HCC invasive margin. *Cell* 186:3686-3705 e3632.
15. Harmon, C., A. Zaborowski, H. Moore, P. St Louis, K. Slattery, D. Duquette, J. Scanlan, H. Kane, B. Kunkemoeller, C. L. McIntyre, A. N. Scannail, B. Moran, A. C. Anderson, D. Winter, D. Brennan, M. A. Brehm, and L. Lynch. 2023. gammadelta T cell dichotomy with opposing cytotoxic and wound healing functions in human solid tumors. *Nat Cancer* 4:1122-1137.
16. de Vries, N. L., J. van de Haar, V. Veninga, M. Chalabi, M. E. Ijsselsteijn, M. van der Ploeg, J. van den Bulk, D. Ruano, J. G. van den Berg, J. B. Haanen, L. J. Zeverijn, B. S. Geurts, G. F. de Wit, T. W. Battaglia, H. Gelderblom, H. M. W. Verheul, T. N. Schumacher, L. F. A. Wessels, F. Koning, N. de Miranda, and E. E. Voest. 2023. gammadelta T cells are effectors of immunotherapy in cancers with HLA class I defects. *Nature* 613:743-750.
17. Beucke, N., and K. Wistuba-Hamprecht. 2021. Accurate determination of gammadelta T cells in multi-channel mass and flow cytometry. *Cytometry. Part B, Clinical cytometry* 100:288-289.

18. Wistuba-Hamprecht, K., G. Pawelec, and E. Derhovanessian. 2014. OMIP-020: phenotypic characterization of human gammadelta T-cells by multicolor flow cytometry. *Cytometry. Part A : the journal of the International Society for Analytical Cytology* 85:522-524.
19. Silva-Santos, B., S. Mensurado, and S. B. Coffelt. 2019. gammadelta T cells: pleiotropic immune effectors with therapeutic potential in cancer. *Nature reviews. Cancer* 19:392-404.
20. Davey, M. S., C. R. Willcox, S. Hunter, S. A. Kasatskaya, E. B. M. Remmerswaal, M. Salim, F. Mohammed, F. J. Bemelman, D. M. Chudakov, Y. H. Oo, and B. E. Willcox. 2018. The human Vdelta2(+) T-cell compartment comprises distinct innate-like Vgamma9(+) and adaptive Vgamma9(-) subsets. *Nature communications* 9:1760.
21. Karunakaran, M. M., C. R. Willcox, M. Salim, D. Paletta, A. S. Fichtner, A. Noll, L. Starick, A. Nohren, C. R. Begley, K. A. Berwick, R. A. G. Chaleil, V. Pitard, J. Dechanet-Merville, P. A. Bates, B. Kimmel, T. J. Knowles, V. Kunzmann, L. Walter, M. Jeeves, F. Mohammed, B. E. Willcox, and T. Herrmann. 2020. Butyrophilin-2A1 Directly Binds Germline-Encoded Regions of the Vgamma9Vdelta2 TCR and Is Essential for Phosphoantigen Sensing. *Immunity* 52:487-498 e486.
22. Rigau, M., S. Ostrouska, T. S. Fulford, D. N. Johnson, K. Woods, Z. Ruan, H. E. G. McWilliam, C. Hudson, C. Tutuka, A. K. Wheatley, S. J. Kent, J. A. Villadangos, B. Pal, C. Kurts, J. Simmonds, M. Pelzing, A. D. Nash, A. Hammet, A. M. Verhagen, G. Vairo, E. Maraskovsky, C. Panousis, N. A. Gherardin, J. Cebon, D. I. Godfrey, A. Behren, and A. P. Uldrich. 2020. Butyrophilin 2A1 is essential for phosphoantigen reactivity by gammadelta T cells. *Science* 367.
23. Davey, M. S., C. R. Willcox, S. P. Joyce, K. Ladell, S. A. Kasatskaya, J. E. McLaren, S. Hunter, M. Salim, F. Mohammed, D. A. Price, D. M. Chudakov, and B. E. Willcox. 2017. Clonal selection in the human Vdelta1 T cell repertoire indicates gammadelta TCR-dependent adaptive immune surveillance. *Nature communications* 8:14760.
24. Tan, L., A. S. Fichtner, E. Bruni, I. Odak, I. Sandrock, A. Bubke, A. Borchers, C. Schultze-Florey, C. Koenecke, R. Forster, M. Jarek, C. von Kaisenberg, A. Schulz, X. Chu, B. Zhang, Y. Li, U. Panzer, C. F. Krebs, S. Ravens, and I. Prinz. 2021. A fetal wave of human type 3 effector gammadelta cells with restricted TCR diversity persists into adulthood. *Sci Immunol* 6.
25. Wistuba-Hamprecht, K., A. Martens, K. Haehnel, M. Geukes Foppen, J. Yuan, M. A. Postow, P. Wong, E. Romano, A. Khammari, B. Dreno, M. Capone, P. A. Ascierto, I. Demuth, E. Steinhagen-Thiessen, A. Larbi, B. Schilling, D. Schadendorf, J. D. Wolchok, C. U. Blank, G. Pawelec, C. Garbe, and B. Weide. 2016. Proportions of blood-borne Vdelta1+ and Vdelta2+ T-cells are associated with overall survival of melanoma patients treated with ipilimumab. *European journal of cancer* 64:116-126.
26. Kinkhabwala, A., C. Herbel, J. Pankratz, D. A. Yushchenko, S. Ruberg, P. Praveen, S. Reiss, F. C. Rodriguez, D. Schafer, J. Kollet, V. Dittmer, M. Martinez-Osuna, L. Minnerup, C. Reinhard, A. Dzionek, T. D. Rockel, S. Borbe, M. Buscher, J. Krieg, M. Nederlof, M. Jungblut, D. Eckardt, O. Hardt, C. Dose, E. Schumann, R. P. Peters, S. Miltenyi, J. Schmitz, W. Muller, and A. Bosio. 2022. MACSima imaging cyclic staining (MICS) technology reveals combinatorial target pairs for CAR T cell treatment of solid tumors. *Sci Rep* 12:1911.
27. Nagel, A., C. Mobs, H. Raifer, H. Wiendl, M. Hertl, and R. Eming. 2014. CD3-positive B cells: a storage-dependent phenomenon. *PloS one* 9:e110138.
28. Lee, A. Y. S. 2022. CD20(+) T cells: an emerging T cell subset in human pathology. *Inflamm Res* 71:1181-1189.
29. Vlaming, M., V. Bilemjian, J. A. Freile, H. J. Lourens, N. van Rooij, G. Huls, T. van Meerten, M. de Bruyn, and E. Bremer. 2021. CD20 positive CD8 T cells are a unique and transcriptionally-distinct subset of T cells with distinct transmigration properties. *Sci Rep* 11:20499.
30. Wesch, D., D. Kabelitz, and H. H. Oberg. 2020. Tumor resistance mechanisms and their consequences on gammadelta T cell activation. *Immunological reviews* 298:84-98.
31. Lo Presti, E., F. Dieli, J. J. Fournie, and S. Meraviglia. 2020. Deciphering human gammadelta T cell response in cancer: Lessons from tumor-infiltrating gammadelta T cells. *Immunological reviews*.
32. Hayday, A. C. 2019. gammadelta T Cell Update: Adaptate Orchestrators of Immune Surveillance. *Journal of immunology* 203:311-320.
33. Bruni, E., M. M. Cimino, M. Donadon, R. Carriero, S. Terzoli, R. Piazza, S. Ravens, I. Prinz, V. Cazzetta, P. Marzano, P. Kunderfranco, C. Peano, C. Soldani, B. Franceschini, F. S. Colombo, C. Garlanda, A. Mantovani, G. Torzilli, J. Mikulak, and D. Mavilio. 2022.

Intrahepatic CD69(+)Vdelta1 T cells re-circulate in the blood of patients with metastatic colorectal cancer and limit tumor progression. *J Immunother Cancer* 10.
34. Foord, E., L. C. M. Arruda, A. Gaballa, C. Klynning, and M. Uhlin. 2021. Characterization of ascites- and tumor-infiltrating gammadelta T cells reveals distinct repertoires and a beneficial role in ovarian cancer. *Science translational medicine* 13.
35. Rampoldi, F., L. Ullrich, and I. Prinz. 2020. Revisiting the Interaction of gammadelta T-Cells and B-Cells. *Cells* 9.
36. Babaei, S., J. Christ, A. Makky, M. Zidane, K. Wistuba-Hamprecht, C. M. Schürch, and M. Claassen. 2023. S³-CIMA: Supervised spatial single-cell image analysis for the identification of disease-associated cell type compositions in tissue. *bioRxiv*:2023.2003.2017.533167.

Funding
This work was partially funded by the DFG (WI 5021-21–FOR2799; KW-H), the Medical Faculty of the University of Tübingen (2509-0-0; KW-H) and the EXC 2180 Image-Guided and Functionally Instructed Tumor Therapies (Deutsche Forschungsgemeinschaft (DFG, German Research Foundation) under Germany's Excellence Strategy – EXC2180 – 390900677); BR, MWL, MC, KW-H). MB was supported by EXC 2064: Machine Learning: New Perspectives for Science (DFG) and the International Max Planck Research School for Intelligent Systems (IMPRS-IS).

Acknowledgements
We thank all patients for their support and participation in this study. Materials for this study were retrieved from the Central Biobank of the CCC Tübingen with ethics approval No. 508/2016BO1.

Conflict of Interest Disclosure
Markus W. Löffler reports personal fees from Boehringer Ingelheim for lectures / consultancy and is listed as a co-inventor on several patents owned by Immatics Biotechnologies, concerning peptides for use in immunotherapies.

Authorship
Conceptualization: NH, MB, SB, MWL, MC & KW-H
Investigation: NH, JS, AC, CY, PJ, MWL, MC & KW-H
Data curation—formal analysis: NH, MB, SB, JS, MC & KW-H
Project Administration/oversight: MWL, MC, KW-H
Writing—original draft: KW-H, MWL, MC
Writing—review, editing, and revision: NH, MB, SB, JS, AC, CY, SS, CS, BR, AK, PJ, MWL, MC & KW-H

Figures

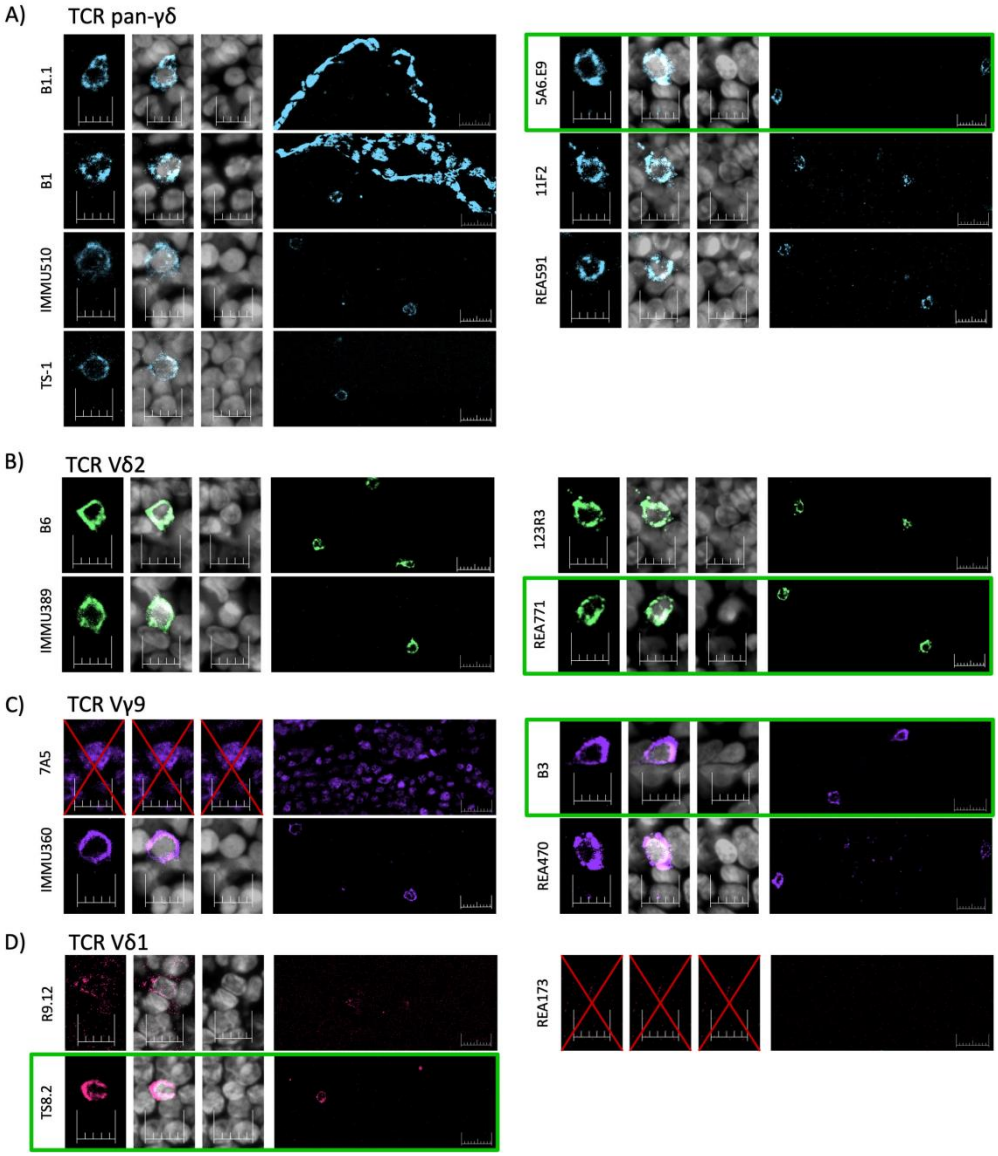

Figure 1: Identification of γδ T cells and their major subsets visualized in a fresh frozen human adenoid tissue sample using commercially available antibody clones. The identified staining patterns of 7 TCR pan-γδ antibody clones are shown in A). Detection of the TCR Vδ2 using 4 different antibody clones is displayed in B), those specific for TCR Vγ9 in C) and 3 TCR Vδ1+ binding antibody clones in D). Each panel depicts the fluorescent image of the respective antibody clone, an overlay on the DAPI stain, the blank DAPI stain and a larger section of the imaged tissue (left to right).

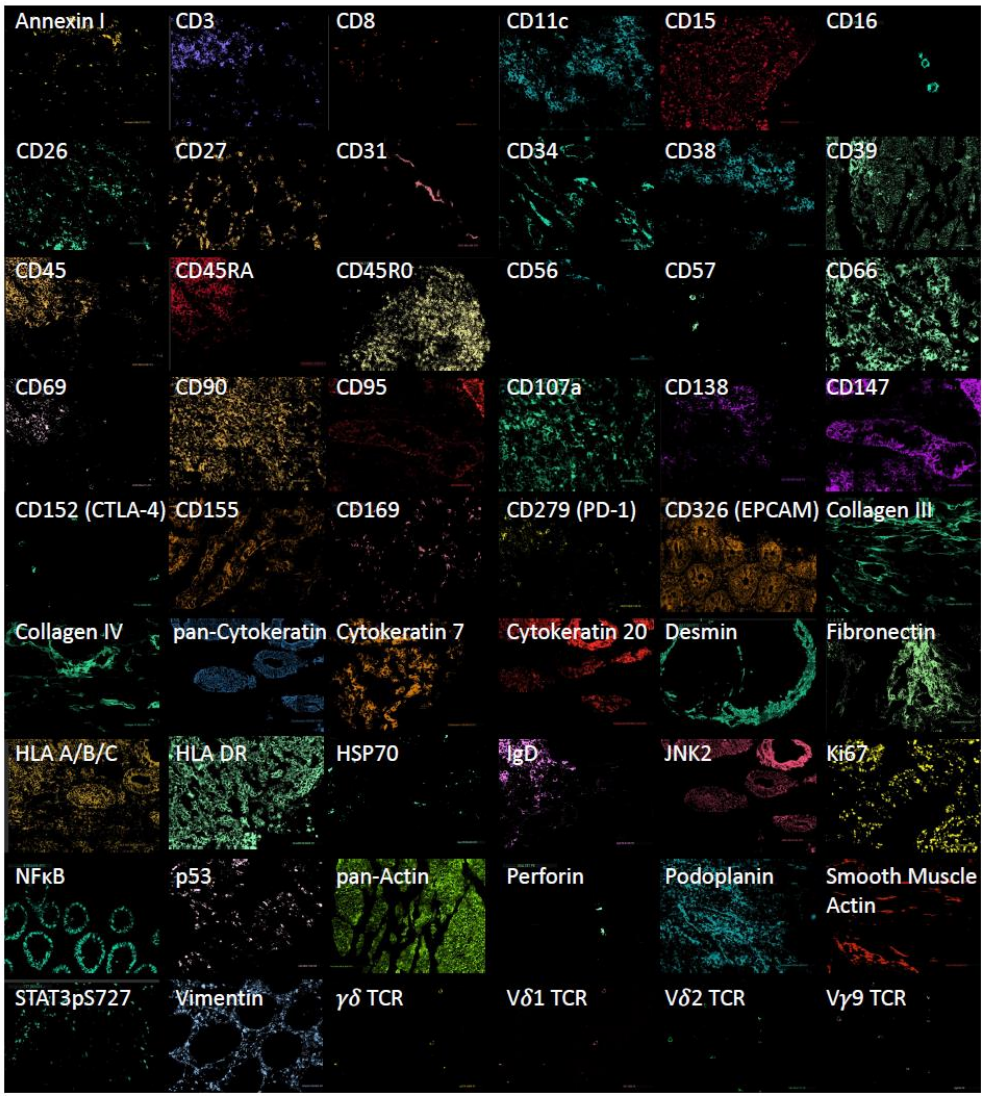

Figure 2: Antibody panel for high-dimensional proteomic MACSima imaging of the γδ T cell neighborhood. Representative pseudocolor images of each marker are shown corresponding to different tissue sections and/or field of views.

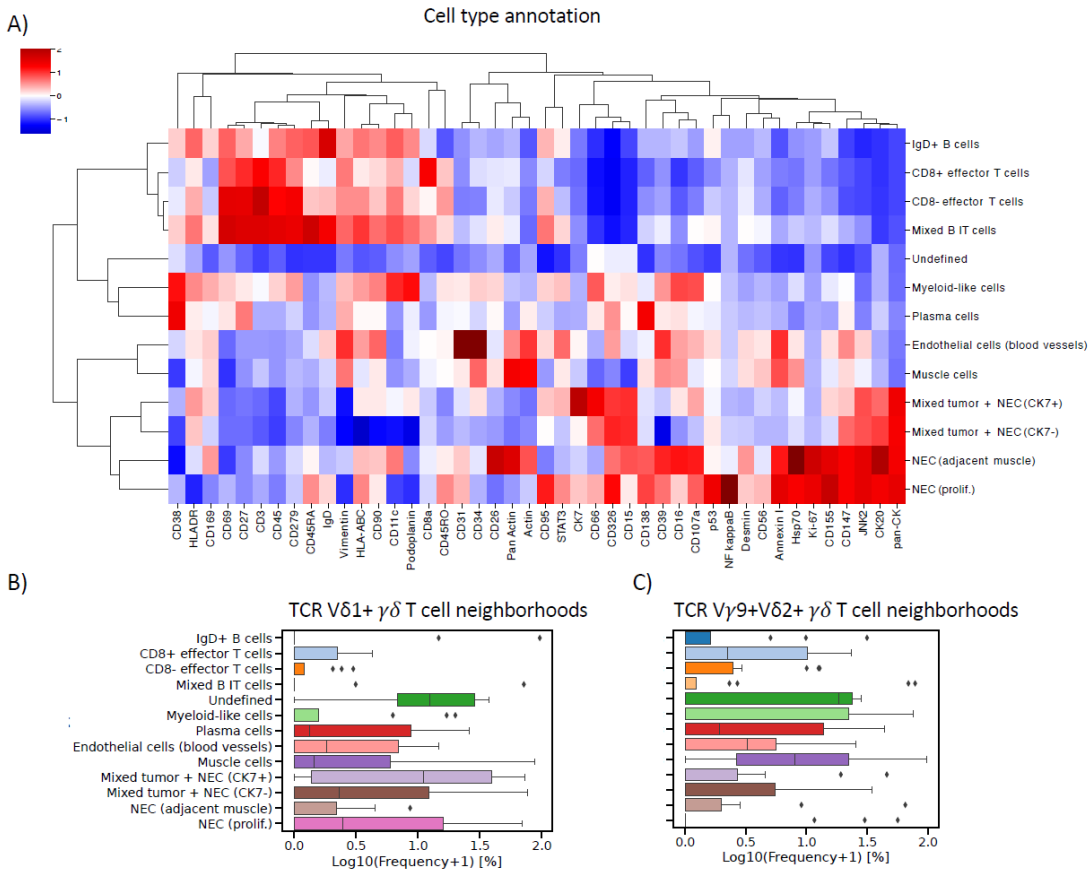

Figure 3: Characterization of the investigated 28 exemplary TiMEs. Median marker expression of identified cell types in the γδ T cell microenvironments (A). Cell type frequency distribution in microenvironment across the considered 11 TCR Vδ1+ γδ T cell (B) and 17 TCR Vγ9+Vδ2+ γδ T cells neighborhoods (C). The x-label "Log10(Frequency+1) [%]" indicates that the data plotted on the x-axis is the logarithm (base 10) of the frequency values, incremented by 1, and expressed as percentages. NEC – normal epithelial cells

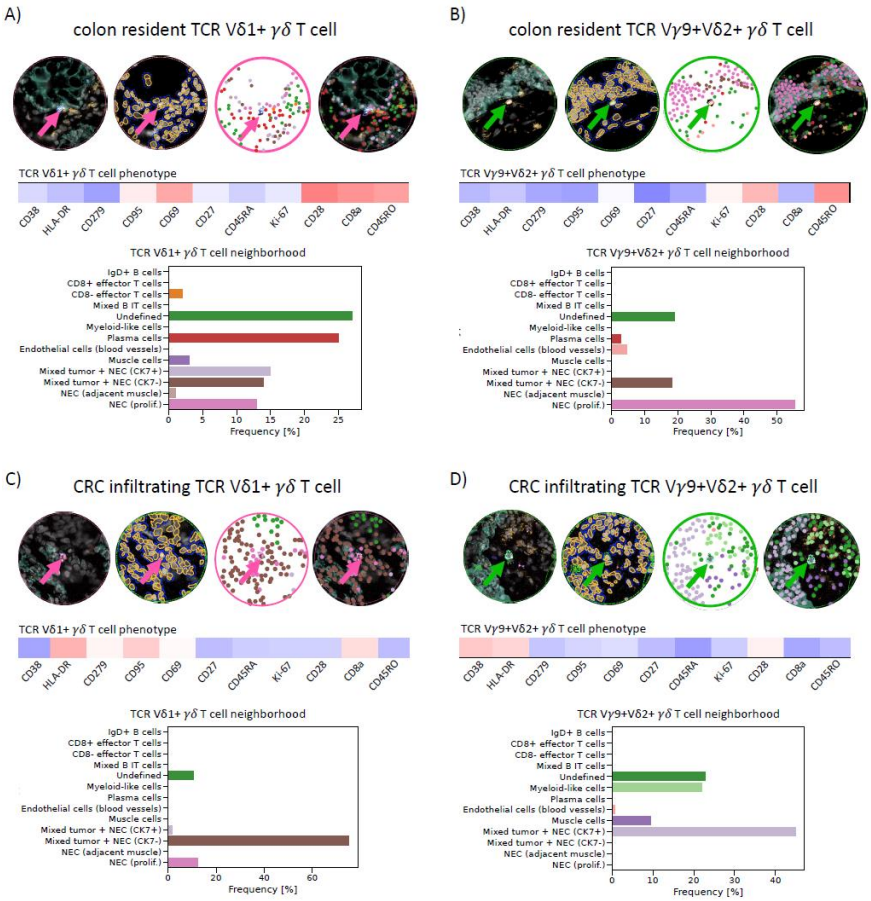

Figure 4: Selected γδ T cell example microenvironments in normal and CRC tissues. Pseudocolor overlay images illustrate the identified γδ T cells (arrows) and their TiME, grey coloring visualizes the DAPI stain, petrol indicates pan-Cytokeratin expression, yellow CD45 expression, purple TCR Vδ1 expression, green TCR Vδ2 expression and salmon TCR Vγ9 expression. Segmented cells are framed in yellow. The projection of the identified cells in the neighborhood is color coded according to the bar chart labels. Overlay of the IHC image and the neighborhood projection (left to right A -D). Heatmap indicates respective γδ T cell phenotypes and bar plots display the relative cell type distribution for the respective example microenvironments. NEC – normal epithelial cells

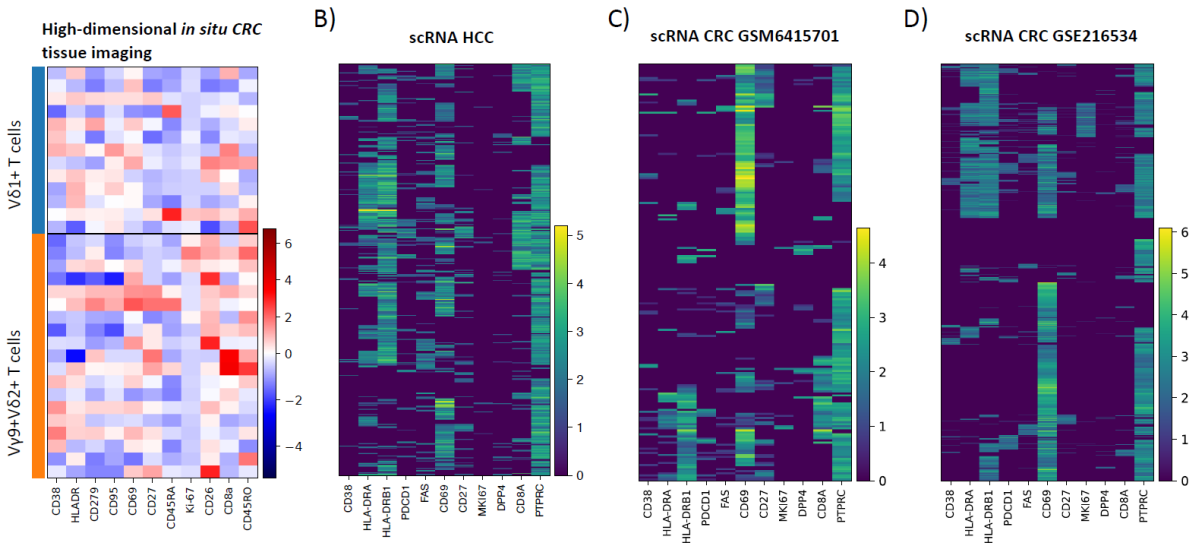

Figure 5: Phenotyping of colon / colorectal carcinoma (CRC) and hepatocellular carcinoma (HCC) tissue invasive γδ T cells. Relative protein expression determined by high-dimensional *in situ* proteomics imaging. Scaling of color coding derived from visualization of all assessed cells see Supplementary Figure 2 (A). Respective gene expression (read counts) of the corresponding markers in HCC (dbGaP; accession number: phs003279.v1.p1) (B) and publicly available colon / CRC tissue GSE210040 (C), GSE216534 (D) invasive γδ T cells. PTPRC corresponds to CD45, PDCD1 to PD-1, FAS to CD95, MKI67 to Ki67 and DPP4 to CD26.

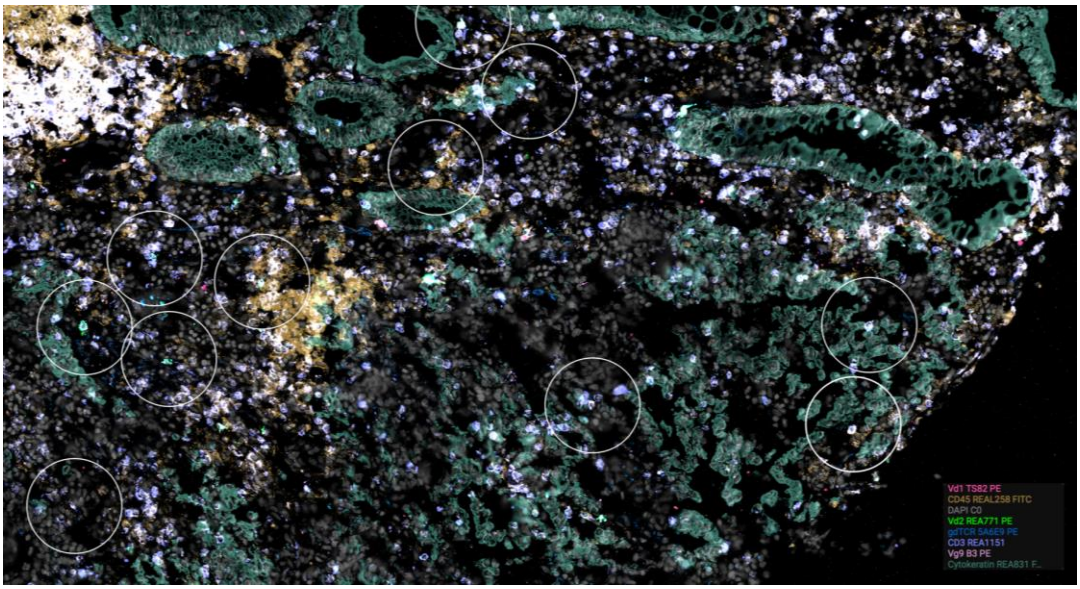

Supplementary Figure 1: Representative example visualizing the selection of $\gamma\delta$ T cell neighborhoods in a 5 μm thick tissue section of a tumor invasive front in colorectal cancer

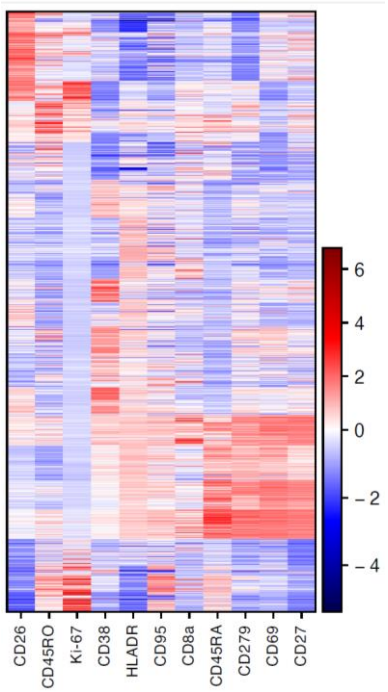

Supplementary Figure 2: Distribution of phenotypic markers relevant for the characterization of immune cells visualized for all cells within the observed $\gamma\delta$ T cell neighborhoods.

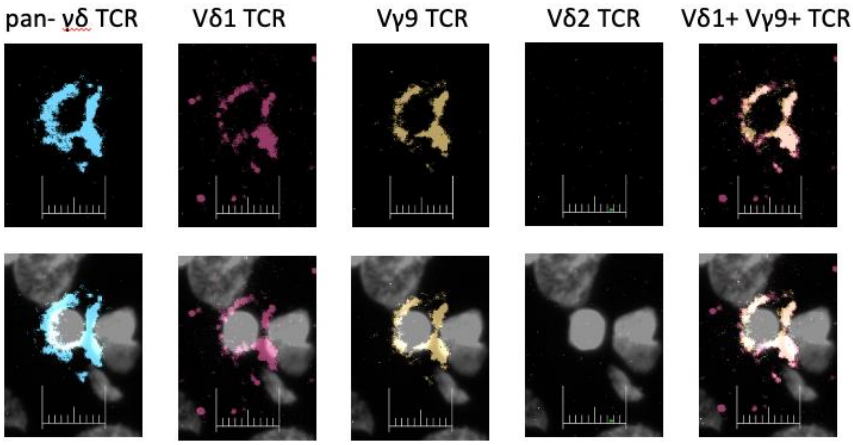

Supplementary Figure 3: Visualization of a rare tissue resident Vδ1+Vγ9+ $\gamma\delta$ T cell. IHC staining of the respective markers is depicted in the upper row, overlay of the latter with the respective DAPI image is shown in the bottom row.

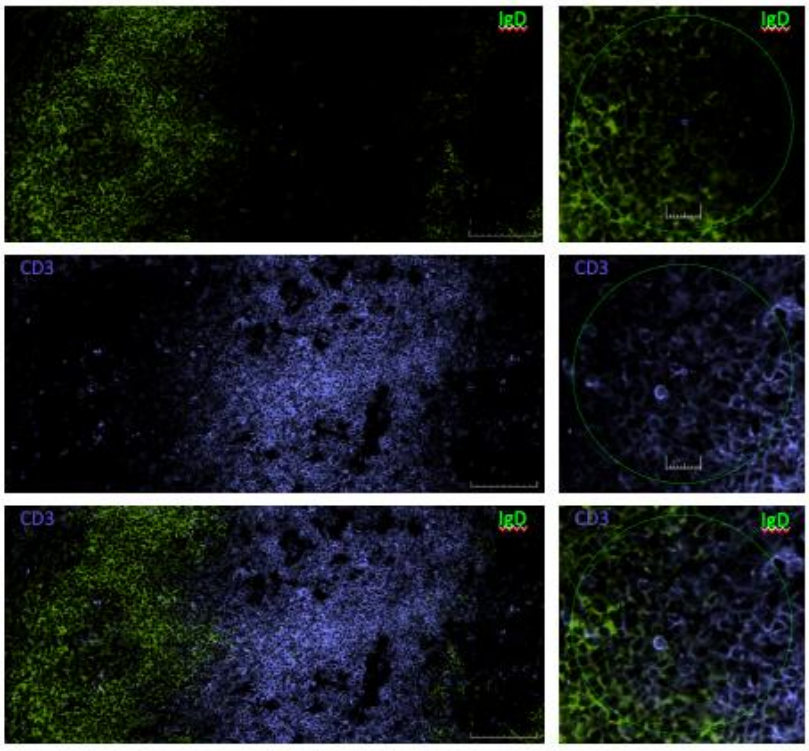

Supplementary Figure 4: Example image to visualize overlapping signals of IgD- (green) and CD3- (purple) specific antibodies in B and T cell dense tissue regions.

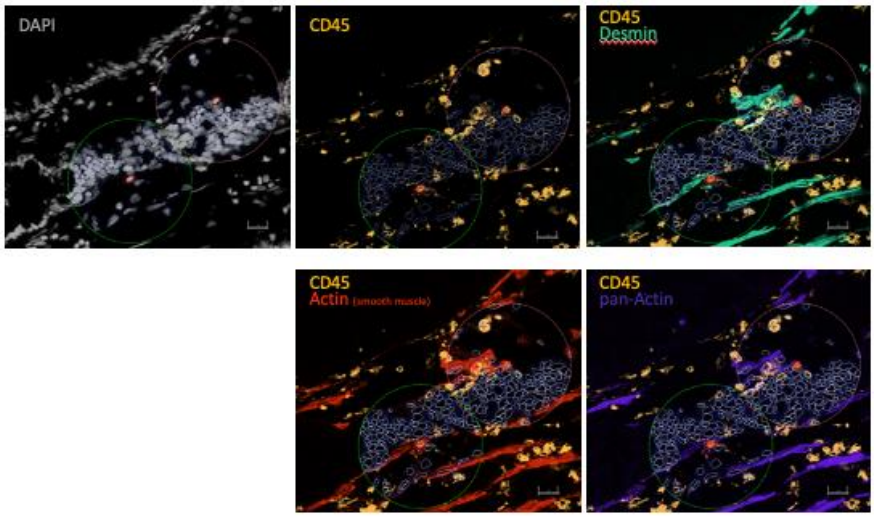

Supplementary Figure 5: Overlay of CD45 and muscle tissue markers.

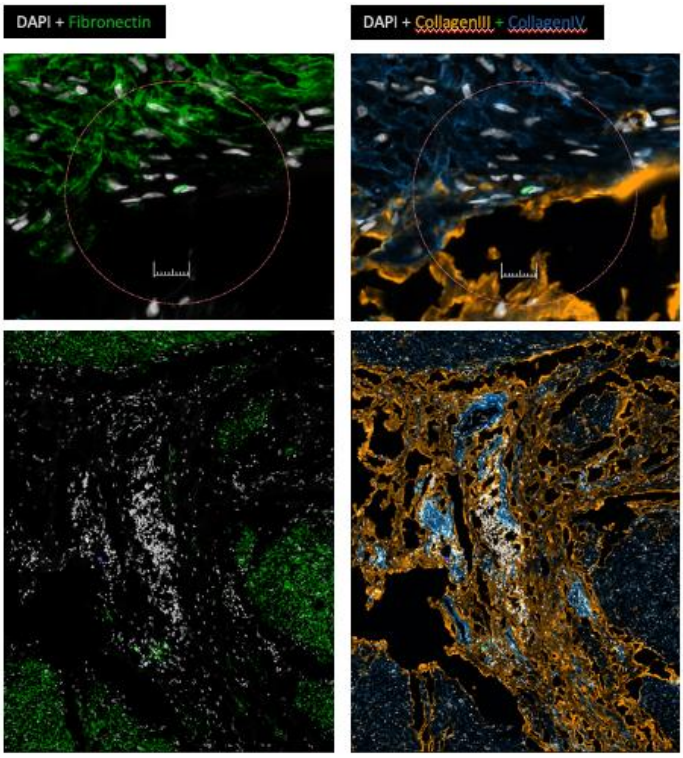

Supplementary Figure 6: Cells surrounded by extracellular matrix.

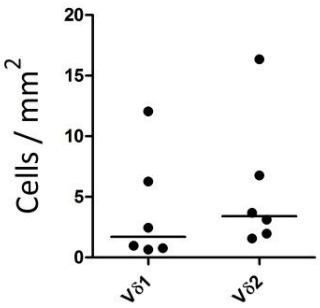

Supplementary Figure 7: Number of $V\delta1$ and $V\delta2$ T cells per area. Each dot represents one ROI.

Title: A Vδ1 T cell subset is responsive to PD-1 blockade and associated with survival in melanoma

Authors:

Nicola Herold[1,2,3], Jonas Bochem[1,2,3], Johanna Leyens[1], Svenja Wingerter[1], Stephan Forchhammer[1], Janine Spreuer[1,2,3], Malte Deseke[4], Can Yurttas[5], Paola Nocerino[6], Rita Antunes dos Reis[6], Teresa Amaral[1], Nikolaus B. Wagner[7], Karolin Thiel[5], Daniel Soffel[1], Kristin Bieber[8], Patrick Terheyden[9], Daniela Wesch[10], Hans-Heinrich Oberg[10], Susanne Sebens[11], Manfred Claassen[2,3,12,13,14], Alfred Königsrainer[5,14], Claus Garbe[1], Graham Pawelec[15,16], Friedegund Meier[17,18], Markus W. Löffler[5,14,15,19], Benjamin Weide[1], Immo Prinz[4,20], Sarina Ravens[4], Shahram Kordasti[6,21,22], Thomas K. Eigentler[1,23], Kilian Wistuba-Hamprecht[1,2,3,14,15]*

Affiliations:

[1]Department of Dermatology, University Hospital Tübingen; Tübingen, 72076, Germany.

[2]Section for Clinical Bioinformatics, Department of Internal Medicine I, University Hospital Tübingen; Tübingen, 72076, Germany.

[3]M3 Research Center, University Hospital Tübingen; Tübingen, 72076, Germany.

[4]Institute of Immunology, Hannover Medical School; Hannover, 30625, Germany.

[5]Department of General, Visceral and Transplant Surgery, University Hospital Tübingen; Tübingen, 72076, Germany.

[6]Systems Cancer Immunology, Comprehensive Cancer Centre, King's College London; London, WC2R 2LS, United Kingdom.

[7]Department of Dermatology, Venereology and Allergology, Kantonsspital St. Gallen; St. Gallen, 9007, Switzerland.

[8]Department of Internal Medicine II, University Hospital Tübingen; Tübingen, 72076, Germany.

[9]Department of Dermatology, University of Lübeck; Lübeck, 23562, Germany.

[10]Institute of Immunology, University Medical Center Schleswig-Holstein, Campus Kiel, Christian-Albrechts University; Kiel, 24105, Germany.

[11]Institute for Experimental Cancer Research, Kiel University and University Hospital Schleswig-Holstein, Campus Kiel; Kiel, 24105, Germany.

[12]Department of Computer Science, University of Tübingen; Tübingen, 72074, Germany.

[13]Institute for Bioinformatics and Medical Informatics, University of Tübingen; Tübingen, 72074, Germany.

[14]Cluster of Excellence iFIT (EXC2180) 'Image-Guided and Functionally Instructed Tumor Therapies', University of Tübingen; Tübingen, 72076, Germany.

[15]Department of Immunology, Institute for Cell Biology, University of Tübingen; Tübingen, 72076, Germany.

[16]Health Sciences North Research Institute; Sudbury, Ontario, ON P3E 2H3, Canada.

[17] Department of Dermatology, Faculty of Medicine and University Hospital Carl Gustav Carus, Technische Universität Dresden; Dresden, 01307, Germany.

[18] Skin Cancer Center at the University Cancer Center Dresden and National Center for Tumor Diseases, Dresden, 01307, Germany.

[19]Department of Clinical Pharmacology, University Hospital Tübingen; Tübingen, 72076, Germany.

[20]Institute of Systems Immunology, Hamburg Center for Translational Immunology (HCTI), University Medical Center Hamburg-Eppendorf, Hamburg, 20246, Germany.

[21]Department of Clinical and Molecular Sciences, Università Politecnica delle Marche; Ancona, 60121, Italy.

[22]Haematology Department, Guy's Hospital; London, SE1 9RT, United Kingdom.

[23]Department of Dermatology, Venereology, and Allergology, Charité – Universitätsmedizin Berlin, corporate member of Freie Universität Berlin and Humboldt-Universität zu Berlin; Berlin, 10117, Germany.

*Corresponding author. Email: kilian.wistuba-hamprecht@uni-tuebingen.de

One Sentence Summary: Vδ1 T cells are associated with phenotypic alterations and overall survival in melanoma supporting the ongoing development of Vδ1-targeted therapies.

Abstract:

Although most studies of anti-cancer T cell immunity focus on αβ T cells, γδ T cells are attracting increasing attention due to their involvement in anti-tumor immune responses in various cancer entities, including melanoma. While immune checkpoint blockade (ICB) using the antagonistic Programmed Cell Death Protein 1 (PD-1) antibodies nivolumab and pembrolizumab significantly improved the survival of melanoma patients with distant metastasis, prognosis remains poor. PD-1 is not only expressed by αβ T cells but also by γδ T cells, making this numerically minor population of unconventional T cells, whose role in melanoma is still elusive, a target of ICB. Here, we present a detailed γδ T cell profiling study in late-stage melanoma at single cell level using mass and polychromatic flow cytometry, T cell receptor repertoire analyses and immunohistochemistry. Our analyses link high frequencies of peripheral Vδ1 T cells before the start of anti-PD-1 therapy to a significantly reduced overall survival. In these patients, the Vδ1 compartment is dominated by a late-differentiated senescent-like phenotype that is presumably unresponsive to therapy. This phenotype is less prevalent at the tumor site and analysis of RNA sequencing data revealed that the abundance of Vδ1 T cells within the tumor was positively associated with survival. Our study suggests that a subset of responsive Vδ1 T cells expands under ICB and enters the tumor to contribute to cancer immunosurveillance. Thus, we propose Vδ1 T cells as promising candidates for novel cancer immunotherapy approaches.

Graphical Abstract

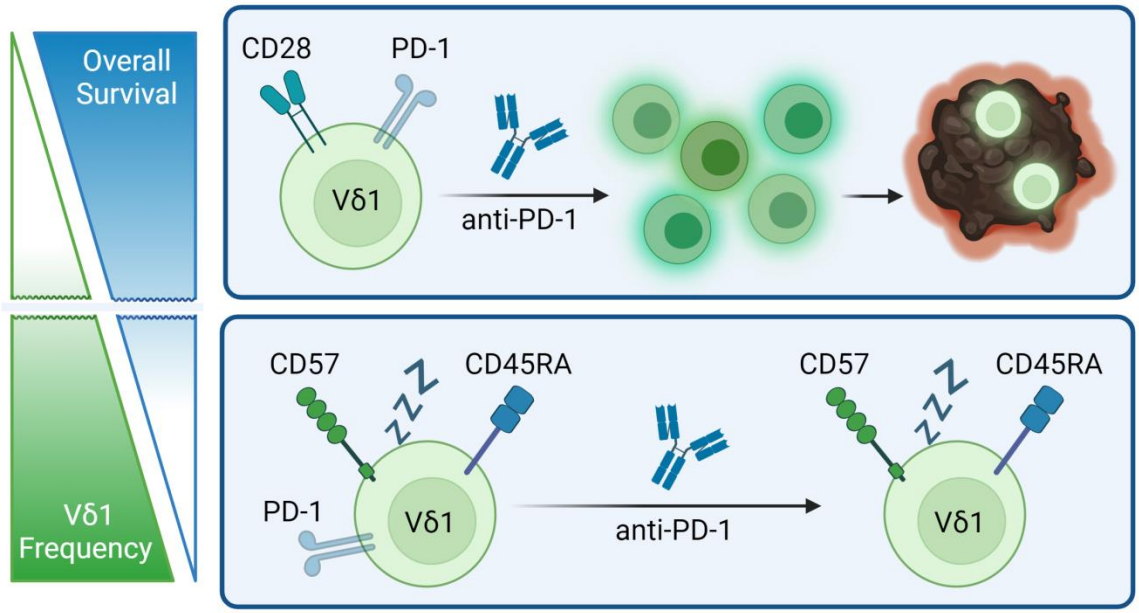

INTRODUCTION

Immune checkpoint blockade, reinvigorating the anti-tumor T cell response, induces durable remissions in advanced melanoma, albeit only in a minority of patients (*1*). Nowadays, therapeutic blockade of the immune checkpoint programmed cell death receptor 1 (PD-1) alone or in combination with targeting cytotoxic T-lymphocyte-associated protein-4 (CTLA-4) is standard-of-care treatment for metastatic melanoma. However, immune-related adverse events of treatment and disease-associated mortality resulting in a 5-year survival rate of around 50% (*2*), underline the urgent need to decipher the mechanisms determining clinical responses (*3*).

The inhibitory receptor PD-1 is expressed transiently on activated T cells, though persistent expression has been associated with T cell dysfunction (*4, 5*). Engagement of the ligands programmed cell death 1 ligand 1 (PD-L1) or PD-L2 results in impaired T cell function, thereby regulating the immune response in order to maintain self-tolerance (*6*). This mechanism can be hijacked by cancers promoting immune evasion and providing the rationale for treatment with antagonistic antibodies (*7*). Besides αβ T cells, PD-1 is expressed on γδ T cells (*8*) making this non-classical T cell population a further target of anti-PD-1 therapy.

γδ T cells are, alongside αβ T cells and B cells, an evolutionarily conserved third subset carrying an antigen receptor assembled via somatic rearrangement (*9*). This unconventional, numerically minor T cell subset utilizes a non-MHC-restricted mode of antigen recognition and is considered an orchestrator of immune surveillance (*10*). The γδ T cell compartment comprises distinct subsets with substantial functional diversity and is commonly delineated into innate-like Vγ9Vδ2 T cells and adaptive-like non-Vγ9Vδ2 T cells primarily encompassing Vδ1 T cells. Vγ9Vδ2 T cells are the predominant subset in peripheral blood, harbor a semi-invariant TCR repertoire (*11*)

and display phosphoantigen reactivity in a butyrophilin-dependent manner involving germline-encoded regions of the Vγ9 chain (*12, 13*). Microbial infections or metabolic changes due, for instance, to a dysregulated mevalonate pathway in cancer cells leading to the accumulation of phosphorylated intermediates (termed phosphoantigens) are sensed by these cells (*14*). The Vδ1 subset is enriched in barrier tissues and is characterized by a private, highly diverse TCR repertoire typically showing stable clonotypic expansions (*15*). Ligands recognized by Vδ1 T cells include stress-induced antigens and MHC-like or -related molecules. Atypical binding modes as well as the involvement of germline-encoded regions have been described (*16-18*). In addition to their somatically-rearranged TCR, γδ T cells express natural cytotoxicity receptors and natural killer receptors (*19*). Both subsets show functional plasticity and a diverse array of anti-tumor functions has been documented, ranging from direct tumor killing via TRAIL or FASL and cytotoxic effector functions to antibody-dependent cellular cytotoxicity, antigen presentation capacity and interaction with B cells (*20*). However, also tumor promoting effects mediated, inter alia, by IL-17, IL-4 and galectins have been reported (*20, 21*).

γδ T cells infiltrate primary melanomas as well as metastases (*22*). While higher proportions of intratumoral γδ T cells were linked to prolonged overall survival (OS) (*23*), high frequencies of circulating Vδ1 T cells were negatively associated with survival in cutaneous melanoma (*24*). Knowledge regarding the role of PD-1 and the impact of immune checkpoint blockade on γδ T cells, especially with respect to the Vδ1 subset, is limited. PD-1 is transiently upregulated on γδ T cells upon stimulation (*25, 26*) and PD-1 expression has been described on γδ T cells residing at the tumor site (*27-30*). In vitro studies demonstrated a diminished cytotoxic function of Vδ2 T cells in the presence of PD-L1, which could be reversed by an anti-PD-L1 mAb, suggesting the presence of a functional PD-1/PD-L1 system in these cells (*31*). Furthermore, in an

immunodeficient prostate cancer mouse model anti-PD-1 treatment enhanced anti-tumor immunity of adoptively transferred Vγ9Vδ2 T cells (*25*). We have reported previously that high frequencies of Vδ1 T cells were associated with a late-differentiated phenotype and poor OS in melanoma patients treated with ipilimumab (*32*).

In the present study we investigated the phenotype, functionality and TCR repertoire of peripheral blood and tumor-infiltrating γδ T cells in late stage melanoma patients receiving anti-PD-1 therapy, in order to further dissect their role and potential for exploitation in cancer immunotherapy.

RESULTS

Anti-PD-1 therapy modulates γδ T cells

Since γδ T cells have been largely neglected in the context of immune checkpoint blockade (ICB), we have undertaken a comprehensive analysis of peripheral blood and tumor tissue samples from late-stage melanoma patients undergoing PD-1 blockade to obtain novel insights into the complex network of ICB modulation of cancer immunosurveillance.

Expression of PD-1 on γδ T cells from melanoma patients prior to as well as during anti-PD-1 therapy was analyzed by flow cytometry. PD-1 expression on patients' peripheral blood γδ T cells at baseline (BL) before the start of therapy was comparable to healthy donors (HD) with a median of 23.8% for Vδ1 and 12.0% for Vδ2 T cells (fig. S1A). Using an indirect staining approach utilizing therapeutic antibodies we found a significant decrease in the frequency of PD-1^{+} Vδ1 and Vδ2 T cells early during anti-PD-1 immunotherapy (at a median of 46 days after starting therapy; Fig. 1A). Furthermore, in follow-up (FU) samples collected during therapy, we detected therapeutic antibody bound to cell-surface PD-1 on Vδ1 T cells (fig. S1B). This confirms γδ T cells as direct targets of immune checkpoint blockade and suggests a modulation of both major γδ T cell subsets.

Mass cytometry reveals differences in Vδ1 profiles associated with survival

The phenotypic profile of γδ T cells in the blood of late-stage melanoma patients (table S1) was characterized at high resolution using mass cytometry (CyTOF). Amongst all T cells, the median frequencies of Vδ1 and Vδ2 T cells were 0.56% and 0.88%, respectively (fig. S2). Clinical data revealed a significant association of the abundance of Vδ1 T cells with OS ($p = 0.033$). Above-median Vδ1 frequencies (Vδ1^{high}) before the start of anti-PD-1 monotherapy were linked to poor

OS, while patients with equal or lower than median Vδ1 frequencies ($V\delta1^{low}$) had a prolonged OS (Fig. 1B). No association of survival with Vδ2 T cell frequencies was observed (fig. S3). High dimensional analysis showed that Vδ1 T cells strongly expressing CD25, CD197, CD27, CD28 or CD127 were enriched in the $V\delta1^{low}$ group, whereas high expression of CD57, CD45RA and perforin was more prominent in the $V\delta1^{high}$ group (Fig. 1C). Of particular note is the patient P1 in the bottom row of the $V\delta1^{high}$ heatmap with a phenotypic profile similar to the $V\delta1^{low}$ group and having the lowest Vδ1 frequency (0.68%) within the $V\delta1^{high}$ group: this patient had an above median OS of 657 days. Cells from BL and FU samples were clustered unsupervised using FlowSOM and the resulting six clusters were projected onto a t-distributed stochastic neighbor embedding (tSNE) visualization (Fig. 1D). Highlighting the BL samples for the $V\delta1^{low}$ and $V\delta1^{high}$ groups in a density visualization of the tSNE plot revealed an opposing distribution (Fig. 1D); a similar pattern was observed under therapy (fig. S4A). Cluster 3 and 6 showed the highest expression of CD27, CD28 and CD127, indicating early differentiated T cells (Fig. 1E, fig. S5). High expression of NKG2D (CD314) and intermediate levels of CD27 and CD127 are characteristic for clusters 4 and 5. These four clusters had a significantly higher abundance in patients of the $V\delta1^{low}$ group (Fig. 1F). High levels of CD45RA and Perforin together with low levels of CD27 and CD28, implying late-differentiated T cells, characterize cluster 1 and 2. Furthermore, the NK cell-related markers CD56, CD161 and NKG2A (CD159a) are upregulated in these two clusters. The Vδ1 T cells from $V\delta1^{high}$ patients constitute the vast majority of cluster 1, while being almost absent from the other clusters, stressing the differences in the phenotypic profiles between long- and short-term survivors. Comparison of the cluster frequencies revealed no distinct changes between BL and FU (fig. S4B).

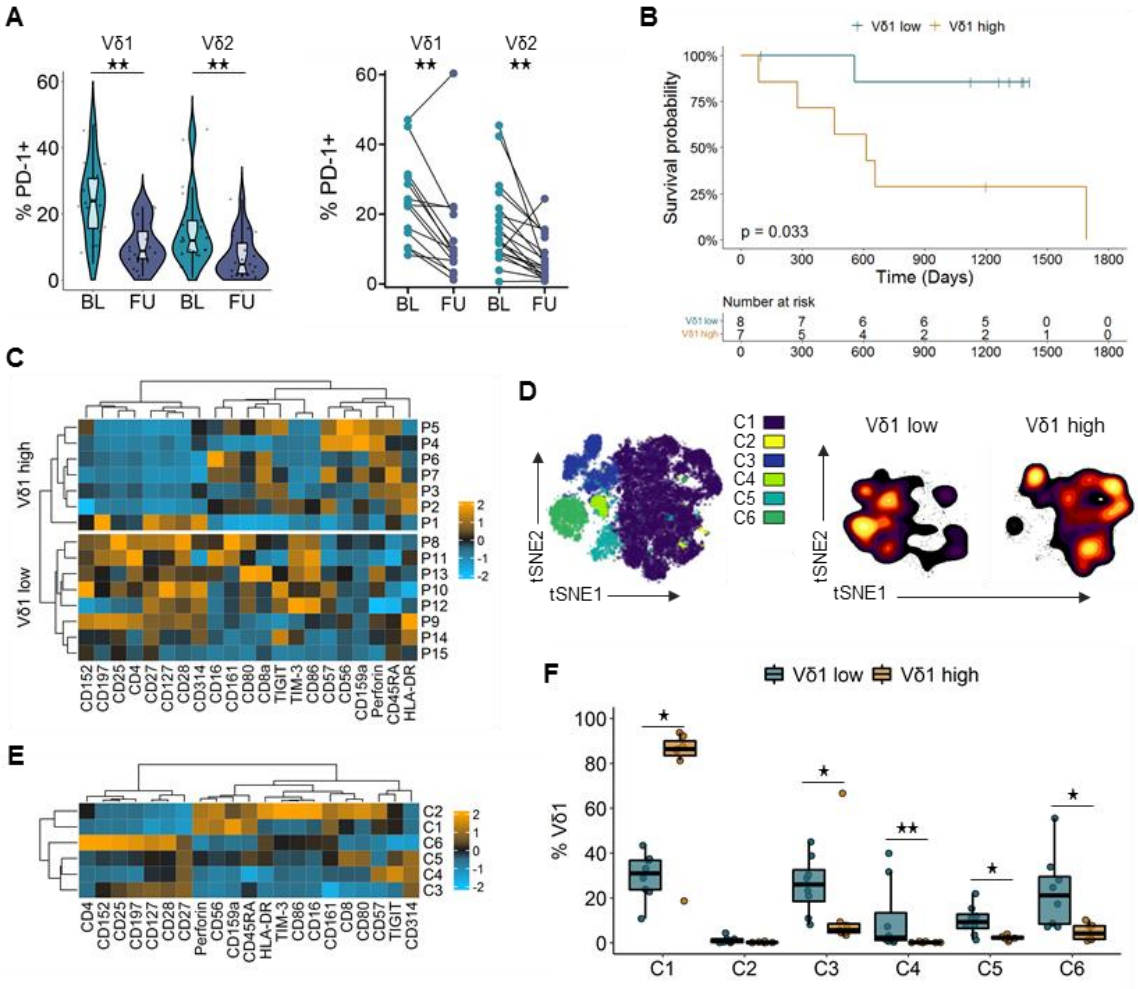

Fig.1 Vδ1 T cell frequencies are associated with survival and different phenotypic profiles. (**A**) PD-1 expression on Vδ1 and Vδ2 T cells before the start of anti-PD-1 therapy at baseline (BL; n = 20 to 25) and at follow-up (FU; n = 16 to 19) under therapy. (**B**) Overall survival of late-stage melanoma patients dichotomized based on the BL median Vδ1 frequency (0.56%) determined by mass cytometry. Survival compared by log rank test. (**C**) Heat map of phenotypic marker expression on Vδ1 T cells. Each row represents the BL sample of one patient, heatmaps are divided based on median Vδ1 frequency. (**D**) tSNE visualization of Vδ1 T cells from BL and FU samples color coded by clusters identified using FlowSOM. Smoothed contour plots show BL samples of the patient groups with lower and higher than median Vδ1 frequencies. (**E**) Heat map depicting the phenotypic marker expression of the FlowSOM clusters identified in D. Only BL samples are shown. (**F**) Abundance of the identified FlowSOM clusters in the BL samples for the $Vδ1^{low}$ and $Vδ1^{high}$ group. Groups compared by Man-Whitney-U test, for paired analysis by Wilcoxon matched pairs signed rank test *P < 0.05, **P < 0.01. Heat maps display marker expression, which was arcsinh-transformed and normalized to a mean of 0 and a standard deviation of 1. Relative overexpression indicated in orange, relative underexpression in blue.

Vδ1 T cells from short-term survivors are dominated by late-differentiated and replicative-senescent phenotypes

To validate these findings and further explore phenotypic variation, two independent cohorts of late-stage melanoma patients (table S1) were investigated by polychromatic flow cytometry and stratified according to the previously determined Vδ1 cut-off frequency of 0.56%. Survival analysis confirmed the association of low Vδ1 frequencies with an improved OS under anti-PD-1 monotherapy (Fig. 2A, $p = 0.018$), as well as in patients receiving either anti-PD-1 monotherapy or combination treatment with ipilimumab targeting CTLA-4 (Fig. 2B, $p = 0.0094$). Significantly higher levels of naive ($CD27^+CD45RA^+$), central memory (CM; $CD27^+CD45RA^-$) and effector memory (EM; $CD27^-CD45RA^-$) Vδ1 T cells were observed in $V\delta1^{low}$ patients (Fig. 2C). In contrast to the rather balanced distribution of memory differentiation phenotypes in these patients, the $V\delta1^{high}$ group was dominated by terminally differentiated effector memory cells re-expressing CD45RA (TEMRA; $CD27^-CD45RA^+$) at a median frequency of 71.8%. This is in line with the high abundance of the late-differentiated cluster 1 in $V\delta1^{high}$ patients (Fig. 1F). Of note, no differences in PD-1 expression were observed between the two groups (Fig. 2C). While some patients exhibited changes in their memory differentiation profile from BL to FU, overall a clear trend towards an increase or a decrease of a certain memory phenotype was lacking (fig. S6). Expression of CD57, a putative marker for replicative senescence, on Vδ1 T cells at BL was comparable to HD (fig. S7A), while patients´ Vδ2 T cells showed elevated percentages (fig. S7B). Comparing the $V\delta1^{low}$ to the $V\delta1^{high}$ group, significantly higher percentages of $CD57^+$ cells were detected in the latter (Fig. 2D). Under therapy, a decrease of $CD57^+$ Vδ1 T cells was observed in both groups (Fig. 2D), whereas this was not seen for Vδ2 T cells (fig. S7).

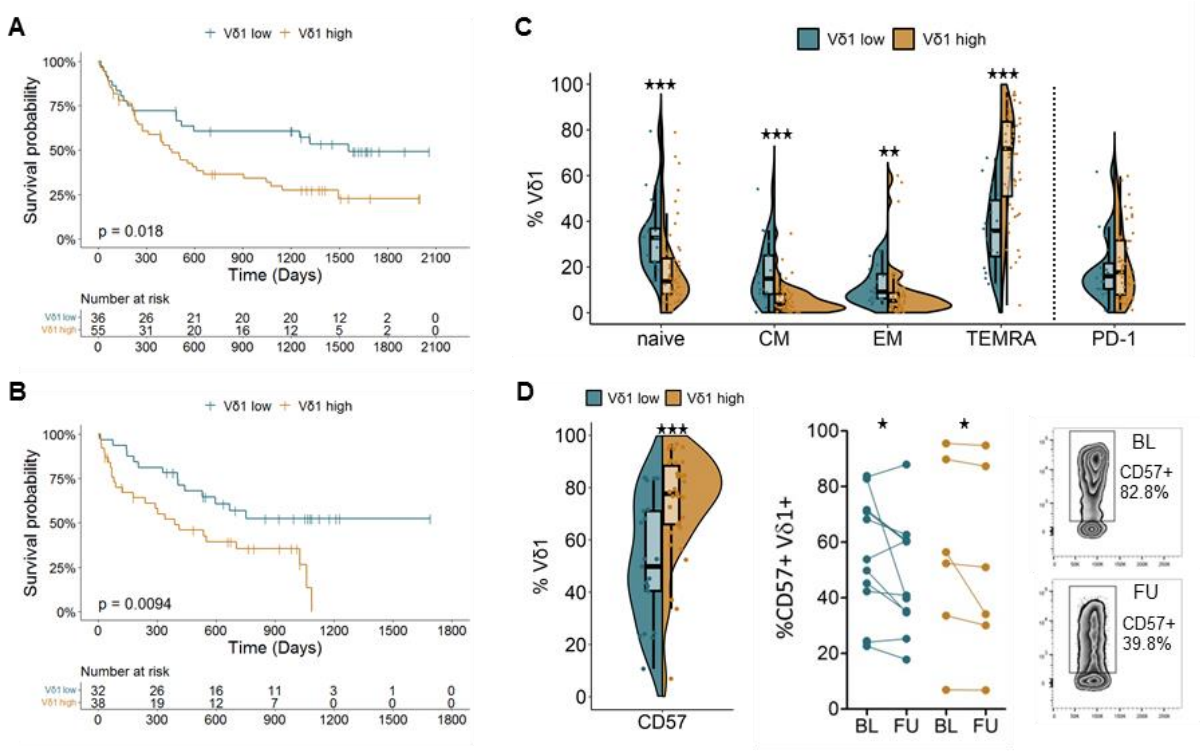

Fig. 2 Flow cytometry reveals association of high Vδ1 T cell frequencies with a TEMRA-like phenotype and high CD57 expression.

(**A**) Overall survival of late-stage melanoma patients in a validation cohort receiving anti-PD-1 monotherapy and **(B)** a second cohort treated either with anti-PD-1 alone or in combination with ipilimumab targeting CTLA-4. Patients were dichotomized based on the predetermined Vδ1 cutoff frequency of 0.56% amongst all T cells. Survival compared by log rank rest. (**C**) Distribution of memory differentiation profiles and PD-1 expression in the $V\delta1^{low}$ and $V\delta1^{high}$ group at BL for the cohort described in A (n = 72). (**D**) Expression of CD57 at BL (n = 56) and changes in expression under therapy (n = 17) in the $V\delta1^{low}$ and $V\delta1^{high}$ group of the cohort described in B. Groups compared by Man-Whitney-U test, for paired analysis by Wilcoxon matched pairs signed rank test. *P < 0.05, **P < 0.01, ***P < 0.001.

Functionality of γδ T cells is altered in late-stage melanoma

We next sought to address whether the functional capacity of γδ T cells is altered in melanoma patients and/or by anti-PD-1 therapy. Overall, low percentages of Vδ1 T cells expressed the degranulation marker CD107a and the cytokines IFN-γ and TNF in response to stimulation with PMA/ionomycin. Expression levels in patients at BL and FU were comparable to HD (Fig. 3A) and also similar between the $V\delta1^{low}$ and $V\delta1^{high}$ group (Fig. 3B). However, patients with low Vδ1 frequencies tended to have a higher polyfunctionality index (*33*), which takes the co-expression pattern of CD107a, IFN-γ and TNF into account (Fig. 3C). The functional response pattern of Vδ2 T cells differed from that of Vδ1 T cells and depended on the type of stimulus. While patients had a significantly higher proportion of CD107a-expressing cells at BL and FU in response to PMA/ionomycin when compared to HD, there were no differences in cytokine expression (Fig. 3D). In contrast, after stimulation with zoledronate we observed lower levels of CD107a, IFN-γ and TNF in patients before and under therapy than in healthy individuals (Fig. 3D). This might be due to the different modes of action of these two stimuli. Whereas zoledronate leads to an accumulation of phosphoantigens, which indirectly activate the Vγ9Vδ2 T cells via interaction of their TCRs with butyrophilins, PMA and ionomycin mimic TCR signaling, but bypass the receptor itself. We also investigated proliferative potential using a dye dilution assay. The Vδ2 subset generally displayed a higher proliferation index than the Vδ1 subset (Fig. 3E, 3F). For both subsets, we observed significantly diminished proliferation in patients compared to HD after stimulation with an anti-TCRγδ antibody (IMMU510) or zoledronate.

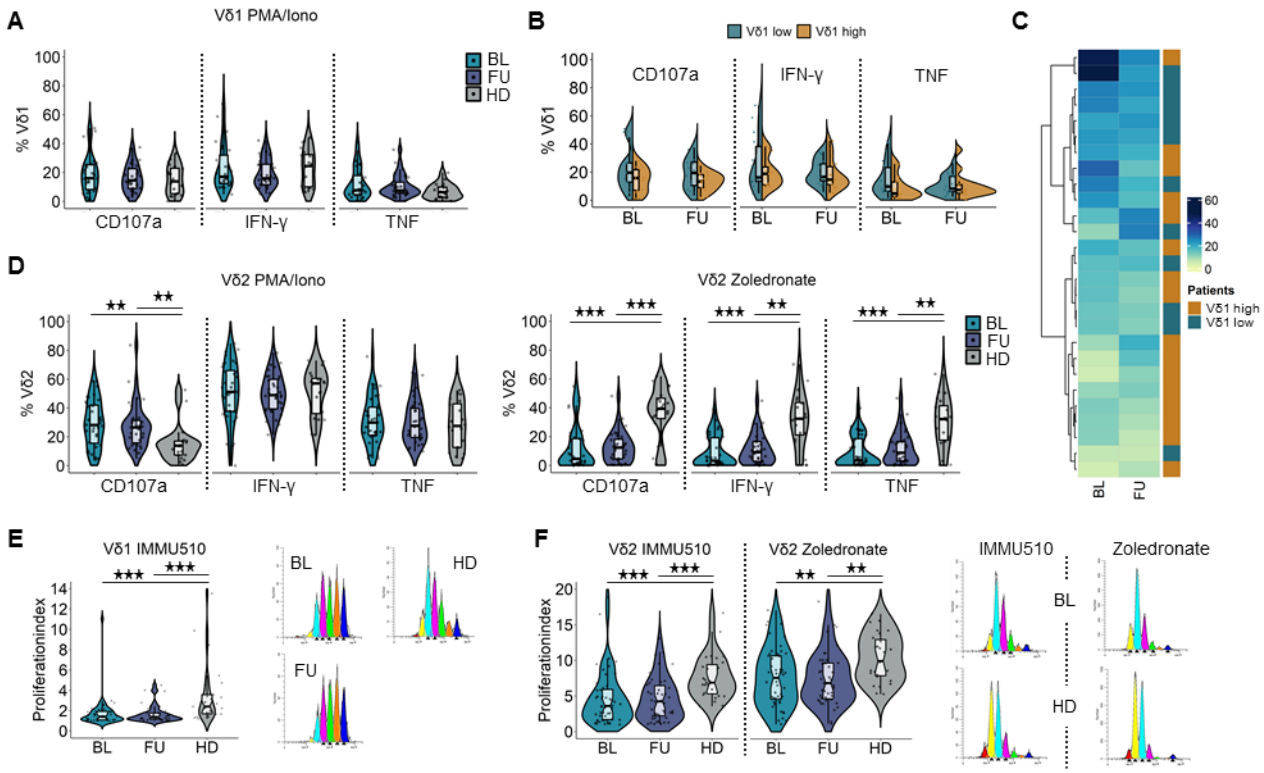

Fig.3 Functional analyses show altered cytokine expression and impaired proliferative capacity of γδ T cells in melanoma patients.

(**A**) Cytokine and CD107a expression in Vδ1 T cells after 12 h stimulation of peripheral blood mononuclear cells (PBMCs) from patients (BL: n = 27; FU: n = 30) and healthy donors (HD; n = 20) with PMA and ionomycin (Iono) in the presence of Golgi inhibitors. (**B**) Comparison of cytokine and CD107a expression between the Vδ1^{low} and Vδ1^{high} group. (**C**) Heatmap visualizing the polyfunctionality index (CD107a, IFN-γ, TNF) for Vδ1 T cells at BL and FU. Each row represents one patient. Heatmap divided by k-means clustering. (**D**) Cytokine and CD107a expression in Vδ2 T cells after 12 h stimulation of PBMCs from patients and HD (n = 20) with PMA and Iono or Zoledronate (BL: n = 36; FU: n = 32 to 34) in the presence of Golgi inhibitors. (**E**) Proliferation index for Vδ1 and (**F**) Vδ2 T cells determined by flow cytometry based on dye dilution. PBMCs from patients (BL: n = 44 to 49; FU: n = 37 to 46) and HD (n = 25 to 27) were cultured for 5 days in the presence of an anti-TCRγδ antibody (IMMU510) or Zoledronate. Groups compared by Man-Whitney-U test. *P < 0.05, **P < 0.01, ***P < 0.001.

Increase in clonal diversity of the TRDV1 repertoire early under anti-PD-1 therapy

Sorted peripheral blood γδ T cells were bulk sequenced in order to investigate the composition of the TCR δ-chain (TRD) repertoire. Diversity of the TRDV1 repertoire was evaluated using the Gini-Simpson index, with a higher index representing higher diversity. We observed a significant increase in diversity early under therapy, especially in patients with low Gini-Simpson indices before the start of therapy (Fig. 4A). A higher Gini-Simpson index is associated with a more equitable representation of clonotypes, as illustrated by the treemaps showing two patients with a strong increase in repertoire diversity in Fig. 4B, indicating an ICB-induced polyclonal expansion of Vδ1 T cells. No public Vδ1 sequences or sequence motifs were identified in this patient cohort, in agreement with the high magnitude of junctional combinations of the TCR δ gene (*34, 35*). Even though Vδ2 T cells express PD-1 and expression declined under therapy (Fig. 1 A), no changes were detected with regard to TRDV2 repertoire diversity (fig. S8), underlining the divergent biology of this innate-like γδ T cell subset. Comparison of the $V\delta1^{low}$ to the $V\delta1^{high}$ group revealed no differences in TRDV1 diversity, neither at BL nor at FU (Fig. 4C). However, a significant increase in the Gini-Simpson index under therapy was seen only in the $V\delta1^{low}$ group, consistent with the observed lower prevalence of late-differentiated or replicatively-senescent cells, while the $V\delta1^{high}$ group displayed alterations in both directions (Fig. 4C). Analysis of CDR3 length distribution revealed no differences between patients and HD and no influence of anti-PD-1 therapy (fig. S9A). Furthermore, the $V\delta1^{low}$ and $V\delta1^{high}$ group presented a similar pattern at BL and FU (fig. S9B). Skewing or reshaping of the CDR3 spectratype would be characteristic of an oligoclonal expansion. The 1-Pielou's index was utilized to assess clonality of the TRDV1 repertoire. We noted a trend towards a higher clonality in the $V\delta1^{high}$ group at BL ($p = 0.056$) as well as at FU ($p = 0.055$) (Fig. 4D), hinting at a higher prevalence of expanded clones

in this patient group. Comparison of BL and FU samples showed mixed alterations in both groups (fig. S9C).

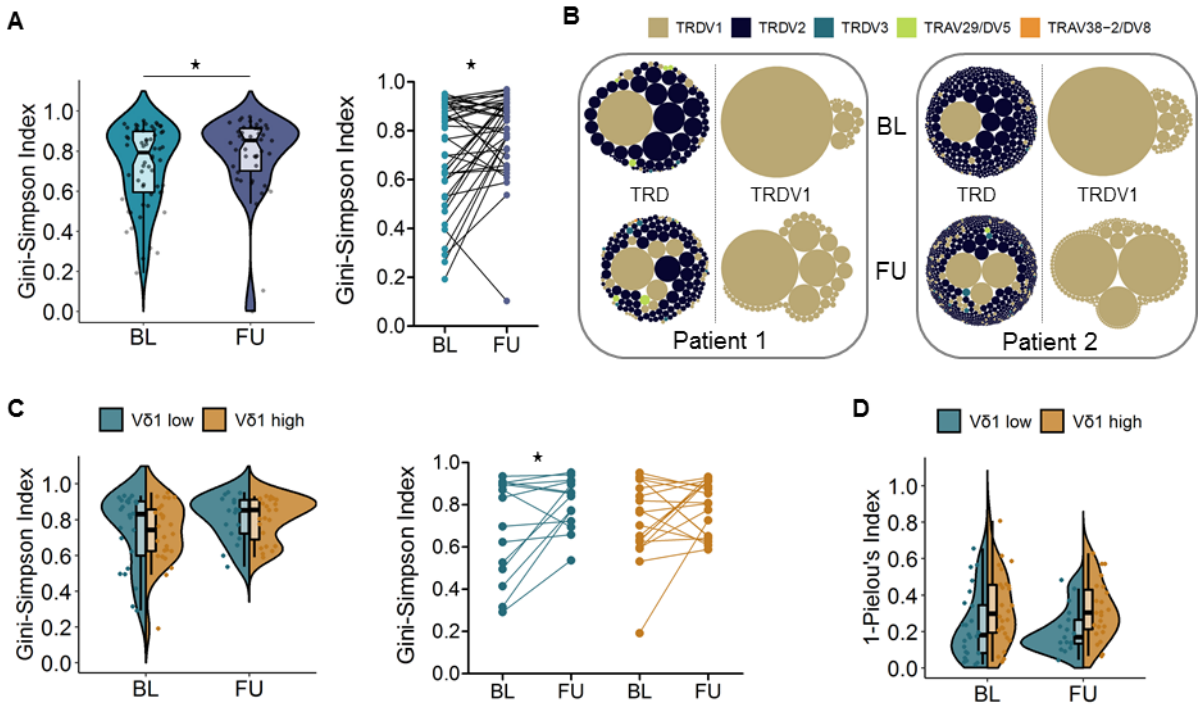

Fig.4 Diversity of the TRDV1 repertoire increases under anti-PD-1 therapy.
(**A**) TRDV1 repertoire diversity in PBMCs from melanoma patients at BL (n = 60) and FU (n = 50) represented by the Gini-Simpson index. (**B**) Tree maps illustrating the TRD and TRDV1 repertoire composition of two patients with a high increase of the Gini-Simpson index under therapy. (**C**) Comparison of TRDV1 repertoire diversity and changes therein in the $V\delta1^{low}$ (BL: n = 24; FU: n = 17) and $V\delta1^{high}$ (BL: n = 26; FU: n = 23) group. (**D**) Clonality (1 – Pielou's index) of the TRDV1 repertoire in the $V\delta1^{low}$ (BL: n = 24; FU: n = 17) and $V\delta1^{high}$ (BL: n = 26; FU: n = 23) group. Phenotypic data allowing assignment to the $V\delta1^{low}$ or $V\delta1^{high}$ group were not available for all patients. Groups compared by Man-Whitney-U test, for paired analysis by Wilcoxon matched pairs signed rank test. *P < 0.05.

TCR repertoire of tumor-infiltrating γδ T cells overlaps with peripheral blood

The intratumoral presence of γδ T cells in melanoma metastases was assessed by immunohistochemistry (IHC). Three-quarters of the studied samples showed γδ T cell infiltration and in about half of the remainder no T cells were detected, while the rest was infiltrated by non-γδ T cells (Fig. 5A). Quantitative analysis revealed a low abundance of γδ T cells (Fig. 5B), which represented less than 2.0% of infiltrating T cells (Fig. 5C). Next, the TRD repertoire of paired peripheral blood mononuclear cell (PBMC) and tumor-infiltrating lymphocyte (TIL) samples was analyzed. TRDV2 sequences dominated in most patients, although two had a high abundance of TRDV1 clonotypes (Fig. 5D). Overall, the TRD distribution was similar between the peripheral blood and TILs in each individual patient. As illustrated by the Venn diagrams, clonotypes overlapped between these two compartments, implying an exchange between blood and tumor (Fig. 5D). The pairwise similarity between the PBMC and TIL TRD repertoire was assessed using the Morisita-Horn-Index (MHI) with an index of 1 representing identical repertoires and 0 no overlap between clonotypes. The MHI was above 0.5, with two exceptions, and dominant clonotypes were shared, further supporting trafficking of γδ T cells between periphery and tumor. More in-depth analysis revealed that up to 28 clonotypes were shared between the TILs of two patients and some clonotypes were present in several patients. However only TRDV2 CDR3 sequences were shared, while TRDV1 and TRDV3/TRDV5/TRDV8 clonotypes were private (Fig. 5E). The TRDV2 CDR3 amino acid sequence "CACDTLGDTDKLIF" was detected in the TILs of 5 patients and, with one exception, was also present in the corresponding PBMC samples. This public clonotype with no N additions has been described previously in the peripheral blood by Papadopoulou et al. in 9 out of 14 samples from 10-week old donors (*36*), by Kakimi et al. in 2 out of 5 non-small cell lung cancer patients (*37*) and by Deng et al. in 76 out of 89 individuals including newborns, infants and adults (*38*).

Intratumoral Vδ1 T cells are positively associated with survival and a lower prevalence of CD57$^+$ cells

Due to the limited availability of tumor samples, we sought to expand our analyses and assess the role of Vδ1 T cells in the tumor utilizing a public dataset from The Cancer Genome Atlas (TCGA) Skin Cutaneous Melanoma (SKCM) project. Following Wu et al. (*39*), TRDV1 expression was used as proxy for Vδ1 T cells and patients were stratified based on median expression. In contrast to peripheral blood, high TRDV1 expression in the tumor was significantly associated with favorable OS in stage IIIc and IV patients (Fig. 5F). This potential paradox could be resolved by investigating CD57 expression on paired peripheral blood and tumor samples (Fig. 5G). For the Vδ1 as well as for the Vδ2 (Fig. 5E) subset we observed significantly lower percentages of CD57$^+$ cells in the tumor, indicating a different subset composition and a higher proliferative potential in the tumor compartment.

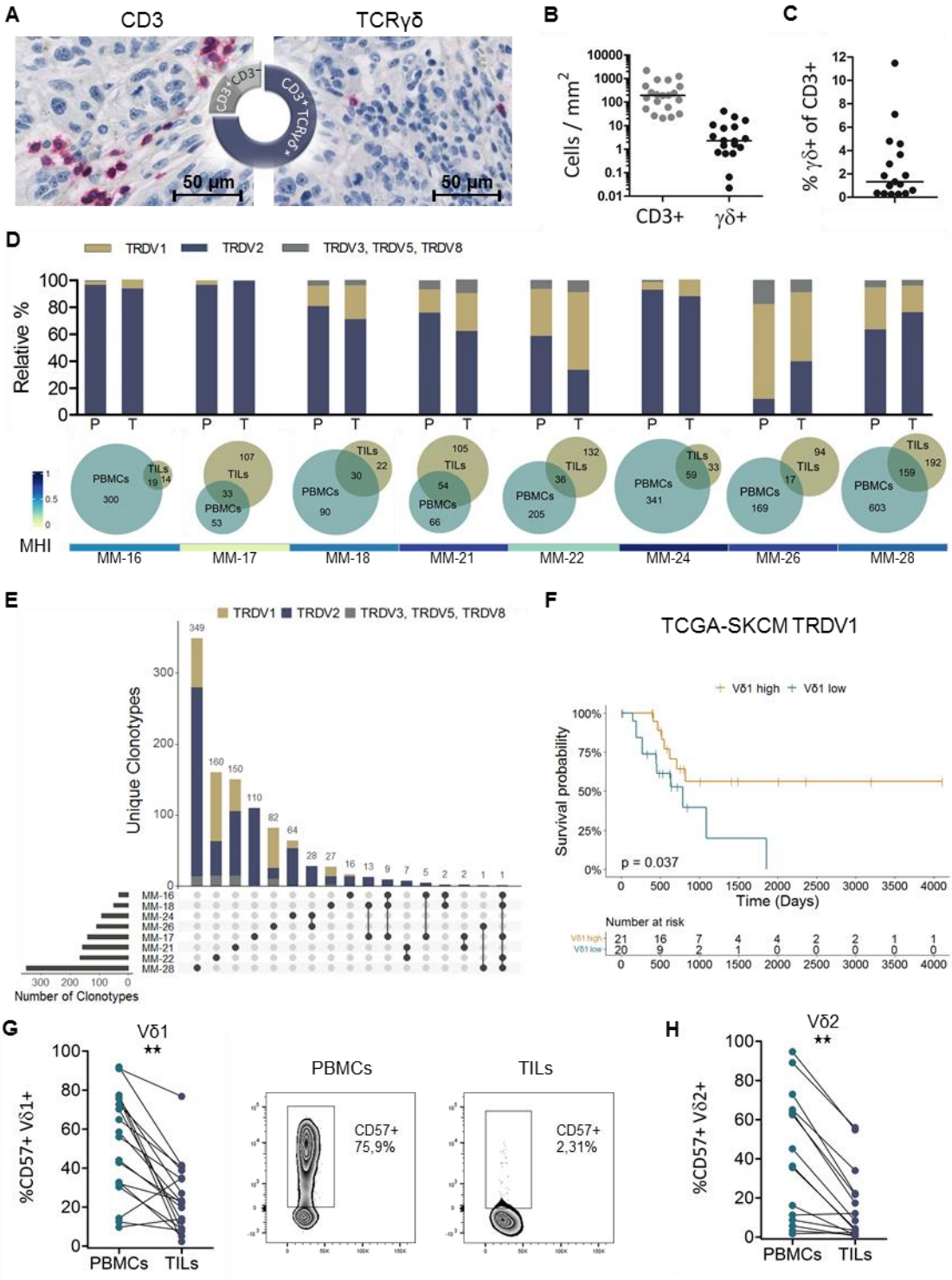

Fig.5 Melanoma- infiltrating Vδ1 T cells are positively associated with survival and a lower CD57 frequency.

(**A**) Representative IHC staining of CD3 and TCRγδ. Pie chart depicts the proportion of metastatic tumor samples showing infiltration with γδ T cells, non-γδ T cells only or no T cell infiltration (n = 24). (**B**) Number of $CD3^+$ and $TCR\gamma\delta^+$ cells per area. (**C**) Percentage of γδ T cells amongst all T cells estimated from serial sections. (**D**) Relative frequencies of TRDV1, TRDV2

and TRDV3/TRDV5/TRDV8 clonotypes in paired samples of **P**BMCs and tumor infiltrating lymphocytes (**T**ILs). Proportional Venn diagrams illustrate the number of detected clonotypes and the proportion of overlapping clonotypes between PBMCs and TILs for each patient. The heatmap displays pairwise TRD repertoire similarity between PBMCs and TILs assessed using the Morisita-Horn index (MHI). (**E**) Clonotype intersections between tumor-infiltrating TCRγδ T cells of metastatic tumor samples. Vertical bar chart represents unique clonotypes and clonotype composition, horizontal bar chart shows the number of clonotypes per patient. Connected dots indicate shared clonotypes. (**F**) Overall survival of stage IIIc and IV patients from the cancer genome atlas (TCGA) skin cutaneous melanoma (SKCM) data set dichotomized based on median TRDV1 expression. Survival distribution compared by log rank test. Frequency of $CD57^+$ cells in paired PBMC and TIL samples for Vδ1 **(G)** and Vδ2 **(H)** T cells (n = 18). Groups compared by Wilcoxon matched pairs signed rank test. **P < 0.01.

DISCUSSION

Despite recent advances in cancer immunotherapy, prognosis of melanoma patients with distant metastases remains poor and only a minority of patients achieves a durable response. γδ T cells mediate mostly anti-tumor and more rarely pro-tumor functions and have been associated with both favorable and unfavorable clinical outcome in different cancer entities (*20, 40*). By comparing the periphery and tumor, we extend previous observations and resolve the apparent paradox of a negative survival association of the Vδ1 frequency in the blood, while a higher abundance of Vδ1 T cells in the tumor is beneficial.

PD-1 blockade reinvigorates exhausted CD8 T cells; this mechanism of action likely extends to other subsets and is not restricted to the tumor microenvironment, but depends on immunomodulation of the peripheral blood and lymphoid compartment (*41*). T cell exhaustion occurs in adaptation to persistent stimulation and is a dynamic process whereby long-lived PD-$1^{intermediate}$ progenitor exhausted cells with low cytotoxicity give rise to short-lived terminally exhausted PD-1^{high} cells. The latter subset is characterized by high cytotoxic activity and the expression of multiple inhibitory receptors including PD-1, TIM-3 and CTLA-4. While progenitor exhausted cells can be reinvigorated by PD-1 blockade, terminally exhausted cells are considered unresponsive (*42*) and melanoma patients with higher proportions of progenitor exhausted cells in pre-therapy biopsies experienced a longer OS under combination therapy (*43*). Our CyTOF experiments did not indicate co-expression of inhibitory receptors, especially not in cluster 1, which distinguished the Vδ1^{high} group. Moreover, the percentage of PD-1^{+} Vδ1 T cells was similar in the two patient groups. Therefore, the level of exhaustion does not seem to differ and is unlikely to account for the differences in OS under anti-PD-1 immunotherapy.

Alongside exhaustion, T cell senescence is another crucial state to consider in the context of dysfunctional tumor immunity (*44*). High levels of senescent peripheral T cells have been associated with poor OS in patients undergoing chemoradiotherapy, PD-(L)1 blockade or cancer vaccination in various solid cancer entities (*45*). T cell senescence is marked by shortened telomeres and a loss of proliferative capacity. Characteristic phenotypic alterations include downregulation of the costimulatory receptors CD27 and CD28, and high expression of CD57 and KLRG1 (*44*). CD57 has been linked to replicative senescence and likely has the same implication for γδ T cells, since $CD57^+$ γδ T cells possess shorter telomeres and have low proliferative potential (*46*). In addition to higher proportions of cells with a TEMRA-like phenotype, we detected higher percentages of $CD57^+$ cells in the $V\delta1^{high}$ group and an overall diminished proliferation of γδ T cells. Furthermore, senescent T cells show an upregulation of a variety of activating and inhibitory NK cell receptors (*47, 48*), increased expression of granzyme B and perforin, and secrete high levels of pro-inflammatory cytokines (*49*). Cluster 1, dominating the $V\delta1^{high}$ group, displayed high expression of the NK cell-related markers CD56, NKG2A and CD161 as well as high perforin levels. The cytokine expression profile was not different between the patient groups or in comparison to HD, though PMA/ionomycin might not be optimal for assessing such differences since these stimuli bypass the TCR. Together, this implies an enrichment of senescence-associated features in patients with high Vδ1 frequencies. Being aware of the limitation that there are no mutually exclusive and inclusive phenotypic markers defining exhausted or senescent T cells, we propose the term “late-differentiated senescent-like” phenotype.

CD28 has been described as the primary target for PD-1-mediated T cell suppression (*50*) and $CD28^+$ CD8 T cells were the pre-dominant subset proliferating under PD-1 blockade in lung cancer patients (*51*). Nonetheless, recent work indicates that CD28 is not required for

responsiveness, but serves as a marker for cells responsive to PD-1 blockade (*52*). Vδ1^{high} patients are characterized by increased levels of late-differentiated senescent-like cells that have lost CD28 expression. Expression of NK-related markers hints at an NK cell-like functionality, which could be advantageous due to a broadening of protective functions (*47*). However, loss of CD28 likely marks these cells as unresponsive to anti-PD-1 therapy, so high percentages of these cells might be disadvantageous in the current immunotherapy setting. For example, in advanced non-small cell lung cancer, elevated frequencies of CD28^{-}CD57^{+}KLRG1^{+} CD8 T cells were associated with poor OS in patients receiving anti-PD-(L)1 therapy (*53*).

In melanoma patients under anti-PD-1 therapy we observed a decrease in the percentage of CD57^{+} Vδ1 T cells, an increase in TRDV1 repertoire diversity but no skewing of the CDR3 spectratype, suggesting polyclonal expansions of less-abundant CD57^{-} Vδ1 clones. Since TRDV1 repertoires would be expected to remain stable over the investigated period (median of 43 days) (*54*), we conclude that a direct or indirect therapy-induced change in TCR repertoires was responsible. This increase in repertoire diversity was only significant in the Vδ1^{low} group, in line with a reduced number of PD-1 blockade-responsive cells in Vδ1^{high} patients. Clonality tended to be higher in the Vδ1^{high} group, which displayed elevated frequencies of CD57^{+} cells, consistent with oligoclonal expansions predominantly described in the CD57^{+} CD8 T cells (*55*).

IHC confirmed that γδ T cells infiltrate melanoma metastases (*22, 23, 56*) and the substantial numbers of shared clonotypes between TILs and PBMCs as well as the degree of TRD repertoire similarity support an ongoing exchange between the peripheral blood and tumor. Within the tumor infiltrating γδ T cells we detected several shared Vδ2 clonotypes including the public clonotype “CACDTLGDTDKLIF” previously described by others (*37, 38, 57*). In contrast, no

Vδ1 clonotypes were shared between the eight studied patients, similar to a recent report by Wu et al. (*58*). In choroidal melanomas the presence of Vδ1 T cells in the tumor correlated positively with survival (*59*). Higher numbers of effector memory Vδ1 T cells in the tumor as well as tissue-resident memory Vδ1 T cells in non-malignant lung tissue were associated with a significantly longer relapse-free survival in resected non-small cell lung cancer (*39*). Furthermore, reanalysis of RNA sequencing data from the INSPIRE trial (*60*), evaluating the effect of pembrolizumab treatment across a variety of advanced solid cancers including melanoma, showed that higher than median TRDV1 expression in tumor biopsies was linked to prolonged OS (*39*). These reports are in line with our analysis of the TCGA SKCM dataset showing a favorable OS in late-stage patients with above median TRDV1 expression. The significantly lower percentage of $CD57^+$ cells within the Vδ1 population in TILs compared to peripheral blood implies a lower prevalence of the late-differentiated senescent-like phenotype in the tumor. In patients with higher frequencies of this phenotype in the blood, the Vδ1 compartment might have a limited potential to expand in the tumor microenvironment and therefore poorer chances of mounting or orchestrating an efficient anti-tumor response.

With regard to the Vδ2 subset, our data revealed no association with clinical outcome and no alterations under anti-PD-1 therapy. This suggests a minor role of this subset in the studied setting, although it is clear that Vδ2 T cells are able to exert anti-tumor effector functions (*20, 61*). However, Vδ2 T cells of melanoma patients showed an altered phenotype with increased levels of $CD57^+$ cells and an impaired functionality in response to phosphoantigen stimulation compared to HD, confirming findings from previously published studies in a more comprehensive and detailed manner (*62-64*).

The main focus of γδ T cell immunotherapy has been on targeting Vδ2 T cells either through stimulation with aminobisphosphonates or in an adoptive transfer setting, although more recently the focus has shifted to the Vδ1 subset (*65-67*). Human melanoma-derived Vδ1 T cell lines mediated cytotoxicity against a melanoma cell line (*68*) and Vδ1 T cells have been shown to traffic to the tumor site and reduce tumor growth in a human melanoma xenograft SCID mouse model (*69*). The results of clinical trials investigating Vδ2 T cells have been disappointing so far (*67*). Since Vδ1 T cells are considered naturally tissue resident, they might be better equipped to traffic to and cope with the hardships of the tumor microenvironment. In addition, based on their MHC independence, γδ T cells are being considered in allogeneic transfer settings even as off-the-shelf products (*70*). There are several ongoing clinical trials and an increasing number of companies utilizing Vδ1 T cells for adoptive transfer or antibody-based strategies to target solid cancer (*71*). Our data, linking Vδ1 T cells to survival outcome and demonstrating a high prevalence of a presumably ICB-unresponsive phenotype in poor survivors encourage these approaches. However, with regard to adoptive cell therapy (chimeric antigen receptor / engineered TCR / Delta One T cell therapy (*72, 73*)) the phenotype of the expanded product should be carefully evaluated, because high proportions of late-differentiated senescent-like cells are likely disadvantageous. Moreover, this supports allogeneic approaches, since in the autologous setting one is restricted by the patients' phenotypic profile. Furthermore, a better understanding of the mechanisms underlying senescence might allow targeting of this dysfunctional state (*45*).

A limitation of our study is that knowledge of T cell exhaustion and senescence stems from investigation of αβ T cells and it remains unclear to which extent these concepts apply to γδ T cells. Nevertheless, there is increasing evidence that Vδ1 T cells follow an adaptive

differentiation process analogous to CD8 T cells (*15*, *74*), indicating parallels in the underlying biology. Furthermore, the precise therapeutic setting of the patients in the TCGA SKCM dataset is unknown and might not be directly comparable to our patient cohorts. Thus, a larger number of tumor samples and phenotypic markers, ideally in situ, would need to be examined to explore associations with clinical outcome related to anti-PD-1 therapy and how the abundance and composition of tumor-infiltrating γδ T cells relates to the phenotypic profile in peripheral blood.

In conclusion, we report a robust association of high peripheral Vδ1 frequencies and poor OS of late-stage melanoma patients undergoing PD-1 blockade. These results are similar to our previous observations in patients receiving ipilimumab (31). The present study extends these findings to reveal that these Vδ1 T cell populations are enriched in cells exhibiting a late-differentiated senescent-like phenotype. Such cells may be dysfunctional and resistant to reactivation by anti-PD-1 therapy. In contrast, enrichment of Vδ1 T cells in the tumor itself was found to be associated with prolonged OS. The majority of tumor-infiltrating Vδ1 T cells did not exhibit a senescent-like phenotype. Thus, we hypothesize that the tumor microenvironment in patients responding to ICB was more conducive to selecting functional, presumably therapy-responsive clones. Consistent with this, we show an alteration of the TRDV1 repertoire composition early under therapy, suggesting ICB-related polyclonal expansions. Altogether, our data support the exploitation of Vδ1 T cells for novel cancer immunotherapy approaches utilizing T cell engagers or adoptive cell therapy as a promising avenue.

MATERIALS AND METHODS

Study design

The aim of this study was to investigate the role of γδ T cells in late-stage melanoma and the influence of anti-PD-1 therapy on this unconventional T cell subset. Peripheral venous blood samples collected before the start of and under therapy were studied and correlated with clinical data. Via high-dimensional single cell analysis the immune signature of γδ T cells was explored in a discovery cohort. Flow cytometric analysis of two further independent patient cohorts (table S1) was performed to validate the findings. Furthermore, cytokine secretion and the proliferative capacity of γδ T cells were determined. The infiltration of γδ T cells into melanoma metastases was assessed by immunohistochemistry and flow cytometry. TCR sequencing was utilized to examine the TRD repertoire of peripheral blood and tumor-infiltrating γδ T cells.

Ethical approval and human samples

EDTA blood was obtained from healthy donors (median age: 61 (range 42-89), 61.8% male, 38.2% female) and late-stage melanoma patients before the start of and under anti-PD-1 therapy. Patients receiving aminobisphosphonate therapy were excluded. Tumor specimens from surgically resected melanoma metastases and paired contemporaneous (-1 to +26 days after surgery) blood samples were collected. Since these samples were processed and measured over a 6-year period, tumor/blood pairs were only compared in a pairwise, but not in a groupwise manner. Bio-banked FFPE blocks of melanoma metastases resected before the start of anti-PD-1 therapy were acquired. This study was conducted in accordance with the Declaration of Helsinki and applicable laws and regulations and has been approved by the Ethics Committee of the University Hospital Tübingen (Project numbers: 315/2018BO2, 280/2022BO2, 633/2019BO2, 652/2026BO2). Written informed consent was obtained from all study participants.

PBMC and TIL isolation

PBMCs were isolated from EDTA blood by Ficoll-Hypaque density gradient centrifugation (FicoLite-H, LINARIS), cryopreserved in RPMI-1640 (Sigma) containing 20% FCS (Sigma) and 10% DMSO (SERVA) and stored in liquid nitrogen. Fresh tumor tissue from surgically resected metastases was finely minced and dissociated using the enzymes H and A from the human Tumor Dissociation Kit (Miltenyi) and a gentleMACS Dissociator (Miltenyi). The cell suspension was passed through a 100 µm cell strainer and washed with RPMI-1640. Freshly isolated TILs were either immediately stained for fluorescence-activated cell sorting or cryopreserved as described above. Sorted γδ T cells were stored in RLT buffer (Qiagen) at -80°C for bulk TCR sequencing.

Lymphocyte activation assay

Thawed, rested PBMCs were seeded in X-Vivo 15 medium (Lonza) and stimulated with 20 ng/ml PMA (Sigma) and 750 ng/ml ionomycin (Merck) or 10 µM zoledronate (Hexal) for 12 h in the presence of Brefeldin A (GolgiPlug, BD) and Monensin (GolgiStop, BD). CD107a Pacific Blue (H4A3, BioLegend) was added directly to the culture medium. Subsequently cells were stained for flow cytometry (fig. S10). The polyfunctionality index was calculated using the following algorithm: $\sum_{i=0}^{n} F_i * \left(\frac{i}{n}\right)$, with n being the number of studied mediators and F_i the frequency of cells expressing i mediators (*33*).

Proliferation assay

Cryopreserved PBMCs were thawed and rested in X-Vivo 15 medium before labeling with 5 µM CellTraceViolet (Invitrogen). Rested, labeled cells were stimulated with 5 µg/ml PHA-L (Roche) or 2.5 µg/ml zoledronate and 30 U/ml IL-2 (Proleukin S, Novartis) or 1 µg/ml immobilized anti-γδTCR mAb (IMMU510, Beckman) and 30 U/ml IL-2. After 5 days of culture, cells were stained

for flow cytometry. Data was analyzed using FlowJo v10.8.0 (BD, fig. S11) and ModFit LT (Version 5.0, Verity Software House) was used to determine the proliferation index. PHA-L stimulation was used as positive control and populations containing less than 100 events were excluded from proliferation analysis.

Flow cytometry and fluorescence-activated cell sorting

Freshly isolated, frozen or cultured PBMCs and TILs were surface stained for lineage and differentiation markers. Cells were incubated with an Fc-receptor-blocking reagent (Gammunex, Grifols) and ethidium monoazide (EMA, Biotium) to label dead cells, or with LIVE/DEAD fixable red (Thermo Fisher Scientific) followed by Fc receptor blocking. An indirect staining approach utilizing the therapeutic antibodies pembrolizumab and nivolumab for detection of PD-1 using anti-human IgG4-PE (Southern Biotech) was applied (*75*). For staining of the γδ TCR an unconjugated antibody in combination with a secondary antibody (*76*) or , to improve the stain index, a streptavidin-biotin based protocol was used (*77*). Cell surface antigens were stained with antibodies directed against CD3 BV510 or Alexa700 (UCHT1 or OKT3), CD27 APC (O323), CD45 BV785 (HI30), CD45RA Pacific Blue (HI100), CD28 PE (CD28.2), CD57 APC or PacificBlue (HCD57), Vδ2 PerCP (B6), PD-1 BV711 (EH12.2H7), Streptavidin-PE; all BioLegend. TCRγδ purified (11F2); BD. TCRγδ Biotin (11F2), Vδ1 FITC (REA173), Vδ2 APC (123R3); all Miltenyi. Vδ1 FITC (TS8.2), F(ab')2-goat anti-mouse IgG Pacific Orange; all Invitrogen. For intracellular cytokine staining cells were fixed and permeabilized with the Cytofix/Cytoperm Fixation/Permeabilization Solution Kit (BD) and stained with IFN-γ PE-Cy7 (B27) and TNF Alexa700 (Mab11) from BioLegend. Cells were acquired on an LSR II flow cytometer (BD) with FACSDiva software v6.1.3 (BD). For fluorescence-activated cell sorting a FACSAria II or FACSAria IIIu (BD) running on FACSDiva software v.8.0.1 or v.9.0.1 (BD) was

used. Data were analyzed with FlowJo (gating strategies see fig. S10-S13) and populations with less than 100 events were excluded from further subset analysis.

Mass cytometry

CyTOF analysis followed established protocols (*78*) and was performed on a partially overlapping cohort of a recent study from Bochem et al. [manuscript in preparation]. In brief, cryopreserved PBMC samples were thawed and 1.5 – $3x10^6$ cells were used for analysis. Rhodium was used as a dead cell marker and Fcγ receptors were blocked using Fcγ receptor blocking reagent (Kioving, Baxter). Surface antibody staining was performed in cell staining medium (CSM) at room temperature. Samples were treated with a fixation/permeabilization kit (Thermo Fisher Scientific), following the manufacturer's instructions, before intracellular antibody staining at 4°C. Samples were then resuspended in PBS containing 4% PFA and stored over night at 4°C. On the next day, each sample was individually incubated with 1 x Iridium intercalator (Fluidigm) and buffered in H_2O. Four element EQ beads (Fluidigm) were added directly before acquisition on a Helios mass cytometer (Fluidigm) at the Flow Cytometry Core Facility, King's College London. Per batch up to five samples were sequentially acquired. FCS files were generated using the Helios software (Fluidigm) and the MATLAB tool from Finck et al. was utilized to normalize for potential batch effects based on the 4 elements EQ beads (*79*). Quality control, data clean-up, concatenations, down-sampling and visualization was done using FlowJo v.10.8.1 (BD, fig. S14). Only samples with >400 Vδ1 T cell counts were considered for analyses. viSNE plots were calculated for data visualization, FlowSOM (*80*) clustering was performed to identify cell subsets of interest and results were overlaid on the respective tSNE plot using Cytobank (Beckmann Coulter). To visualize the cluster distributions of the individual patient samples, the cell counts per sample were downsampled to 433 cells (sample with the

lowest counts). Next, concatenation of the Vδ1^{high} and Vδ1^{low} samples, followed by downsampling to 3031 cells per group was performed for data visualization using density tSNE plots. Heatmaps were generated using the mean of arcsinh(5) transformed marker expressions normalized to a mean of 0 and a standard deviation of 1 per marker.

TCR sequencing

RNA was isolated from sorted γδ T cells using the RNAeasy Micro Kit (Qiagen), followed by cDNA synthesis with the SuperScript reverse transcriptase (Invitrogen). For analysis of the TRD repertoire, CDR3 regions of the δ-chain were amplified via a multiplex PCR approach as described previously (*54*). Paired-end sequencing with 500 cycles was performed at the Illumina MiSeq platform.

TCR repertoire analysis

Repertoire diversity represented by the Gini-Simpson index and clonality represented by 1-Pielou's index were both calculated in Microsoft Excel. Pairwise similarity between repertoires described by the Morisita-Horn index was determined utilizing the R package divo v.1.0.1. Circular tree maps were created with the R package packcircles v.0.3.4, Venn diagrams were generated using BioVenn (*81*). Shared and unique clonotypes of TILs were visualized using the R package UpSetR v.1.4.0 (*82*).

Immunohistochemistry

Serial sections (3 µm) of FFPE tissue were stained with anti-CD3 (SP7; Thermo Scientific), anti-TCRγδ (H-41; Santa Cruz Biotechnology) or the corresponding isotype controls rabbit IgG (SP137; abcam), mouse IgG1 (11711; R&D Systems). Whole slide scans were acquired using a

NanoZoomer 2.0-HT digital slide scanner (Hamamatsu). Hematoxylin and eosin stained slide scans were examined by a histopathologist to identify tumor regions. Quantitative detection of $CD3^+$ and $TCR\gamma\delta^+$ cells was performed using QuPath v.0.2.3 (*83*).

TCGA analysis

Clinical data and HTSeq-Counts from the TCGA-SKCM project were acquired using R software v.4.2.0 and the R/Bioconductor package TCGAbiolinks v.2.24.3 (*84*). To compile a cohort comparable to the patients analyzed in this study (described in table S1) only patients with "AJCC pathologic stage" IV or IIIC were included. Patients with lymph nodes as the "site of resection or biopsy" were excluded. Normalization of HTSeq-Counts was performed using the variance stabilizing transformation included in the R package DESeq2 v.1.36.0 (*85*). Based on the median TRDV1 expression patients were stratified into $V\delta1^{high}$ and $V\delta1^{low}$. "Days to death", "days to last follow up" and "vital status" were used for survival analysis.

Statistical analysis

Heatmaps were generated using the R package ComplexHeatmap v.2.12.1 (*86*). Statistical significance was determined by Mann-Whitney test, Wilcoxon matched-pairs signed rank test or log-rank rest using SPSS Statistics v.28 (IBM), Prism v.5.04 (GraphPad) or the R packages survival v.3.4-0 and survminer v.0.4.9. P-values were adjusted for multiple testing using the Benjamini-Hochberg procedure. A p-value < 0.05 was considered significant.

List of Supplementary Materials

References and Notes

1. J. D. Wolchok, V. Chiarion-Sileni, R. Gonzalez, J. J. Grob, P. Rutkowski, C. D. Lao, C. L. Cowey, D. Schadendorf, J. Wagstaff, R. Dummer, P. F. Ferrucci, M. Smylie, M. O. Butler, A. Hill, I. Marquez-Rodas, J. Haanen, M. Guidoboni, M. Maio, P. Schoffski, M. S. Carlino, C. Lebbe, G. McArthur, P. A. Ascierto, G. A. Daniels, G. V. Long, T. Bas, C. Ritchings, J. Larkin, F. S. Hodi, Long-Term Outcomes With Nivolumab Plus Ipilimumab or Nivolumab Alone Versus Ipilimumab in Patients With Advanced Melanoma. *J Clin Oncol* **40**, 127-137 (2022).
2. J. Larkin, V. Chiarion-Sileni, R. Gonzalez, J. J. Grob, P. Rutkowski, C. D. Lao, C. L. Cowey, D. Schadendorf, J. Wagstaff, R. Dummer, P. F. Ferrucci, M. Smylie, D. Hogg, A. Hill, I. Marquez-Rodas, J. Haanen, M. Guidoboni, M. Maio, P. Schoffski, M. S. Carlino, C. Lebbe, G. McArthur, P. A. Ascierto, G. A. Daniels, G. V. Long, L. Bastholt, J. I. Rizzo, A. Balogh, A. Moshyk, F. S. Hodi, J. D. Wolchok, Five-Year Survival with Combined Nivolumab and Ipilimumab in Advanced Melanoma. *N Engl J Med* **381**, 1535-1546 (2019).
3. A. C. Huang, R. Zappasodi, A decade of checkpoint blockade immunotherapy in melanoma: understanding the molecular basis for immune sensitivity and resistance. *Nat. Immunol.* **23**, 660-670 (2022).
4. E. J. Wherry, M. Kurachi, Molecular and cellular insights into T cell exhaustion. *Nature Reviews Immunology* **15**, 486-499 (2015).
5. A. Schietinger, P. D. Greenberg, Tolerance and exhaustion: defining mechanisms of T cell dysfunction. *Trends Immunol* **35**, 51-60 (2014).
6. M. E. Keir, M. J. Butte, G. J. Freeman, A. H. Sharpel, PD-1 and its ligands in tolerance and immunity. *Annual Review of Immunology* **26**, 677-704 (2008).
7. W. P. Zou, L. P. Chen, Inhibitory B7-family molecules in the tumour microenvironment. *Nat. Rev. Immunol.* **8**, 467-477 (2008).
8. E. Catafal-Tardos, M. V. Baglioni, V. Bekiaris, Inhibiting the Unconventionals: Importance of Immune Checkpoint Receptors in gamma delta T, MAIT, and NKT Cells. *Cancers* **13**, (2021).
9. A. C. Hayday, gamma delta cells: A right time and a right place for a conserved third way of protection. *Annu. Rev. Immunol.* **18**, 975-1026 (2000).
10. A. C. Hayday, gamma delta T Cell Update: Adaptate Orchestrators of Immune Surveillance. *J. Immunol.* **203**, 311-320 (2019).
11. M. S. Davey, C. R. Willcox, S. Hunter, S. A. Kasatskaya, E. B. M. Remmerswaal, M. Salim, F. Mohammed, F. J. Bemelman, D. M. Chudakov, Y. H. Oo, B. E. Willcox, The human Vdelta2(+) T-cell compartment comprises distinct innate-like Vgamma9(+) and adaptive Vgamma9(-) subsets. *Nat Commun* **9**, 1760 (2018).
12. M. M. Karunakaran, C. R. Willcox, M. Salim, D. Paletta, A. S. Fichtner, A. Noll, L. Starick, A. Nohren, C. R. Begley, K. A. Berwick, R. A. G. Chaleil, V. Pitard, J. Dechanet-Merville, P. A. Bates, B. Kimmel, T. J. Knowles, V. Kunzmann, L. Walter, M. Jeeves, F. Mohammed, B. E. Willcox, T. Herrmann, Butyrophilin-2A1 Directly Binds Germline-Encoded Regions of the Vgamma9Vdelta2 TCR and Is Essential for Phosphoantigen Sensing. *Immunity* **52**, 487-498 e486 (2020).
13. M. Rigau, S. Ostrouska, T. S. Fulford, D. N. Johnson, K. Woods, Z. Ruan, H. E. G. McWilliam, C. Hudson, C. Tutuka, A. K. Wheatley, S. J. Kent, J. A. Villadangos, B. Pal, C. Kurts, J. Simmonds, M. Pelzing, A. D. Nash, A. Hammet, A. M. Verhagen, G. Vairo, E. Maraskovsky, C. Panousis, N. A. Gherardin, J. Cebon, D. I. Godfrey, A. Behren, A. P. Uldrich, Butyrophilin 2A1 is essential for phosphoantigen reactivity by gammadelta T cells. *Science* **367**, (2020).
14. H. J. Gober, M. Kistowska, L. Angman, P. Jeno, L. Mori, G. De Libero, Human T cell receptor gammadelta cells recognize endogenous mevalonate metabolites in tumor cells. *J. Exp. Med.* **197**, 163-168 (2003).
15. M. S. Davey, C. R. Willcox, S. P. Joyce, K. Ladell, S. A. Kasatskaya, J. E. McLaren, S. Hunter, M. Salim, F. Mohammed, D. A. Price, D. M. Chudakov, B. E. Willcox, Clonal selection in the human Vdelta1 T cell repertoire indicates gammadelta TCR-dependent adaptive immune surveillance. *Nat Commun* **8**, 14760 (2017).
16. M. Wegrecki, T. A. Ocampo, S. D. Gunasinghe, A. von Borstel, S. Y. Tin, J. F. Reijneveld, T. P. Cao, B. S. Gully, J. Le Nours, D. B. Moody, I. Van Rhijn, J. Rossjohn, Atypical sideways recognition of CD1a by autoreactive gammadelta T cell receptors. *Nat. Commun.* **13**, 3872 (2022).
17. J. Le Nours, N. A. Gherardin, S. H. Ramarathinam, W. Awad, F. Wiede, B. S. Gully, Y. Khandokar, T. Praveena, J. M. Wubben, J. J. Sandow, A. I. Webb, A. von Borstel, M. T. Rice, S. J. Redmond, R. Seneviratna, M. L. Sandoval-Romero, S. Li, M. N. T. Souter, S. B. G. Eckle, A. J. Corbett, H. H. Reid, L.

Liu, D. P. Fairlie, E. M. Giles, G. P. Westall, R. W. Tothill, M. S. Davey, R. Berry, T. Tiganis, J. McCluskey, D. G. Pellicci, A. W. Purcell, A. P. Uldrich, D. I. Godfrey, J. Rossjohn, A class of gammadelta T cell receptors recognize the underside of the antigen-presenting molecule MR1. *Science* **366**, 1522-1527 (2019).
18. C. D. Castro, C. T. Boughter, A. E. Broughton, A. Ramesh, E. J. Adams, Diversity in recognition and function of human gammadelta T cells. *Immunol. Rev.* **298**, 134-152 (2020).
19. A. E. Simoes, B. Di Lorenzo, B. Silva-Santos, Molecular Determinants of Target Cell Recognition by Human gamma delta T Cells. *Frontiers in Immunology* **9**, (2018).
20. B. Silva-Santos, S. Mensurado, S. B. Coffelt, gammadelta T cells: pleiotropic immune effectors with therapeutic potential in cancer. *Nat. Rev. Cancer* **19**, 392-404 (2019).
21. D. Wesch, D. Kabelitz, H. H. Oberg, Tumor resistance mechanisms and their consequences on gamma delta T cell activation. *Immunol. Rev.* **298**, 84-98 (2020).
22. H. Bachelez, B. Flageul, L. Degos, L. Boumsell, A. Bensussan, TCR gamma delta bearing T lymphocytes infiltrating human primary cutaneous melanomas. *J. Invest. Dermatol.* **98**, 369-374 (1992).
23. P. Girard, J. Charles, C. Cluzel, E. Degeorges, O. Manches, J. Plumas, F. De Fraipont, M. T. Leccia, S. Mouret, L. Chaperot, C. Aspord, The features of circulating and tumor-infiltrating gammadelta T cells in melanoma patients display critical perturbations with prognostic impact on clinical outcome. *Oncoimmunology* **8**, 1601483 (2019).
24. K. Wistuba-Hamprecht, S. Di Benedetto, B. Schilling, A. Sucker, D. Schadendorf, C. Garbe, B. Weide, G. Pawelec, Phenotypic characterization and prognostic impact of circulating gammadelta and alphabeta T-cells in metastatic malignant melanoma. *Int. J. Cancer* **138**, 698-704 (2016).
25. M. H. Nada, H. Wang, A. J. Hussein, Y. Tanaka, C. T. Morita, PD-1 checkpoint blockade enhances adoptive immunotherapy by human Vgamma2Vdelta2 T cells against human prostate cancer. *Oncoimmunology* **10**, 1989789 (2021).
26. T. Hoeres, E. Holzmann, M. Smetak, J. Birkmann, M. Wilhelm, PD-1 signaling modulates interferon-gamma production by Gamma Delta (gamma delta) T-Cells in response to leukemia. *Oncoimmunology* **8**, (2019).
27. B. Castella, M. Foglietta, P. Sciancalepore, M. Rigoni, M. Coscia, V. Griggio, C. Vitale, R. Ferracini, E. Saraci, P. Omede, C. Riganti, A. Palumbo, M. Boccadoro, M. Massaia, Anergic bone marrow V gamma 9V delta 2 T cells as early and long-lasting markers of PD-1-targetable microenvironment-induced immune suppression in human myeloma. *Oncoimmunology* **4**, (2015).
28. G. M. Hu, P. Wu, P. Cheng, Z. G. Zhang, Z. Wang, X. Y. Yu, X. Shao, D. Wu, J. Ye, T. Zhang, X. C. Wang, F. M. Qiu, J. Yan, J. Huang, Tumor-infiltrating CD39(+) gamma delta Tregs are novel immunosuppressive T cells in human colorectal cancer. *Oncoimmunology* **6**, (2017).
29. A. Dondero, F. Pastorino, M. Della Chiesa, M. V. Corrias, F. Morandi, V. Pistoia, D. Olive, F. Bellora, F. Locatelli, A. Castellano, L. Moretta, A. Moretta, C. Bottino, R. Castriconi, PD-L1 expression in metastatic neuroblastoma as an additional mechanism for limiting immune surveillance. *Oncoimmunology* **5**, (2016).
30. E. Foord, L. C. M. Arruda, A. Gaballa, C. Klynning, M. Uhlin, Characterization of ascites- and tumor-infiltrating gamma delta T cells reveals distinct repertoires and a beneficial role in ovarian cancer. *Sci. Transl. Med.* **13**, (2021).
31. M. Iwasaki, Y. Tanaka, H. Kobayashi, K. Murata-Hirai, H. Miyabe, T. Sugie, M. Toi, N. Minato, Expression and function of PD-1 in human gammadelta T cells that recognize phosphoantigens. *Eur J Immunol* **41**, 345-355 (2011).
32. K. Wistuba-Hamprecht, A. Martens, K. Haehnel, M. Geukes Foppen, J. Yuan, M. A. Postow, P. Wong, E. Romano, A. Khammari, B. Dreno, M. Capone, P. A. Ascierto, I. Demuth, E. Steinhagen-Thiessen, A. Larbi, B. Schilling, D. Schadendorf, J. D. Wolchok, C. U. Blank, G. Pawelec, C. Garbe, B. Weide, Proportions of blood-borne Vdelta1+ and Vdelta2+ T-cells are associated with overall survival of melanoma patients treated with ipilimumab. *Eur. J. Cancer* **64**, 116-126 (2016).
33. M. Larsen, D. Sauce, L. Arnaud, S. Fastenackels, V. Appay, G. Gorochov, Evaluating Cellular Polyfunctionality with a Novel Polyfunctionality Index. *PLoS One* **7**, (2012).
34. E. P. Rock, P. R. Sibbald, M. M. Davis, Y. H. Chien, Cdr3 Length in Antigen-Specific Immune Receptors. *J. Exp. Med.* **179**, 323-328 (1994).
35. M. M. Davis, P. J. Bjorkman, T-cell antigen receptor genes and T-cell recognition. *Nature* **334**, 395-402 (1988).
36. M. Papadopoulou, T. Dimova, M. Shey, L. Briel, H. Veldtsman, N. Khomba, H. Africa, M. Steyn, W. A. Hanekom, T. J. Scriba, E. Nemes, D. Vermijlen, Fetal public Vgamma9Vdelta2 T cells expand and gain potent cytotoxic functions early after birth. *Proc. Natl. Acad. Sci. U.S.A.* **117**, 18638-18648 (2020).

37. K. Kakimi, H. Matsushita, K. Masuzawa, T. Karasaki, Y. Kobayashi, K. Nagaoka, A. Hosoi, S. Ikemura, K. Kitano, I. Kawada, T. Manabe, T. Takehara, T. Ebisudani, K. Nagayama, Y. Nakamura, R. Suzuki, H. Yasuda, M. Sato, K. Soejima, J. Nakajima, Adoptive transfer of zoledronate-expanded autologous V gamma 9V delta 2 T-cells in patients with treatment-refractory non-small-cell lung cancer: a multicenter, open-label, single-arm, phase 2 study. *J. Immunother. Cancer* **8**, (2020).
38. L. H. Deng, A. Harms, S. Ravens, I. Prinz, L. K. Tan, Systematic pattern analyses of V delta 2(+) TCRs reveal that shared "public" V delta 2(+) gamma delta T cell clones are a consequence of rearrangement bias and a higher expansion status (vol 13, 960920, 2022). *Front. Immunol.* **13**, (2022).
39. Y. Wu, D. Biswas, I. Usaite, M. Angelova, S. Boeing, T. Karasaki, S. Veeriah, J. Czyzewska-Khan, C. Morton, M. Joseph, S. Hessey, J. Reading, A. Georgiou, M. Al-Bakir, N. J. Birkbak, N. McGranahan, M. Jamal-Hanjani, A. Hackshaw, S. A. Quezada, A. C. Hayday, C. Swanton, T. Consortium, A local human V delta 1 T cell population is associated with survival in nonsmall-cell lung cancer. *Nat. Cancer* **3**, 696-+ (2022).
40. G. Chabab, C. Barjon, N. Bonnefoy, V. Lafont, Pro-tumor gamma delta T Cells in Human Cancer: Polarization, Mechanisms of Action, and Implications for Therapy. *Frontiers in Immunology* **11**, (2020).
41. N. Budimir, G. D. Thomas, J. S. Dolina, S. Salek-Ardakani, Reversing T-cell Exhaustion in Cancer: Lessons Learned from PD-1/PD-L1 Immune Checkpoint Blockade. *Cancer Immunol. Res.* **10**, 146-153 (2022).
42. W. Q. Jiang, Y. J. He, W. G. He, G. S. Wu, X. L. Zhou, Q. S. Sheng, W. X. Zhong, Y. M. Lu, Y. F. Ding, Q. Lu, F. Ye, H. J. Hua, Exhausted CD8+T Cells in the Tumor Immune Microenvironment: New Pathways to Therapy. *Front. Immunol.* **11**, (2021).
43. B. C. Miller, D. R. Sen, R. Al Abosy, K. Bi, Y. V. Virkud, M. W. LaFleur, K. B. Yates, A. Lako, K. Felt, G. S. Naik, M. Manos, E. Gjini, J. R. Kuchroo, J. J. Ishizuka, J. L. Collier, G. K. Griffin, S. Maleri, D. E. Comstock, S. A. Weiss, F. D. Brown, A. Panda, M. D. Zimmer, R. T. Manguso, F. S. Hodi, S. J. Rodig, A. H. Sharpe, W. N. Haining, Subsets of exhausted CD8(+) T cells differentially mediate tumor control and respond to checkpoint blockade. *Nat. Immunol.* **20**, 326-336 (2019).
44. Y. J. Zhao, Q. X. Shao, G. Y. Peng, Exhaustion and senescence: two crucial dysfunctional states of T cells in the tumor microenvironment. *Cellular & Molecular Immunology* **17**, 27-35 (2020).
45. J. Zhang, T. H. He, L. X. Xue, H. Y. Guo, Senescent T cells: a potential biomarker and target for cancer therapy. *EBioMedicine* **68**, (2021).
46. W. Xu, G. Monaco, E. H. Wong, W. L. W. Tan, H. Kared, Y. Simoni, S. W. Tan, W. Z. Y. How, C. T. Y. Tan, B. T. K. Lee, D. Carbajo, G. S. K, I. C. H. Low, E. W. H. Mok, S. Foo, J. Lum, H. L. Tey, W. P. Tan, M. Poidinger, E. Newell, T. P. Ng, R. Foo, A. N. Akbar, T. Fulop, A. Larbi, Mapping of gamma/delta T cells reveals Vdelta2+ T cells resistance to senescence. *EBioMedicine* **39**, 44-58 (2018).
47. B. I. Pereira, R. P. H. De Maeyer, L. P. Covre, D. Nehar-Belaid, A. Lanna, S. Ward, R. Marches, E. S. Chambers, D. C. O. Gomes, N. E. Riddell, M. K. Maini, V. H. Teixeira, S. M. Janes, D. W. Gilroy, A. Larbi, N. A. Mabbott, D. Ucar, G. A. Kuchel, S. M. Henson, J. Strid, J. H. Lee, J. Banchereau, A. N. Akbar, Sestrins induce natural killer function in senescent-like CD8(+) T cells. *Nat. Immunol.* **21**, 684-694 (2020).
48. R. Tarazona, O. DelaRosa, C. Alonso, B. Ostos, J. Espejo, J. Pena, R. Solana, Increased expression of NK cell markers on T lymphocytes in aging and chronic activation of the immune system reflects the accumulation of effector/senescent T cells. *Mech. Ageing Dev.* **121**, 77-88 (2000).
49. A. N. Akbar, S. M. Henson, A. Lanna, Senescence of T Lymphocytes: Implications for Enhancing Human Immunity. *Trends Immunol.* **37**, 866-876 (2016).
50. E. F. Hui, J. Cheung, J. Zhu, X. L. Su, M. J. Taylor, H. A. Wallweber, D. K. Sasmal, J. Huang, J. M. Kim, I. Mellman, R. D. Vale, T cell costimulatory receptor CD28 is a primary target for PD-1-mediated inhibition. *Science* **355**, 1428-+ (2017).
51. A. O. Kamphorst, A. Wieland, T. Nasti, S. Yang, R. Zhang, D. L. Barber, B. T. Konieczny, C. Z. Daugherty, L. Koenig, K. Yu, G. L. Sica, A. H. Sharpe, G. J. Freeman, B. R. Blazar, L. A. Turka, T. K. Owonikoko, R. N. Pillai, S. S. Ramalingam, K. Araki, R. Ahmed, Rescue of exhausted CD8 T cells by PD-1-targeted therapies is CD28-dependent. *Science* **355**, 1423-1427 (2017).
52. K. H. Kim, H. K. Kim, H. D. Kim, C. G. Kim, H. Lee, J. W. Han, S. J. Choi, S. Jeong, M. Jeon, H. Kim, J. Koh, B. M. Ku, S. H. Park, M. J. Ahn, E. C. Shin, PD-1 blockade-unresponsive human tumor-infiltrating CD8(+) T cells are marked by loss of CD28 expression and rescued by IL-15. *Cell. Mol. Immunol.* **18**, 385-397 (2021).
53. R. Ferrara, M. Naigeon, E. Auclin, B. Duchemann, L. Cassard, J. M. Jouniaux, L. Boselli, J. Grivel, A. Desnoyer, L. Mezquita, M. Texier, C. Caramella, L. Hendriks, D. Planchard, J. Remon, S. Sangaletti, C. Proto, M. C. Garassino, J. C. Soria, A. Marabelle, A. L. Voisin, S. Farhane, B. Besse, N. Chaput,

Circulating T-cell Immunosenescence in Patients with Advanced Non-small Cell Lung Cancer Treated with Single-agent PD-1/PD-L1 Inhibitors or Platinum-based Chemotherapy. *Clin. Cancer Res.* **27**, 492-503 (2021).
54. S. Ravens, C. Schultze-Florey, S. Raha, I. Sandrock, M. Drenker, L. Oberdorfer, A. Reinhardt, I. Ravens, M. Beck, R. Geffers, C. von Kaisenberg, M. Heuser, F. Thol, A. Ganser, R. Forster, C. Koenecke, I. Prinz, Human gammadelta T cells are quickly reconstituted after stem-cell transplantation and show adaptive clonal expansion in response to viral infection. *Nat Immunol* **18**, 393-401 (2017).
55. J. K. Morley, F. M. Batliwalla, R. Hingorani, P. K. Gregersen, Oligoclonal Cd8(+) T-Cells Are Preferentially Expanded in the Cd57(+) Subset. *J. Immunol.* **154**, 6182-6190 (1995).
56. M. Donia, E. Ellebaek, M. H. Andersen, P. T. Straten, I. M. Svane, Analysis of Vdelta1 T cells in clinical grade melanoma-infiltrating lymphocytes. *Oncoimmunology* **1**, 1297-1304 (2012).
57. M. Papadopoulou, T. Dimova, M. Shey, L. Briel, H. Veldtsman, N. Khomba, H. Africa, M. Steyn, W. A. Hanekom, T. J. Scriba, E. Nemes, D. Vermijlen, Fetal public Vgamma9Vdelta2 T cells expand and gain potent cytotoxic functions early after birth. *Proc Natl Acad Sci U S A* **117**, 18638-18648 (2020).
58. Y. Wu, F. Kyle-Cezar, R. T. Woolf, C. Naceur-Lombardelli, J. Owen, D. Biswas, A. Lorenc, P. Vantourout, P. Gazinska, A. Grigoriadis, A. Tutt, A. Hayday, An innate-like V delta 1(+) gamma delta T cell compartment in the human breast is associated with remission in triple-negative breast cancer. *Sci. Transl. Med.* **11**, (2019).
59. A. A. Bialasiewicz, J. X. Ma, G. Richard, alpha/beta and gamma/delta TCR+ lymphocyte infiltration in necrotising choroidal melanomas. *Br. J. Ophthalmol.* **83**, 1069-1073 (1999).
60. S. Y. Cindy Yang, S. C. Lien, B. X. Wang, D. L. Clouthier, Y. Hanna, I. Cirlan, K. Zhu, J. P. Bruce, S. El Ghamrasni, M. A. J. Iafolla, M. Oliva, A. R. Hansen, A. Spreafico, P. L. Bedard, S. Lheureux, A. Razak, V. Speers, H. K. Berman, A. Aleshin, B. Haibe-Kains, D. G. Brooks, T. L. McGaha, M. O. Butler, S. V. Bratman, P. S. Ohashi, L. L. Siu, T. J. Pugh, Pan-cancer analysis of longitudinal metastatic tumors reveals genomic alterations and immune landscape dynamics associated with pembrolizumab sensitivity. *Nat. Commun.* **12**, 5137 (2021).
61. V. Cazzetta, E. Bruni, S. Terzoli, C. Carenza, S. Franzese, R. Piazza, P. Marzano, M. Donadon, G. Torzilli, M. Cimino, M. Simonelli, L. Bello, A. Villa, L. K. Tan, S. Ravens, I. Prinz, D. Supino, F. S. Colombo, E. Lugli, E. Marcenaro, E. Vivier, S. Della Bella, J. Mikulak, D. Mavilio, NKG2A expression identifies a subset of human V delta 2 T cells exerting the highest antitumor effector functions. *Cell Rep.* **37**, (2021).
62. I. Petrini, S. Pacini, S. Galimberti, M. R. Taddei, A. Romanini, M. Petrini, Impaired function of gamma-delta lymphocytes in melanoma patients. *Eur J Clin Invest* **41**, 1186-1194 (2011).
63. K. Argentati, F. Re, S. Serresi, M. G. Tucci, B. Bartozzi, G. Bernardini, M. Provinciali, Reduced number and impaired function of circulating gamma delta T cells in patients with cutaneous primary melanoma. *J. Invest. Dermatol.* **120**, 829-834 (2003).
64. F. Re, A. Donnini, B. Bartozzi, G. Bernardini, M. Provinciali, Circulating gammadelta T cells in young/adult and old patients with cutaneous primary melanoma. *Immun. Ageing* **2**, 2 (2005).
65. D. Kabelitz, R. Serrano, L. Kouakanou, C. Peters, S. Kalyan, Cancer immunotherapy with gammadelta T cells: many paths ahead of us. *Cell. Mol. Immunol.*, (2020).
66. F. Toia, A. B. Di Stefano, S. Meraviglia, E. Lo Presti, R. Pirrello, G. Rinaldi, F. Fulfaro, F. Dieli, A. Cordova, Gammadelta T Cell-Based Immunotherapy in Melanoma: State of the Art. *J Oncol* **2019**, 9014607 (2019).
67. Z. Sebestyen, I. Prinz, J. Dechanet-Merville, B. Silva-Santos, J. Kuball, Translating gammadelta (gammadelta) T cells and their receptors into cancer cell therapies. *Nat Rev Drug Discov*, (2019).
68. A. Cordova, F. Toia, C. La Mendola, V. Orlando, S. Meraviglia, G. Rinaldi, M. Todaro, G. Cicero, L. Zichichi, P. L. Donni, N. Caccamo, G. Stassi, F. Dieli, F. Moschella, Characterization of Human gamma delta T Lymphocytes Infiltrating Primary Malignant Melanomas. *Plos One* **7**, (2012).
69. F. Lozupone, D. Pende, V. L. Burgio, C. Castelli, M. Spada, M. Venditti, F. Luciani, L. Lugini, C. Federici, C. Ramoni, L. Rivoltini, G. Parmiani, F. Belardelli, P. Rivera, S. Marcenaro, L. Moretta, S. Fais, Effect of human natural killer and gamma delta T cells on the growth of human autologous melanoma xenografts in SCID mice. *Cancer Res.* **64**, 378-385 (2004).
70. X. C. Y. Amani Makkouk, Taylor Barca, Anthony Lucas, Mustafa Turkoz, Jonathan T S Wong, Kevin P Nishimoto, Mary M Brodey, Maryam Tabrizizad, Smitha R Y Gundurao, Lu Bai, Arun Bhat, Zili An, Stewart Abbot, Daulet Satpayev, Blake T Aftab and Marissa Herrman, Off-the-shelf Vδ1 gamma delta T cells engineered with glypican-3 (GPC-3)-specific chimeric antigen receptor (CAR) and soluble IL-15 display robust antitumor efficacy against hepatocellular carcinoma. (2021).

71. J. Saura-Esteller, M. De Jong, L. A. King, E. Ensing, B. Winograd, T. D. De Gruijl, P. W. H. I. Parren, H. J. van der Vliet, Gamma Delta T-Cell Based Cancer Immunotherapy: Past-Present-Future. *Front. Immunol.* **13**, (2022).
72. B. Di Lorenzo, A. E. Simoes, F. Caiado, P. Tieppo, D. V. Correia, T. Carvalho, M. G. da Silva, J. Dechanet-Merville, T. N. Schumacher, I. Prinz, H. Norell, S. Ravens, D. Vermijlen, B. Silva-Santos, Broad Cytotoxic Targeting of Acute Myeloid Leukemia by Polyclonal Delta One T Cells. *Cancer Immunol. Res.* **7**, 552-558 (2019).
73. S. Mensurado, R. Blanco-Dominguez, B. Silva-Santos, The emerging roles of gammadelta T cells in cancer immunotherapy. *Nat. Rev. Clin. Oncol.* **20**, 178-191 (2023).
74. J. L. McMurray, A. von Borstel, T. E. Taher, E. Syrimi, G. S. Taylor, M. Sharif, J. Rossjohn, E. B. M. Remmerswaal, F. J. Bemelman, F. A. Vieira Braga, X. Chen, S. A. Teichmann, F. Mohammed, A. A. Berry, K. E. Lyke, K. C. Williamson, M. J. T. Stubbington, M. S. Davey, C. R. Willcox, B. E. Willcox, Transcriptional profiling of human Vdelta1 T cells reveals a pathogen-driven adaptive differentiation program. *Cell Rep.* **39**, 110858 (2022).
75. H. Zelba, J. Bochem, G. Pawelec, C. Garbe, K. Wistuba-Hamprecht, B. Weide, Accurate quantification of T-cells expressing PD-1 in patients on anti-PD-1 immunotherapy. *Cancer Immunol Immunother*, (2018).
76. K. Wistuba-Hamprecht, G. Pawelec, E. Derhovanessian, OMIP-020: Phenotypic characterization of human gammadelta T-cells by multicolor flow cytometry. *Cytometry A* **85**, 522-524 (2014).
77. N. Beucke, D. Wesch, H. H. Oberg, C. Peters, J. Bochem, B. Weide, C. Garbe, G. Pawelec, S. Sebens, C. Rocken, H. Hashimoto, M. W. Loffler, P. Nocerino, S. Kordasti, D. Kabelitz, K. Schilbach, K. Wistuba-Hamprecht, Pitfalls in the characterization of circulating and tissue-resident human gammadelta T cells. *J. Leukoc. Biol.*, (2020).
78. S. Kordasti, B. Costantini, T. Seidl, P. Perez Abellan, M. Martinez Llordella, D. McLornan, K. E. Diggins, A. Kulasekararaj, C. Benfatto, X. Feng, A. Smith, S. A. Mian, R. Melchiotti, E. de Rinaldis, R. Ellis, N. Petrov, G. A. Povoleri, S. S. Chung, N. S. Thomas, F. Farzaneh, J. M. Irish, S. Heck, N. S. Young, J. C. Marsh, G. J. Mufti, Deep phenotyping of Tregs identifies an immune signature for idiopathic aplastic anemia and predicts response to treatment. *Blood* **128**, 1193-1205 (2016).
79. R. Finck, E. F. Simonds, A. Jager, S. Krishnaswamy, K. Sachs, W. Fantl, D. Pe'er, G. P. Nolan, S. C. Bendall, Normalization of mass cytometry data with bead standards. *Cytometry A* **83**, 483-494 (2013).
80. S. Van Gassen, B. Callebaut, M. J. Van Helden, B. N. Lambrecht, P. Demeester, T. Dhaene, Y. Saeys, FlowSOM: Using self-organizing maps for visualization and interpretation of cytometry data. *Cytometry A* **87a**, 636-645 (2015).
81. T. Hulsen, J. de Vlieg, W. Alkema, BioVenn - a web application for the comparison and visualization of biological lists using area-proportional Venn diagrams. *BMC Genom.* **9**, (2008).
82. A. Lex, N. Gehlenborg, H. Strobelt, R. Vuillemot, H. Pfister, UpSet: Visualization of Intersecting Sets. *IEEE Trans Vis Comput Graph* **20**, 1983-1992 (2014).
83. P. Bankhead, M. B. Loughrey, J. A. Fernandez, Y. Dombrowski, D. G. McArt, P. D. Dunne, S. McQuaid, R. T. Gray, L. J. Murray, H. G. Coleman, J. A. James, M. Salto-Tellez, P. W. Hamilton, QuPath: Open source software for digital pathology image analysis. *Sci Rep* **7**, 16878 (2017).
84. A. Colaprico, T. C. Silva, C. Olsen, L. Garofano, C. Cava, D. Garolini, T. S. Sabedot, T. M. Malta, S. M. Pagnotta, I. Castiglioni, M. Ceccarelli, G. Bontempi, H. Noushmehr, TCGAbiolinks: an R/Bioconductor package for integrative analysis of TCGA data. *Nucleic Acids Res.* **44**, e71 (2016).
85. M. I. Love, W. Huber, S. Anders, Moderated estimation of fold change and dispersion for RNA-seq data with DESeq2. *Genome Biol.* **15**, (2014).
86. Z. G. Gu, R. Eils, M. Schlesner, Complex heatmaps reveal patterns and correlations in multidimensional genomic data. *Bioinformatics* **32**, 2847-2849 (2016).

Acknowledgments:

Cell sorting was done on shared instruments of the Flow Cytometry Core Facility Tübingen. Acquisition of mass cytometry experiments was performed at the advanced cytometry platform at King's College London. Many thanks to Susanne Heck, Richard J Ellis, Rianne Wester and Cynthia Bishop for their excellent support and the scientific discussions. Thanks to Dieter Kabelitz and Christian Peters for scientific discussions and to Petra Leber for performing the IHC staining. Furthermore, we would like to thank the Study Center at the University Hospital Tübingen, Department of General, Visceral and Transplant Surgery, particularly Silvia Wagner and Jürgen Winter for their assistance regarding sample collection. We thank all patients and volunteers for their support and participation in this study.

Funding:

Deutsche Forschungsgemeinschaft (DFG)(WI 5021/1-1 FOR2799); KW-H

DFG (WI 5021/2-1 FOR2799); KW-H

DFG, Cluster of Excellence iFIT (EXC2180) 'Image-Guided and Functionally Instructed Tumor Therapies', University of Tübingen, Tübingen, Germany; S.54.10087; KW-H, MWL & MC

Medical Faculty of the University of Tübingen (F1261355); KW-H

Medical Faculty of the University of Tübingen (2509-0-0); KW-H

Klaus Tschira Foundation, Germany (03.132.2017); KW-H

Klaus Tschira Foundation, Germany (000.316.2017); KW-H

CRUK City of London Centre Award at KCL (CTRQQR-2021/100004); SK, RAR

Author contributions:

Conceptualization: KW-H

Investigation: NH, JB, JL, SW, SF, JS, MD, CY, PN, TA, NBW, KT, DS, KB, FM, MWL, SR, SK, TKE, KW-H

Data curation – formal analysis: NH, JB, SW, SF, MD, MWL, SR, SK, KW-H

Project administration: KW-H

Writing – original draft: NH

Writing – review & editing: NH, JB, JL, SW, RAR, KB, PT, DW, HHO, SS, MC, AK, CG, GP, FM, MWL, BW, IP, SR, SK, TKE, KW-H

Competing interests:

SF has received personal fees from Kyowa Kirin, Takeda Pharamceuticals and Recordati Pharma GmbH (speaker′s honoraria), as well as institutional grants from NeraCare, SkylineDX and BioNTech outside the submitted work. NBW has received advisor's honoraria from Pierre-Fabre and advisor's honoraria as well as speaker's fees from Novartis and Sanofi outside the submitted work.PT has received travel support or/and speaker´s fees or/and advisor´s honoraria from Almirall Hermal, Biofrontera, Bristol-Myers Squibb, CureVac, Kyowa Kirin, Merck, Merck Sharp & Dohme, Novartis, Pierre-Fabre, Roche, Sanofi, 4SC. FM has received travel support or/and speaker's fees or/and advisor's honoraria by Novartis, Roche, BMS, MSD, Pierre Fabre, Sanofi and Immunocore and research funding from Novartis and Roche. MWL has received travel support by RanD S.p.A. and is an inventor of patents owned by Immatics Biotechnologies, further he has acted as a speaker and paid consultant in cancer immunology for Boehringer Ingelheim. TKE is/was a consultant for Novartis, MSD, Merck, CureVac, Bristol-Myers Squibb, Sanofi, Immunocore, Pierre Fabre, Almirall Hermal. The other authors declare that they have no competing interests.

Data and materials availability:

All data are available in the main text or the supplementary materials or upon reasonable request from the corresponding author.

Table S1: Patients characteristics

Factor	Category	Cohort 1 "CyTOF" n = 15		Cohort 2 "Differentiation" n = 91		Cohort 3 "CD57" n = 70	
		n	%	n	%	n	%
Clinical Site	Tübingen	15	100	63	69.2	51	72.9
	Dresden	0	0	17	18.7	16	22.9
	Lübeck	0	0	11	12.1	3	4.2
Treatment	anti-PD-1	15	100	91	100	25	35.7
	anti-PD-1 + anti-CTLA-4	0	0	0	0	45	64.3
Sex	Female	5	33.3	33	36.3	29	41.4
	Male	10	66.7	58	63.7	41	58.6
Stage	III	3	20.0	14	15.4	6	8.6
	IV	12	80.0	77	84.6	64	91.4
M category (AJCC)	M1a	2	13.3	12	13.2	6	8.6
	M1b	3	20.0	16	17.6	7	10.0
	M1c	9	60.0	53	58.2	53	75.7
	unknown	1	6.7	10	11.0	4	5.7
Age	Median	77		74		72	
	Range	65-82		36-94		23-89	

Table S2: Panel for mass cytometry

Specificity	Label	Clone	Manufacturer
TCR Vδ2	141Pr	B6	BioLegend
CD57	142Nd	HCD57	Fluidigm
CD45RA	143Nd	HI100	Fluidigm
CD4	145Nd	RPA-T4	Fluidigm
CD8a	146Nd	RPA-T8	Fluidigm
CD25	149Sm	2A3	Fluidigm
CD161	150Nd	HP-3G10	BioLegend
CD14	151Eu	M5E2	Fluidigm
TIM-3	153Eu	F38-2E2	Fluidigm
TIGIT	154Sm	MBSA43	Fluidigm
CD86	156Gd	IT2.2	Fluidigm
CD33	158Gd	WM53	Fluidigm
CD197	159Tb	G043H7	Fluidigm
anti-FITC	160Gd	FIT-22	Fluidigm
CD152*	161Dy	14D3	Fluidigm
CD80	162Dy	2D10.4	Fluidigm
CD56	163Dy	NCAM16.2	Fluidigm
CD28	164Dy	CD28.2	BioLegend
CD314	166Er	ON72	Fluidigm
CD27	167Er	L128	Fluidigm
CD159a	169Tm	Z199	Fluidigm
CD3	170Er	UCHT1	Fluidigm
HLA-DR	174Yb	L243	Fluidigm
Perforin*	175Lu	B-D48	Fluidigm
CD127	176Yb	A019D5	Fluidigm
CD16	209Bi	3G8	Fluidigm
CD45	89Y	HI30	Fluidigm
TCR Vδ2	FITC	TS8.2	Life Technologies

* Intracellular detection

Supplementary Figures

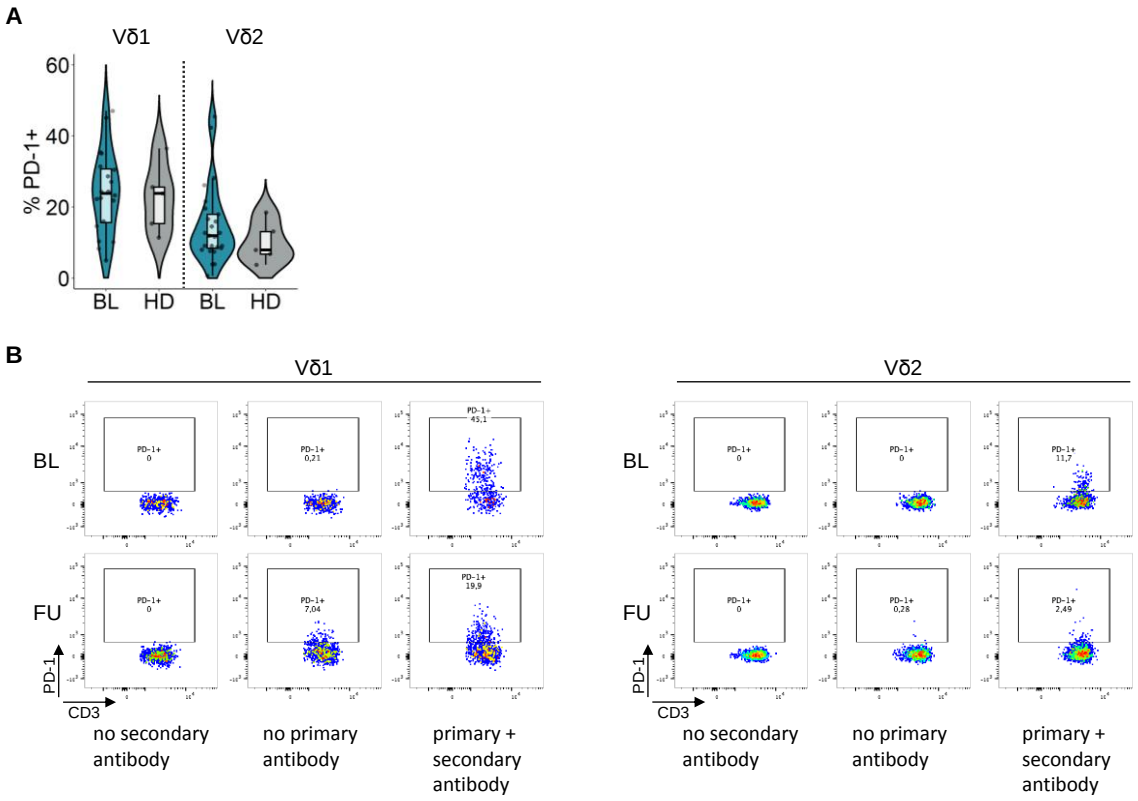

Fig. S1 PD-1 expression on γδ T cells.
(A) Percentage of PD-1-expressing Vδ1 and Vδ2 T cells in patients before the start of therapy (BL) and healthy donors (HD). **(B)** Analysis of PD-1 expression in patients at follow-up (FU) under anti-PD-1 therapy. Flow cytometric detection of therapeutic antibody (Pembrolizumab) on Vδ1 and Vδ2 T cells using an anti-IgG4 PE antibody.

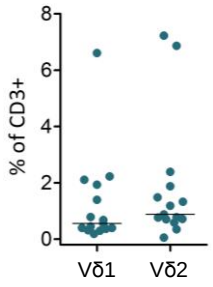

Fig. S2 Frequency of Vδ1 and Vδ2 T cells within all T cells.
Percentage of CD3+ cells expressing Vδ1 or Vδ2 in melanoma patients before the start of therapy. Horizontal lines denote the median.

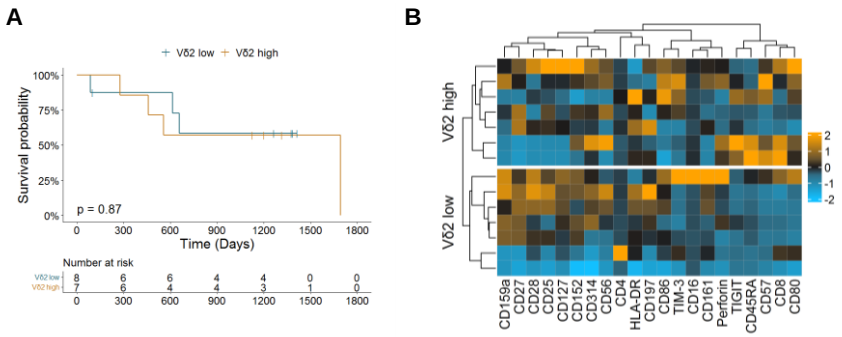

Fig. S3 Vδ2 T cell frequencies are not associated with survival.
(A) Overall survival of late-stage melanoma patients dichotomized based on the BL median Vδ2 frequency (0.88 %) determined by mass cytometry. Survival distribution compared by log rank rest. **(B)** Heat map of phenotypic marker expression on Vδ2 T cells. Each row represents the BL sample of one patient, heatmaps are divided based on median Vδ2 frequency. Marker expression was arcsinh-transformed and normalized to a mean of 0 and a standard deviation of 1. Relative overexpression indicated in orange, relative underexpression in blue.

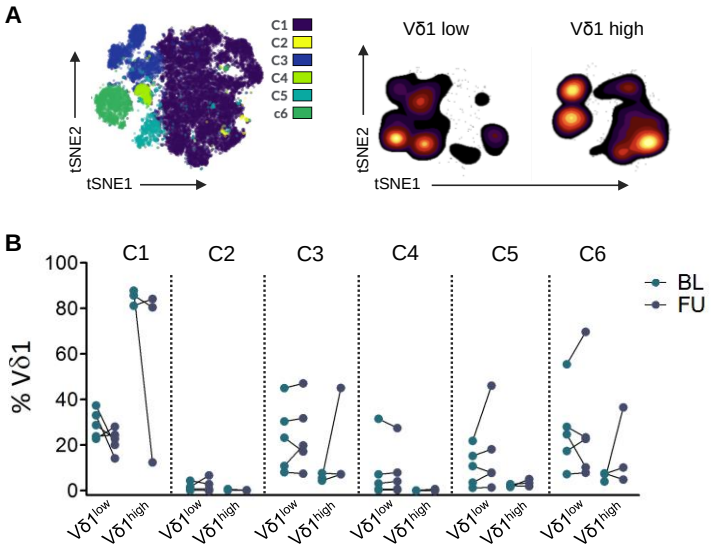

Fig. S4 Changes in Vδ1 cluster frequencies under therapy.
(**A**) tSNE visualization of Vδ1 T cells from BL and FU samples. Clusters were annotated using FlowSOM. Smoothed contour plots show FU samples of the patient groups with lower and higher than median Vδ1 frequencies at BL. **(B)** Change of the Vδ1 FlowSOM cluster frequencies from BL to FU for patients with high and low Vδ1 frequencies.

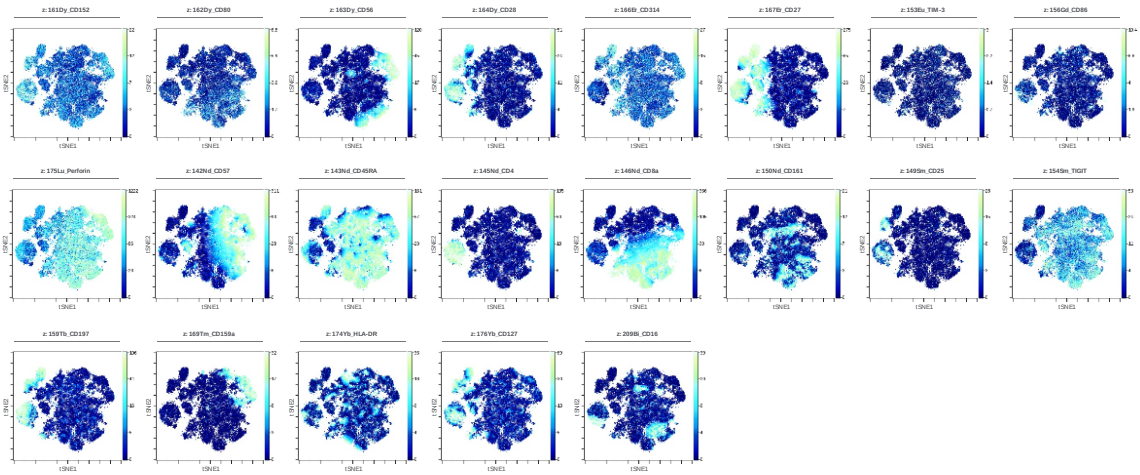

Fig. S5 Expression profile of Vδ1 T cells determined by mass cytometry.
Distribution of relative arcsinh-transformed marker expression intensities for Vδ1 T cells in all investigated samples projected on the tSNE visualization.

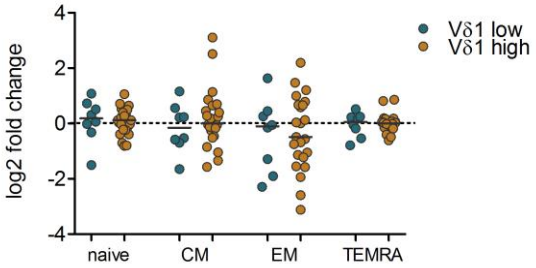

Fig. S6 Fold change in Vδ1 memory differentiation profile.
Log2 fold change between BL and FU for naive, central memory (CM), effector memory (EM) and TEMRA Vδ1 T cells for patients with high and low Vδ1 frequencies.

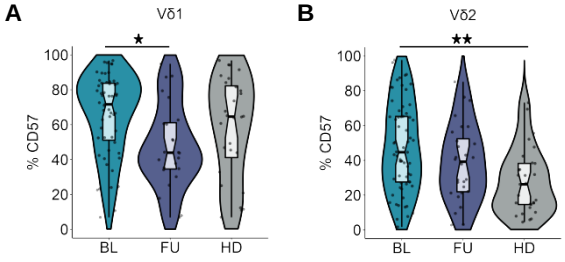

Fig. S7 CD57 expression in patients and healthy donors.
(A) Expression of CD57 on Vδ1 and **(B)** Vδ2 T cells in patients at BL and FU and in healthy donors. Groups compared by Man-Whitney-U test. *P < 0.05, **P < 0.01.

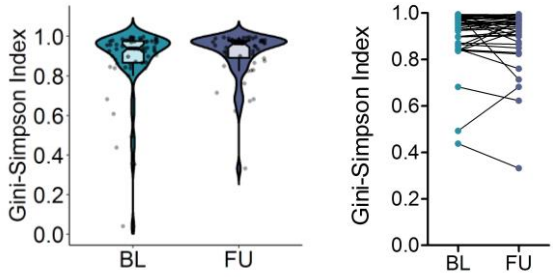

Fig. S8 Diversity of the TRDV2 repertoire.
TRDV2 repertoire diversity in PBMCs from melanoma patients at BL and FU represented by the Gini-Simpson index.

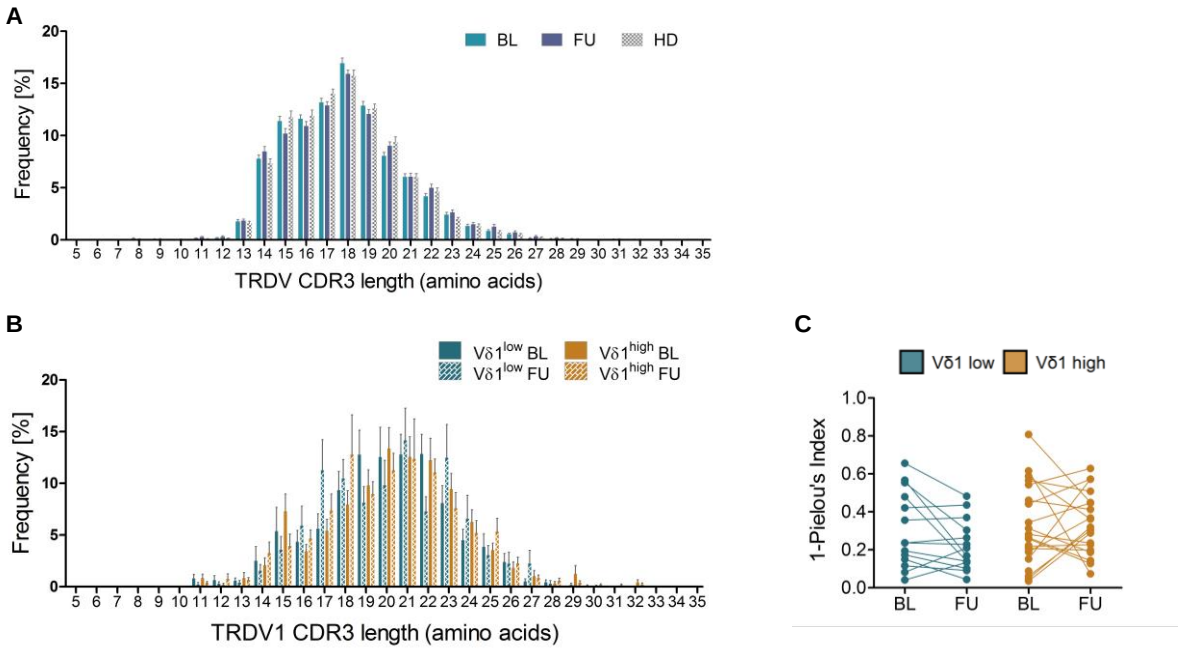

Fig. S9 Composition of the TRDV1 repertoire.
(**A**) Comparison of the TRDV repertoire CDR3 length distribution between patients at BL and FU and healthy donors. (**B**) Comparison of the TRDV1 repertoire CDR3 length distribution between BL and FU and the Vδ1^{low} and Vδ1^{high} group. (**C**) Changes in TRDV1 repertoire clonality (1-Pielou's Index) under therapy in the Vδ1^{low} and Vδ1^{high} group. Bars indicate mean, whiskers standard error of the mean.

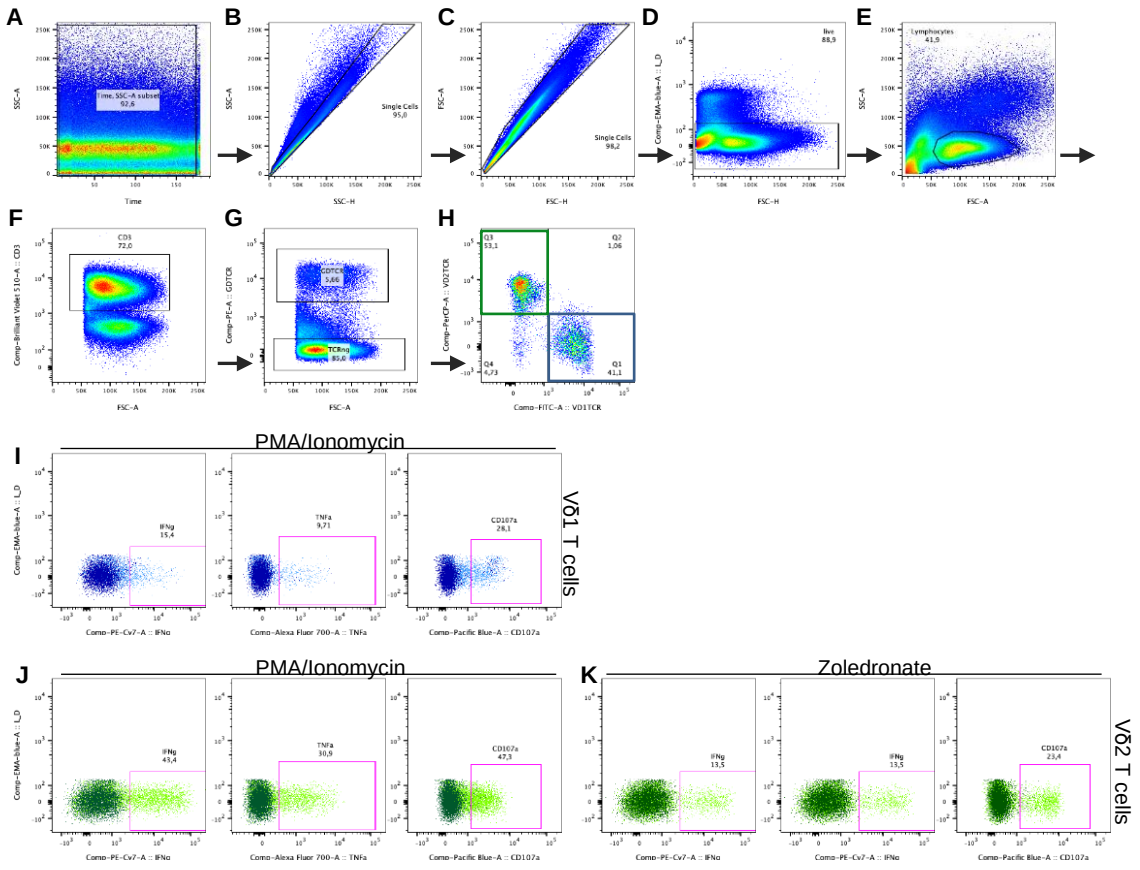

Fig. S10 Gating strategy for functional analysis.

(**A**) Gating started with a time gate to monitor potential fluctuations in the pressure system and exclude cross-contamination from the previous sample. (**B**)(**C**) Singlets were selected and (**D**) dead cells excluded, followed by (**E**) lymphocyte gating. (**F**) CD3+, (**G**) TCRγδ+ cells were subdivided into (**H**) Vδ1+ and Vδ2+ cells. Expression of functional markers (IFNγ, TNF & CD107a) was quantified relative to the not stimulated sample (dark versus light coloring in the overlayed dot plots) for PMA/Ionomycin stimulation of Vδ1+ **(I)** Vδ2+ T cells (**J**) and for zoledronate stimulation of Vδ2 T cells (**K**).

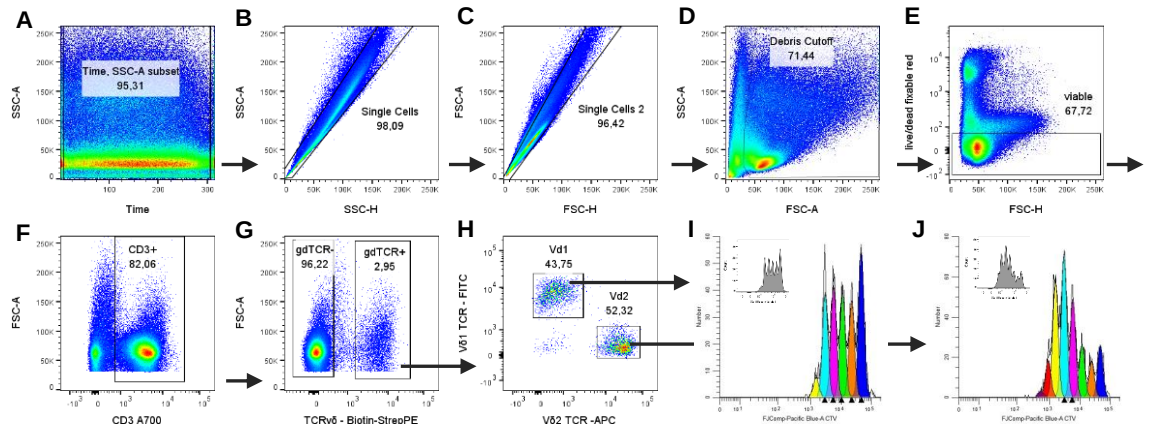

Fig. S11 Gating strategy for proliferation analysis.
(**A**) Gating started with a time gate to monitor potential fluctuations in the pressure system and exclude cross-contamination from the previous sample. (**B**)(**C**) Singlets were selected. (**D**) Debris was excluded and no lymphocyte gate applied to avoid bias, because proliferating cells deviate in size and granularity from non-proliferating lymphocytes. (**E**) Dead cells were excluded. (**F**) CD3+, (**G**) TCRγδ+ cells were subdivided into (**H**) Vδ1+ and Vδ2+ cells. (**I**)(**J**) Proliferation of both subsets was examined using the ModFit proliferation analysis tool.

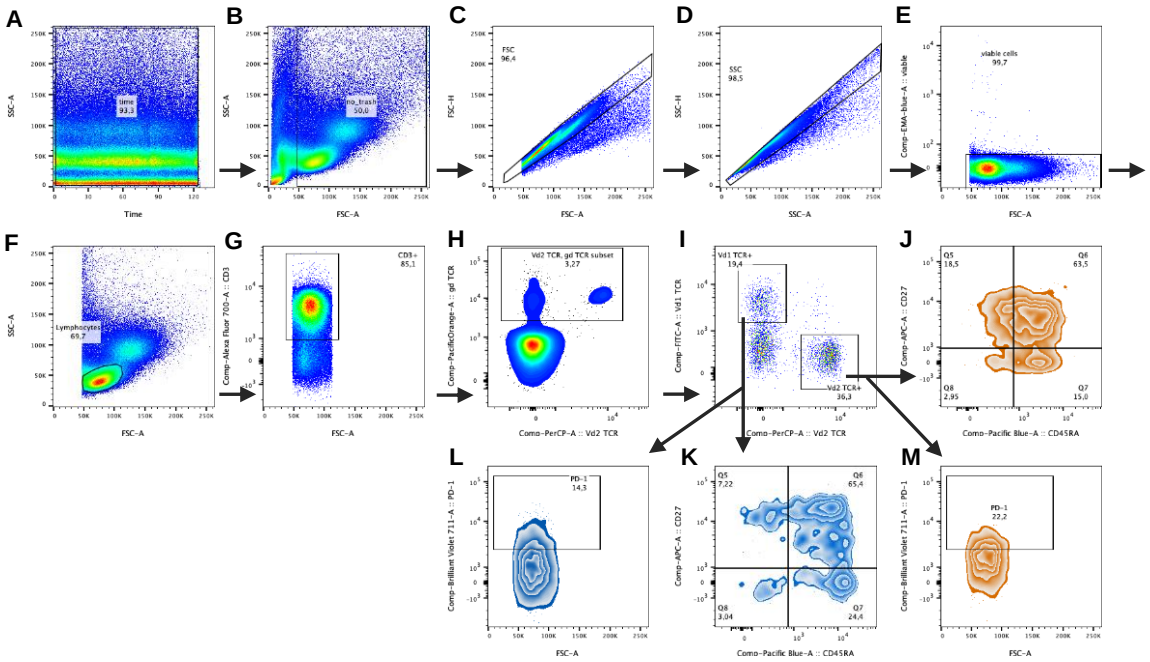

Fig. S12 Gating strategy differentiation panel.
(**A**) Gating started with a time gate to monitor potential fluctuations in the pressure system and exclude cross-contamination from the previous sample. **(B)** Debris was excluded. (**C**)(**D**) Singlets were selected and (**E**) dead cells excluded, followed by (**F**) lymphocyte gating. (**G**) CD3+, (**H**) TCRγδ+ cells were subdivided into (**I**) Vδ1+ and Vδ2+ T cells. (**J**)(**K**) Differentiation subsets were gated based on differential expression of CD27 and CD45RA. (**L**)(**M**) PD-1 expression was quantified on Vδ1+ and Vδ2+ T cells.

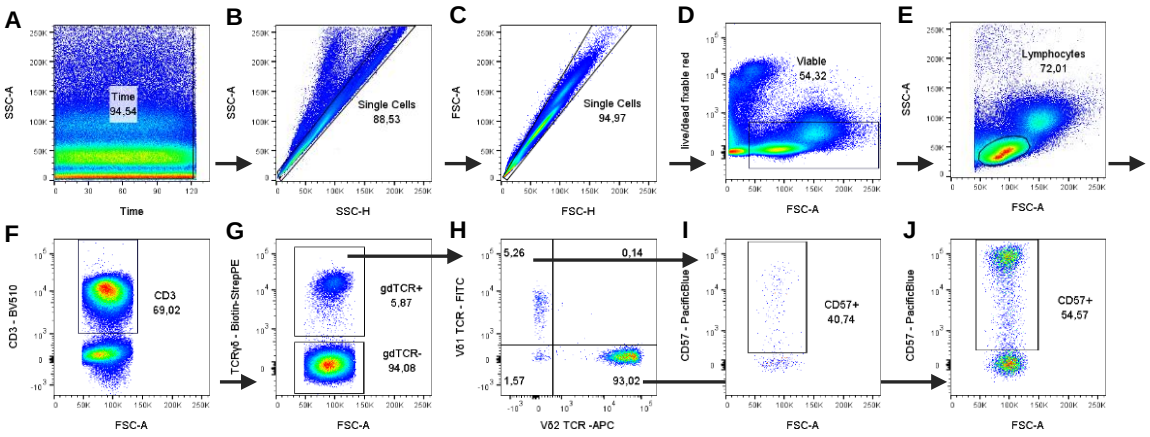

Fig. S13 Gating strategy phenotypic panel.
(**A**) Gating started with a time gate to monitor potential fluctuations in the pressure system and exclude cross-contamination from the previous sample. (**B**)(**C**) Singlets were selected and (**D**) dead cells excluded, followed by (**E**) lymphocyte gating. (**F**) CD3+, (**G**) TCRγδ+ cells were subdivided into (**H**) Vδ1+ and Vδ2+ cells. (**I**)(**J**) CD57 expression on both subsets was examined.

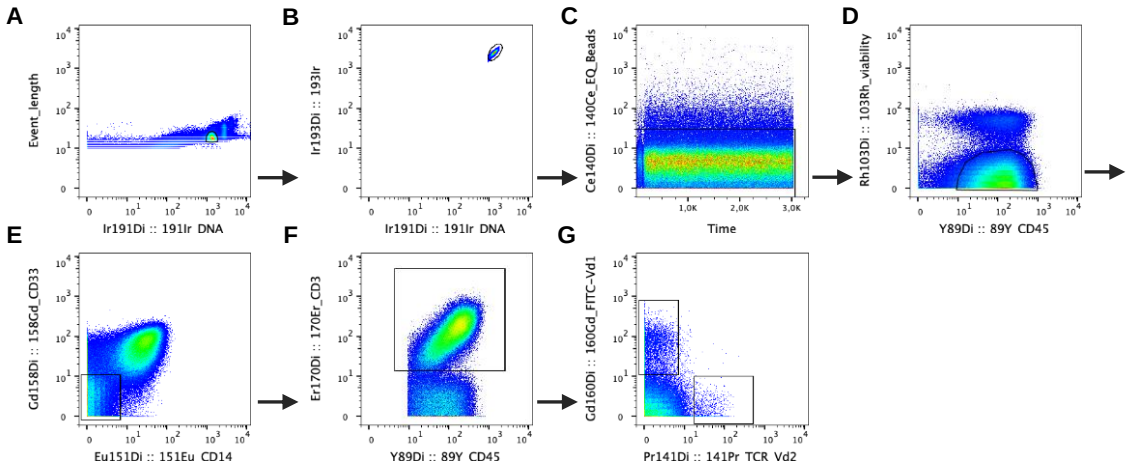

Fig. S14 Gating strategy for mass cytometry.
(**A**) Intact cells were identified based on event length and Ir-191, (**B**) followed by Ir193 versus Ir191. (**C**) Exclusion of EQ beads. (**D**) Viable, rhodium negative CD45+ cells were selected. (**E**) Cells expressing CD33 and/or CD14 were excluded. (**F**) CD3+ cells were subdivided into (**G**) Vδ1+ and Vδ2+ cells.